IMPACT OF NOVEL CAVEOLIN-1 FRAMESHIFT MUTANTS ON CAVEOLAE ASSEMBLY AND FUNCTION

By

Courtney Amanda Copeland

Dissertation

Submitted to the Faculty of the

Graduate School of Vanderbilt University

in Partial Fulfillment of the Requirements

for the Degree of

DOCTOR OF PHILOSOPHY

in

Molecular Physiology and Biophysics

May 2017

Nashville, Tennessee

Approved:

Roger Colbran, Ph.D.

David Harrison, M.D.

Aurelio Galli, Ph.D.

Ambra Pozzi, Ph.D.

Todd Graham, Ph.D.

DEDICATION

I dedicate this dissertation to my loving parents, who have always been my inspiration. My mom and dad have always shown me unwavering support throughout my life and especially during my pre-doctoral fellowship here at Vanderbilt. My parents have been the greatest support system and always provide me with wisdom and motivation that helps me get through the ups and downs of life. They have been there every step of the way and I am thankful they have been at my side through all of my challenges and all of my accomplishments. ESPECIALLY THIS ONE!!!!!!!!

Love you, Mom and Dad!

ACKNOWLEDGEMENTS

I have been very fortunate to have a tremendous amount of support from people in my life, especially here at Vanderbilt. I am forever grateful for their contributions and guidance that have been essential throughout this process and for my success in earning my doctoral degree.

I thank my mentor Anne Kenworthy, for her guidance and support during my time in her lab. My development as a scientist has been deeply influenced by her insight and her confidence in me to allow me to have independence in my projects. I admire her as a scientist and her many contributions to the field. I would also like to acknowledge Roger Colbran, David Harrison, Aurelio Galli, Ambra Pozzi and Todd Graham for serving on my thesis committee, and their wisdom over the years.

I would also like to thank my past and current lab members for their help, and friendship. Bing Han and I worked closely together on our projects and he was also extremely helpful to me as a graduate student. The molecular biology advise of Ajit Tiwari helped me not pull all of my hair out during my time generating mutants for my research projects and the friendship we developed was an added benefit. And last but not least, Krish Raghunathan, for all of his wisdom in coding, statistical analysis, and image analysis, not to mention the countless hours of great conversation and advice over the years.

To Tim Sparer, Tom Masi and Pranay “P-Dog” Dogra, thank you all for your friendship and helping me realize my potential as a scientist while at the University of Tennessee as a lab technician. I would not be here without you guys!!!

To my extraordinary parents David and Susan, as well as the rest of my family and friends, thank you all from the bottom of my heart. You guys mean the world to me and helped me stay grounded throughout life and while in graduate school.

ACKNOWLEDGEMENT OF FUNDING

This research was funded through the National Institutes of Health (R01 HL111259-01S1) awarded to Dr. Anne Kenworthy.

PUBLICATIONS

The contents of Chapter III were published in *Traffic* (2016 Dec; 17(12): 1297-1312. doi: 10.1111/tra.12452).

Additional Publications are as follows:

1. Tiwari, A., Copeland, C. A., Han, B., Hanson, C. A., Raghunathan, K. and Kenworthy, A. K. (2016). Caveolin-1 is an aggresome-inducing protein. *Scientific Reports*, *6*, 38681. http://doi.org/10.1038/srep38681

2. Han, B., Copeland, C. A., Kawano, Y., Rosenzweig, E. B., Austin, E. D., Shahmirzadi, L., Tang, S., Raghunathan, K., Chung, W. K. and Kenworthy, A. K. (2016). Characterization of a caveolin-1 mutation associated with both pulmonary arterial hypertension and congenital generalized lipodystrophy, *Traffic*, 17(12): 1297–1312. doi: 10.1111/tra.12452

3. Dogra, P., Miller-Kittrell, M., Pitt, E., Jackson, J., Masi, T., Copeland, C., Wu, S., Miller, W. and Sparer, T. J. (2016) *Gen. Virol.* 97(11): 2957-2972 doi:10.1099/jgv.0.000603

4. Han, B., Copeland, C. A., Tiwari, A. and Kenworthy, A. K. (2016). Assembly and Turnover of Caveolae: What Do We Really Know? *Frontiers in Cell and Developmental Biology*, *4*, 68. http://doi.org/10.3389/fcell.2016.00068

5. Doyle, J. D., Stencel-Baerenwald, J. E., Copeland, C. A., Rhoads, J. P., Brown, J. J., Boyd, K. L. and Dermody, T. S. (2015). Diminished Reovirus Capsid Stability Alters Disease Pathogenesis and Littermate Transmission. *PLoS Pathogens*, *11*(3), e1004693. http://doi.org/10.1371/journal.ppat.1004693

6. Day, C. A., Baetz, N. W., Copeland, C. A., Kraft, L. J., Han, B., Tiwari, A. and Kenworthy, A. K. (2015). Microtubule Motors Power Plasma Membrane Tubulation in Clathrin-Independent Endocytosis. *Traffic (Copenhagen, Denmark)*, *16*(6), 572–590. http://doi.org/10.1111/tra.12269

7. Nicholas, K. J., Zern, E. K., Barnett, L., Smith, R. M., Lorey, S. L., Copeland, C. A. and Kalams, S. A. (2013). B Cell Responses to HIV Antigen Are a Potent Correlate of Viremia in HIV-1 Infection and Improve with PD-1 Blockade. *PLoS ONE*, *8*(12), e84185. http://doi.org/10.1371/journal.pone.0084185

TABLE OF CONTENTS

Page

LIST OF TABLES

LIST OF FIGURES

LIST OF SUPPLEMENTARY FIGURES

(APPENDIX A)

CHAPTER 1

INTRODUCTION

The goal of this work has been to delineate the impact of novel caveolin-1 frameshift mutants on the assembly and function specialized invaginated membrane microdomains called caveolae. Caveolae are found in many cell types [1, 2] and are important platforms for cell signaling, mechano-protection and maintaining lipid homeostasis [3-6]. Oligomers of the scaffolding protein Caveolin-1 provide the structural framework of caveolae needed to support their characteristic morphology [7-9] (Figure 1). Expression, oligomerization and trafficking of Caveolin-1 is required for the formation of stable caveolae [8]. Caveolin-1 deficiency compromises the formation, abundance and functions of caveolae at the plasma membrane [10-12] giving rise to hyperproliferative cells with altered lipid composition and increased sensitivity to mechanical stress [3-6].

Recently, two novel heterozygous *Caveolin-1* frameshift mutations were identified in a family of patients with pulmonary arterial hypertension (PAH; CAV1-P158) and patient with both PAH and congenital generalized lipodystrophy (CGL; CAV1-F160X) [13-16]. Reduced CAV1 protein levels were reported in these preliminary studies; however, how this impacts caveolae formation and function is not known [14-16]. It is therefore important to characterize the behavior of these mutants and their impact on caveolae in order to begin determining how they give rise to disease. Here, the expression, oligomerization, trafficking, and assembly of caveolae were examined in patient cells and *caveolin-1*$^{-/-}$ murine embryonic fibroblasts (MEFs) transfected with the mutant proteins. These studies indicate that neither mutant completely ablates caveolae formation and both are capable of co-assembling into complexes with wild type Caveolin-1 that are required for caveolae formation; however, they are biochemically unstable. CAV1-P158 behaves as a dominant negative, reduces caveolae formation and disrupts the mechano-protective function of caveolae. CAV1-F160X is incorporated into caveolae with no affect on their abundance or mechano-protection, but the

incorporation of this mutant with wild type Caveolin-1 in caveolae results in the formation of less stable caveolae with an altered composition [13]. This is a novel example of a disease-associated Caveolin-1 mutant that has no effect on the density of caveolae in cells despite causing a more severe phenotype. Thus, abnormal stability and composition of caveolae are contributing factors to the development of PAH and CGL.

In this chapter, caveolae/CAV1 the concept of membrane microdomains will be introduced with an emphasis on caveolae membranes and their essential protein components. The implications and proposed roles of caveolae/CAV1 in human diseases will be discussed with a primary focus on PAH, CGL and the CAV1 mutants investigated in these studies.

1.1 Membrane Microdomains

The **plasma membrane** functions as a barrier between the extracellular environment and the cytoplasmic contents of the cell and is found in living organisms. The plasma membrane (PM) is composed of a diverse milieu of lipid species that form a continuous lipid bilayer that also contains cholesterol and membrane proteins, which are laterally dispersed throughout the bilayer. Membrane fluidity is a property of the PM that allows lipids and membrane proteins to laterally diffuse across the plasma membrane. However, nano-scale clustering within the bilayer promoted by lipid-lipid, lipid-protein and protein-protein interactions gives rise to distinct transient fluid-phase ***microdomains*** and generates heterogeneity/asymmetry within the plasma membrane [17, 18].

Microdomains are further divided into two categories that have distinct properties: **i)** ***non-lipid rafts*** are detergent-soluble portions of the membrane composed of lipids and proteins that display high lateral mobility and are considered liquid-disordered (L_d) membranes. **ii)** ***Lipid rafts*** are planar membrane domains ranging from ~5-20 nm in diameter that are enriched in cholesterol and sphingomyelin [19]. The enrichment of

these types of lipids in rafts promotes the tight packing between other raft-associated lipids/proteins and reduces their lateral mobility. Tight association between lipid raft components also decreases membrane fluidity, promoting the characteristic properties of increased detergent-insolubility and liquid-order (L_o). The compartmentalization of lipids and proteins within rafts is believed to be an important contributing factor for their proposed functions in trans-/endo-/exocytosis, membrane trafficking and modulating protein activity and cell signaling events [20].

In addition to *planar* lipid rafts, invaginated structures highly enriched in cholesterol and sphingolipids called ***caveolae*** are another specialized membrane microdomain with raft-like properties and functions. Unlike dynamic, transient planar lipid rafts, omega-shaped caveolae membranes are generally larger diameter than planar lipid rafts and are characteristically highly immobile structures [21]. The biogenesis and functions of caveolae are discussed in detail in section 1.2 below.

1.2 Caveolae: Components Required for Assembly and Stability

Caveolae are 50-100 nm invaginations found at the plasma membrane of many cell types including adipocytes, smooth muscle and endothelial cells [1, 2] (Figure 1). Caveolae are specialized membrane domains enriched in cholesterol and sphingolipids implicated in numerous cellular events: **i) Endocytosis** of caveolae is required for repairing wounded regions of the plasma membrane, internalization and recycling of excess lipids [22-24]. **Transcytosis** in endothelial cells occurs in a caveolae-dependent manner and plays a role in maintaining tight junctions [22]. Caveolae can also negatively regulate clathrin-independent endocytosis [25]. **ii)** Caveolae modulate activity and localization of extracellular and intracellular signaling molecules to maintain their appropriate spatial distribution, thereby integrating **signal transduction** events [26]. **iii) Fatty acid and lipid uptake** occurs in caveolae, and caveolae involvement in lipid storage/metabolism is critically important for adipose tissue function [27, 28]. **iv)** In environments when the plasma membrane is under high amounts of mechanical tension, caveolae flattening **buffers** the membrane to prevent cells from rupturing and

caveolae are involved in **mechano-transduction** [25, 29-31]. Exactly how these events are regulated by caveolae, however, is not fully understood but currently is extensively investigated in the field. In order to understand the requirements necessary for caveolae function, many groups have focused on identifying the protein composition of these structures and the critical components involved in caveolae formation.

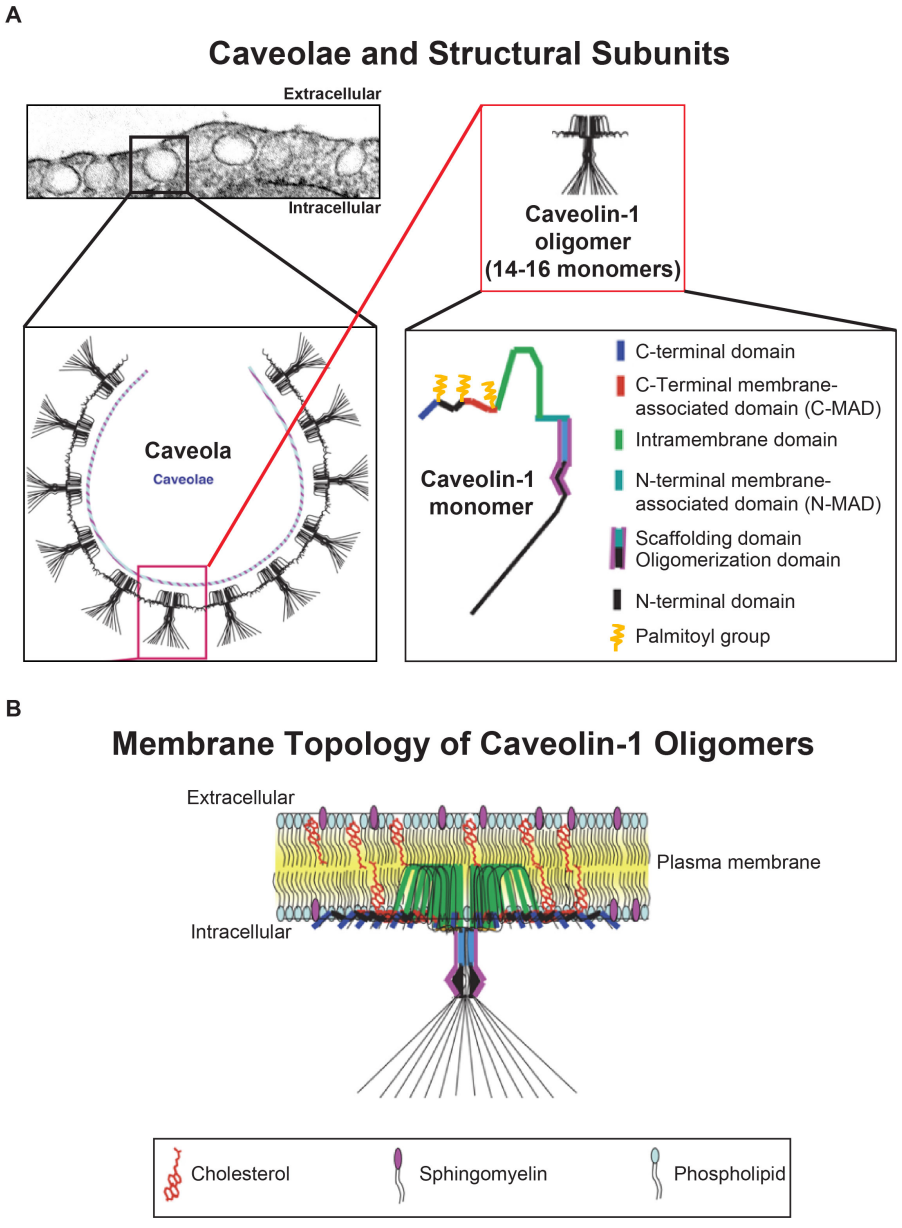

Figure 1. Caveolae and Caveolin-1 Organization. (A) Electron micrograph depicting caveolae in human dermal fibroblasts. The arrangement of Caveolin-1 oligomers within caveolae, composition of caveolae oligomers and the subdomains of Caveolin-1 monomers are also shown. **(B)** A Cartoon showing the topology of Caveolin-1 oligomers in a lipid bilayer. Adapted from Mercier et al., 2009 [32].

1.2.1 The Caveolin Family of Proteins

Caveolins are conserved in many species and comprise a family of hairpin-like integral membrane proteins with cytoplasmic N- and C-termini. Caveolins contain four domains: the N-terminal domain (NTD), scaffolding domain (CSD), intramembrane domain (IMD) and C-terminal domain (CTD) [33-35] (Figure 2). Three mammalian caveolin family members (1, 2, and 3) are expressed in a variety of tissues and the formation of caveolae critically depends on the expression of these proteins. Caveolin-1 and Caveolin-2 are expressed together in most cell types, while Caveolin-3 is specifically expressed in skeletal, smooth and cardiac muscle [25, 26]. Unlike Caveolin-1/3, the assembly of caveolin-2 into complexes that are recruited to caveolae is dependent on the expression of and oligomerization with Caveolin-1/3. In the absence of caveolin-1 expression, caveolin-2 is unable to exit the Golgi complex and is rapidly degraded [11]. Caveolins also undergo post-translational modifications: all caveolins are palmitoylated on three homologous cysteine residues found in the C-terminal domain of the proteins and caveolin-1 and caveolin-2 can be phosphorylated on multiple residues (Figure 1 and 2) [29-32].

Table 1. Caveolins Proteins (Human; Full-Length)

Name	Tissue Distribution	Size	Molecular weight	% Similarity (Identity) to CAV1	% Similarity (Identity) to CAV2
Caveolin-1/ CAV1 NP_001744.2	Most tissues	178 aa.	21-24 kDa	100% (100%)	-
Caveolin-2/ CAV2 NP_001224.1	Most Tissues	162 aa.	18-21 kDa	74% (41%)	100% (100%)
Caveolin-3/ CAV3 NP_001225.1	Muscle	151 aa.	~21 kDa	87% (64%)	72% (39%)

http://fasta.bioch.virginia.edu/fasta_www2/fasta_www.cgi

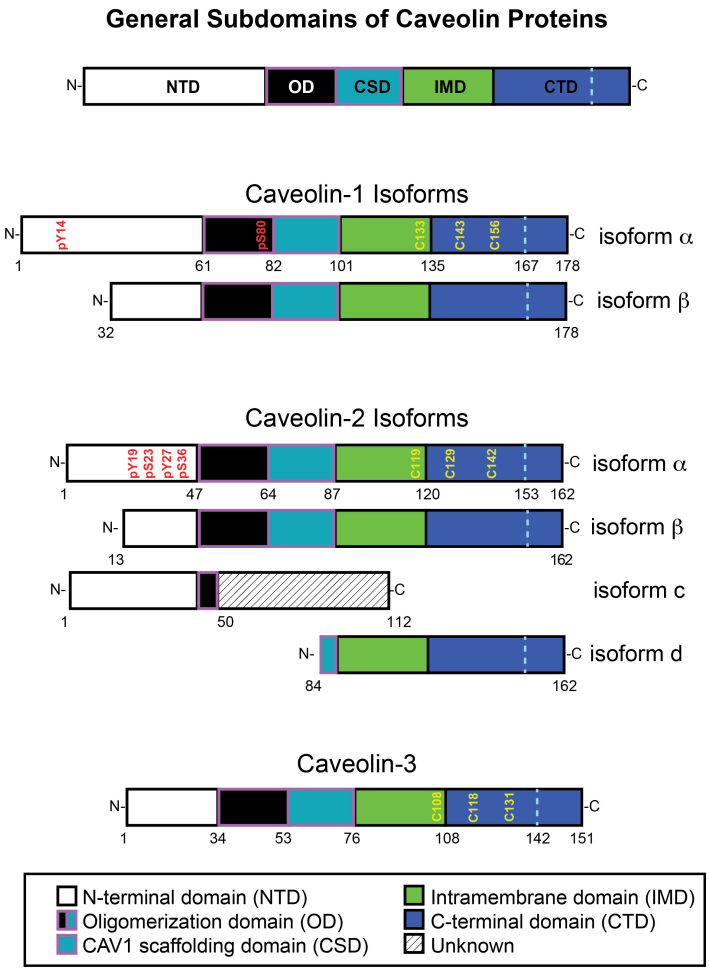

Figure 2. Caveolin Proteins: Subdomains, Family Members and Isoforms. The subdomains conserved in all caveolins are shown. Red text indicates phosphorylation sites. Yellow text indicates conserved cysteine residues that are palmitoylated. Adapted from Sverdlov et al., 2007 [36].

1.2.2 Caveolin-1 (CAV1)

CAV1 is the family member that is primarily discussed for the remainder of this dissertation. The *CAV1* gene encodes a 178 amino acid protein that has an approximate molecular weight of 22 kDa (Table 1). There are two isoforms of CAV1: **1)** the full-length alpha isoform (**CAV1α**) and **2)** the beta isoform (**CAV1β**; 32-178), which lacks the first thirty-one amino acids due to an alternative start site at an internal methionine residue [37] (Figure 2). While there is some overlap in the subcellular distribution of the two isoforms, differences have been reported in the way the isoforms affect the structure and depth of caveolae, and how they influence the activity of growth factor receptors [37-40]. CAV1α associates with deeper caveolae unlike

CAV1β, which is incorporated into shallower caveolae and reportedly has an inhibitory effect on the signaling activity of a growth factor receptor [38, 40]. Aside from these findings, a deeper understanding of differential behaviors of CAV1α/β requires further investigation.

As mentioned above, caveolin proteins contain several structural domains. The CAV1 NTD (residues 1-81) contains the oligomerization domain (OD, residues 61-81), which is essential for the assembly of complexes that serve as building blocks of caveolae [41]. CAV1 is thought to negatively regulate the activity of many signaling molecules through interactions with the CSD (residues 82-101) [42, 43]; however, whether specific binding sites in CAV1/binding partners exist remains controversial. The IMD of CAV1 (residues 102-134) is composed of two α-helices that are separated by a 3-residue linker region containing a proline residue (P110) that induces a ~50° angle between the two α-helices [44, 45]. This allows CAV1 to adopt a hairpin topology in the lipid bilayer such that both N- and C- termini are exposed to the cytoplasmic interior of the cell [45-47] (Figure 1). The CTD (residues 135-178) is important for oligomer-oligomer interactions (residues 168-178) [48] and contains three cysteine residues that are palmitoylated (C133, C143 and C156) that are thought to mediate membrane attachment. However, they are not required for the trafficking or plasma membrane targeting of CAV1 [49].

1.2.3 Caveolin-2 (CAV2)

Like CAV1, CAV2 is detected in several isoforms from the result of transcript variants and initiation of translation from internal methionines that serve as alternative start sites (Figure 2). The alpha isoform (**CAV2α**) encodes the full-length (162 amino acids) protein (Table 1) and the beta isoform (**CAV2β**), lacking the first twelve amino acids of the full-length N-terminus, is 149 amino acids in length. Differences in the subcellular distribution of the α and β isoforms have been reported [50]; however, an in depth understanding of the behaviors of all CAV2 isoforms is currently lacking.

Both CAV1 and CAV2 are located on same chromosome and have overlapping tissue distributions. CAV2 can assemble into homo-dimers as well as hetero-oligomers with CAV1 [51, 52]. CAV2 expression levels, trafficking and caveolae targeting is critically dependent on CAV1 expression. For example, in cells isolated from *Cav1*$^{-/-}$ mice, Cav2 remains in the Golgi and is unable to form caveolae [53, 54]. *Cav2* deficiency in mice has no effect on caveolae formation; however, in these animals, Cav1 expression levels are reportedly 50% lower than their wild type counterparts and have pulmonary abnormalities [52, 54]. Due to the overlap in tissue distribution and dependence on CAV1 expression, it is difficult to independently study CAV2 and rule out any influence from CAV1. However, despite the difficulties of independently assessing CAV2, some groups have begun to tease out CAV2-specific roles in promoting caveolae formation [55], modulating tumor angiogenesis [56], protecting lung tissue from pharmacologically induced fibrosis [57], negative regulation of proliferation [58, 59], insulin signaling [33], and preventing injury/permeability along the gastro-intestinal tract [60].

1.2.4 Caveolin-3 (CAV3)

Caveolae in muscle cells are primarily composed of CAV3, the muscle-specific family member [61] (Table 1; Figure 2). While predominantly in cardiac and skeletal muscle, CAV3 can also be detected in smooth muscle cells [62]. CAV3 is located on an entirely different chromosome (locus 3p25) than CAV1/2 [63] and currently no isoforms have been reported. The molecular characterization of human CAV3 and investigation of *Cav3*$^{-/-}$ mice has shown that this family member plays a role in the fusion of myoblasts into myotubes during development, and in the biogenesis of transverse-tubules (T-tubules) during muscle differentiation [64-66]. Following maturation of myotubes into mature muscle fibers, CAV3 is most prominently found in the sarcolemma and influences glucose uptake, energy metabolism [67], hypertrophy-promoting signaling pathways [68] and contractility. Alterations in CAV3 expression levels are associated with altered insulin signaling in the muscle [69] and several identified CAV3 mutations are implicated in many muscle-related diseases including limb-girdle muscular dystrophy (LGMD), Duchenne muscular dystrophy (DMD), rippling muscle disease (RMD) and abnormally high serum creatine kinase levels (hyperCKemia) [63, 70-72].

Cav3-deficient mice have skeletal muscle abnormalities that mirror muscular dystrophy-like pathology and these mice suffer from cardiac abnormalities [66, 68]. The expression of some dominant negative CAV3 mutants associated with disease that are rapidly degraded and abnormally trafficked can cause haploinsufficiency [63, 70, 72-74]. Despite an obvious importance for CAV3 in maintaining normal muscle cell homeostasis, the molecular basis of how CAV3 or mutant forms of the protein contribute to these processes and the pathogenesis of diseases is not fully understood.

1.3 Caveolae Accessory Proteins

In addition to caveolins being a primary structural component of caveolae, several accessory proteins that further promote caveolae formation, stability and function have been identified [75-77]. These proteins comprise what is often referred to as the "*caveolar coat*". The caveolar coat is composed of proteins that have roles in stabilizing the caveolae by mediating interactions with the actin cytoskeleton and sculpting caveolar membranes. Some of these proteins include EHD-2, PACSIN2, and the cavin family of proteins. CAV1, the cavins and PACSIN2 are essential for the formation and function of caveolae and without their expression an absence of detectible caveolae or inability to form normal caveolae is observed [77, 78].

1.3.1 EHD2 and its Role in Reducing Lateral Mobility of Caveolae

E**ps-15 **h**omology **d**omain* (EHD 1-4***) containing proteins are a mammalian family of dynamin-like ATPases that regulate endocytic processes and intracellular trafficking [79]. There is a high amount of homology among the EHD family members, which contain an ATP-binding (*G*) domain that is flanked by two helical regions, and a C-terminal *EH* domain that binds *NPF* motifs found in proteins like PACSIN2 [80]. **EHD2** (61 kDa) is a 534 amino acid protein that directly interacts with CAV1 and is therefore localized to caveolae but caveolae still form in the absence of EHD2 [79]. Dimerization of EHD2 and recruitment to the necks of caveolae occurs in an ATP-dependent manner [79]. Caveolae must be intact and decorated with the caveolae accessory protein Cavin-

1 in order for EHD2 to be targeted to caveolae [79]. Thus, EHD2 is often used as a marker of caveolae in microscopy-based experiments. Based on computational analysis of membrane shaping physical models, EHD2 is predicted to play a role in the fission of tubulated membranes [81]. However, caveolae-associated EHD2 is tethered to the actin cytoskeleton and immobilizes caveolae to prevent fission. In concert with this, loss of EHD2 increases the mobility and turnover of caveolae at the plasma membrane [82] (Figure 3A).

1.3.2 PACSIN2 and its Role in Stabilizing the Curvature of Caveolae

Protein kinase C and casein kinase substrate in neurons 2 (***PACSIN2***, also known as *syndapin 2*, 56 kDa) is a 486 amino acid protein that is ubiquitously expressed and is a member of a family of highly conserved mammalian proteins (PACSINs 1-3) involved in bending and sculpting membranes [83]. The protein is comprised of an N-terminal *F-BAR* domain, a C-terminal Src Homology 3 domain (*SH3*) that mediates adaptor protein and kinase binding, in addition to Asn-Pro-Phe (*NPF*) motifs found throughout the protein, which are important for protein-protein interactions. Originally identified in Bin-Amphiphysin-RVS (*BAR*) proteins, BAR domains dimerize generating a highly curved surface with inherent lipid-binding properties and a high affinity for positively or negatively curved membranes [84]. The degree of curvature in BAR domain-containing proteins varies, but F-BAR domains have a shallower curve and bind positively curved membranes. The F-BAR domain of PACSIN2 is essential for its recruitment to caveolae and is established through interactions with CAV1 [84]. PACSIN2 colocalizes with a subset of caveolae and is thought to be important for stabilizing newly formed caveolae [85]. In addition to forming and sculpting caveolae, PACSIN2 recruits dynamin-2 to the necks of caveolae to initiate scission and internalization of caveolae from the plasma membrane; without PACSIN2, caveolae take on an abnormal morphology with reduced dynamin-2 recruitment [77] (Figure 3B).

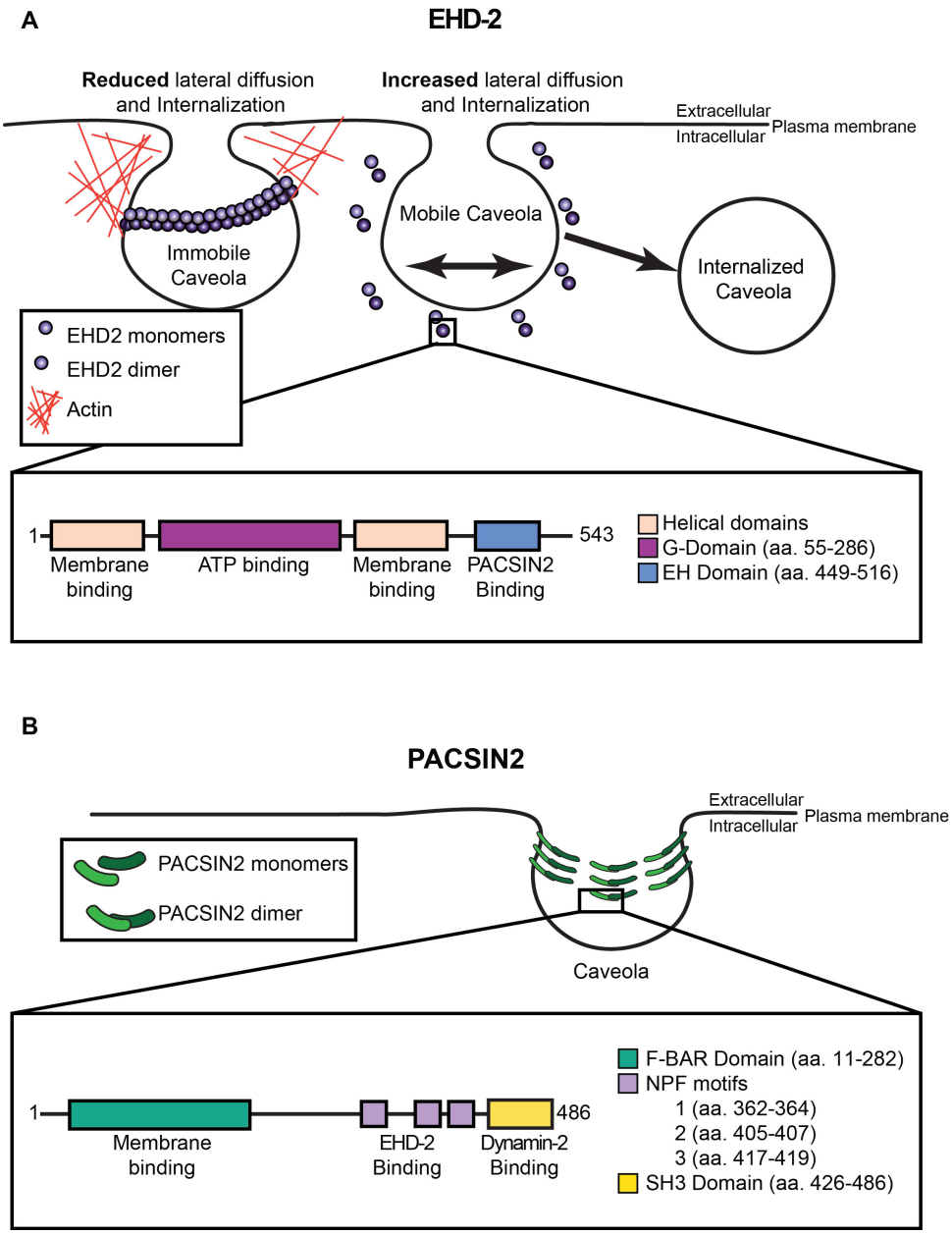

Figure 3. Caveolae Accessory Proteins: EHD-2 and PACSIN2. A) The ATPase EHD2 tethers caveolae to the actin cytoskeleton. Dimers of EHD-2 are recruited to the necks of caveolae and interact with actin through the adaptor protein, Filamin-A (not shown) [79, 82] **B)** PACSIN2 binds to curved membranes through the F-BAR domain, and additionally sculpts membranes to induce curvature due to intrinsic properties of their curved structure. PACSIN2 is found in the necks of caveolae and can interact with EHD-2 via NPF motifs in addition to binding Dynamin-2 via the SH3 domain to mediate scission [77].

1.3.3 The Caveolar Coat: Cavin Family of Proteins

A group of peripheral membrane proteins **PTRF**, **SDPR**, **SRBC** and **MURC** have been designated **Cavins 1-4**, respectively (Figure 4). These lipid-binding proteins share

sequence homology and conserved structural domains in their predicted secondary structure [86]. The structural features of Cavins include N- and C-terminal disordered regions (*D1, 3*) and two helical regions (*H1, 2*) that are separated by another disordered region (*D2*). All Cavin proteins contain numerous phosphorylation sites and contain Pro-Glu-Ser-Thr (*PEST*) domains that undergo proteolytic cleavage/degradation and leucine-zipper (*LZ*) domains that mediate protein-binding interactions. Multiple cleavage products have been observed associated with caveolae and Cavins can form homo- and hetero-oligomers [87]. In addition, both Cavin-1 and -4 contain nuclear localization sequences (*NLSs*).

Cavin-1/PTRF. Originally named ***p****olymerase-I and* ***t****ranscript* ***r****elease* ***f****actor* (*PTRF*) for its role in regulating gene transcription and RNA Polymerase 1 activity [88-90], Cavin-1 is now widely recognized as a major component of caveolae [91, 92]. The *Cavin-1* gene encodes a 390 amino acid protein with a predicted molecular weight of 43 kDa, though on SDS-PAGE the protein is typically observed to migrate between 50-60 kDa. Like EHD-2, Cavin-1 is used as a marker of caveolae and highly colocalizes with CAV1. The leucine-zipper domain of Cavin-1 (a subtype of coiled-coil domains) is important for oligomerization of Cavin molecules and is required for caveolae localization; however, there is no direct interaction between CAV1 and Cavin-1 [93, 94]. It is thought that Cavin-1 associates with membranes through a phosphatidylinositol 4,5-bisphosphate/PtdIns (4,5) P2 (PIP_2) and phosphotidylserine (*PS*) binding sites. Cavin-1 does not associate with intracellular pools of CAV1 and only colocalizes with CAV1 in caveolae at the plasma membrane or with caveolae that were recently internalized and fused to early endosomes [75]. In cells lacking Cavin-1, caveolae are not detectible and CAV1 distribution is diffuse in the plasma membrane; therefore, cavin-1 is required for caveolae formation but not trafficking of CAV1 to the cell surface. When Cavin-1 dissociates from caveolae, the domains flatten and the diffusional mobility and turnover rate of the remaining CAV1 in the membrane increases [75, 95]. Alterations in Cavin-1 expression levels are also implicated in the development of some cancers [75], muscular dystrophies [96, 97], and dyslipidemias [98] (Figure 4).

Cavin-2/ SDPR. S*erum* ***d****eprivation* ***p****rotein* ***r****esponse* (*SDPR*) whose expression is modulated by serum concentration [99] was later alternatively named Cavin-2 after being identified as an additional caveolar coat protein and has high structural similarity with other Cavin proteins [100] (Figure 4). Like Cavin-1, Cavin-2 is also a PS-binding protein [101] and also contains a leucine-zipper domain [102]. Cavin-2 appears to promote the tubulation of caveolae membranes, but the functional significance of this is unclear [100].

Cavin-3/ SRBC. The gene expression of ***s****erum deprivation response (****S****DR)-****r****elated gene product that* ***b****inds to* ***c****-kinase* (*SRBC*) is much like Cavin-2 in addition to similarities in amino acid sequence and response to serum starvation [87]. After being identified as a caveolae-associated protein in co-localization and co-immunoprecipitation studies conducted in human fibroblasts and *Cav1*$^{-/-}$ MEFs, and based on its high structural similarity with Cavin-1, SRBC is now recognized as Cavin-3 [103]. It is not clear if Cavin-3 structurally stabilizes caveolae, but it is thought to destabilize caveolae and mediate interactions with microtubules in order for internalization to occur [103]. In support of this, caveolae trafficking becomes perturbed when Cavin-3 expression is reduced or lost [103] (Figure 4).

Cavin-4/ MURC. Mu*scle-****r****estricted putative* ***c****oiled-coil protein* (*MURC*) was identified last as a member of the Cavin family of proteins. This protein is muscle specific and only found in skeletal, cardiac muscle and vascular smooth muscle cells in a subset of tissues [104]. The structural moiety responsible for targeting Cavin-4 to caveolae is the coiled-coil domain [105]. In muscle cells, Cavin-4 localizes to the sarcolemma along with CAV3 within caveolae. As such, alterations in expression levels and mutations are associated with diseases that affect the heart [104, 106] and skeletal muscle [107] (Figure 4).

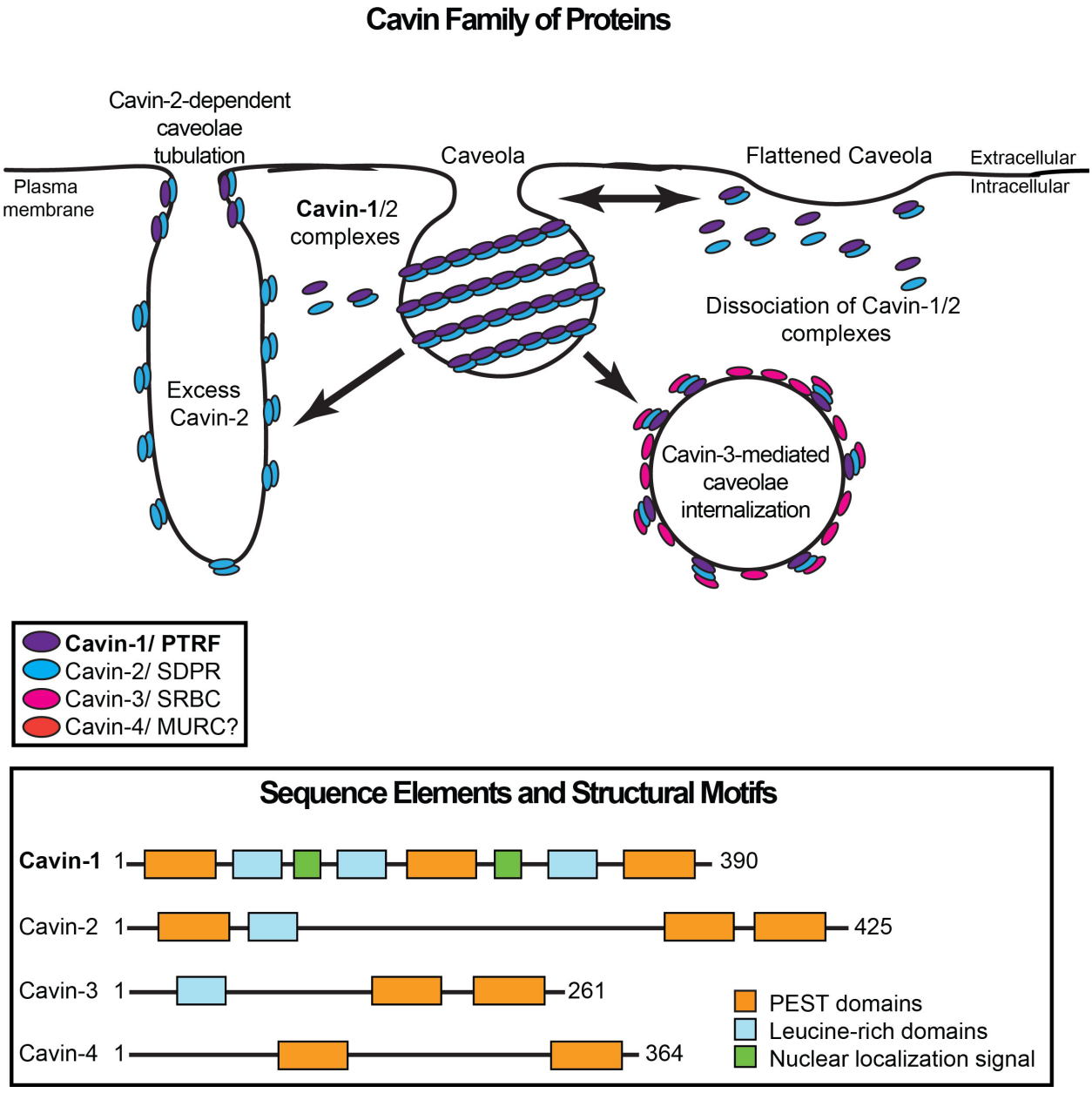

Figure 4. The Cavin Family of Proteins: Proposed Interactions with Caveolae and Conserved Structural Domains. Recruitment of Cavin-1 homodimers and Cavin-1/2 heterodimers to caveolae provides structural stability to caveolae and prevents caveolae from flattening. Cavin-2 has a tubulating effect on caveolae membranes and Cavin-3 is implicated in the internalization of budded off caveolae. All cavins have PEST domains but not all contain NLSs or leucine-rich domains [79, 78].

1.4 Assembly and Disassembly of Caveolae

1.4.1 Assembly and Trafficking of Higher-Order CAV1 Complexes

Caveolae formation begins with the biosynthesis of CAV1. Nascent peptides generated by the translation of CAV1 transcripts are co-translationally inserted into the outer ER membrane where the newly synthesized protein quickly oligomerizes into 8S complexes comprised of 14-16 CAV1 monomers [9, 41] (Figure 5). Glycosphingolipids have been shown to enhance the stability of CAV1 oligomers [108]. These 8S complexes can be found as homo-oligomers of CAV1 or hetero-oligomers of CAV1/2 and are characteristically resistant to detergent solubilization. Organization of CAV1 monomers into 8S complexes is reportedly required for ER-exit [8]. Following entry into the Golgi complex, the 8S complexes serve as building blocks of larger 70S caveolin complexes that are assembled in late Golgi compartments, where they become enriched in cholesterol, lose their diffusional mobility and become increasingly detergent resistant [8] (Figure 5).

Multiple studies have evaluated the requirements for different domains of CAV1 in various aspects of caveolae biogenesis [8, 48, 109-111]. Earlier work from the Lisanti group using a CAV1 construct lacking the C-terminus (aa. 1-140) highlighted the importance of this domain for mediating homotypic interactions between the C-termini of CAV1 in adjacent 8S complexes in order to form 70s complexes [111]. This final round of oligomerization is very important for Golgi-to-PM sorting into detergent-resistant caveolae membranes [111, 112]. Once trafficked to the plasma membrane through a poorly understood process, filament-like 70S CAV1 complexes serve as the structural framework for caveolae and provide stability necessary for the formation of caveolae [8] (Figure 5).

Upon transport from the Golgi complex and fusion of CAV1 carriers to the PM, the CAV1-enriched membranes are sculpted into caveolae following the recruitment of the previously described accessory proteins [8]. Here, fully assembled, mature caveolae become tethered to the actin cytoskeleton by interactions mediated by the milieu of

accessory/adaptor proteins recruited to caveolae thus causing them to be confined in highly immobile invaginated raft-like domains [76, 113]. As a result of caveolin biogenesis and trafficking, CAV1 has a characteristic subcellular distribution and is readily observed in the Golgi complex, trans-Golgi network (*TGN*), early endosomes, and in punctate or streak like pattern at the plasma membrane under steady-state conditions. CAV1 isoforms contain N-terminal di-acidic ER-exit signals (*DXE*) to promote ER-exit and it is thought that newly synthesized CAV1 is rapidly exported from the ER to the Golgi in a COP II-dependent manner, as very little CAV1 is detectible in the ER under normal conditions.

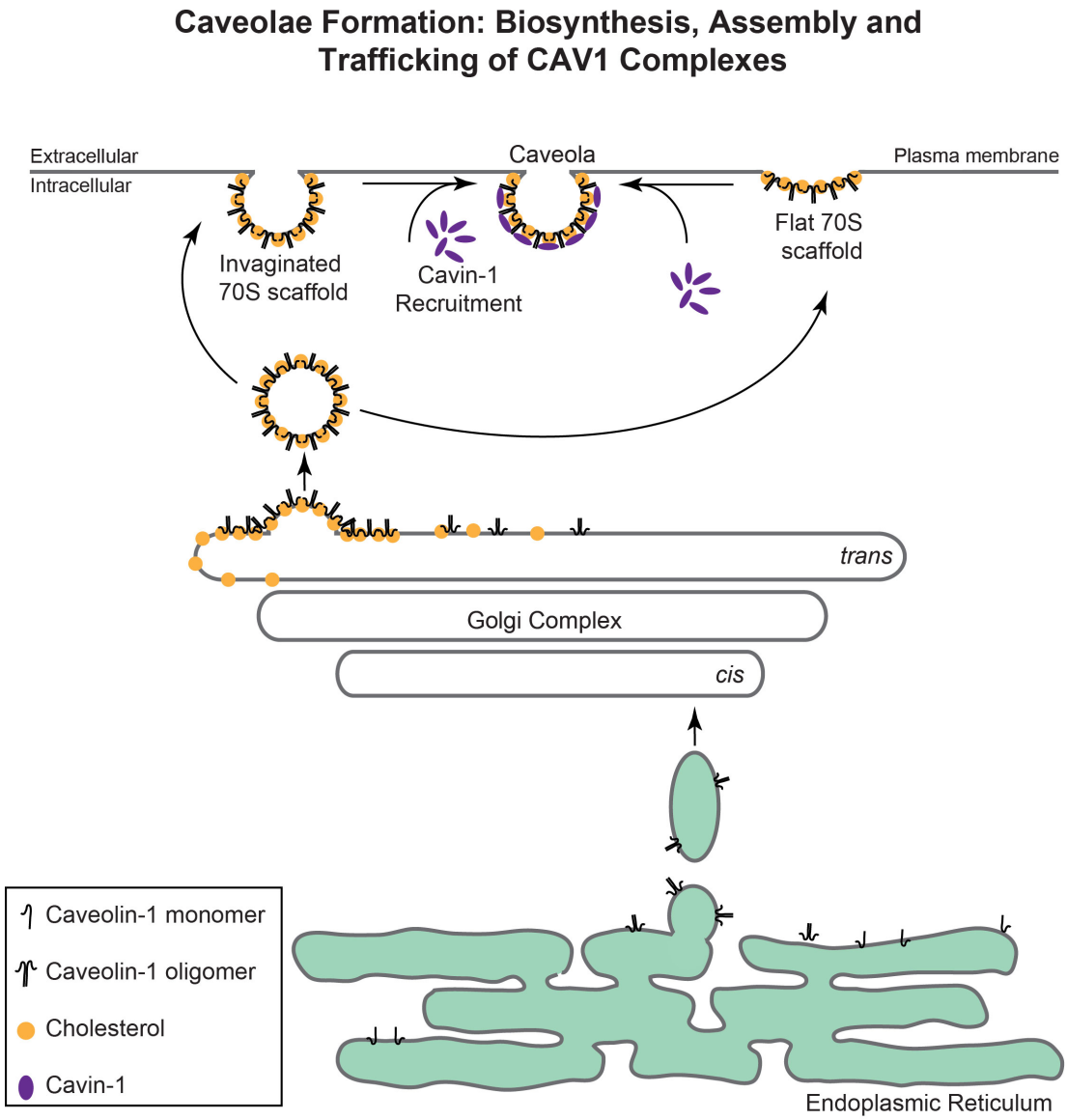

Figure 5. Model of the Assembly of CAV1 Complexes and Caveolae Biogenesis. Newly synthesized CAV1 oligomerizes and assembles into higher-order complexes as it transits through the ER and Golgi complex. In a final round of cholesterol-mediated organization, the "70S" domains are budded off of the Golgi membrane into vesicles and transported to the plasma membrane. Cavin-1 is either recruited to invaginated CAV1 domains where it stabilizes the caveolae or it is recruited to flattened CAV1 domains where it induces invagination. Adapted from Hayer et al., 2010 [8].

1.4.2 Removing Caveolae: Disassembly of CAV1 Complexes and Degradation

Due to the stable and immobile nature of caveolae, endogenous CAV1 has a long half-life on the order of 36 hours in CV1 cells [95]. However, caveolins can be targeted for degradation under physiological conditions that promote caveolae flattening or induce caveolae internalization (Figure 6). Caveolae flattening/internalization is dependent on

tyrosine phosphorylation of oligomerized 8S CAV1 at tyrosine-14 (*pY14*) and results in both flattening and endocytosis [114-117]. Src-dependent CAV1 phosphorylation on tyrosine-14 results from a variety of cellular stimuli including cellular response to mechanical stress [116, 118], insulin signaling [119] and activation of G-protein subunits [120]. The close proximity of negatively charged phosphate groups generates repulsive forces between adjacent caveolin molecules causing them to spread apart. This spatial rearrangement resulting in the apparent flattening and appearance of distended caveolae [121] leaves CAV1 proteins open for ubiquitination [95].

Though not fully understood, these physical changes to caveolae are followed by the dissociation of caveolae accessory proteins allowing for the recruitment of dynamin-2 to the necks of caveolae to mediate vesicular fission. The internalized caveolar vesicles are recruited to early endosomes in an actin- and microtubule-dependent manner. Unlike other accessory proteins, Cavins can remain associated with some internalized caveolae and evidence suggests that if cavin is not removed from these early endosome-associated caveolae, they are recycled back to the plasma membrane [95] which may occur in a cell type-specific manner [122]. Once Cavin-1 dissociates from internalized caveolae, CAV1 oligomers can become ubiquitinated while in early endosomes. CAV1 ubiquitination can also occur at the plasma membrane in disassembled caveolae domains before trafficking to early endosomes. From this compartment, ubiquitinated CAV1 is packaged into intraluminal vesicles in an ESCRT-dependent manner and targeted for lysosomal degradation [95]. Cholesterol depletion and mechanical stress cause caveolae to flatten while caveolae endocytosis can be stimulated by SV40 viral infection or treatment with albumin, known caveolae cargos.

Alternatively, mutant forms of caveolins and membrane-associated caveolins in cells exposed to excessive amounts of reactive oxygen/nitrogen species are targeted for proteasomal degradation. In response to oxidative/nitrosative stress, proteasomes degrade proteins that have become oxidated or S-nitrosylated on sulfurhydryl group-containing amino acids (*SNO*, a reversible post-translational modification) [123, 124]. CAV1 is targeted for proteasomal degradation in response to oxidative stress in skeletal

muscle cells [125]. In addition, increased reactive oxygen species as a result of overproduction of nitric oxide leads to the S-nitrosylation of CAV1 on Cysteine-156. *SNO-CAV1* is later phosphorylated (pY14), mono-ubiquitinated on lysine-86 and degraded by the proteasome in pulmonary arterial endothelial cells [126]. Caveolin mutants that are intracellularly retained in compartments such as the Golgi complex and rapidly turned-over are also degraded in a proteasome-dependent manner, following ubiquitination [70, 127].

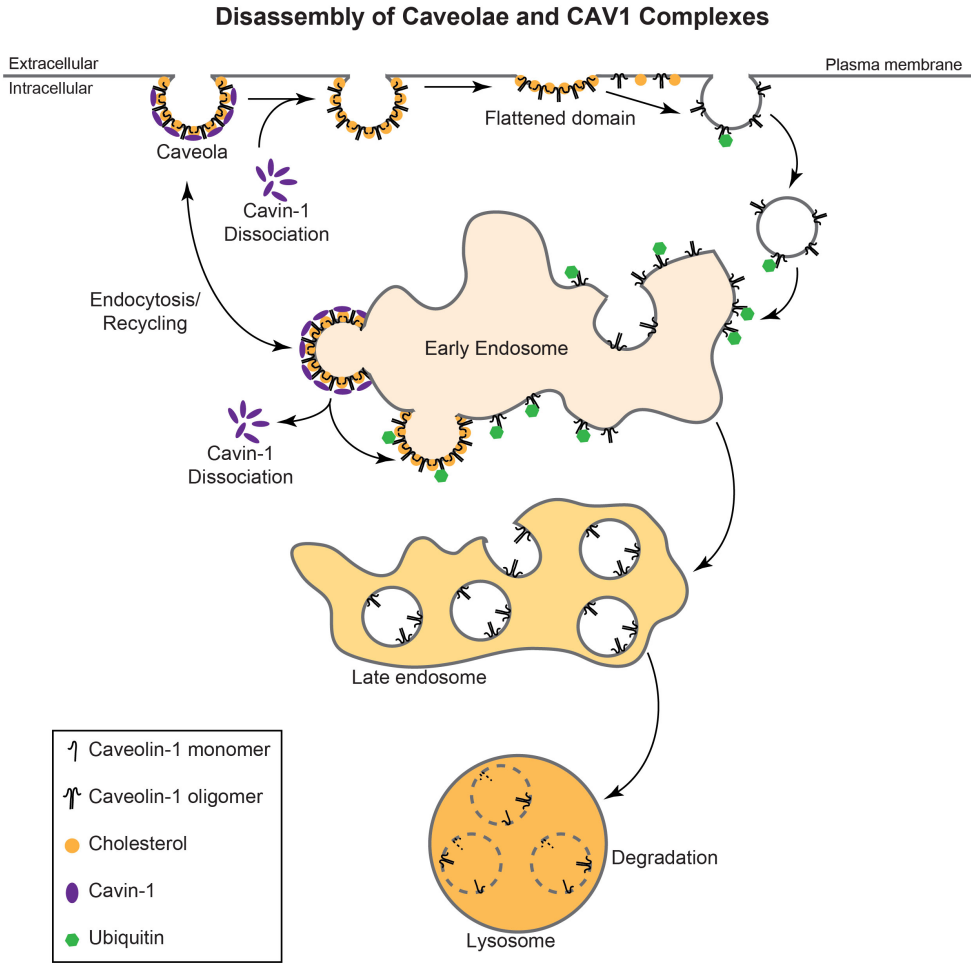

Figure 6. Model Summarizing the Turnover of Caveolae and the Breakdown of CAV1 Complexes for Degradation. Caveolae become destabilized following Cavin-1 dissociation. The exposed "70S" disassembles into 8S caveolar complexes either at the plasma membrane or in the early endosome after internalization of a budded caveolae vesicle. 8S complexes of CAV1 are ubiquitinated and targeted to the lysosome for degradation. Adapted from Hayer et al., 2010 [87].

1.5 Phenotypes Associated with *Caveolin-1* Gene Disruption in Mice

The phenotypes resulting from loss of caveolae as a direct consequence of *Cav1* gene deletion in animal models have established the physiological importance of caveolae in numerous cell types. Although the underlying molecular mechanisms are not fully understood [128], it is clear that caveolae and CAV1 are important for regulating signaling pathways involving vascular tone, tissue remodeling, lipid metabolism and proliferation. As such, *Cav1*$^{-/-}$ mice display several pathological phenotypes across multiple tissue systems and are often studied as models for human diseases.

1.5.1 Pulmonary-Vascular Defects in Cav1$^{-/-}$ *Mice*

Endogenous Cav1 is heavily expressed in lungs, primarily in cells of the vascular endothelium where it plays a role in maintaining pulmonary architecture and vascular tone by modulating pathways associated with proliferation, matrix deposition and vaso-reactivity. The characterization of *Cav1*-null mice helped identify these proposed functions of Cav1/caveolae. Lungs from Cav1-deficient animals show signs of hypercellularity and alveolar constriction due to septal thickening. There is also evidence of pre-capillary vessel remodeling due endothelial dysfunction and hyperproliferation cell types within the pulmonary endothelium. These pathological abnormalities narrow vessel diameter and increase arterial pressure and cardiac output. As a consequence, the mice develop pulmonary hypertension (PH), as evidenced by elevated arterial pressure, right ventricular dilation, cardiac dysfunction, and exercise intolerance [11].

In addition to creating a permissive environment for the development of PH, Cav1 deficiency conversely results in enhanced vascular relaxation (which is predicted to counteract some of the symptoms of PH observed in the mice). Cav1 regulates vascular contractility by tonic inhibition of the vasoreactive enzyme, *endothelial nitric oxide synthase* (*eNOS*). When eNOS is activated in response to mechanical stress, Ca^{2+} influx, or growth factor stimulation (VEGF) it enzymatically catalyzes the reaction that produces nitric oxide (NO), a potent vasodilator that promotes vascular relaxation. Cav1

negatively regulates eNOS in caveolae, thereby preventing the production of NO to maintain contractile tone in the vasculature. However, the localization of eNOS to caveolae is required for its proper activation. Constitutive production of NO in the lungs of *Cav1*$^{-/-}$ mice results in aortic dilation with impaired contractility in response to pharmacological stimulation [11, 129-131]. Thus, the severity of the PH-like diseases appears to be partially dampened by the persistent production of NO and the resulting vascular relaxation.

Interestingly, *Cav2*-null mice (which still express Cav1 and caveolae) show a pulmonary phenotype that mirrors Cav1 ablation suggesting that Cav2 may play a regulatory role in modulating pathways that are involved in pulmonary-vascular homeostasis in mice [54]. This also suggests that some of the pulmonary defects observed in *Cav1*-null mice, which also have significantly reduced Cav2 expression, may be perpetuated by Cav2 deficiency.

1.5.2 Cardiac Abnormalities in Cav1$^{-/-}$ *Mice*

The heart is primarily composed of **cardiomyocytes**, **cardiac fibroblasts** and **endothelial cells** that line the chambers of the heart. Together, these cells establish mechanical, chemical and electrical properties of cardiac tissue through coordinated autocrine and paracrine modulation that are essential for normal heart function. Cav1 is found in all three cell types; however, its role in the myogenic cells of the heart is not fully understood [129, 132, 133]. *Cav1* gene disruption in mice results in several defects in cardiac fibroblasts and cardiac endothelial cells that negatively affect the architecture and functional capacity of heart [11, 129, 134-137].

eNOS activity and eNOS-dependent NO production by endothelial cells is regulated by Cav1/caveolae and influences the contractile tone in vessels and tissues. Cav1 deficiency in murine **cardiac endothelial cells** results in hyperactive eNOS and overproduction of NO. The relaxing effect of NO reduces ventricular contractility and can cause systolic dysfunction. Additionally, abnormally high levels of NO and resulting generation of reactive nitrogen species causes nitrosative stress, which can damage

exposed cells and promote apoptosis [138]. While it is possible that other cells that produce NO in the heart contribute to these pathological processes in Cav1-deficient mice, evidence suggests that the main culprits are dysfunctional cardiac endothelial cells.

Cardiac fibroblasts produce and remodel the extracellular matrix in cardiac tissue. These processes are important for maintaining the morphology of the heart and during wound healing of injured tissue. Furthermore, autocrine and paracrine regulation of cardiac cells is mediated by factors produced by cardiac fibroblasts. In cardiac fibroblasts, Cav1 negatively regulates many signaling pathways including those involved in proliferation and fibrogenesis. The hyperactivation of the pro-proliferative p42/MAPK pathway is associated with cardiac hypertrophy and myocardial interstitial fibrosis [129]. In interstitial fibrotic lesions and cardiac fibroblasts isolated from Cav1-deficient mice, this pathway is upregulated [129]. Evidence suggests that Cav1-deficient fibroblasts promote hypertrophic growth in surrounding cardiomyocytes. Not surprisingly, cardiac hypertrophy of the left and right ventricles with a high incidence of cardiac fibrosis compared to control mice is observed in these animals [129].

In vivo studies carried out in these mice have shown that Cav1 is a critical component in the maintenance of cardiac function, tissue organization and structure. The hypertrophic phenotype observed in both ventricles perpetuated by aberrant tissue remodeling due to endothelial, myocyte and fibroblast dysfunction is the result of Cav1 deficiency. Additionally, the mice show evidence of ventricular dilation, which often develops during decompensation in the progression of cardiac hypertrophy. However, because these mice also have PH, the observed right ventricular dilation is possibly a secondary consequence of elevated pulmonary vascular resistance and increased cardiac output in $Cav1^{-/-}$ mice [11, 129-131]. Eventually, hypertrophy/fibrosis-induced cardiac stiffening, dilation and reduced contractility gradually abrogate cardiac function, ultimately progressing to heart failure and death [139].

In summary, the observed heart-related phenotypes of *Cav1*$^{-/-}$ mice have established a link between Cav1/caveolae and their role in the maintenance cardiac tissue homeostasis. However, the underlying mechanisms promoting these abnormalities resulting from Cav1 deficiency are not entirely understood.

1.5.3 Dyslipidemia in Cav1$^{-/-}$ *Mice*

Cav1-null mice are resistant to diet-induced obesity, insulin resistant, and are under weight [140]. An underlying defect contributing to these abnormalities is impaired preadipocyte differentiation [140] giving rise to cells that are prone to apoptosis [141] with diminished ability to store and metabolize lipids. Under metabolic stress, adipose tissue from *Cav1*-null mice becomes inflamed and is susceptible to atrophy, autophagy and fibrosis [142, 143]. The influence of Caveolin-1 on glucose transport [144], insulin signaling, and lipid metabolism in adipose tissue likely plays a role in the development of metabolic abnormalities in these mice.

1.6 Functions of CAV1 and Caveolae at the Cellular Level

It is often difficult to distinguish whether the abnormalities observed in Cav1-deficient mice are purely due to a loss of caveolae or functions of CAV1 that lie outside of caveolae. Although some investigators have begun to implement the use of techniques that allow for distinction between caveolae-associated and non-caveolar CAV1 functions, whether the reported functions of CAV1 are specific to caveolae, non-caveolar CAV1 or secreted CAV1 remains unclear. It should also be noted that many of the proposed functions of CAV1/caveolae discussed below are controversial [128] (Figure 7).

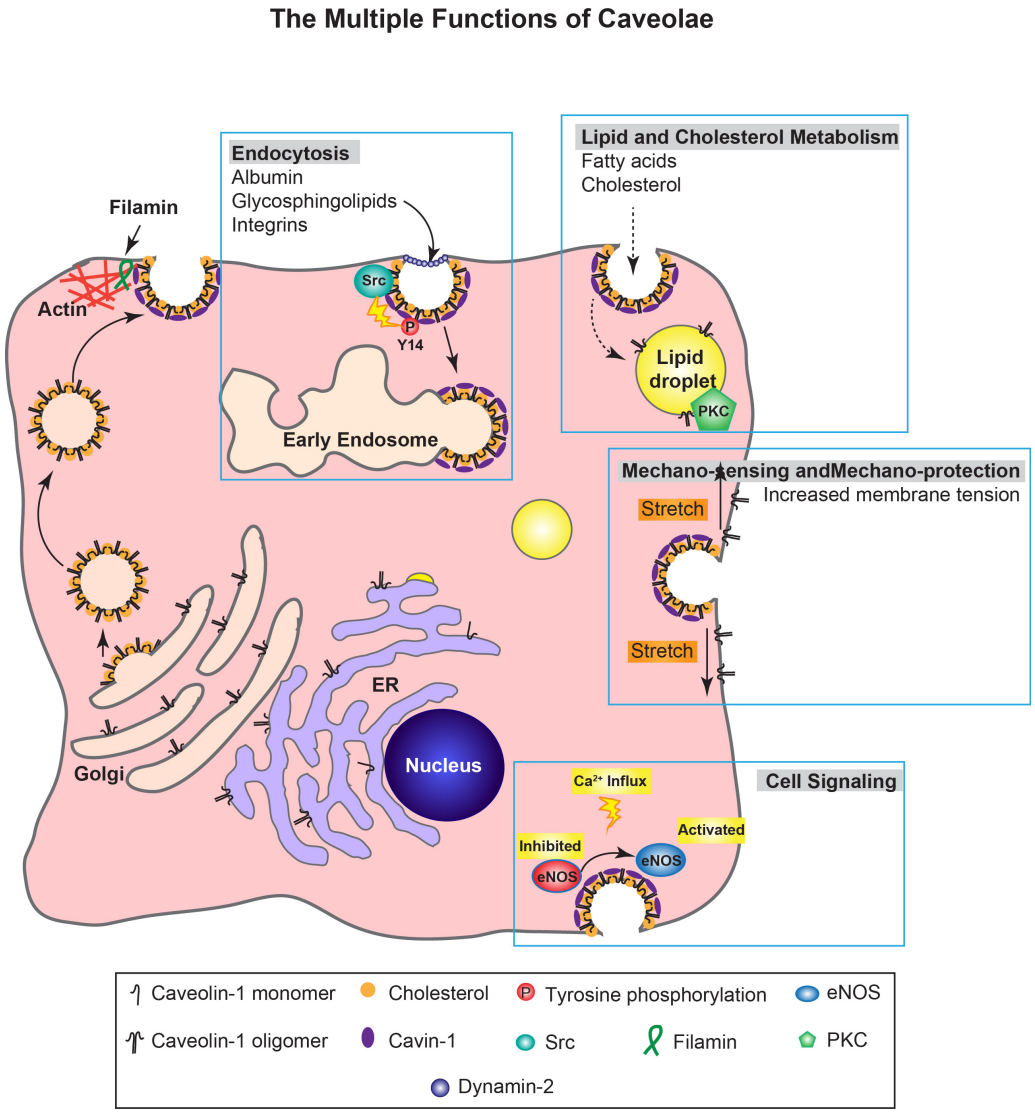

Figure 7. Cartoon Depicting Known Functions of Caveolae. Dynamin-dependent budding of caveolae is important for the endocytosis of albumin, glycosphingolipids and integrins. Src-dependent phosphorylation of CAV1 stimulates caveolae internalization. Uptake of cholesterol and free fatty acids occurs through caveolae and caveolae are also involved in lipid droplet function. Caveolae flattening protects cells from mechanical stress and prevents membrane rupture. Several signaling molecules are localized to caveolae in order to be properly regulated and to coordinate signal transduction. eNOS is inhibited in caveolae through direct interactions with CAV1, but this association is also required to coordinate the proper activation of the enzyme in a calcium-dependent manner. Adapted from Bastiani et al., 2010 [145].

1.6.1 Cell Signaling

In order for cells to maintain homeostasis, and respond to metabolic or environmental stimuli, biochemical and mechanical signals generated within a cell or received from other cells are transduced into a cellular response. Receptor-mediated signal

transduction generally results in the initiation of a signaling cascade of a particular pathway depending on the stimulus. In the plasma membrane, lipid rafts can serve as epicenters of signaling activity. Receptors that reside at the plasma membrane as well as intracellular signaling molecules are often spatially confined to subdomains in the membrane, including caveolae, spatio-temporal modulation of their signaling activity. Caveolae-associated CAV1 is thought to negatively regulate cell signaling based on evidence suggesting that different receptors and signaling molecules are in an inhibitory state when confined to caveolae via the scaffolding domain of CAV1 (Figure 7) [146].

The following intracellular signaling proteins are known to associate with and be inhibited by CAV1/caveolae: protein kinase-C (*PKC*) [147], endothelial nitric oxide synthase (*eNOS*) [148], cSrc, Ras proteins [29] and G-protein subunits [42, 43]. Their activity and downstream signal transduction is modulated by the localization of these molecules to caveolae. eNOS, cSrc, Ras proteins, and G-protein subunits are post-translationally acylated in order to be properly targeted to caveolae [36, 37, 130, 131]. The palmitoylation of CAV1 at cysteine-156 is thought to play an important role recruiting acylated proteins to caveolae [126,127]. In addition to lipid modification, the association of some proteins with caveolae is mediated through interactions with the scaffolding domain of CAV1 [37]. eNOS has also been shown to directly bind to and be inhibited by the scaffolding domain of CAV1, which abrogates the production of the NO [149]. Some examples of receptor tyrosine kinases (*RTKs*) found in caveolae are platelet-derived growth factor receptors (*PDGFR*) [150], epidermal growth factor receptors (*EGFR*) [151], type-1 tumor growth factor receptor beta (*TGFβR1*) [152], and type-2 bone morphogenetic protein receptors (*BMPR2*) [136]. As mentioned above, CAV1/caveolae-localized signaling molecules are inactive in most cases and access to activating phosphorylation cites is limited. However, upon Src-dependent phosphorylation of CAV1 on tyrosine-14, the inhibitory effect of CAV1 is lost, allowing previously inhibited molecules to be come activated [150, 153, 154]. Modulation of these signaling molecules/RTKs by caveolae can have diverse effects on proliferation/differentiation, cell mobility, endocytosis, lipid transport, buffering cellular

membranes, vascular tone, and adipose tissue homeostasis, which will be discussed further in depth in the sections to follow.

1.6.2 CAV1 Functions as a Tumor Suppressor

Cells that are terminally differentiated have a low proliferative capacity and often express high levels of caveolin-1 [155-157]. Conversely, hyperplastic cells that are mitotically active or have undergone oncogenic transformation express low levels of CAV1 [158]. The activation of cSrc and AKT promotes signal transduction through pathways that promote cell proliferation and survival [159, 160]. CAV1 negatively regulates these molecules to prevent aberrant proliferation that is associated with benign and malignant hyperplasias [161, 162] implicated in tumor growth and cancer progression [163, 164]. Many tissues in *Cav1*$^{-/-}$ mice display signs of hypercellularity and hyperplasia with a concomitant increase in the activity of cSrc and other signaling pathways that promote proliferation [10, 134, 137]. The *CAV1* gene is located downstream of a commonly deleted region within a candidate tumor suppressor locus of human chromosome 7 (D7S522/7q31.1) [165]. Because of chromosomal localization and pattern of expression described above, CAV1 is often described as a tumor suppressor and negative regulator of proliferation in normal cells. Oncogenes that are upregulated during cellular transformation can transcriptionally repress *CAV1* expression. It has also been shown that loss of the well-known tumor suppressor p53 results in reduced CAV1 expression levels [166]. Silencing of *CAV1* by DNA hypermethylation has also been observed in some cancer cells as another means of gene regulation [165]. The CAV1-P132L mutant is the result of a somatic point mutation that was identified in a small subset of breast cancer patients [10, 167]. This dominant negative mutant reduces caveolae density as a result of forming abnormal aggregate-prone oligomers that are retained in the Golgi complex and aggresomes [168-170]. Therefore CAV1-P132L is unable to assemble into caveolae [171, 172]. Phosphorylation of CAV1 is another mechanism to reduce the density of caveolae at the membrane and therefore CAV1 expression levels. Upregulation of Src-tyrosine kinase activity is observed in cancers and it phosphorylates CAV1 on the tyrosine-14 residue (pY14) [173]. This ultimately results in the internalization of caveolae and targeting of

CAV1 for degradation [121, 126]. Lastly, phosphorylation of CAV1 on serine-80 (pS80) targets the protein for secretion out of the ER [174, 175], thereby reducing intracellular CAV1 protein levels, and preventing the tumor-suppressing role of CAV1. Evidence suggests that cholesterol or PKC epsilon may modulate secretion of CAV1 [176, 177]. Interestingly, the secreted form of caveolin-1 appears to function as a paracrine factor to initiate tumorigenesis in nearby cells [178]. The detection of secreted CAV1 in serum of cancer patients has sparked investigation into its use as a biomarker to predict prostate cancer recurrence [179], to predict breast cancer risk [180], and to track the progression of colorectal cancer [181]. Although it is well known that reduced CAV1 results in loss of caveolae, it is not clear whether oncogenesis is perpetuated by CAV1 independently of caveolae, or in response to changes within caveolae.

1.6.3 Cell Mobility

Cells within tissues and organs are often rendered static by environmental constraints imposed by the local cell density and interactions with the extracellular matrix (ECM). However, some cell types become migratory in response to inflammation, during wound healing, angiogenesis, and tumor cell metastasis. In order for a cell to become migratory, it must become detached from its local environment and degrade the surrounding ECM such that the cell can invade or move freely into other tissues. Cells are attached to the ECM via integrins, which are enriched in attachment sites called focal adhesions (FAs). Cell migration is orchestrated by the dynamic interplay between actin reorganization; cell adhesion rearrangements and ECM remodeling, resulting in an elaborate array of intracellular signaling events. CAV1 is thought to play a role in cell migration by influencing FA organization, dynamics and signaling events that modulate cell mobility and attachment [118, 182]. Static cells have relatively low FA dynamics. However migrating cells have an increased rate of FA assembly and disassembly in order to mediate cell motility. Reduced CAV1 expression disrupts FAs and causes cell detachment [118]. High CAV1 expression is observed in migratory cells and CAV1 tyrosine-14 phosphorylation was found to be important for FA turnover dynamics in these cells [183]. Cells expressing elevated levels of CAV1 have enhanced capacity for migration/invasion and anchorage-independent growth [184, 185]. In fact, in some

metastatic cancer cells, CAV1 expression is elevated compared to tumorigenic cells. CAV1 expression during cancer progression has also been linked to metastatic potential and invasiveness of tumor cells [186]. Thus, the fluctuations of CAV1 expression can create a permissive environment for tumorigenesis or promote tumor metastasis/invasiveness in a cell type/tissue-dependent manner that also depends on the stage in cancer [187].

1.6.4 Endocytosis and Transcytosis

The packaging and internalization of vesicular carriers containing nutrients and macromolecules from the extracellular space is referred to as ***endocytosis***. Regulation of receptor density of at the plasma membrane and cell signaling is also modulated by endocytic activity. Once internalized, endocytic cargo are trafficked to endocytic compartments to be sorted for recycling back to the membrane, or targeted for degradation. Caveolae endocytosis is one of many endocytic pathways and can be stimulated by cholesterol or glycosphingolipid loading as well as other endocytic cargo molecules including SV40 virus. Insulin, albumin and folic acid can also induce caveolae to internalize [188]. Coordinated dynamin-dependent scission and actin reorganization events initiate the budding of caveolae vesicles form the plasma membrane [189, 190]. PKC activity and Src-mediated tyrosine-14 phosphorylation of CAV1 are other important regulators of caveolar endocytosis [29, 162, 163]. Endocytosis of β1 integrins via caveolae modulates extracellular matrix remodeling and may contribute to the development of fibrosis [191]. Another function of caveolae endocytosis is to repair cellular membranes that have become damaged. When the integrity of the plasma membrane becomes compromised following a wounding event, the injured portions of the membrane are internalized in a caveolae-dependent mechanism. The membrane gradually becomes repaired through removal membrane lesions by caveolar endocytosis and resulting resealing of the plasma membrane [22].

Transcytosis involves vesicular transport of cargo similar to endocytosis, but once internalized the endocytic carriers are transported *across* the cell bidirectionally where their contents are then released from the opposite side of the cell. Transcytosis is

particularly important in microvascular **endothelial cells** for mediating transport of macromolecules and nutrients from the plasma/lumen to the underlying tissues [192]. Caveolae-dependent transcytosis has also been shown to regulate endothelial permeability. In *Cav1*$^{-/-}$ animals, endothelial transcytosis of serum albumin is markedly reduced, and increased hyperpermeability was observed [165,166].

Expression of CAV1/3 and cavin-1/3 has also been shown to negatively regulate endocytosis through the *clathrin-independent carriers/GPI-AP enriched early endosomal compartment* (*CLIC/GEEC*) pathway. This conclusion is based on the observation that CLIC/GEEC endocytosis is increased in cells expressing reduced amounts of the caveolae-associated proteins CAV1/3 and cavin-1/3 [25]. Thus, while caveolae play important roles in caveolin-dependent endocytosis and transcytosis, CAV1/caveolae also serve as negative regulators of clathrin-independent endocytosis.

1.6.5 Membrane Lipid Homeostasis and Lipid Metabolism

Cholesterol is a molecule regulated by Caveolin-1 that is an essential precursor for steroid synthesis, involved in cell signaling, and important for maintaining the fluidity of biological membranes. Clustering of cholesterol in sub-compartments within the plasma membrane decreases membrane fluidity giving rise to “liquid ordered” microdomains (also referred to as lipid rafts). CAV1 is a cholesterol-binding protein [193] and caveolae are therefore enriched in cholesterol with raft-like properties. Cholesterol also influences the trafficking of CAV1 from the plasma membrane to intracellular compartments [194]. Caveolae are thought to compartmentalize cholesterol at the plasma membrane in order to modulate membrane fluidity. It has also been shown that CAV1 modulates the bidirectional intracellular trafficking of cholesterol from the ER to the plasma membrane [195]. Loss of CAV1 disrupts trafficking of newly synthesized cholesterol from the ER and results in reduced cellular free cholesterol levels [195]. Caveolin-deficient cells also have impaired sphingolipid trafficking [196], further demonstrating the requirement of CAV1 for maintaining cellular lipid composition and trafficking.

In **white adipose tissue**, lipophilic properties of CAV1/caveolae play another role. Lipid metabolism is an important process in organisms that is necessary for energy consumption/utilization in addition to maintaining biological membranes. In adipose tissue, adipocytes store energy in the form of fat in a large, unilocular lipid droplet. The high density of caveolae in adipocytes is associated with enhanced lipid storage and lipid droplet size in adipose tissue [197]. CAV1/caveolae also modulate fatty acid uptake [198], glucose transport and insulin signaling [144] by compartmentalizing molecules involved in these pathways. Lipid metabolism in adipocytes can generate high amounts of lipid intermediates that require appropriate compartmentalization/storage in lipid droplets to prevent lipotoxicity-induced cell damage and apoptosis. In concert with this, CAV1 expression/caveolae in adipocytes has been shown to provide protection from lipotoxicity [199].

1.6.6 Membrane Buffering and Mechano-transduction

All cells have a unique shape that is bounded by the PM and further stabilized by intracellular networks of cytoskeletal and filamentous elements. Furthermore, hydrostatic pressure, established by the dynamic regulation of cell volume via active and passive transport of solutes/ions/molecules across the PM, exerts forces on the PM and additionally influences cell shape. Fluctuations in tonicity that change the hydrostatic pressure can therefore cause the PM to either shrink or **stretch**. Mechanical stresses derived from extracellular/environmental that deform cells can also mechanically stretch the PM [200, 201]. Some pathophysiological mechanical stressors include but are not limited to: contraction and relaxation (muscle movement, lung respiration, blood vessels), changes in pressure (blood vessels, eyes, joints), and changes in volume (lipid metabolism in adipocytes, systole, diastole) [187]. In order for cells to maintain their normal shape and function while resisting mechanical injury, the PM is equipped with a "**membrane buffering system**" that allows it to accommodate mechanical stretch and serves as a platform to transmit mechanical stimuli into the cell to elicit the appropriate responses required to counteract imposing mechanical stresses [201]. Membrane buffering is particularly important in **endothelial cells** which line blood

vessels that are subject to pressure challenges due to fluctuations in cardiac output and vascular resistance caused by changes in vascular tone.

While the fluid nature of the PM buffers cells from mechanical stresses, sustained exposure can result in membrane rupture/damage and apoptosis. Adipocytes, fibroblasts, muscle and endothelial cells are found in tissue systems under high amounts of mechanical stress during physiological conditions but are generally able to maintain proper function and avoid damage [187]. High expression of CAV1 in these cell types results in an increased density of caveolae that function as membrane reservoirs. When cells are mechanically stretched, the flattening of caveolae increases the surface area of the PM and reduces tension to **buffer** cells from membrane rupture [3, 31, 187, 202].

In response to mechanical stress, cells sense (mechano-sensing) and translate mechanical stimuli into biochemical responses through a process referred to as ***mechano-transduction.*** The resulting activation of stretch-dependent calcium channels and integrin-dependent cell signaling events causes architectural rearrangements to the cytoskeleton that stiffen and contract the cell in order to adapt increases in mechanical stress [187]. Caveolae have been implicated in modulating integrin activity and calcium signaling and are also thought to play a role in mechano-transduction [203] by compartmentalizing and modulating signaling molecules important for mechano-transduction [30, 116, 118, 204]. The presence of caveolae is important for the spatial organization and modulation of mechano-sensitive ion channels, Src-dependent actin reorganization, Rho-dependent actomyosin contraction, and focal adhesion remodeling (ROCK/mDia), which promote cellular stiffening and contraction [21]. These changes help the cell maintain its shape and function during pathophysiological mechanical stresses that stretch the PM. In adipocytes, caveolae additionally play a role in mechano-sensing and serve as a platform for integrating signaling cascades in response to dynamic changes in intracellular volume as a consequence of lipid droplet expansion and depletion associated with routine adipose tissue function [205]

1.7 Role of CAV1 in Human Diseases

CAV1 expression levels and mutations are implicated in many human diseases. CAV1 is downregulated in cancers of the breast, prostate, bladder, ovaries, lung, colorectal, and liver [206]. Tumor progression/invasiveness and enhanced metastatic potential is associated with upregulated CAV1 expression [186]. Decreased CAV1 expression is also observed in patients with fibrotic disorders such as systemic sclerosis/scleroderma (*SSc*) [207] and idiopathic pulmonary fibrosis [208]. Additionally, loss-of-function mutations in CAV1 and CAV3 cause other human diseases including Limb-Girdle muscular dystrophy and other skeletal myopathies, **lipodystrophy** and **pulmonary arterial hypertension** [15, 16, 72]. We have characterized two mutant forms of CAV1 that were identified in patients with pulmonary arterial hypertension (PAH) and congenital generalized lipodystrophy (CGL) that will be discussed in section 1.8. The remaining part of this section focuses on background information regarding CGL and PAH and how CAV1 contributes to these diseases.

1.7.1 Congenital Generalized Lipodystrophy (CGL)

Lipodystrophy is an acquired or congenital condition that results in a complete loss (*generalized*) of subcutaneous adipose tissue, ectopic lipid accumulation in non-adipose tissues and insulin resistance. Adipose tissue depletion can result from an inhibition of preadipocyte differentiation, lipolytic hyperactivity, defective lipogenesis/lipid storage, and increased adipocyte apoptosis. Congenital generalized lipodystrophy is caused by genetic mutations in *AGPAT2, BSCL2, PTRF/Cavin-1, and* ***CAV1*** (Table 2; Chapter 3). *CAV1* mutations are also associated with partial lipodystrophies (Table 2; Chapter 3) and can have a range of effects on adipose tissue ranging from impaired adipose tissue development to an inability to adequately store lipids in lipid droplets (LDs) [209].

1.7.2 Pulmonary Arterial Hypertension (PAH)

PAH is a progressive and fatal disease of the smallest pre-capillary arteries in the pulmonary-vascular system, caused by pathological narrowing of the vessels. PAH can be acquired many ways, but more than 75% of heritable PAH cases are associated with

mutations the *BMPRII* gene and other TGF beta family members (*ALK1, ENG, and SMAD9*) [210]. Heritable forms of PAH display incomplete penetrance; therefore it is believed that additional yet-to-be determined genetic or non-genetic/environmental modifiers increase the mutation carrier's susceptibility to developing PAH. Patients with PAH are susceptible to vascular injury, which then leads to endothelial dysfunction, vascular remodeling, and smooth muscle hypertrophy. Endothelial dysfunction, resulting in an inability to adequately regulate vascular tone, promotes a state in which cells are unable to appropriately respond to environmental stimuli that trigger vasoreactive responses. This can lead to increased vessel resistance and mechanical stress, ultimately causing increased arterial pressure, right ventricular dysfunction and heart failure. The changes in pressure and inability to respond can lead to endothelial damage and injury of underlying tissues. In the current model of PAH, an inability to terminate the injury response and pathological vascular remodeling is due to dysregulated eNOS activity and other signaling pathways that promote proliferation. The cellular basis of PAH is still not well understood and currently there are no cures for this devastating disease.

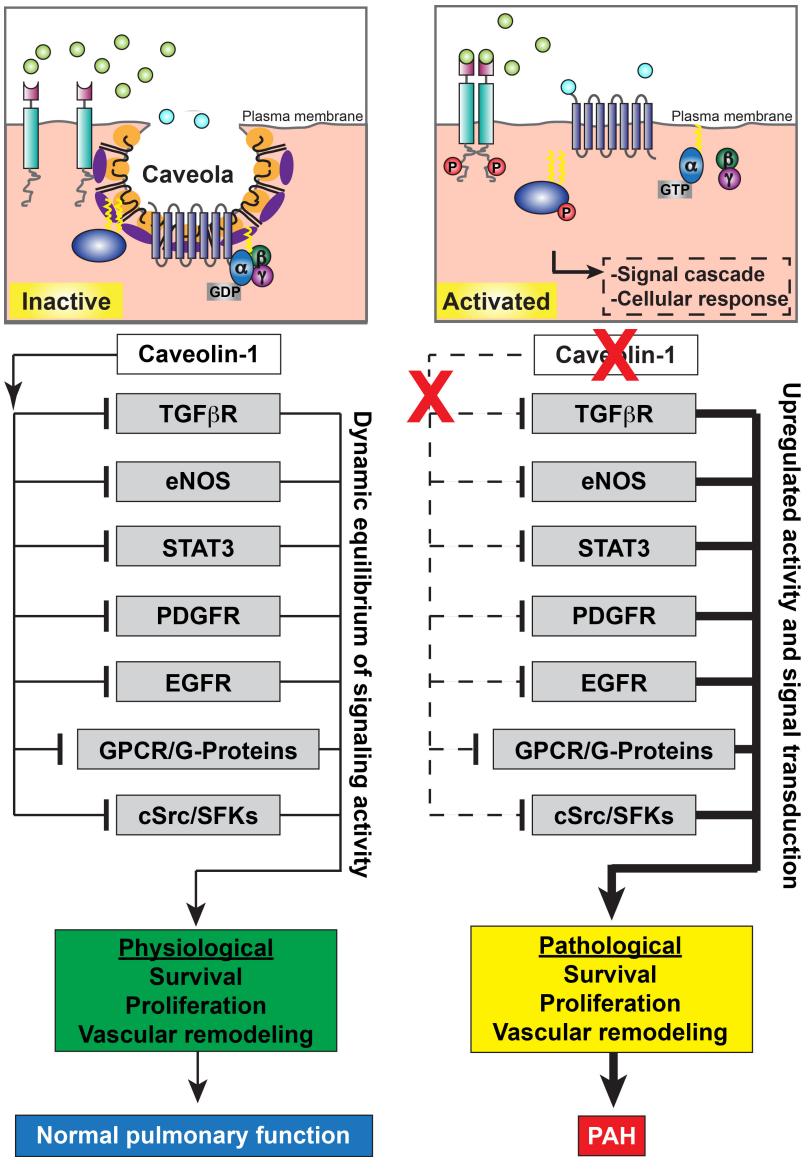

Figure 8. Implications of Reduced CAV1 Expression to the Pathogenesis of PAH. Tonic inhibition of the indicated signaling pathways above occurs in caveolae via direct interaction with the scaffolding domain of CAV1 (Figure 7 shows how molecules are believed to localize to caveolae), in order to maintain vascular homeostasis, and prevent aberrant vascular remodeling. Many of these molecules are lipid-modified, which also influences their association with lipids in raft/caveolae and non-raft membrane domains [146-148]. Loss of caveolae due to CAV1 deficiency liberates these signaling molecules from an inhibited state and leads to dysregulated activity that initiates signaling events involved in promoting pathological vascular remodeling and proliferation associated with the development of PAH [27, 36, 37, 43, 130, 131, 141, 143, 146, 149, 150]. This is discussed in detail in section 1.6.1.

Caveolae influence many signaling pathways that are implicated in PAH, and are important for maintaining normal vascular function (Figure 8). CAV1 and caveolae are markedly reduced in clinical and experimental models of PAH but until recently, no *CAV1* mutations had been described in association with the disease.

1.8 Novel CAV1 Mutations Discovered in Patients with PAH and CGL

Our collaborators Dr. Wendy K. Chung and Dr. Eric Austin discovered three heterozygous frameshift mutations in the *CAV1* gene in patients with idiopathic CGL/PAH and familial PAH. Mutations in other genes commonly associated with CGL and PAH were not detected in the patients and the underlying cause of disease was unclear. To determine if novel mutations in coding genes were contributing factors to the development of disease in these patients, whole exome sequencing (WES) was performed. Numerous genetic variants were detected in the patients but none previously known to be pathogenic. Novel non-synonymous variants were identified after further screening across multiple databases [13, 16]. Of the novel non-synonymous variants identified, the *CAV1* mutations were predicted to more severely impact the protein function due to the resulting changes in the amino acid sequence [14, 16, 211]. Interestingly, all three frameshift mutations in the *CAV1* gene result in the expression of three unique but similar mutant CAV1 proteins, which are further discussed in the next sections. It is thus important to characterize the mutant proteins and how expression of the mutants affects caveolae formation/function in order to elucidate the underlying caveolae defects contributing to disease.

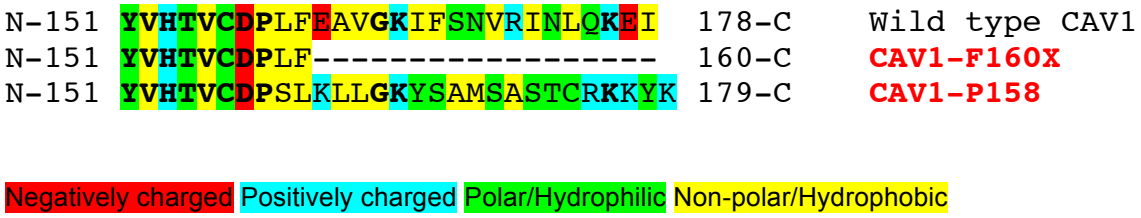

Figure 9. C-terminal Amino Acid Sequence Alignment of Wild type CAV1 and Mutants. This schematic shows the differences and similarities between C-terminus of wild type CAV1 and the mutants characterized in this dissertation. Red, bold text indicates the mutants. Bold, black text indicates conserved residues. Adapted from Austin et al., 2012 [16].

1.8.1 The CAV1-F160X Frameshift Mutant Associated with PAH and CGL

The *de novo* ***CAV1*-F160X** mutation was identified in a patient with PAH and CGL [14, 211] (Table 2; Chapter 3). A di-nucleotide deletion in the *CAV1* gene (c.479_480delTT) introduces a premature stop codon that results in a truncated mutant protein lacking the

last 19 amino acids of wild type CAV1 C-terminus (p.F160X; referred to as F160X) [14, 211] (Figure 9). This mutation has only been identified in one patient, who presented with a variety of abnormalities including a generalized decrease in adiposity, progeroid appearance, low weight, brain abnormalities that suggest cerebral atrophy, elevated fasting triglyceride levels, narrowing of pulmonary arterioles, and elevated mean pulmonary arteriole pressure [13-15]. The parents and siblings of the patient are healthy and there is no prior family history of the diseases. Previous biochemical analysis of lysates derived from the patient and control cells have shown that CAV1 protein levels are reduced in the patient compared to control cells. However, exactly how this mutant affects caveolae, or contributes to the pathogenesis of PAH and CGL has not been fully investigated [14, 211].

1.8.2 The CAV1-P158 Frameshift Mutant Associated with PAH

The **CAV1-P158fsX22** frameshift mutant was identified in a family of patients with PAH. During this time, a very similar mutation was identified in a juvenile patient with idiopathic PAH. The frameshift mutations in the *CAV1* gene (**c.474delA** and c.473delC) produce 179 amino acid mutant proteins with identical novel 21 amino acid C-terminus beyond amino acid residue proline-158 (p.P158P fsX22, referred to as **P158**; p.P158H fsX22) [16] (Table 2; Chapter 3). The novel C-terminus of the mutants contains only four conserved residues in common with the C-terminus of wild type CAV1. The mutant C-terminus also has more charged residues, and fewer hydrophobic residues compared to the C-terminus of the wild type protein [16] (Figure 9). Total CAV1 protein levels were decreased in skin fibroblasts isolated from heterozygous patients expressing P158 compared to control fibroblasts expressing only wild type CAV1 [16]. Whether the mutation induces a novel gain-of-function, leads to haploinsufficiency or behaves in a dominant-negative manner has yet to be explored. Experiments described in this proposal are aimed to determine if expression of this mutant leads to defects in oligomerization and caveolae formation to understand how it contributes to the development of PAH.

1.9 Goals and Summary of Dissertation Research Projects

Studies carried out in the *Cav1*$^{-/-}$ mice and other *in vitro* functional experiments have broadened our understanding of CAV1/caveolae and their roles in modulating proliferation, adipose and vascular homeostasis, and metabolism [11, 212-215]. However, little is known about how the caveolae structure, CAV1 oligomer stability, and composition of caveolae contributes to their proper function during these physiological processes. This is because a major challenge in defining the necessary requirements for caveolae function is that most routine experimental approaches either prevent caveolae formation from occurring or completely disrupt existing caveolae, promoting the disassembly of protein components. Despite the breadth of knowledge gained from experiments that disrupt caveolae, experimental ablation of caveolae as a means for investigation limits the ability to determine whether the morphology, structural stability and composition of caveolae influences their function. The investigation of CAV1 mutants is an alternative approach used to overcome these caveats. Studying mutant forms of CAV1 is useful for delineating the trafficking and assembly of CAV1 complexes in order for caveolae to form without entirely disrupting CAV1 expression.

The identification of new disease-associated mutations in *CAV1* (CAV1-F160X and CAV1-P158) has generated a heightened need for us to expand our understanding of how mutations affect CAV1 and caveolae [13-16]. Reduced CAV1 protein levels were reported in preliminary studies; however, exactly how these newly identified mutant forms of CAV1 impact caveolae formation and function remains to be elucidated [14-16]. Therefore, the goal of this dissertation project was to characterize the behavior of these mutants and their impact on caveolae in order to begin determining how they contribute to disease. As discussed above, CAV1 expression is essential for the formation of caveolae, which have numerous functions, including modulating cell signaling and buffering cells from mechanical stress. Additional work has also highlighted the importance of the C-terminus of CAV1 in the assembly of CAV1 complexes, and trafficking to the plasma membrane. Based on this we hypothesized

that *expression of the CAV1 mutants negatively impacts the trafficking and assembly of CAV1 complexes, which will give rise to caveolar defects.*

To test this hypothesis, we assessed the expression, oligomerization, trafficking, and assembly of caveolae in patient-derived cells and in *Caveolin-1*$^{-/-}$ murine embryonic fibroblasts (MEFs) transfected with the mutant proteins using biochemical, cell and molecular-based approaches. Our results indicated that CAV1-F160X is incorporated into caveolae with no affect on density of caveolae or their mechano-protective properties [13] (Chapter 3). We also show that CAV1-P158 behaves as a dominant negative that reduces caveolae formation and disrupts the mechano-protective function of caveolae (Chapter 4).

Thus, neither mutant completely ablates caveolae formation and both are capable of co-assembling with wild type CAV1 into hybrid complexes that are required for caveolae formation. However, the caveolae formed in cells expressing the mutant proteins are biochemically unstable and appear to have an altered composition, indicating that an intact C-terminus may also be important for normal caveolae function. Furthermore, we show that CAV1-F160X is a novel example of a disease-associated CAV1 mutant that has no effect on the density of caveolae in cells despite being linked to two different diseases. We conclude that the stability of CAV1 complexes and composition of caveolae are contributing factors to the development of PAH and CGL. Thus, the incorporation of CAV1 proteins with C-terminal mutations into caveolae is a critical factor associated with human diseases.

In the next chapters, the experimental methods and results of our experimental characterization of the mutant proteins are discussed.

CHAPTER 2

MATERIALS AND METHODS

2.1 Materials and Reagents

Complete, EDTA-free protease inhibitor cocktail tablets were purchased from Roche (Indianapolis, IN). RIPA cell lysis buffer, and phosphatase inhibitor cocktail 2 and 3 were purchased from Sigma-Aldrich (St. Louis, MO). ProLong® Gold Antifade Mountant and Lipofectamine 2000 transfection reagent were purchased from Life Technologies (Grand Island, NY). DRAQ5 (#4084) far-red nuclear stain was purchased from Cell Signaling Technology (Danvers, MA). Restriction enzymes were purchased from New England BioLabs.

2.2 Antibodies

Anti-Caveolin-1$\alpha/\beta^{aa.1\text{-}97}$ rabbit polyconal (610060), anti-Caveolin-1$\alpha^{aa.1\text{-}24}$ monoclonal, clone 2234 (610494), anti-Caveolin-1$\alpha/\beta^{aa.61\text{-}71}$ monoclonal, clone 2297 (610406) anti-Caveolin-2 monoclonal (610684), anti-GM130 monoclonal (610822) and anti-EEA1 monoclonal (610457) antibodies were purchased from BD Transduction Laboratories. Anti-Caveolin-1 $\alpha/\beta^{C\text{-}term}$ [E249] rabbit monoclonal (ab32577), anti-Caveolin-2 [EPR2220] rabbit monoclonal (ab79397), anti-Cavin-1/PTRF rabbit polyclonal (ab48824), and anti-EHD2 goat polyclonal (ab23935) antibodies were purchased from Abcam. Anti-Golgin97 monoclonal [CDF4] (A-21270) and all Alexa-Fluor dye conjugated secondary antibodies were purchased from Thermo Scientific. Anti-β-tubulin monoclonal [E7] (AB_2315513) antibody was purchased from the University of Iowa Developmental Studies Hybridoma Bank. Anti-Myc monoclonal [9B11] (#2276) and anti-HA-tag monoclonal [6E2] (#2367) antibodies purchased from Cell Signaling Technology. Anti-ADRP guinea pig polyclonal [hNT] (GP46) antibody was purchased from PROGEN Biotechnik. QuickChange Site-Directed mutagenesis kit was purchased from Agilent Technologies, Santa Clara, CA.

2.3 Cell Culture

Skin biopsy specimens were obtained via a sterile 3 mm punch skin biopsy technique from the patients and primary skin fibroblasts isolated as described previously [16]. Healthy control primary skin fibroblasts derived from skin biopsies were previously described [16]. Cells were cultured using standard methods in Dulbecco's Modified Eagle Medium (DMEM) (4.5g/L glucose, L-glutamine, and sodium pyruvate) supplemented with 20% heat-inactivated fetal bovine serum (FBS), 1% penicillin-streptomycin, and 1% L-Glutamine from Invitrogen (Grand Island, NY). Wild type and *Cav1*$^{-/-}$ MEFs were obtained from ATCC and cultured in DMEM (with 4.5 g/L glucose, L-glutamine, and sodium pyruvate) supplemented with 10% FBS. All the cultures were maintained at 37°C in an atmosphere of 5% CO_2 in air with 95% relative humidity.

2.4 Plasmids and Site-Directed Mutagenesis

2.4.1 Plasmids

mCherry-LAMP1 (Addgene No.55073), Caveolin-1-mEmerald N10 (Addgene No.54026) and mEmerald-Caveolin-1 C-10 (Addgene No.54025) were gifts from Dr. Mike Davidson. pCMV-HA-N (No. 82017) empty vector plasmid DNA was used to generate HA-tagged constructs (ThermoFisher Scientific, Rockford, IL).

2.4.2 Site-directed Mutagenesis

Standard PCR, site-directed mutagenesis and subcloning were used to generate novel constructs to further study the PAH mutant. The naturally occurring PAH-associated frameshift mutation in the *CAV1* gene (c.Δ474A/ p.P158fsX22 single nucleotide deletion) was mutagenized into both mEmerald-Caveolin-1 C-10 and Caveolin-1-mEmerald N-10 constructs (5' ACACCGTCTGTGACCCCTCTTTGAAGCTGTTG 3') with site-directed mutagenesis. Further mutagenesis was required to put the C-terminal mEmerald tag in frame and terminate the reading frame of the N-terminally tagged mutant construct.

2.4.3 CAV1-P158-mEmerald

The reading frame of C-terminal tag in construct was corrected by inserting the nucleotides “TATAAA” at the end of the CAV1 coding sequence with NheI and AgeI restriction sites, just before the start of the linker region that separates *CAV1-P158* and *mEmerald*. This was performed by GenScript USA Inc.

2.4.4 mEmerald-CAV1-P158

Similar methods used for correcting the reading frame of CAV1-P158-mEmerald described in section 2.4.3 were used to insert the stop codon “TGA” at the end of the coding sequence of mutant *CAV1* with BglII and PstI restriction sites in order to terminate translation at the appropriate site and prevent translation beyond the mutant *CAV1* insert.

2.4.5 HA-CAV1-Wt

Wild type full-length *CAV1* was excised from an untagged Caveolin-1-mEmerald N10 construct generated with the primer 5’ GCAGAAAGAAATATAGCTCCGGAGGGG 3’ to insert a stop codon to prevent the reading of the mEmerald fusion protein tag. The excised CAV1 fragment was subcloned into the linearized pCMV-HA-N vector using BamHI and NheI restriction enzyme sites. A single nucleotide was inserted in the linker region between the *HA* and *CAV1* coding sequences with the primer 5’ GCTAGCCACCGCCACC 3’ to put CAV1 in frame.

2.4.6 HA-CAV1-P158

Identical methods used to generate HA-CAV1-Wt were used to make HA-CAV1-P158 but an untagged version CAV1-P158-mEmerald mutagenized with the 5’ CAGAAAGAAATATAAATAGCTCCGGAGGGGATC 3’ primer to terminate translation of mEmerald was used instead as template to be inserted into pCMV-HA-N vector using BamHI and NheI restriction enzyme sites.

2.4.7 HA-CAV1-P158-AAYK (K176-177A)

For the first lysine to alanine substitution at amino acid position 176, HA-CAV1-P158 was mutagenized with the primer 5' CATCAACTTGCAGAGCGAAATATAAATAGC 3'. The resulting product was mutated a second time with the primer 5' CATCAACTTGCAGAGCGGCATATAAATAGC 3' to mutate the lysine at amino acid position 177 to an alanine to disrupt the ER-retention/retrieval signal.

2.4.8 HA-CAV1-P158-ΔKKYK (R175X or Δ176-179)

The HA-CAV1-P158 construct was further mutagenized by GenScript USA Inc. to mutate the codon encoding *K176* to a "TAG" stop codon using NheI and BamHI restriction enzyme sites to truncate the *KKYK* ER-retention/retrieval in the protein product.

2.4.9 HA-CAV1-KKYK

Wild type mEmerald-Caveolin-1 C-10 plasmid DNA was sent to GenScript USA Inc. for the *KKYK* peptide to be added using BglII and SacII restriction enzyme sites in order to induce an ER-retention/ retrieval signal into the C-terminus of the wild type CAV1 protein. The mEmerald-CAV1-KKYK was digested with BglII and EcoRI and the fragment containing *CAV1-KKYK* was ligated to the linearized pCMV-HA-N empty vector cut with BamHI and EcoRI. A single nucleotide was inserted in the linker region between the *HA* and *CAV1* coding sequences with the primer 5' CTCGAGGGATTCTGGCAGC 3' to put CAV1 in frame.

2.4.10 HA-CAV1-F160X

The identical frameshift mutation of the patient (c.479-480ΔTT/ p.F160X) was first mutagenized into wild type mEmerald-Caveolin-1 C-10 site-directed mutagenesis (primer: 5' GACCCACTCTGAAGCTGTTG 3'). The CAV1-F160X-coding fragment of mEmerald-CAV1-F160X was then excised out of the mEmerald C-10 vector backbone with BglII and EcoRI and subcloned into the pCMV-HA-N destination vector that had been linearized with BamHI and EcoRI restriction enzyme digest. Site-directed

mutagenesis was used to insert a nucleotide in the linker region between the HA-tag and CAV1 coding sequence in HA-CAV1-F160X in order to put CAV1 in frame for proper translation (5' CTCGAGGGATTCTGGCAGC 3').

2.4.11 Untagged CAV1-F160X

Caveolin-1-mEmerald N-10 was used as template, and the same primer that was used to generate mEmerald-CAV1-F160X was used on this construct to generate the same mutation, which also effectively terminated reading into the mEmerald fusion protein tag (5' GACCCACTCTGAAGCTGTTG 3').

2.4.12 Myc-CAV1-Wt

This construct was generated by GenScript USA Inc. Briefly, in order to generate an N-terminally Myc-tagged CAV1, an oligo encoding the Myc-tag sequence (5'GAACAGAAACTGATTAGCGAAGAAGATCTG3') was inserted upstream of wild type human CAV1 coding region in a CAV1-mEmerald N-10 construct that had been mutated to terminate reading for the mEmerald fusion protein (5'GCAGAAAGAAATATAGCTCCGGAGGGG3'). Site-directed mutagenesis (5'CACCGCCACCATGGAACAGAAAC3') was later performed to insert an initiator methionine before the Myc-tag sequence to initiate translation.

2.5 Transfections

Cav1$^{-/-}$ MEFs were trypsinized, seeded onto glass coverslips in a 6-well dish at a density of 1.5×10^5 cells per well, and allowed to incubate overnight in complete growth medium. The cells were then transfected according to the manufacture's protocol with Lipofectamine 2000 reagent. Before the transfection reaction mixture was added to the cells, they were placed in Opti-MEM low serum medium. After 4-6 hours, the transfection medium was removed and replaced with fresh growth medium and incubated for a total of 24 hours.

2.6 Immunofluorescence Microscopy

Cells were plated on No.1.5 glass coverslips, and allowed to adhere for 24-48 hours. Coverslips were fixed in 4% PFA for 15 minutes at room temperature, washed, and blocked for an hour in 1% BSA, 5% glycerol, 0.1% glycine, 0.04% sodium azide, 0.01% saponin, and 5% normal sera (IF buffer). Cav1 N-term polyclonal (1:300), anti-Cav1 clone 2234 (1:50), Cav2 monoclonal (1:50), C-term rabbit monoclonal (1:50), Cav2 rabbit monoclonal (1:50), Cavin1/PTRF polyclonal (1:100), EHD2 goat polyclonal (1:250), GM130 (1:100), and β-tubulin monoclonal (1:100) primary antibodies were diluted in IF blocking buffer, and incubated from 1-24 hours and washed. For incubations longer than 1 hour, coverslips were placed in a humid chamber and incubated at 4°C. Alexa Fluor-conjugated secondary antibodies (1:500, Thermo-Fisher Scientific) were diluted in IF blocking buffer containing 1:1000 DRAQ5 far-red nuclear stain (Cell Signaling Technology) if the far-red channel was not used to image an immunostained protein, and incubated for 1 hour at room temperature while protected from light. Following secondary incubation, coverslips were washed, and mounted with Prolong® Gold Anti-fade mounting agent. Slides were imaged on a Zeiss LSM510 inverted laser-scanning confocal microscope. Images were acquired using a 100× 1.4 N/A Plan Apochromat DIC oil objective. Argon, HeNe1, and HeNe2 lasers were used to excite Alexa-fluor 488, 546 and 633/647, respectively.

2.7 Colocalization Analysis

Colocalization analysis was performed using Macbiophotonics ImageJ and "Intensity Correlation Analysis" plugin using a semi-automated procedure. Analysis was performed on 4× zooms collected at 22.5 μm × 22.50 μm. A region of interest (ROI) containing the cell was manually defined on each image and only the ROI was used for colocalization analysis. For each set of comparisons, at least 30 images were used for measurement from at least 3 independent experiments, unless stated otherwise in the

figure legends. Pearson's correlation coefficients are reported as the mean ± standard deviation for all the ROIs. A Student's T-test was used to calculate p-values.

2.8 Transmission Electron Microscopy

Cells were grown to confluency in 10 cm culture plates, washed in 0.1 M Cacodylate buffer, fixed in 2.5% gluteraldehyde diluted in 0.1 M Cacodylate buffer and stored at 4º C. Thereafter, fixed cells were scraped, pelleted, post-fixed in osmium tetroxide, stained with Uranyl acetate *en bloc* to enhance membrane contrast, and epon embedded. Blocks were thin sectioned and counter-stained with lead citrate. Images were acquired on a Philips/Tecnai FEI T-12 transmission electron microscope operated at 80kV at 30,000× magnification. Control and patient fibroblasts were imaged in at least 3 independent experiments.

2.9 Quantification of Caveolae

25 images of cell sections from each sample were captured, and caveolae were counted. Caveolae were defined as 50-80nm diameter, PM attached, or internalized vesicles, no more than 200nm from the PM. The number of caveolae counted was normalized to the total length of plasma membrane from a minimum of 25 cells in each sample, from three independent experiments.

2.10 Western Blotting

Whole cell lysates were generated from control and patient primary human skin fibroblasts cultured to confluence in 15 cm tissue culture dishes (Corning, New York) or transfected *Cav1*$^{-/-}$ MEFs. Once confluent or 24 hours-post transfection, cultures were chilled on ice for 5 minutes and washed three times in phosphate-buffered saline (PBS) from Corning. Cells were lysed with 0.5 mL of 50 mM Tris-HCL, pH 8.0, 150 mM, 1.0% Igepal Ca-630 (NP-40), 0.5% sodium deoxycholate, 0.1% SDS plus phosphatase inhibitors from (Sigma-Aldrich) and protease inhibitors (Roche). Following 5 min

incubation on ice, the lysed cells were scraped and transferred to new tubes. To clear the lysates, the samples were flash frozen in liquid nitrogen and allowed to thaw at room temperature. Thawed lysates were spun at 13,000 rpm at 4°C for 10 minutes to pellet the debris. The protein concentration of supernatant was quantified with BCA protein assay (Thermo Scientific Pierce). Equal amounts of protein from each sample were mixed with reducing reagent and loading buffer (Life Technologies) and boiled for 10 min.

SDS-PAGE was conducted using the Novex® NuPAGE® SDS-PAGE Gel System (Life Technologies). NuPAGE® 4–12% and 4-20% Bis-Tris gels (Life Technologies) were used for the protein separation. SeeBlue® Pre-stained Protein was used to evaluate the molecular weight. The Bio-Rad Mini-PROTEAN System and 12% tris-glycine hand- and 12%TGX pre-cast gels were used for transfected *Cav1*$^{-/-}$ MEFs. A Mini Trans-Blot® Electrophoretic Transfer Cell (Bio-Rad) was used for the electrophoretic transfer. The PVDF membranes (Millipore) were de-stained with methanol. Secondary antibodies and blocking buffer were obtained from LI-COR and imaging was performed using the LI-COR Odyssey system. Densitometry analysis was conducted using ImageJ software (http://fiji.sc/Fiji).

2.11 Blue Native-PAGE

BN-PAGE was performed as recently described [13]. Briefly, BN-PAGE was conducted by using the NativePAGE™ Bis-Tris Gel System (Life Technologies). Cell lysis buffer (NativePAGE 1× sample buffer, complete protease inhibitor cocktail from Roche and 1% digitonin) was made according to the NativePAGE Sample Prep Kit's manual book. Fibroblast cells were lysed at 4°C for 30 min. Then, a 30-minute centrifugation at 16,100×*g* (centrifuge 5415D, Eppendorf) was performed at 4°C. The pellet was discarded and the supernatant was used for further analysis. Protein concentrations were determined using a BCA Assay Kit from Thermo Scientific. 4–16% NativePAGE gels (Life Technologies) were used for electrophoretic separation of the proteins. Equal amounts of protein were loaded on the same gel as determined by BCA (10 µg for each

lane). NativeMark ™ unstained protein standards (Life Technologies) were used to evaluate the molecular weight.

2.12 Velocity Gradient Centrifugation for Isolation of 8S and 70S Complexes

Velocity gradient centrifugation was performed as recently described [13]. Briefly, about 1×10^6 fibroblasts or 4×10^6 *Cav1*$^{-/-}$ MEFs were lysed at room temperature for 20 min in 330 µL of 0.5% Triton-X-100 in TNE [100 mM NaCl, 20 mM Tris–HCl pH 7.5 and 5 mM ethylenediaminetetraacetic acid (EDTA)] buffer, supplemented with 'Complete' protease inhibitors cocktail (Roche). Post-nuclear supernatants (PNSs) were prepared by a 5-min centrifugation at 1,100×*g*. Three hundred microliters of the PNSs was loaded onto linear 10–40% sucrose gradients containing 0.5% Triton-X-100, 20 mM Tris–HCl pH 7.5, 100 mM NaCl, 5 mM EDTA and protease inhibitors cocktail. After centrifugation in an SW55 rotor (OptimaTM LE-80K Ultracentrifuge, Beckman) for 5 hours at 48,000 rpm at 4°C, fourteen 360µL fractions were collected from the top to the bottom and analyzed by SDS–PAGE/western blot with an equal loading volume. Western blots were imaged and quantified as indicated above.

2.13 Detergent-Resistant Membrane Fractionation

Preparation of detergent resistant membrane fractions was performed as recently described [13]. Briefly, about 1×10^6 fibroblast cells or 1.6×10^7 *Cav1*$^{-/-}$ MEFs were suspended in 300 µL of cold 0.5% (or 1%) Triton-X-100 in TNE [100 mM NaCl, 20 mM Tris–HCl pH7.5 and 5 mM EDTA], supplemented with 'Complete' protease inhibitors cocktail (Roche). Homogenization was performed in a cold room using pre-cooled equipment by passing the cell solution 10 times through a 1-mL syringe with a 27-gauge stainless steel needle (BD Biosciences). The homogenate was adjusted to about 40% sucrose by the addition of 700 µL of 60% sucrose prepared in TNE and placed at the bottom of an ultracentrifuge tube. A 5–35% linear sucrose gradient was formed above the homogenate and centrifuged at 40,100 rpm and 4°C for 16 hours in a SW55 rotor (Optima LE-80K Ultracentrifuge, Beckman). Fourteen 360-µL fractions were collected

from the top and analyzed by SDS–PAGE/western blotting with an equal loading volume. Western blots were imaged and quantified as indicated above.

2.14 Osmotic Swelling and Cell Viability

2.14.1 Osmotic swelling

Cells were plated in Matte® dishes at 60% confluence two days prior to the experiment. The growth medium was removed and replaced with 2 ml of 0.1X hypotonic serum free DMEM medium (10-fold dilution in water) and incubated at 37°C for 10 min.

2.14.2 Viability assay

The hypotonic medium was carefully removed and then cell viability was assessed using LIVE/DEAD® Viability/Cytotoxicity kit (Molecular Protest, Invitrogen Detection Technologies) as directed by the manufacturer protocol. Twelve fields of cells were analyzed at 10× magnification for each cell line. Confocal images were acquired using the previously mentioned inverted Zeiss LSM 510 confocal microscope (Plan-NEOFLUAR 10× 0.3 N/A objective). Calcium AM-positive live cells (green) and ethidium homodimer-1-positive dead cells (red) were counted using ImageJ software. A Student's T-test was used to analyze the data with GraphPad Prism 7.0 software; values reported are the mean ± the standard deviation of three replicate experiments.

CHAPTER 3

CHARACTERIZATION OF A PAH AND CGL-ASSOCIATED CAVEOLIN-1 MUTANT [1]

3.1 Introduction

Flask-shaped membrane invaginations known as caveolae are thought to function as key regulators of cholesterol and lipid metabolism as well as to maintain proper function of the vascular system [187, 197]. Congenital generalized lipodystrophy (CGL) and pulmonary arterial hypertension (PAH), diseases of the adipose tissue and vascular endothelium, respectively, have been associated with mutations in caveolin-1 (CAV1), a protein required for the formation of caveolae [15, 16]. CAV1 and caveolae are abundant in cell types linked to CGL and PAH, including adipocytes, endothelial cells, and smooth muscle cells [197, 214, 216]. Mutations in another caveolae-stabilizing protein, cavin-1/PTRF, have also been linked to lipodystrophy, further highlighting the importance of these structures in the maintenance of lipid homeostasis [97, 98, 217-221].

So far, there has been one reported case of a patient with congenital generalized lipodystrophy (CGL) with a homozygous CAV1 mutation (E38X) [222], and three individuals with heterozygous mutations in CAV1 (I134 fsdelA-X137 and -88delC) with atypical partial lipodystrophy [12] (Table 2; Figure 10). Through whole exome sequencing, our group identified two novel frameshift heterozygous mutations in CAV1, c.474delA (p.P158PfsX22) and c.473delC (p.P158HfsX22), in patients lacking other known PAH-associated mutations, such as BMPR2 [16]. These two different CAV1 mutations have nearly the same effect on the protein by introducing a frameshift after amino acid 158 and inserting the same 21 novel amino acids after amino acid 158. However, exactly how these CAV1 mutations contribute to the development of PAH or

1. ***Han B**, ***Copeland CA**, Kawano Y, Rosenzweig EB, Austin ED, Shahmirzadi L, Tang S, Raghunathan K, Chung WK and Kenworthy AK. Characterization of a caveolin-1 mutation associated with both pulmonary arterial hypertension and congenital generalized lipodystrophy, Traffic. 2016; 17(12): 1297-1312. [13]. *, These authors contributed equally to this manuscript.

lipodystrophy, and why different CAV1 mutations are linked to different diseases is currently unclear.

Recently, a new heterozygous CAV1 nonsense mutation, c.479_480delTT (p.F160X), was reported in a patient with both pulmonary hypertension and CGL by two groups [14, 15] (Table 2; Figure 10). The two-base-pair deletion induces a premature stop codon, and is predicted to generate a C-terminally truncated mutant protein designated F160X. In the first study reporting the mutation, morphologically defined caveolae were observed by electron microscopy in skin fibroblasts isolated from the patient, but little CAV1 was detectible by immunofluorescence microscopy [15]. The second study reported reduced CAV1 protein levels by Western blotting as well as decreased co-localization of CAV1 with the caveolae accessory protein cavin1 in patient fibroblasts [179]. Besides these initial findings, how heterozygous expression of the F160X mutant protein impacts caveolae formation and function remains otherwise unknown.

Table 2. Summary of *CAV1* Mutations, Mode of Inheritance and Phenotype

CAV1 mutation	F160X	Q142X	E38X	I134 fsdelA-X137	−88delC	P158P fsX22	P158H fsX22
Mode of inheritance	Heterozygous	Heterozygous	Homozygous	Heterozygous	Heterozygous	Heterozygous	Heterozygous
Lipodystrophy	Congenital generalized lipodystrophy	Congenital generalized lipodystrophy	Congenital generalized lipodystrophy	Congenital partial lipodystophy	Adult-onset partial lipodystrophy	Absent	Absent
PAH	Present	Absent	Absent	Absent	Absent	Present	Present
Reference	This study, 4,16	4	14	15	15	3	3

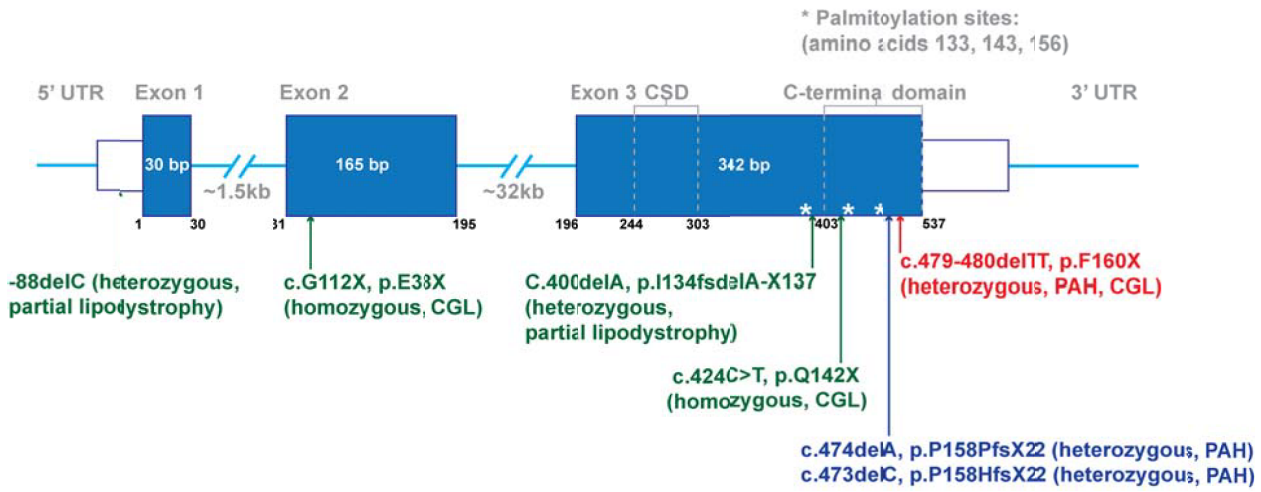

Figure 10. CAV1 Gene Organization and Reported CAV1 Mutations Associated with PAH and CGL in Humans. Exons are shown in blue. *, Protein palmitoylation sites. CSD, caveolin scaffolding domain. (Bing Han, Ph.D.)

The assembly and targeting of CAV1 to caveolae is known to be a stepwise process involving oligomerization of newly synthesized CAV1 monomers, assembly of oligomers into high-molecular-weight complexes and trafficking to the plasma membrane [8]. In this pathway, CAV1 forms an 8S core complex consisting of homo-oligomers and hetero-oligomers with CAV2 in the endoplasmic reticulum before being transported to the Golgi complex [8]. There, the 8S core complexes assemble to 70S complexes that become enriched in cholesterol [8]. Finally, 70S complexes are transported to plasma membrane and induce caveolae formation [8] with the help of the cavin family of proteins as well as other accessory proteins such as EHD-2 and PACSIN2 [75-77, 79, 85, 86, 223-226]. The C-terminal domain of CAV1 (amino acids 135-178) has been reported to be important for interactions between adjacent homo-oligomers of CAV1 that are necessary for forming the higher-order CAV1 oligomers that ultimately become incorporated into caveolae [48, 111]. Thus, the F160X mutation could potentially influence on the assembly of CAV1 oligomers as well as possibly disrupt caveolae formation per se.

Here, we report the independent identification and characterization of caveolae in the patient with both PAH and CGL linked to a heterozygous F160X mutation in CAV1. We show that caveolae are present in skin fibroblasts isolated from the patient and that

putative caveolae can be reconstituted by co-expression of wild type CAV1 and CAV1-F160X in *Cav1*$^{-/-}$ murine embryonic fibroblasts (MEFs). The ability of caveolae to confer mechano-protection against hypo-osmotic shock was unaffected in patient cells. However, expression of the CAV1-F160X mutant was found to reduce the levels of cavin-1 associated with CAV1, significantly impair the stability of both core CAV1 oligomers and higher-order CAV1 complexes, and decrease the association of CAV1 with detergent resistant membranes. Thus, though caveolae are present in patient cells, they are not completely normal. These findings suggest that the formation of aberrant caveolae may contribute to the development of both PAH and CGL and broaden our knowledge of disease-associated CAV1 mutations.

3.2 Results

3.2.1 Clinical Description

The patient is a three-year-old girl with CGL and PAH. She was born full-term with a birth weight of 2466 grams (<5th percentile), length of 46 cm (<5th percentile), and head circumference of 35.5 cm (65th percentile). At birth, she was found to have a triangular face, a large anterior fontanelle, and cutis marmorata telangiectatica congenita over her entire body.

She was noted to have generalized absence of subcutaneous fat from birth and was therefore diagnosed with CGL. Her fasting triglyceride level was elevated at 168 mg/dL (normal 30-150 mg/dL) at 27 months, but a repeat test at 30 months was normal. Her cholesterol and LDL have been normal, though her HDL has been consistently low. Her leptin at 30 months was 1.0 ng/mL (normal 0.6-16.8 ng/mL) and insulin at 35 months was low at 1.3 mcU/mL (normal 2.6-24.9 mcU/mL). Abdominal ultrasound at 27 months showed no signs of fatty infiltration of the liver.

Her weight has remained below the 5th percentile since 3 months of age, while her height and head circumference have remained at the 50th percentile. Her clinical course is notable for episodes of abdominal pain and diarrhea occurring once a month,

and she has been hospitalized on two occasions, at 15 months and 27 months, for dehydration due to these episodes. A duodenal biopsy performed at 27 months showed mild villous atrophy, crypt hyperplasia, and epithelial lymphocytosis, interpreted as a Marsh IIIA lesion [227] suspicious for celiac disease though a tissue transglutaminase IgA antibody done at the time was negative.

She was diagnosed with pulmonary hypertension by echocardiogram at 15 months of age. Due to her unusual systemic disease, a lung biopsy was performed at 18 months showed changes consistent with mild pulmonary hypertension, including focal thickening of the smooth muscle in preacinar pulmonary arterioles. While she had no symptoms of syncope, dyspnea, or exercise intolerance, persistent abnormalities on echocardiogram led to further work up for pulmonary hypertension including cardiac catheterization. At 35 months, cardiac catheterization confirmed a diagnosis of PAH with a mean pulmonary artery pressure (mPAP) of 33 mmHg, pulmonary capillary wedge pressure of 11 mmHg, and pulmonary vascular resistance (PVR) of 3.97 Wood units. Acute vasodilator testing was notable for an acute response to 80 ppm of NO and 100% FiO2 with mPAP reduced to 21 mmHg and PVR to 2.07 Wood units.

Developmentally, she has met her milestones on time and has a non-focal normal neurological examination. However, MRI of her brain at 7 months showed global cerebral atrophy.

The family history is unrevealing for cardiopulmonary disease, lipodystrophy, or other related concerns. Her parents, two older brothers and younger sister are all in good health, and there is no family history of lipodystrophy or pulmonary hypertension. Whole exome sequencing revealed a de novo heterozygous c.479_480delTT (p.F160X) mutation in CAV1 (Table 2; Figure 10) and no other suspected pathogenic, rare or novel variants to explain either her lipodystrophy or PAH. The family of the patient confirmed that she is the same patient described in two previous studies [14, 15].

3.2.2 CAV1 and Caveolae Accessory Proteins are Expressed in Patient Skin Fibroblasts

Previous studies have shown that caveolae are present in skin fibroblasts isolated from this patient [176] and that CAV1 can be detected in skin fibroblasts albeit at reduced levels by Western blotting [179]. In order to determine if CAV1 protein was being expressed in the patient identified here, we performed Western blot analysis using two different antibodies, an N-terminally directed antibody that detects both wild type CAV1 and the F160X mutant, and a C-terminally directed antibody that only recognizes wild type CAV1 (Figure 11). Similar levels of total CAV1 were observed in patient cells and control fibroblasts using the N-terminal antibody, whereas slightly decreased levels of wild type CAV1 were detected by the C-terminal antibody in the patient cells versus controls (Figure 11, Supplementary Figure 1A-D). Because the mutant protein is predicted to lack its C-terminus, this difference implies that the mutant protein is expressed in patient cells. We also analyzed levels of CAV2 and the caveolae accessory proteins cavin-1, EHD-2, and PACSIN2, and found that they were present at either similar or slightly lower levels in patient cells as well (Figure 11). Finally, levels of flotillin-1 and flotillin-2, proteins are that are non-caveolae lipid raft markers, were similar in patient and control cells (Figure 11).

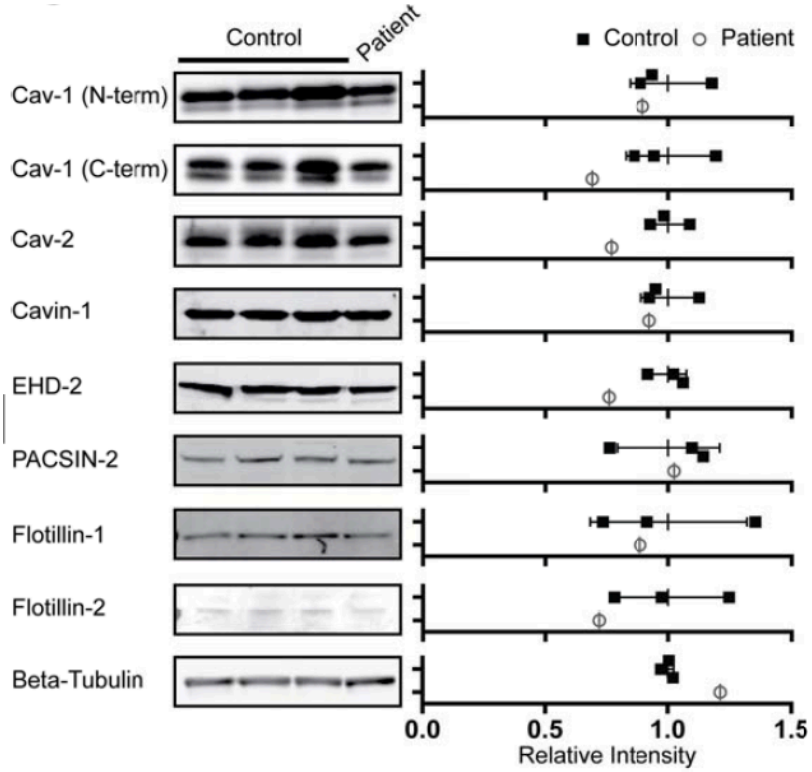

Figure 11. CAV1 and Caveolar Accessory Proteins are Present in Patient Skin Fibroblasts at Levels Similar to Wild Type. (**Left**) Protein levels were measured in three control cell lines and the F160X patient cell line by SDS-PAGE and Western blotting. Representative Western blots for the indicated proteins are shown. (**Right**) The relative densitometries of the protein bands were quantified to estimate protein levels in control (closed squares) and patient skin fibroblasts (open circles). The data were normalized to the averaged value for the three control cell lines for each protein. Error bars are the mean ± SD of intensity for the three control lines. Data is representative of 3 independent experiments. (Bing Han, Ph.D.)

3.2.3 CAV1 Forms 8S and 70S Complexes with Reduced Detergent-Resistance in Patient Fibroblasts

CAV1 undergoes a series of oligomerization events that are required for the proper assembly of caveolae. To test whether this process occurs correctly in patient cells, we first examined the biochemical properties of 8S oligomeric complexes formed by CAV1 and CAV2 using Blue-Native polyacrylamide gel electrophoresis (BN-PAGE) [109, 228-230]. We previously reported that CAV1 and CAV2 form complexes with an apparent size of 600-800 kDa in several cell types using this method [229]. CAV1 and CAV2 were detected in complexes of similar molecular weights in both control and patient skin fibroblasts (Figure 12A). To assess the assembly of higher order CAV1 oligomers in patient cells, we fractionated 8S and 70S complexes on sucrose gradients by velocity

gradient centrifugation [8]. Both 8S and 70S complexes were detected in control cells, with the majority of CAV1 being detected in 70S complexes (Figure 12B). CAV1 and CAV2 were also associated with both 8S and 70S complexes in patient fibroblasts. However, a larger fraction of CAV1 was found in 8S complexes compared to controls, suggesting that 70S complexes either form less efficiently or are less stable in patient cells (Figure 12B). To further assess the stability of the 8S complexes, we extracted cells using an SDS-containing lysis buffer (0.2% Triton X-100 + 0.4% SDS), which was previously shown to completely disassemble the 70S complexes to 8S oligomer units [8]. Under these conditions, almost all of the CAV1 complexes were disassembled to monomers or small oligomers in patient cells, whereas the CAV1 from control cell lines remained associated with intact 8S oligomers (Figure 12C). Thus, the stability of the 8S complexes is decreased in patient cells.

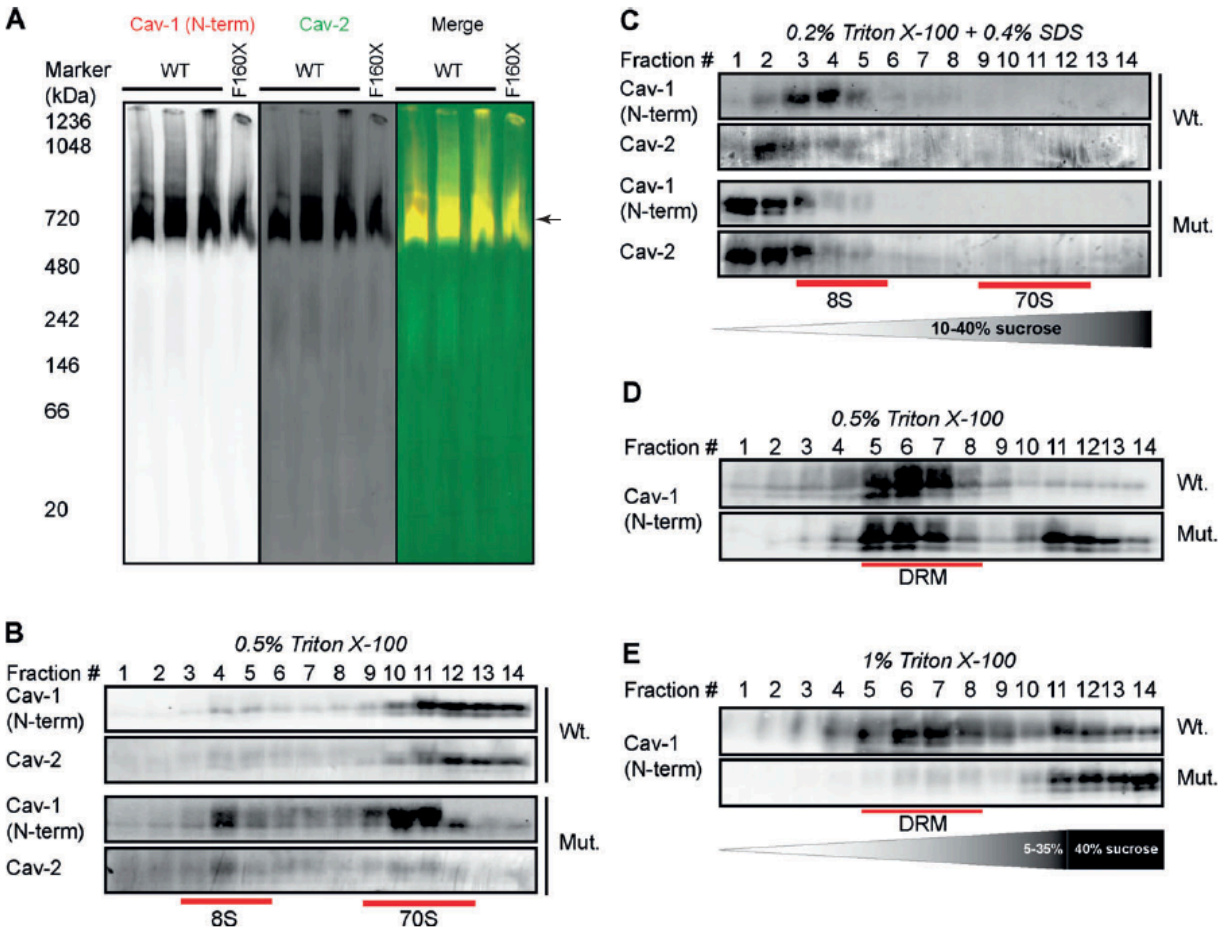

Figure 12. CAV1 Associates with High-Molecular-Weight Complexes and Detergent-Resistant Membranes in Patient Fibroblasts. (A) BN-PAGE and Western blotting was used to measure CAV1 in high-molecular-weight oligomers in control and patient skin fibroblasts. CAV proteins were detected with CAV1 N-terminal (red in merge) and CAV2 antibodies (green in merge). The position of the putative 8S complexes is marked with an arrow. **(B)** CAV1 and CAV2 fractionate as 8S and 70S complexes in both control and patient skin fibroblasts. Positions of the 8S and 70S complexes on the gradient are indicated with red lines. Note the increased amounts of 8S complexes present in the patient fibroblasts. **(C)** CAV1 oligomers dissolve into SDS-resistant 8S oligomers in control cells but form even smaller oligomers in patient cells. CAV2 was also assessed. Fractions containing 8S and 70S complexes are indicated with red lines on the gradient. **(D)** CAV1 associates with DRMs isolated using 0.5% TX-100 in both control and patient fibroblasts. Fractions enriched in DRMs are indicated with the red lines. **(E)** CAV1 is excluded from DRMs isolated using 1% TX-100 in patient fibroblasts but retains its detergent resistance in control fibroblasts under these conditions. All data sets shown are representative of 2 independent experiments. (Bing Han, Ph.D.)

It is well known that caveolae have detergent resistant properties and CAV1 is predominantly found in detergent resistant membranes [231]. Biochemical fractionation of detergent resistant membranes (DRMs) on sucrose gradients by buoyant density is thus commonly used to analyze CAV1 and caveolae. CAV1 was detectible in DRM fractions (fractions 5-8) in both wild type and patient cells extracted using 0.5% Triton X-

100 (TX100) (Figure 12D). However, when the detergent concentration was increased to solubilize weakly associated DRM components, CAV1 was predominantly associated with detergent soluble fractions in patient cells. Thus, expression of CAV1-F160X reduces the DRM affinity of CAV1 (Figure 12E).

3.2.4 Caveolae are Present in Patient Cells

The presence of 8S and 70S CAV1 complexes and acquisition of detergent resistance does not necessarily mean that CAV1 is normally associated with caveolae [229]. We thus next tested whether CAV1 is trafficked correctly and assembles into caveolae in patient cells at the cellular level. Similar densities of caveolae were readily observed in patient and control cells by transmission electron microscopy ($p=0.28$) (Figure 13A,B). Consistent with this, using immunofluorescence microscopy, CAV1 staining was observed in punctate structures characteristic of caveolae in both control and patient cells labeled with an N-terminal CAV1 antibody that detects both wild type and mutant CAV1 (Figure 13C). CAV1 staining also strongly co-localized with caveolin-2 (Figure 13D, E) and the caveolae accessory proteins cavin-1 and EHD-2 (Figure 14A-D) in both control and patient cells.

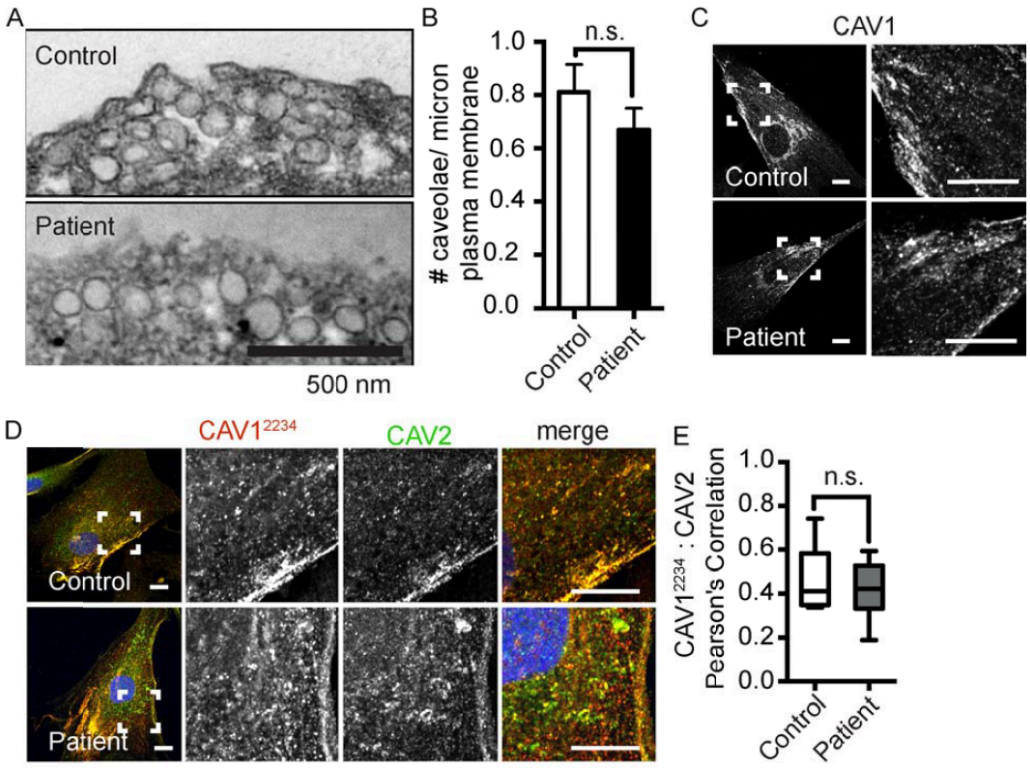

Figure 13. CAV1, CAV2 and Caveolae are Detectible in Patient Skin Fibroblasts. **(A)** Caveolae are detected in control and patient fibroblasts by transmission electron microscopy. Scale bar, 500 nm. Note that these images represent regions of high caveolae density for illustration purposes and are not representative of average densities of caveolae. **(B)** The patient's cells contain comparable amounts of caveolae as control cells (p= 0.28, Student T-test). A minimum of 25 images collected at 30,000X magnification per experiment were analyzed across three independent experiments for both the control and patient cell lines. **(C)** Representative immunofluorescence images of control and patient fibroblasts labeled with an N-terminally directed CAV1 antibody that detects both wild type and mutant F160X CAV1. The subcellular distribution of CAV1 in patient cells is similar to control cells. Scale bars, 10 mm. **(D)** Representative images of control and patient cells dually labeled with a CAV1a antibody (epitope = residues 1-24) in green and CAV2 antibody (red in merged image). Scale bars, 10 mm. **(E)** CAV1 and CAV1 exhibit similar levels of colocalization in control and patient fibroblasts as quantified using Pearson's correlation coefficient (n = 15 ROIs from 2 independent experiments.) n.s., not significant (Student's T-test).

However, the colocalization of CAV1 and cavin-1 was slightly albeit significantly reduced in patient cells compared to controls (Figure 14B). PACSIN2 colocalization with CAV1 was low but not significantly different between wild type and patient cells (Figure 14E, F).

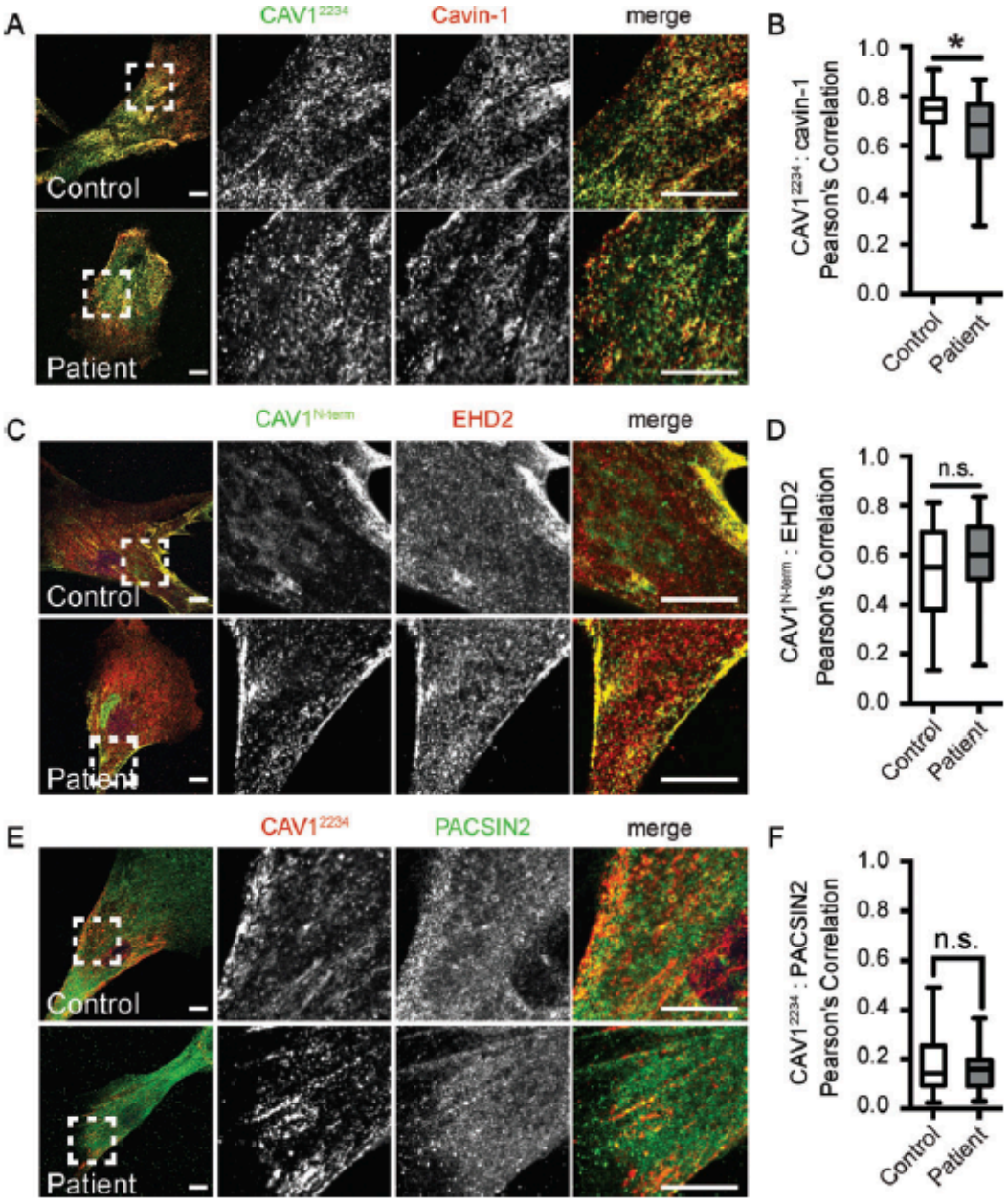

Figure 14. Caveolae Accessory Proteins are Localized Correctly in Patient Skin Fibroblasts. (A, B) Cavin-1 labeling (green) colocalizes with CAV1a staining ((red), albeit at reduced levels in patient cells compared to controls (n = 31 ROIs from 3 independent experiments) . *, p=0.012, Student's T-test. **(C, D)** CAV1 (green) and EHD-2 (red) colocalize to similar extents in control and patient fibroblasts (n = 21 ROIs from 2 independent experiments.) n.s., not significant (Student's T-test) **(E, F)** CAV1α (red) and PACSIN2 (green) exhibit low levels of colocalization in both in control (n=40) and patient (n=31) fibroblasts (n = 40 or 31 ROIs from 3 independent experiments.) n.s., not significant (Student's T-test). Scale bars, 10 mm.

To further test whether CAV1 is localized normally in patient cells, we performed immuno-staining with a C-terminally directed antibody. Typically, the C-terminus of CAV1 is only accessible in the Golgi complex where the protein is not fully oligomerized,

and is masked within caveolae [7, 194]. In agreement with this, we found that this antibody labeling was predominantly restricted to the GM130-labeled Golgi complex in control fibroblasts (Figure 15A, top panel). Strikingly, in patient cells, in addition to Golgi labeling a significant amount of labeling of extra-Golgi puncta was also observed, leading to a drop in the overall level of colocalization of C-terminal CAV1 labeling with GM130 (Figure 15A, bottom panel and 15B). The staining pattern observed with the C-terminal antibody in patient cells highly colocalized with an N-terminally directed antibody that normally detects CAV1 at the plasma membrane, suggesting that the non-Golgi puncta labeled by this antibody in patient cells are caveolae (Figure 15C, D). Since the C-terminal antibody only detects wild type CAV1 and not the F160X mutant (Supplementary Figure 2A-D), these findings imply that in patient cells the C-terminus of wild type CAV1 is accessible at the cell surface, possibly within hybrid caveolae composed of both F160X (which lacks the C-terminal domain) and wild type CAV1.

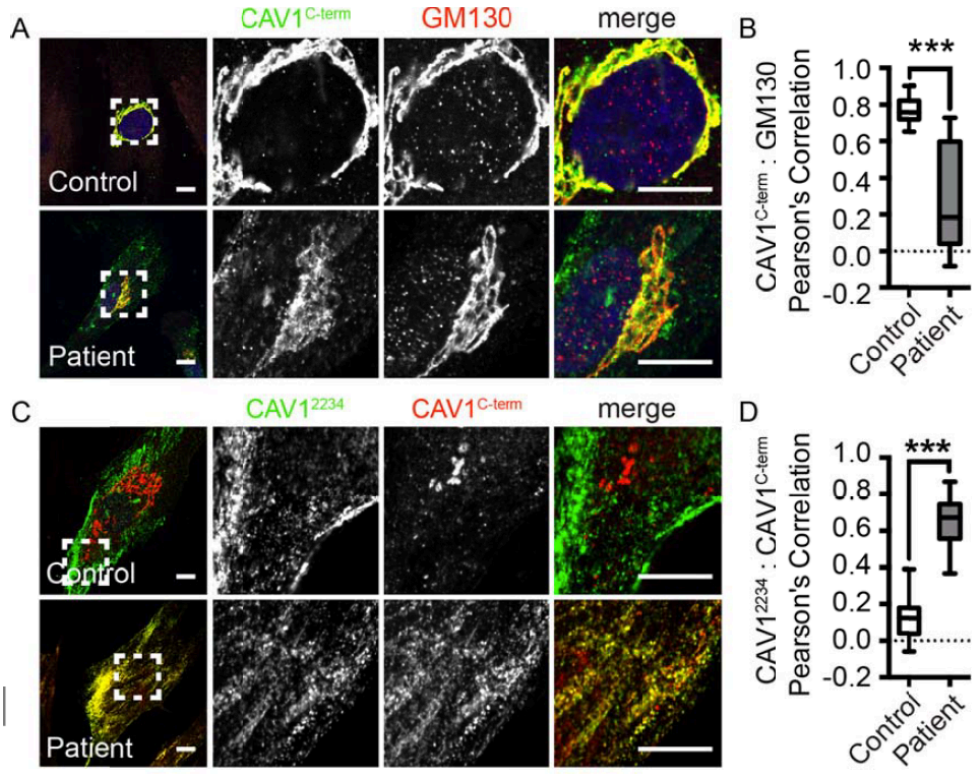

Figure 15. The C-terminus of CAV1 is Exposed Outside of the Golgi Complex in Patient Fibroblasts. (A, B) In control fibroblasts, a $CAV1^{Cterm}$ antibody (green) predominantly stains wild type CAV1 in the Golgi complex (red), whereas in patient cells $CAV1^{Cterm}$ antibody labeling is also observed in punctate structures outside of the Golgi complex. Quantification of colocalization is shown for n = 19 or 20 ROIs from 2 independent experiments. ***, $p < 0.0001$, Student's T-test. **(C, D)** In patient cells, punctate staining by the $CAV1^{Cterm}$ antibody (red) colocalizes with staining by an N-terminally directed $CAV1\alpha/\beta^{Cterm}$ antibody (green). In contrast, no colocalization of the staining patterns by these two CAV1 antibodies is observed in control cells. Quantification of colocalization is shown for n=14 or 15 ROIs from 2 independent experiments. Scale bars, 10 mm.

To further assess possible differences in the organization of CAV1 oligomers in patient cells, we probed Western blots from the BN-PAGE experiments with antibodies against two different regions of CAV1, the oligomerization domain (mAb 2297) and the C-terminus (C-term). Both the F160X mutant and Wt CAV1 contain the complete N-terminus and oligomerization domain, and thus theoretically mAb 2297 will be able to detect total CAV1. In contrast, the C-term antibody only detects Wt CAV1. Despite this, in patient cells mAb 2297 did not detect the complexes as efficiently as did the C-terminal antibody (compare ratio of red and green signals in the merged images of panels left versus middle and right) (Supplementary Figure 1). These findings imply that the organization of CAV1 may differ somewhat in these oligomeric complexes in the

patient cells in a manner that alters accessibility of the oligomerization domain to antibody labeling.

3.2.5 F160X Forms Putative Caveolae Independently or in Combination with Wild Type CAV1

To directly test whether wild type and CAV1-F160X are capable of co-assembling to form caveolae, we carried out reconstitution studies in *Cav1*$^{-/-}$ MEFs. Re-expression of wild type CAV1 into this cell line supports caveolae formation [75, 232]. The presence of caveolae at the cellular level can be assayed by monitoring colocalization of endogenous cavin-1 with exogenous CAV1 in punctae. This is because cavin-1 is only recruited newly formed caveolae and otherwise does not associate with the plasma membrane in the absence of CAV1 [75]. It has further been shown that cavin-1 only associates with membranes of invaginated caveolae and not with flattened CAV1 membrane domains using FRET and electron microscopy [75]. We therefore used cavin-1/CAV1 colocalization as a reporter of caveolae formation [3, 7, 31, 233, 234].

We first tested whether CAV1-F160X is capable of recruiting cavin-1 in the absence of wild type CAV1. Consistent with this possibility, when we expressed epitope tagged CAV1-F160X in these cells, we observed the formation of punctate structures that co-stained for endogenous cavin-1, similar to the behavior of wild type CAV1 (Figure 16A-C). Thus, CAV1-F160X itself has the propensity to form putative caveolae. We did note however that CAV1-F160X did not co-localize as strongly with cavin-1 as did Wt CAV1 despite similar expression levels of endogenous cavin-1 protein (Figure 16D, E).

Previous studies have shown that FRET can be observed between CAV1 and cavin-1 in caveolae [31, 75]. Thus, to further test for possible defects in the recruitment of cavin1 to CAV1-F160X, we attempted to set up a confocal FRET experiment between mEmerald-tagged CAV1 constructs and mCherry-tagged cavin1. Because the F160X mutation impacts the C-terminus of CAV1, we utilized N-terminally tagged CAV1 constructs for these studies. In control studies, we first verified that the mEmerald-CAV1 construct was not trapped in the perinuclear region of *Cav1*$^{-/-}$ MEFs, unlike some

other tagged CAV1 constructs are when overexpressed in this cell type [235]. Next, we co-expressed either mEmerald-CAV1 or mEmerald-CAV1-F160X with mCherry-cavin-1. As expected, mEmerald-CAV1 and mCherry-cavin-1 strongly colocalized in cell surface puncta (Figure 16F). mEmerald-CAV1-F160X was poorly expressed, but in cells where it was present it was found in punctate structures. However, these structures had a different appearance than those observed in cells expressing Wt mEmerald-CAV1 (Figure 16G). Moreover, they were essentially devoid of either mCherry-cavin-1 or endogenous cavin-1 staining (Figure 16G, H; Supplementary Figure 3). Thus, an even more profound defect in cavin-1 recruitment was observed for mEmerald-CAV1-F160X than for epitope tagged CAV1-F160X. Given these dramatic findings, we did not pursue FRET experiments further.

Since CAV1-F160X is co-expressed with wild type CAV1 in heterozygous patient cells, we also performed co-expression studies in *Cav1*$^{-/-}$ MEFs. As expected, co-expressed versions of HA- and myc-tagged wild type CAV1 strongly colocalized with each other (Figure 16I, K) and with cavin-1 (Figure 16I, L). When co-expressed, myc-CAV1 Wt and HA-CAV1-F160X also co-localized both with each other (Figure 16J, K), with endogenous cavin-1 (Figure 16J, L), and with the C-terminal CAV1 antibody (Supplementary Figure 2E-G). This finding supports a model in which wild type CAV1 and CAV1-F160X co-assemble to form hybrid caveolae. However, CAV1-F160X colocalized with endogenous cavin-1 to a lesser extent than did wild type CAV1 (Figure 16L). This again suggests that cavin-1 may not be recruited as strongly to the plasma membrane when CAV1-F160X is present, similar to the results obtained in patient cells (Figure 14B).

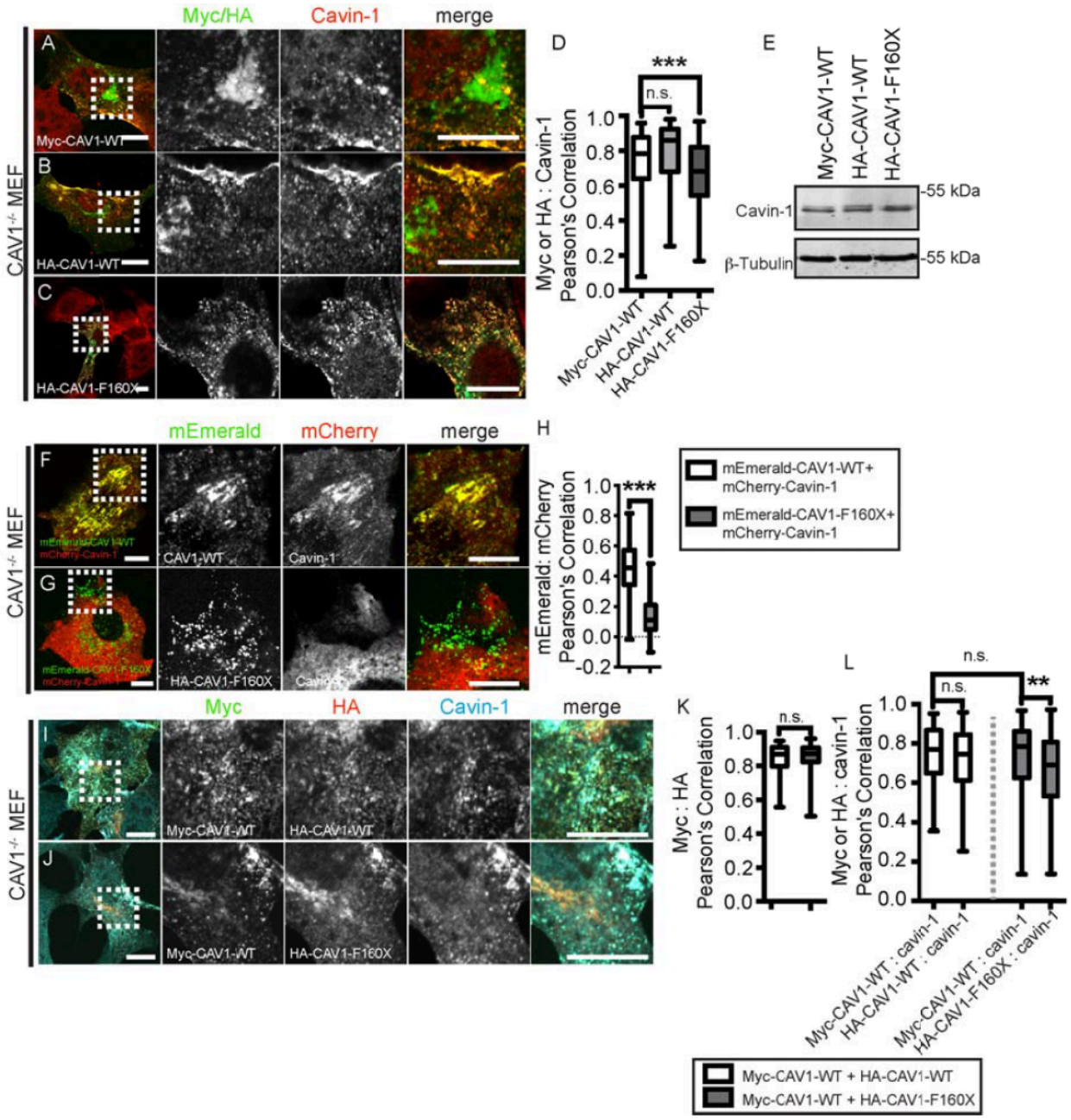

Figure 16. Reconstitution of Caveolae Formation by CAV1-F160X in *Cav1*$^{-/-}$ MEFs. (A-C) Representative images showing colocalization of endogenous cavin-1 (red) with **(A)** wild type Myc-CAV1 (green), **(B)** wild type HA-CAV1 (green), or **(C)** HA-CAV1-F160X (green) in transfected *Cav1*$^{-/-}$ MEFs. Anti-Myc or anti-HA antibodies were used to label CAV1 constructs. **(D)** Quantification of colocalization shows that HA-CAV1-F160X (n=163 ROIs) colocalizes less well with endogenous cavin-1 than does wild type HA-CAV1 (n = 25 ROIs) or Myc-CAV1 (n = 157 ROIs). These results represent data acquired from 3 independent experiments. ***, $p<0.001$, Student T test. **(E)** Western blot of transfected *Cav1*$^{-/-}$ MEFs probed with antibodies to detect endogenous cavin-1 and β-tubulin as a control for equal loading. **(F-G)** Representative live cell images showing colocalization of mCherry-cavin-1 (red) with **(F)** wild type mEmerald-CAV1 (green) or **(G)** mEmerald-F160X (green) in transfected *Cav1*$^{-/-}$ MEFs. Note that mCherry-cavin-1 staining is weak in some regions where mEmerald-F160X spots are visible in this image due to the thinness of the cell at this location. **(H)** Wild type mEmerald-CAV1 strongly colocalizes with mCherry-cavin-1 in *Cav1*$^{-/-}$ MEFs. In contrast, mEmerald-F160X displayed much less colocalization with

Figure 16 Continued. mCherry-cavin-1 (n = 51-81 ROIs from 3 independent experiments) (***, p<0.0001, Student's T-test). Scale bars, 10 mm. (I) Co-transfected Myc-CAV1 (green) and HA-CAV1 (red) colocalize with each other and with endogenous cavin-1 (cyan) in triple labeled *Cav1*$^{-/-}$ MEFs. **(J)** Co-transfected Myc-CAV1 (green) and HA-CAV1-F160X (red) colocalize with each other and with endogenous cavin-1 (cyan) in *Cav1*$^{-/-}$ MEFs. **(K)** Wild type HA-CAV1 and HA-CAV1-F160X both strongly colocalize with wild type Myc-CAV1 in *Cav1*$^{-/-}$ MEFs (n = 114-118 ROIs from 3 independent experiments) (n.s., not significant, Student's T-test). **(L)** In *Cav1*$^{-/-}$ MEFs co-expressing wild type and mutant CAV1, endogenous cavin-1 colocalizes less well with HA-CAV1-F160X than with Myc-CAV1 (**, p=0.0013, Student's T-test). In contrast, endogenous cavin-1 colocalizes equally well with wild type Myc-CAV1 and HA-CAV1 in co-expressing cells (n.s., Student's T-test). Scale bars, 10 mm. (Bing Han, Ph.D.)

Next, we asked whether CAV1-F160X associates with DRMs in reconstituted cells. DRM analysis of *Cav1*$^{-/-}$ MEFs extracted with 0.5% Triton X-100 confirmed the association of CAV1-F160X with DRMs both when expressed individually and when co-expressed with wild type CAV1 (Figure 17). This is consistent with the results obtained in human skin fibroblasts extracted in 0.5% Triton X-100, where CAV1 associated with DRMs in both the mutant and control cell lines (Figure 12D). However, the DRM fractionations for the *Cav1*$^{-/-}$ MEFs were much more sensitive to the number of cells used. This made it difficult to identify detergent extraction conditions that could detect differences in the detergent resistance of wild type and F160X CAV1 in the reconstituted MEFs. We also found that most of the endogenous CAV2 in the *Cav1*$^{-/-}$ MEFs could not be recruited to DRMs when CAV1 was expressed, even for the case of wild type CAV1 (Figure 17). This is probably because CAV2 is trapped in Golgi complex when CAV1 is not expressed [53], and thus is unavailable to form complexes with newly synthesized exogenous CAV1.

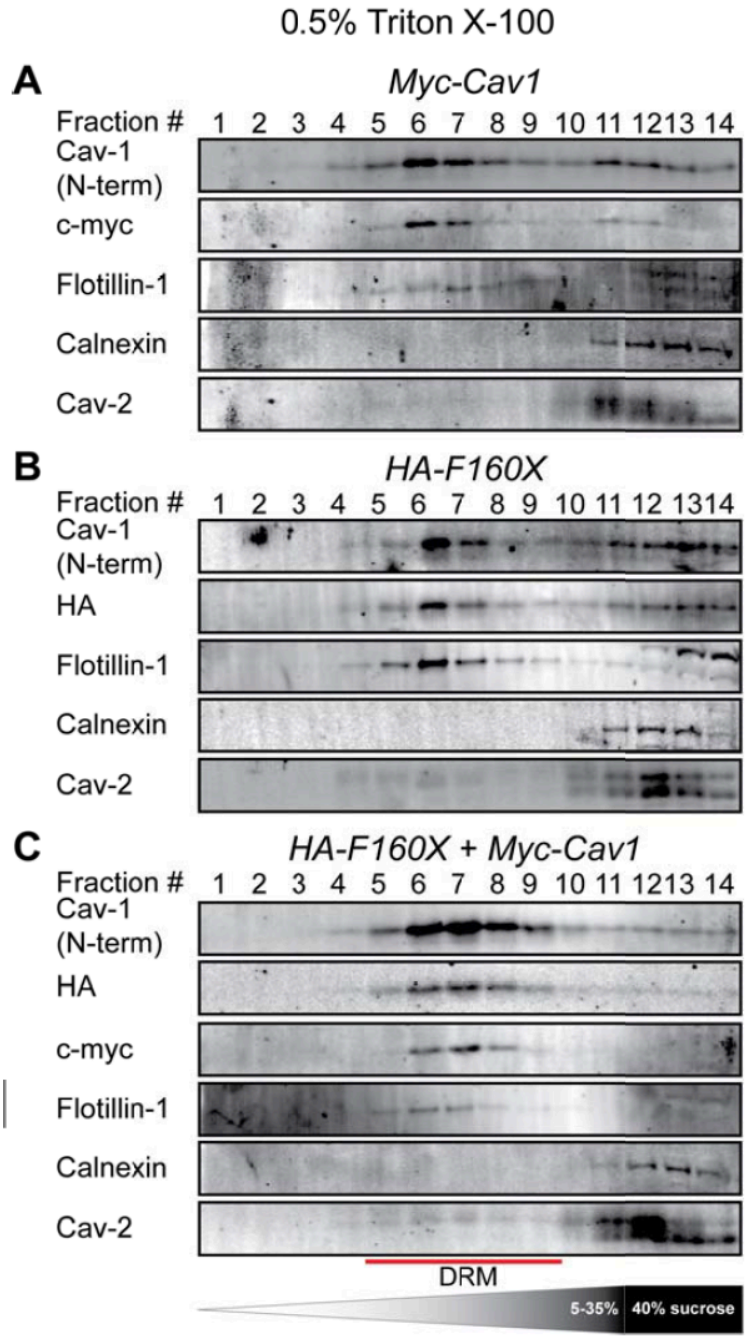

Figure 17. CAV1-F160X Co-Fractionates with Detergent-Resistant Membranes. DRMs isolated using 0.5% Triton X-100 in reconstituted *Cav1*$^{-/-}$ MEFs. DRMs were isolated from *Cav1*$^{-/-}$ MEFs transiently transfected with **(A)** Myc-CAV1, **(B)** HA-CAV1-F160X or **(C)** Myc-CAV1 and HA-CAV1-F160X. Fractions were analyzed by SDS-PAGE/Western blotting. Fractions enriched in DRMs are indicated with the red lines. Data are representative of 2 independent experiments. (Bing Han, Ph.D.)

3.2.6 Reconstituted F160X/CAV1 Complexes Display Decreased Stability

Since the CAV1 complexes in patient cell displayed defects in the stability of 8S and 70S complexes (Figure 12B, C), we conducted corresponding tests on reconstituted cells. We found that CAV1-F160X itself can form both 8S and 70S complexes in *Cav1*$^{-/-}$ MEFs (Figure 18B). However, compared to Wt CAV1, more CAV1-F160X was found in lower molecular weight complexes (Figure 18A, B). This defect was rescued by co-expressing CAV1-F160X with Wt CAV1 (Figure 18C). We also tested the stability of the complexes by dissolving the 70S complexes with SDS-containing lysis buffer (0.2% Triton X-100 + 0.4% SDS) following the approach of Hayer et al [8] (Figure 18D, E, F). Whereas wild type CAV1 accumulated in the form of 8S complexes under these conditions (Figure 18D), CAV1-F160X was dissolved to structures smaller than 8S (Figure 18E). Interestingly, the F160X/CAV1 co-expressing cells displayed an intermediate phenotype (Figure 18F). These findings are in good agreement with the findings in patient cells and suggest that the far end of the CAV1 C-terminus is very important for the stability of CAV1 complexes.

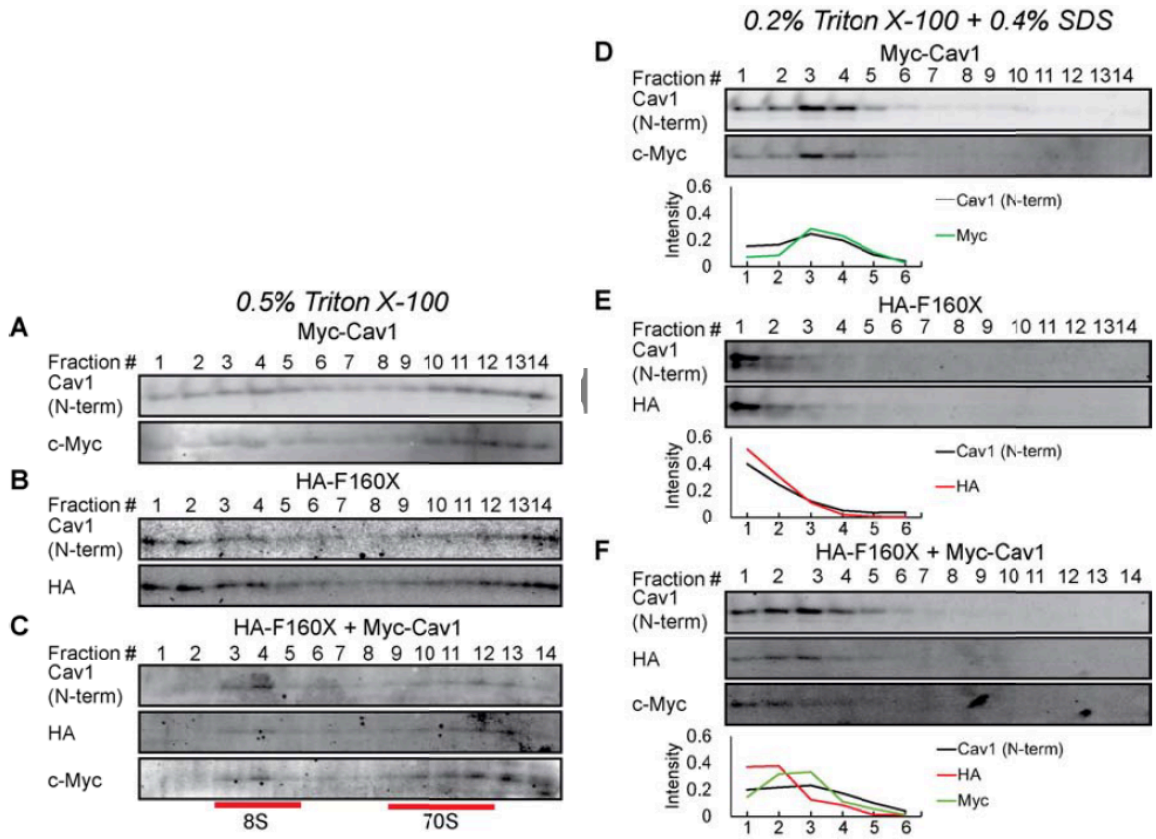

Figure 18. Reduced Stability of CAV1 Complexes Containing CAV1-F160X in Reconstituted *Cav1*$^{-/-}$ MEFs. *Cav1*$^{-/-}$ MEFs expressing **(A, D)** Myc-CAV1, **(B, E)** HA-CAV1-F160X, or **(C, F)** HA-CAV1-F160X and Myc-CAV1 were lysed in either 0.5% Triton X-100 **(A-C)** or 0.2% Triton X-100 and 0.4% SDS **(D-F)** at room temperature. Extracts were run though 10-40% sucrose velocity gradients and fractions were analyzed by SDS-PAGE followed by Western blotting. In **(D-F)**, the proportion of CAV1 in each fraction was quantified by densitometry, and the values for the first 6 fractions are show in line charts below each corresponding Western blot dataset. Data are representative of 2 independent experiments. (Bing Han, Ph.D.)

3.2.7 Caveolae Confer Mechano-Protection Against Hypo-Osmotic Shock in Patient Cells.

Caveolae are now widely recognized for their role as membrane buffers during times when cells are under mechanical stress and cells lacking caveolae are more vulnerable to injury under high mechanical tension [3, 233, 234]. Although the abundance of caveolae was normal in patient cells (Figure 13), we wanted to determine if the presence of CAV1-F160X impacted the ability of caveolae to function as mechanical buffers in patient cells. To address this question, cells were incubated in hypotonic medium to induce osmotic swelling and recapitulate mechanical stress (Figure 19).

Cell viability was determined to assess the ability of cells to survive osmotic swelling. Before treatment, the vast majority of cells was viable and had a normal cellular morphology (Figure 19A). Following ten minutes of osmotic swelling, the number of live cells decreased; however, loss of viability was similar in patient and control cells (Figure 19B). These results indicate that presence of the mutant CAV1 does not compromise the ability of caveolae to function in mechano-protection, at least under the conditions of these experiments.

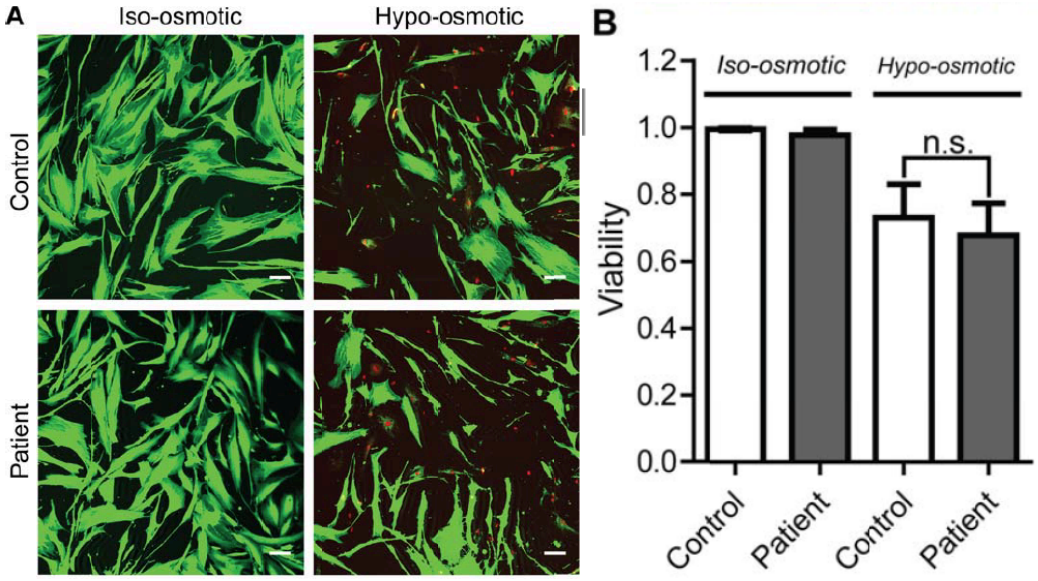

Figure 19. Caveolae Confer Mechano-Protection in Patient Fibroblasts. (A) Representative images of control and patient human skin fibroblasts before and after ten minutes of hypo-osmotic shock. The images were deliberately saturated to enable quantification of the numbers of live (green) and dead (red) cells. Bar, 10 μm. **(B)** Quantification of cell viability. Bars show the mean ± standard deviation from 3 independent experiments. There is no significant difference between the control and patient cell line in either iso-osmotic (p=0.16) or hypo-osmotic (p=0.55) conditions. (Bing Han, Ph.D.)

3.3 Discussion

In the current study, we identified and characterized a F160X mutation in CAV1 in a patient with both PAH and CGL. The F160X CAV1 mutation is predicted to give rise to a truncated protein missing nearly 20 amino acids of the C-terminus. Although recent studies have independently identified this mutation in this patient [15, 16], the effects of the expression of this mutant protein on caveolae formation and function are not yet

fully understood. Using a combination of biochemical approaches, immunofluorescence microscopy, and electron microscopy, we show here that the fundamental building blocks of caveolae are in place and are capable of forming hybrid caveolae in patient skin fibroblasts.

To complement our studies in patient cells, we also assayed the ability of CAV1-F160X to form caveolae in reconstituted *Cav1*$^{-/-}$ MEFs by testing whether it can recruit cavin1 to cell surface puncta. The results of these studies suggest that the mutant protein can drive caveolae formation both on its own and when co-expressed with wild type CAV1, further supporting our findings in the patient cells (summarized in Figure 20A).

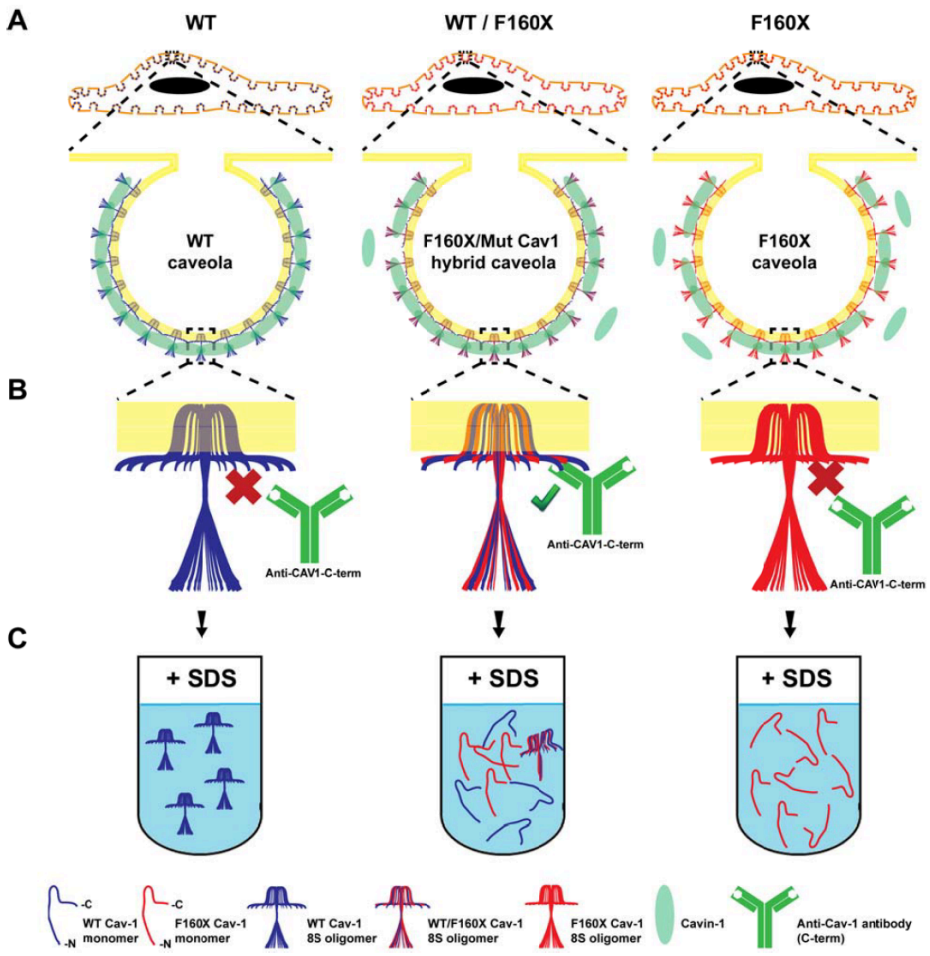

Figure 20. Working Model Depicting Proposed Impact of CAV1-F160X on Caveolae Assembly and Stability. (A) Like wild type CAV1, CAV1-F160X is capable of supporting caveolae formation when expressed on its own. In heterozygous patient cells, CAV1-F160X forms hybrid caveolae with wild type CAV1. **(B)** The C-terminus of wild type CAV1 is normally masked in caveolae due to interactions of adjacent C-termini of CAV1 with one another. However, the absence of the C-terminus of CAV1-F160X exposes the C-terminus of wild type CAV1, making it accessible to detection by antibodies. **(C)** CAV1-F160X can form both 8S and 70S complexes, but these complexes are destabilized compared to those formed by wild type CAV1. (Bing Han, Ph.D.)

The observation that CAV1-F160X itself can form putative caveolae is in line with a recent report showing that a C-terminal truncation mutant of CAV1 (Cav1, aa. 1-147) is capable of generating heterologous caveolae in a model prokaryotic expression system [233]. A potential caveat of using co-localization of CAV1 and cavin-1 as a readout of caveolae formation is that this method does not provide information regarding the morphology of caveolae. Thus, further work will be required to determine whether the putative caveolae formed by heterologous expression of F160X exhibit any morphological defects.

Despite the presence of caveolae in patient fibroblasts, several of their features were altered relative to those found in control cells. First, the degree of co-localization of cavin1 and CAV1 was reduced in both patient cells and reconstituted *Cav1*$^{-/-}$ MEFs (Figure 20A). This phenotype was especially dramatic in *Cav1*$^{-/-}$ MEFs co-expressing mEmerald CAV1-F160X and mCherry-cavin-1; under these conditions, essentially no colocalization of cavin-1 with CAV1-positive puncta was observed. Although cavin-1 is known to be an important CAV1 accessory protein that is essential for caveolae formation, the exact mechanisms by which CAV1 and cavin-1 interact are still unknown [86]. Our current findings suggest that the far end of the CAV1 C-terminus participates in this interaction. We also found that the C-terminus epitope of CAV1, which is normally masked after exiting the Golgi complex [194], was readily accessible in punctate structures at the cell surface. We speculate that the absence of C-terminus of the mutant protein may allow for recognition of the C-terminus of wild type CAV1 within caveolae, which would normally be masked due to interactions with other C-termini (Figure 20B). The formation and/or stability of 70S complexes also appeared to be reduced in patient cells, as evidenced by the increased fraction of 8S complexes. This may reflect a requirement for the C-terminus in homotypic interactions of CAV1 within 70S complexes [111]. We further found that the 8S complexes formed by CAV1-F160X in both re-constituted *Cav1*$^{-/-}$ MEFs and patient cells were readily disassembled into smaller oligomers in the presence of SDS (Figure 20C). This suggests that the C-terminus of CAV1 is not only important for interactions between adjacent homo-oligomers of CAV1, but also important for the stability of the 8S CAV1 homo-oligomer itself. Finally, CAV1 was also less detergent resistant in patient cells than in control cells. Although the cause of this shift in detergent resistance is currently unknown, similar results were reported in studies of C-terminal deletion mutants of CAV1 [111]. It is possible that this is a consequence of changes in the lipid or protein composition of caveolae, or even the plasma membrane itself. Further work will be required to test these possibilities.

Caveolae are thought to function as a cellular buffering system to provide protection from stresses that perturb membrane tension in vitro [3, 233, 234]. This idea was

recently tested in vivo in endothelial cells of the lung and cardiac muscle in mice under treatments to increase cardiac output and shear stress, conditions often associated with PAH and cardiovascular diseases [233]. Here, we tested this hypothesis directly in skin fibroblasts from a patient with PAH and CGL. We found that patient cells showed similar responses to controls under conditions that induced acute mechanical stress on the plasma membrane via a hypo-osmotic shock (Figure 19). Thus, incorporation of CAV1-F160X into the patient's caveolae does not significantly disrupt the functional capacity of caveolae as membrane buffers. However, it remains formally possible that defects in mechano-protection may be more apparent under other conditions or in other cell types. Whether the expression of F160X impacts other caveolae functions will require further examination in future work.

While these studies were in progress, two other groups identified a F160X mutation in CAV1 in a patient presenting with both PAH and CGL [14, 15]. Through informed consent, the family of this patient confirmed that the same patient was studied in all three investigations. It is thus interesting to directly compare the results of each study. In the first study [15], close to wild type numbers of caveolae were observed in patient skin fibroblasts by electron microscopy. However, immunofluorescence staining using an N-terminally directed antibody revealed substantially decreased CAV1 labeling in patient fibroblasts, leading the authors to conclude that the caveolae may being formed in a CAV1-independent manner [15]. In the second study [14], CAV1 protein levels were analyzed by Western blotting and shown to be less than 50% of control values. Immunofluorescence analysis of patient skin fibroblasts using an antibody directed against an internal epitope of CAV1 (residues 34-45) detected CAV1 in puncta. Thus, all three studies reported differential staining of CAV1 in control and patient cells by immunofluorescence, using different combinations of antibodies and labeling conditions. Because the epitope accessibility on CAV1 is known to be heavily dependent on the protein conformation and oligomerization state [194, 234, 235], this strongly suggests that one or more of these factors are altered in patient cells. Furthermore, the decreased colocalization of cavin-1 and CAV1 in patient cells observed both in our study and in a previous report [14] suggests the affinity of cavin-1 for caveolae is

decreased in cells expressing the F160X CAV1 mutant, a result we went on to confirm in reconstituted *Cav1*$^{-/-}$ MEFs. Thus, several key findings have been reproduced across laboratories. Importantly however, in our current study, we have now greatly extended our knowledge about this mutation through our detailed biochemical analysis, reconstitution studies, and functional studies.

It is striking that the F160X mutation is linked to both lipodystrophy and PAH while other CAV1 mutations appear to only correlate with the development of either PAH [16] or lipodystrophy [12, 222]. Why this is the case is not yet entirely clear. It has been shown that reduced caveolae formation disrupts endothelial cell and adipose tissue function. On the basis of our biochemical findings, we speculate that CAV1-F160X may contribute to both diseases by several potential mechanisms. First, changes in the stability of CAV1 oligomers and/or changes in CAV1 organization within caveolae could potentially lead to cellular defects in endothelial cells and adipocytes that promote PAH and CGL. Such changes might impact the ability of caveolae to function as membrane reservoirs, a mechanism that appears to be important in endothelial cells as well as other cell types [3, 31, 187, 202]. Although we did not observed significant defects in mechano-protection in patient skin fibroblasts, they may occur in other cell types or in under more physiological challenges. Changes in the stability of CAV1 oligomers or the organization of CAV1 within caveolae could also potentially alter caveolae dynamics linked to fluctuations in lipid storage in adipocytes [205]. Animal models displaying lipodystrophic- and PAH-like disorders have also been shown to be the result of significantly decreased levels of CAV1 expression [11, 131, 140, 236]. It is thus also possible that changes in CAV1 expression in adipocytes, endothelial cells, smooth muscle cells, or other tissues not examined here may contribute to the development of lipodystrophy and PAH in this patient.

Another interesting possibility that arises from our findings is that the diminished association of cavin-1 with CAV1 in patient cells is related to the development of CGL and/or PAH. *CAVIN1* has been repeatedly identified as a CGL associated gene [97, 217-219] [98, 220, 221] and has recently been shown to function in the control of

ribosomal RNA transcription in adipocytes [237]. Cavin-1 is also involved in the mechanical stress response of caveolae [3]. This suggests that a common CAV1-Cavin1-dependent pathway, perhaps one regulated by the regulated assembly and disassembly of caveolae, may be disrupted in patients with CGL. Additional predisposing mutations may also contribute to the pathophysiology of one or both diseases. For example, mutations in *AGPAT2* and *LPIN1* were hypothesized to contribute to the development of CGL in a patient with an F160X mutation [14]. Whether these variants are truly pathogenic or contributory remains to be determined.

In conclusion, our work adds to the breadth of knowledge of known human phenotypes associated with CAV1 mutations and suggests that the development of lipodystrophy and PAH in the context of a F160X mutation is not the result of the loss of production of CAV1 and caveolae per se but instead may be linked to decreased stability of CAV1 oligomers and/or weakened interactions between cavin-1 and CAV1 in caveolae. Future investigation is needed to understand the varied presentation of disease and differential impact on multiple organ systems of in patients with CAV1 mutations.

CHAPTER 4

INVESTIGATION OF A NOVEL PAH-ASSOCIATED DOMINANT NEGATIVE CAV1 MUTANT

4.1 Introduction

Caveolae are specialized plasma membrane domains rich in cholesterol [25, 187, 238]. Found at the plasma membrane of many cell types, these 50-100 nm invaginations are especially highly abundant in adipocytes, smooth muscle and endothelial cells [216]. Caveolae have numerous cellular functions including buffering cells from mechanical stress, maintaining membrane integrity and regulating clathrin-independent endocytosis [25, 187]. They also are thought to control a variety of signal transduction pathways, by mechanisms that are still somewhat unclear [187, 239].

The primary structural components of caveolae are a family of proteins known as caveolins. Caveolin 1, 2, and 3 are integral membrane proteins whose cytoplasmically oriented N- and C-termini are connected by a predicted hairpin [7]. Caveolin-1 (CAV1) is a 178 amino acid protein that was the first protein identified as a component of caveolae [238] and that also is required for caveolae formation [11, 66, 232]. Caveolae biogenesis begins in the endoplasmic reticulum through a step-wise series of oligomerization events of caveolin monomers [8, 240, 241]. Newly synthesized caveolin becomes incorporated into complexes composed of 14-16 CAV1 monomers [240] that correspond to an 8S complex [8] (Figures 1 and 5). This first oligomerization event occurs in the ER and the oligomers are quickly transported to the Golgi complex for further maturation. In the Golgi compartment, 8S complexes undergo another round of oligomerization to form 70S scaffolds of CAV1 oligomers that become enriched in cholesterol and lipids before being trafficked to the plasma membrane [8]. Proper caveolae assembly also requires the presence of several accessory proteins, including the Cavins, PACSIN2, and EHD-2 [75-77, 79, 85, 86, 92, 224, 242].

The 178 amino acid CAV1 protein consists of an N-terminal domain, scaffolding domain, intramembrane domain, and C-terminal domain [7, 45]. The functions of the various domains of CAV1 have been extensively studied via truncation and mutagenesis experiments [48, 243]. For example, the C-terminus of CAV1 (residues 135-178) is important for membrane attachment, exit from the Golgi complex and homotypic interactions between caveolin complexes to form 70S scaffolds [8, 109, 243]. The C-terminus is also palmitoylated, which allows the protein to interact more strongly with membranes (Figure 1), and is important for interactions with other lipid-modified proteins such as the tyrosine kinase Src [244]. This portion of CAV1 is also speculated to be important for proper trafficking of the protein, because C-terminal truncations and other mutant forms of CAV1 often accumulate in the Golgi compartment or aggresomes when ectopically expressed [170, 245].

The functions of both CAV1 and caveolae have been extensively studied using knockout mice, and work in this animal model has highlighted an importance for CAV1 in modulating proliferation, adipose and vascular homeostasis, and metabolism [11, 212-215]. CAV1 and caveolae have been linked to a number of diseases such as lung injury/disease, myopathies, lipodystrophy, cardiovascular disease, and cancer [246, 247]. Known disease-associated mutations of CAV1 include P132L [246] and others [248]. In addition to these disease-associated mutants, mutations that generate poorly folded CAV1 proteins have been shown to cause the protein to be retained intracellularly, and to have dominant-negative effects on wild-type CAV1 [170, 172, 249]. However, the mechanisms by which defects in CAV1 or caveolae give rise to disease are still poorly understood.

One of the many diseases in which CAV1 is implicated is pulmonary arterial hypertension (PAH) [14-16, 126, 250-255]. Pulmonary arterial hypertension (PAH) is a fatal disease arising from progressive right ventricular failure that is induced by progressive increase in pulmonary vascular resistance [256]. Most cases of familial PAH with a known etiology involve mutations in BMPR2 [251], although the details of the molecular and cellular pathogenesis of the disease remain unclear. However, many

of the signaling pathways disrupted in PAH are regulated by caveolin [250, 252], and decreases in the expression of CAV1 and number of caveolae have been reported in endothelial cells in clinical and experimental cases of PAH [126, 236, 251, 253, 257].

Interestingly, recent genetic analysis of PAH patients with both familial and idiopathic forms of PAH has identified novel heterozygous frameshift mutations in CAV1 (CAV1_P158fsX22, and CAV1_H158fsX22, respectively) [16]. Patients are heterozygous for the mutant CAV1 genes. Both frameshift mutations are predicted to generate a mutant form of CAV1 that is one amino acid longer than the wild-type protein and contains a novel C-terminus (residues 159-179) (Figure 9). Remarkably, the predicted protein sequences of the familial and idiopathic mutations are nearly identical with the exception of the first affected residue of the mutant portion of the protein [16]. Immunostaining of tissue sections obtained from a lung biopsy of one of the patients revealed substantially decreased CAV1 levels in endothelial cells compared to healthy controls [16]. Total CAV1 protein levels were also decreased to less than 50% of control levels in skin fibroblasts isolated from patients carrying one wild-type copy of CAV1 and one copy of CAV1_P158fsX22 (here referred to as CAV1-P158) compared to control fibroblasts isolated from healthy subjects expressing only wild-type CAV1 [16]. Very recently, additional mutations of the C-terminus of CAV1 have been linked to PAH, further implicating a critical role for both CAV1 and caveolae in this disease [13-15]. However, how the expression of mutant forms of CAV1 impacts the assembly and function of caveolae and ultimately contributes to PAH have yet to be determined.

Here, we examined the effects of the naturally occurring familial CAV1-P158 frameshift mutation in *CAV1* on caveolae formation using a combination of cell biological and biochemical approaches in patient fibroblasts. We show that in heterozygous patient fibroblasts expressing both mutant and wild copies of the protein, CAV1 is correctly incorporated into caveolae. However, overall levels of CAV1, caveolar accessory proteins, and caveolae are reduced. As a result, patient cells exhibit corresponding defects in the function of caveolae as membrane reservoirs. These findings thus define a new mechanism by which CAV1 mutants disrupt cellular function. They also suggest

that decreased levels of CAV1, caveolae accessory proteins, and/or caveolae may contribute to the development of PAH in patients expressing the CAV1 mutants.

4.2 Results

4.2.1 The Density of Caveolae and CAV1 Protein Levels are Reduced in Patient Fibroblasts Expressing CAV1-P158

In the previous study reporting the identification of CAV1-P158, Western blotting analysis showed that CAV1 expression is reduced in patient skin fibroblasts compared to skin fibroblasts derived from healthy humans that express only wild-type CAV1 [16]. To test whether reduced CAV1 expression decreased the abundance of caveolae, we carried out electron microscopy for higher resolution analysis of morphologically identifiable caveolae in patient fibroblasts and the wild-type controls. Interestingly, characteristic flask-shaped caveolae at the plasma membrane were readily detected in patient cells, and their overall appearance was similar to those observed in control fibroblasts (Figure 21A). We quantified the numbers of caveolae by morphologically defining them as uncoated circular or flask-shaped structures with diameters between 50-80 nm found no more than 200 nm from the plasma membrane. Using these criteria, we found that there were fewer caveolae in patient cells compared to controls (Figure 21B) in agreement with the reduced levels of CAV1 in patient cells previously reported by our collaborators [16].

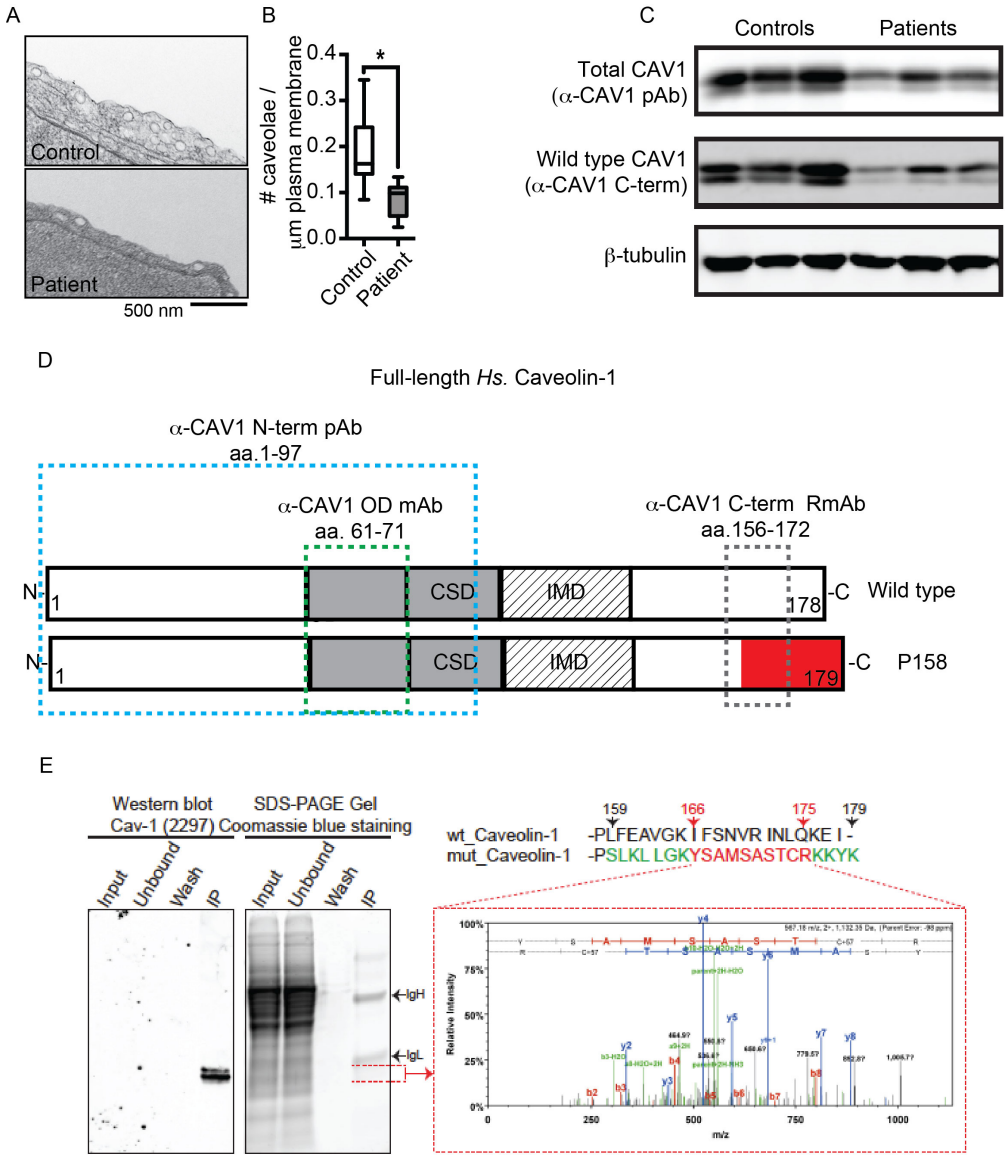

Figure 21. Caveolae and CAV1 Levels are Reduced in Patient Fibroblasts Expressing CAV1-P158. **(A)** Representative, cropped electron micrographs of control and patient skin fibroblasts. Images were acquired at 30,000x magnification. For purposes of illustration, the density of caveolae in these images is higher than the average values quantified in panel B. Scale bar, 500 nm. **(B)** Quantification of number of caveolae per micrometer membrane in patient and control fibroblasts. Caveolae were counted in 25 images each from 3 patient and 3 control cell lines in two independent experimental replicates and one experiment for 1 control and 1 patient cell line. *, $p < 0.01$, Students T-test. **(C)** Western blots of CAV1 in control and patient fibroblasts using N-term (anti-CAV1 pAb) and C-term (anti-CAV1 RmAb) specific antibodies, β-tubulin is the loading control. Data are representative of 3 independent experiments. **(D)** Schematic of full-length type and mutant CAV1 with the novel mutant C-terminus in red and epitopes recognized by N-terminal and C-terminal CAV1 antibodies. Both N-terminus antibodies (pAb aa. 1-97-blue dashed box; mAb aa.61-71-green dashed box) can recognize mutant and wild-type CAV1α/β. The C-terminal CAV1 (aa.156-172) antibody recognizes the region of wild-type CAV1α/β (grey dashed box) that is unique from the CAV1 frameshift mutant. **(E)** Tandem mass spectrometry was used to determine if CAV1-P158 was expressed in patient fibroblasts. CAV1 protein from lysates of a patient fibroblast cell line was immunoprecipitated using anti-CAV1 (aa. 1-97), separated by SDS-PAGE and coomassie stained. Immunoprecipitated CAV1 was also detected in immunoblots with anti-CAV1 α/β (aa. 61-71). The region

Figure 21 continued. of the SDS-PAGE gel that corresponded to the position of the CAV1 band in the immunoblot was excised and analyzed by mass spectrometry to determine if unique peptides of the novel C-terminus of CAV1-P158 were detectible in patient cells. **(F)** Peptides from CAV1 mutant's unique C-terminus are detected by MS/MS and are indicated in red in this spectrum. (C, E: Bing Han, Ph.D.)

To estimate the relative expression levels of mutant and wild-type CAV1 in the patient fibroblasts, we took advantage of a commercially available C-terminal antibody that is predicted to specifically only detect the wild-type form of endogenous human caveolin-1 and not the frameshift mutant due to the change in amino acid sequence of the C-terminus. In concert with initial studies showing that patient fibroblasts have decreased total protein levels of CAV1, similar findings were observed when we tested patient samples using the same N-terminal antibody predicted to detect both wild type and mutant CAV1α/β [16]. In addition, even less CAV1 was detected by the C-terminal antibody than by the N-terminal antibody in patient cells relative to controls (Figure 21C). This also suggests that the mutant CAV1 protein is expressed. Assuming that the frameshift mutant is not detected by the C-terminal antibody, we estimate that approximately 25% of the CAV1 protein present in patient cells consists of the mutant form of the protein.

Our western blot data implies that a small amount of the mutant protein is contributing to the total CAV1 protein levels. However we needed to confirm whether the CAV1-P158 protein is actually expressed. The frameshift mutation of CAV1 is predicted to generate a novel protein sequence that is not normally present in the human genome by BLAST analysis. Initial attempts to generate antibodies against this domain of the protein were unsuccessful. We thus tested for the presence of the peptide that corresponds to the region encompassing the mutant C-terminus in patient cells using mass spectrometry as an alternative approach.

For the mass spectrometry experiments, CAV1 was immunoprecipitated using an antibody directed against the N-terminal region of the protein (aa. 1-97), a region that is present in both the wild-type and mutant form of the protein (Figure 21D, E). Immunoprecipitated CAV1 was detected by Western blot with an antibody against a region within the oligomerization domain (aa. 61-71) (Figure 21D, E). The region of the

gel containing immunoprecipitated CAV1 was excised, in-gel trypsin digested and subjected to mass spectrometry analysis (Figure 21E). Three MS/MS spectra were identified that correspond to regions of the novel C-terminus of CAV1-P158 (Figure 21E and data not shown). These findings demonstrate that CAV1-P158 is expressed in the patient fibroblasts.

4.2.2 CAV1-P158 is Expressed at Reduced Levels and is Unable to Traffic to Caveolae in Cav1$^{-/-}$ MEFs

The mass spectrometry data showed that the mutant protein is detectible in heterozygous patient cells (Figure 21E). Several previously characterized caveolin mutants are expressed at low levels and have a shortened half-life [70]. Based on the previous finding of reduced total CAV1 protein levels heterozygous in patient cells [16] (Figure 21C), we wanted to determine if the mutant protein was expressed at decreased levels compared to the wild type protein. Unable to immunologically distinguish the wild type form the mutant protein in heterozygous patient cells, we carried out complimentary studies in *Cav1*$^{-/-}$ MEFs that had been transfected with plasmids encoding various CAV1 proteins. Consistent with a low amount of the mutant protein contributing to the total CAV1 protein levels observed in patient cells (approx. 25%, Figure 21), CAV1-P158 levels were also decreased when transfected into *Cav1*$^{-/-}$ MEFs compared to wild type CAV1 constructs, despite similar transfection efficiencies for each construct (Figure S.4).

We next wanted to determine if the mutant protein was properly localized. In wild type MEFs endogenous Cav1 and cavin-1 (a caveolae accessory protein) normally co-localize in puncta that are presumably caveolae [75] (Figure 22A). *Cav1*$^{-/-}$ MEFs lack endogenous caveolin-1 but still express other caveolae accessory proteins. In *Cav1*$^{-/-}$ MEFs, endogenous cavin-1 is still expressed at low levels but is abnormally diffusely distributed in the cell in the absence of Cav1 (Figure 22B) [75]. We took advantage of this *in vitro* system and generated CAV1-P158 constructs (Figure S.5A; Chapter 2.4) in order to independently assess the localization of the mutant in the absence of the wild type copy of CAV1, which we were unable to do in heterozygous patient cells. When

wild type HA-CAV1 is transfected into *Cav1*$^{-/-}$ MEFs, endogenous cavin-1 redistributes into a punctate pattern and colocalizes with exogenous CAV1 (Figure 22C, D; Figure S.5B, C) similarly to the labeling observed in Figure 22A. HA-CAV1-P158 did not colocalize with cavin-1 and was observed in vesicles and in a reticular distribution (Figure 22E, E', F). When we quantified the colocalization between either of the CAV1 constructs and cavin-1, significantly less CAV1-P158 colocalized with cavin-1, compared to wild type CAV1, suggesting that few or no caveolae formed upon expression of CAV1-P158 (Figure 22F). The inability of CAV1-P158 to form caveolae was further substantiated when caveolae were assessed biochemically by detergent-resistant membrane (DRM) fractionation. While wild type CAV1 was readily detectible in DRMS, little or no CAV1-P158 was observed in DRM fractions (Figure 22G). Based on these findings, we concluded that CAV1-P158 was expressed at low levels and is not able to traffic to the plasma membrane and form caveolae. We carried out the next set of experiments to determine the cause of the trafficking defect in CAV1-P158.

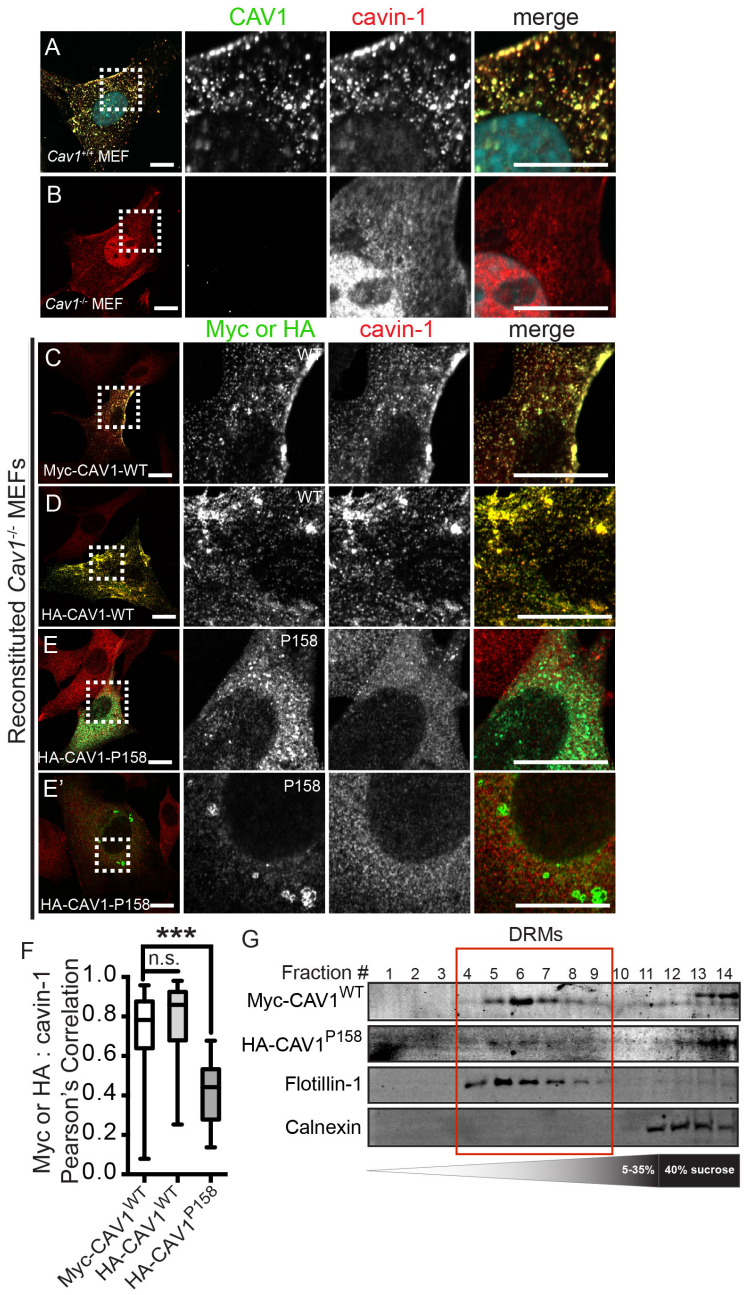

Figure 22. Reconstitution of Wild Type CAV1 Supports Caveolae Formation in *Cav1*$^{-/-}$ MEFs but CAV1-P158 is Unable to form Caveolae. (A) In positive control *Cav1*$^{+/+}$ MEFs, Cav1 (green) colocalizes with cavin-1 (red) in puncta that correspond to caveolae. **(B)** In the absence of Cav1 (green), cavin-1 (red) is diffuse and not recruited to caveolae in *Cav1*$^{-/-}$ MEFs. **(C, D)** Normal distribution of cavin-1/CAV1 and colocalization with **(C)** wild type Myc-CAV1, or **(D)** wild type HA-CAV1. **(E, E')** Two representative images depicting the abnormal distribution observed for CAV1-P158 and the diffuse distribution of cavin-1 immunofluorescence in *Cav1*$^{-/-}$ MEFs. **(F)** Quantification of CAV1/cavin-1 colocalization. p-values were calculated with a two-tailed student's T-test (***, p<0.0001). Data sets were represented in the graphed box-and-whisker plots. Scale bars represent 10μm. **(G)** DRMs isolated from transfected *Cav1*$^{-/-}$ MEFs contain higher amounts of wild type Myc-CAV1 (top panel) compared to DRMs isolated from HA-CAV1-P158 expressing *Cav1*$^{-/-}$ MEFs (panel 2). Fractions rich in the non-caveolae raft protein Flotillin-1 (panel 3) are enriched in DRMs, and non-DRMs correspond to fractions containing the non-raft protein, Calnexin (bottom panel). (G, Bing Han, Ph.D.)

4.2.3 Identification of a de novo ER-Retrieval Signal in the C-terminus of CAV1-P158

C-terminal dilysine motifs (KKXX; KXKXX) ranging form the distal -3 to -5 positions function as sorting signals for the ER-retrieval to maintain the localization of membrane proteins that reside in the ER [258, 259]. Previously published mutational analyses showed that the addition of a C-terminal di-lysine motif to Cav1 promotes ER-retention [211]. The resulting CAV1-KKSL construct is not only retained in the ER but also is targeted to lipid droplets as secondary result of ER accumulation [211]. The subcellular distribution of CAV1-KKSL is similar to the localization of CAV1-P158 mutants that we observe in *Cav1*$^{-/-}$ MEFs (Figure 22E, E'; Figure S.5E). Indeed, CAV1-P158 colocalizes with the ER and lipid droplets (Figure 23C-E) and a similar dilysine *KKXX* motif resembling that of CAV1-KKSL was identified in the distal C-terminus of CAV1-P158 encompassing the -3 and -4 positions of the C-terminus (*KKYK*) (Figures 9 and 23F) [16]. Additionally, the mutant is excluded from lysosomes, early endosomes and recycling endosomes (Figure S.6A-D), while low amounts of CAV1-P158 have an overlapping distribution with the Golgi-marker giantin (~25% transfected cells; Figure S.6D). We determined that the mutant protein predominantly colocalizes with the ER marker calreticulin (~50% transfected cells) and the lipid droplet marker ADRP (~25% transfected cells) (Figure 23E). In contrast, little or no wild type CAV1 is detected in these compartments (Figure 23A, B) and the elevated amount of colocalization of the mutant with the ER or lipid droplet (roughly 30% of transfected cells) markers is statistically significant (Figure 23D, E, F).

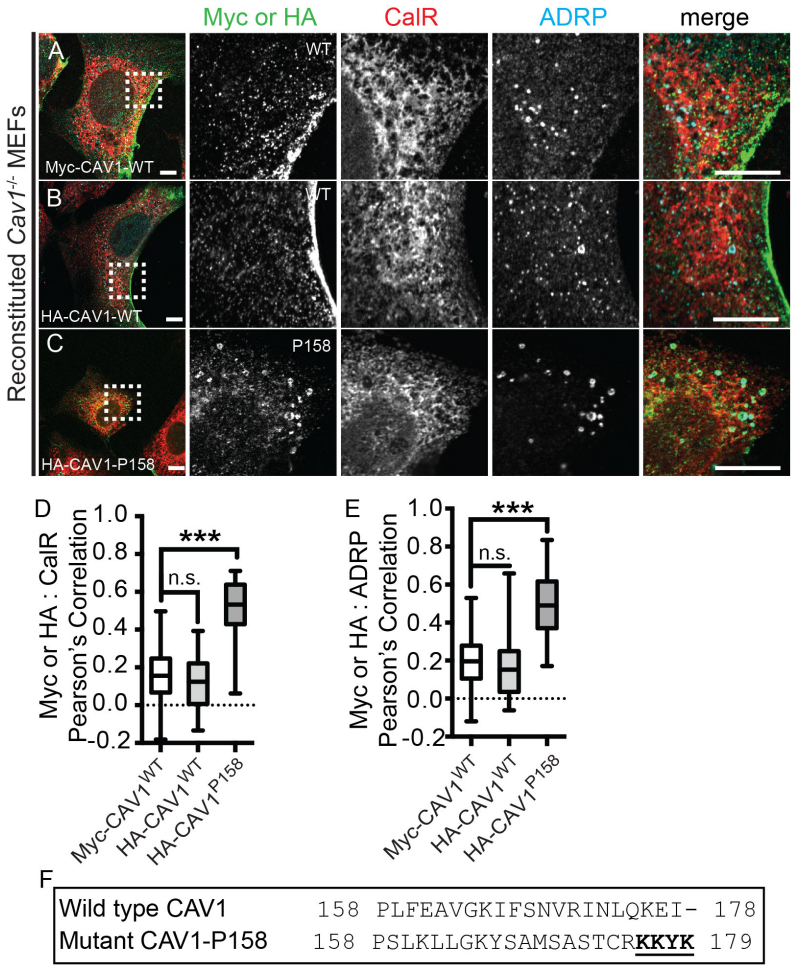

Figure 23. The CAV1-P158 Frameshift Mutant is Localized to the ER and Lipid Droplets and Contains a Putative ER-Retrieval Signal in the form of a C-terminal Dilysine Motif. Immunofluorescence staining of CAV1 constructs (green) in *Cav1*$^{-/-}$ MEFs labeled with the ER marker calreticulin (CalR, red) and the lipid droplet marker ADRP (cyan). **(A, B)** Wild type Myc-CAV1 or HA-CAV1 transfected *Cav1*$^{-/-}$ MEFs (green) does not co-localize with the ER protein calreticulin (CalR, red) or the lipid droplet protein, ADRP (cyan) in transfected *Cav1*$^{-/-}$ MEFs. **(C)** Immunofluorescence staining of HA-CAV1-P158 (green), CalR (red) and ADRP expressed in *Cav1*$^{-/-}$ MEFs. **(D)** Colocalization analysis of wild type and mutant CAV1 constructs with CalR with Pearson's correlation coefficient (PCC). **(E)** Colocalization analysis of wild type and mutant CAV1 constructs with ADRP. Data sets were represented in the graphed box-and-whisker plots. P-values were calculated with a student's T-test (***, p<0.0001). **(F)** Amino acid sequence alignment comparing the distal C-terminus of wild type CAV1 and CAV1-P158 (aa. 158-178/9). The dilysine motif (*KKYK*) in CAV1-P158 is in bold, underlined text. Scale bars represent 10μm.

4.2.4 Mutational Analysis of the Dilysine Motif to Test its Function as an ER-Retrieval Signal

Next, I wanted to test whether or not the putative dilysine motif was functioning as an ER-retrieval signal. ER-retrieval signals must be positioned at the distal C-terminus to

function and are sensitive to substitution and deletion mutations. Tagging membrane proteins that contain dilysine motifs on the C-terminus can also disrupt ER-retrieval. Thus, membrane proteins bearing dilysine motifs that have been mutated/deleted or fused to a C-terminal tag escape ER retention and traffic to the plasma membrane [258-260]. In line with this, a version of the CAV1-P158 mutant tagged on the C-terminus with mEmerald has a normal subcellular distribution, colocalizes with cavin-1 and was detected in DRMs (Figure S.5D, F) similarly to wild type CAV1 (Figure 22C, D, F, G; Figure S.5B, C, F). This is in contrast to the behavior of the N-terminally mEmerald-tagged CAV1-P158 mutant (Figure S.5E).

To further test the function of the putative dilysine motif in CAV1-P158 (*KKYK*; aa. 176-179), I wanted to determine if disrupting the dilysine motif would rescue the trafficking defect of CAV1-P158. To do so, I deleted the amino acids encompassing the dilysine motif (aa. 176-179; CAV1-P158-*ΔKKYK*) or substituted the lysine residues (K176, K177) of the ER-retrieval signal with alanines (CAV1-P158-AAYK) and assessed their subcellular distribution (Figure 24; Chapter 2.4). I found that the CAV1-P158 lysine mutants exhibited little or no colocalization with the ER and LD markers (Figure 24B, C). Quantifying the colocalization between CAV1-P158-AAYK and CAV1-P158-ΔKKYK with either the ER or LD marker revealed that both mutants behave identically to each other and also mirror the localization of wild type CAV1 (Figure 24E, F), suggesting that disrupting the dilysine motif allowed the protein to exit from the ER.

To test if the CAV1-P158 dilysine motif (*KKYK*) is sufficient to target proteins to the ER and lipid droplets, I introduced *KKYK* into the C-terminus of wild type CAV1 (CAV1-KKYK) to determine if this experimental mutant phenocopied the trafficking defect of CAV1-P158 (Figure 24A). CAV1-KKYK colocalizes with ADRP in lipid droplets; however, very little colocalizes with calreticulin in the ER (Figure 24D). This suggested that the rate of ER-to-lipid droplet transport is increased in this construct. Colocalization analysis also indicates that CAV1-KKYK colocalizes with lipid droplets to the same degree as CAV1-P158, and this is significantly higher when compared to wild type CAV1.

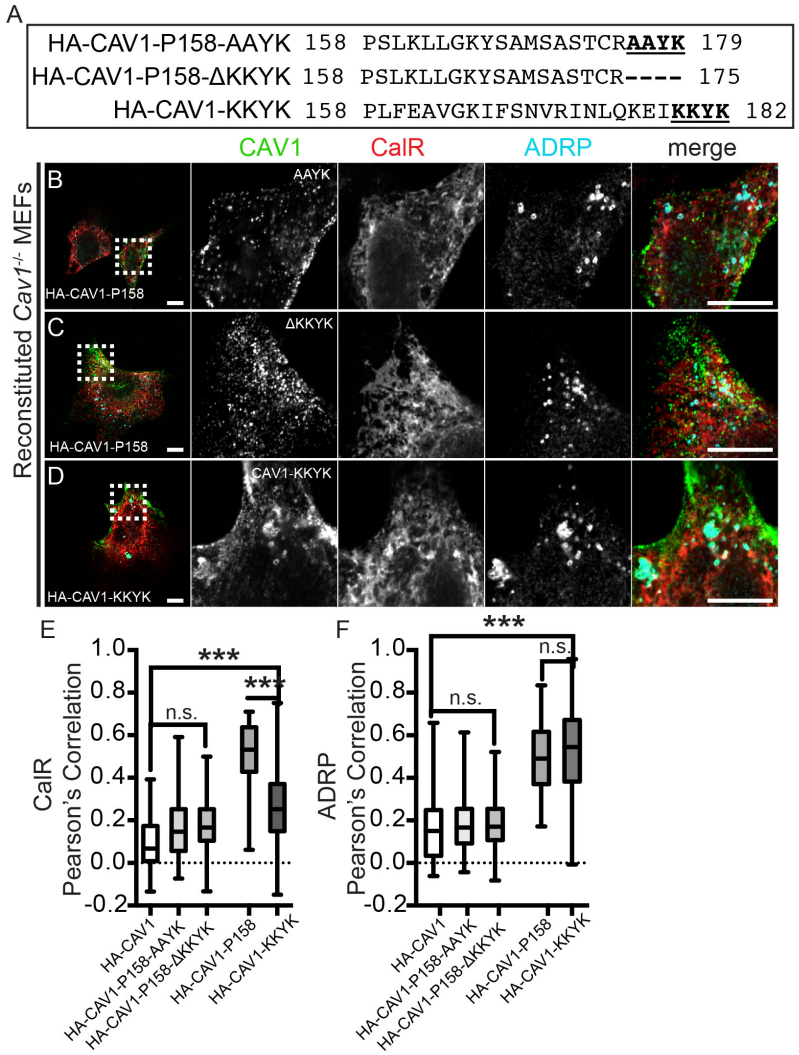

Figure 24. Mutational Analysis Probing the Role of the Dilysine Motif in the Abnormal Localization of CAV1-P158. (A) C-terminal amino acid sequence experimental mutants generated from CAV1-P158 template to disrupt the dilysine motif by alanine substitution (top, HA-CAV1-P158-AAYK; aa. 176-177), truncation (middle, HA-CAV1-P158-ΔKKYK; aa. 176-179) or by introducing the *KKYK* peptide into the C-terminus of wild type CAV1 (bottom, HA-CAV1-KKYK; aa. 179-182). (B-F) *Cav1*$^{-/-}$ MEFs transfected with experimental CAV1 constructs were triple-immuno-labeled with antibodies against tagged CAV1 (green), CalR (red) and ADRP (cyan). **(B)** HA-CAV1-P158-AAYK (green) fluorescence is absent from the ER (red) and lipid droplets (cyan). **(C)** HA-CAV1-P158-ΔKKYK (green) labeling is also absent from the ER (red) and lipid droplets (cyan). **(D)** HA-CAV1-KKYK (green) and **(E)** have an apparent wild type localization (refer to 4B). **(F)** CAV1-KKYK has a distribution that resembles both wild type CAV1 and CAV1-P158. Graphs represent colocalization analysis between CAV1 and CalR **(E)** and ADRP **(F)**. p-values were calculated with a student's T-test, data sets are graphed as box-and-whisker plots. Scale bars represent 10μm.

In order to determine if these mutants were able to form caveolae, I additionally analyzed endogenous cavin-1 immunofluorescence in expressing the experimental

mutants. Cavin-1 is a caveolae accessory protein that is routinely used in immunofluorescence experiments as a marker of caveolae [75, 92, 242]. Similar to wild type CAV1 (Figure 22C, D), both CAV1-P158-AAYK and CAV1-P158-ΔKKYK colocalize with cavin-1 (Figure 25A, B, D) suggesting they are targeted to the PM and recruit the necessary components for caveolae formation. A portion of the CAV1-KKYK mutant also colocalizes with cavin-1 (Figure 25C, D), which is not observed in CAV1-P158 (Figure 22; Figure S.5). This raises the possibility that the unique CAV1-P158 C-terminal residues 158-175 actually may contribute to ER accumulation independently of the ER-retrieval signal (176-179). In support of this, significant amounts of CAV1-P158-AAYK and CAV1-P158-ΔKKYK colocalized with the ER marker compared to wild type CAV1 (Figure 24E).

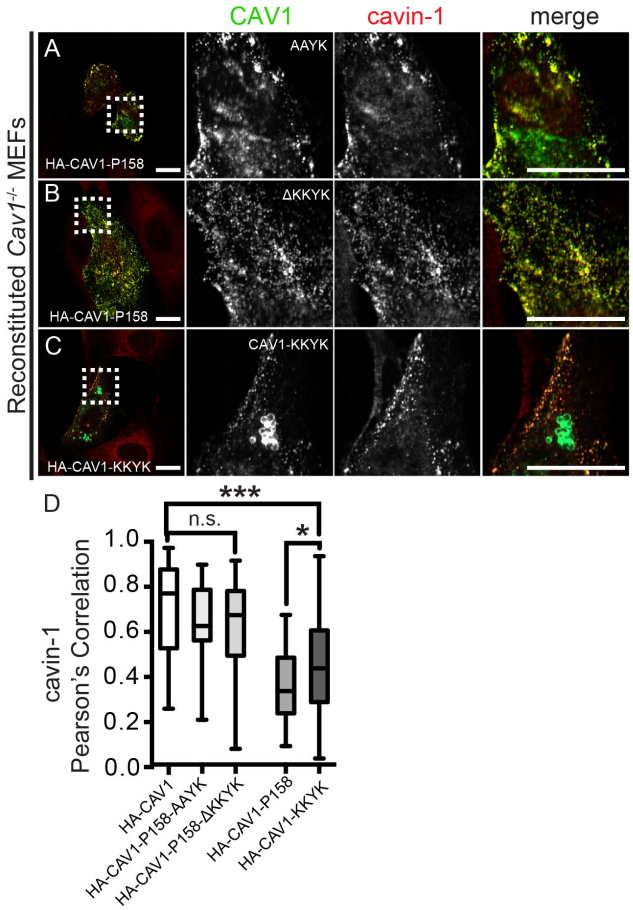

Figure 25. Colocalization of Cavin-1 and Experimental Dilysine Mutants. Colocalization between CAV1 constructs (green) and the caveolae accessory protein cavin-1 (red) in transfected *Cav1*$^{-/-}$ MEFs. **(A)** HA-CAV1-P158-AAYK (green). **(B)** HA-CAV1-P158-Δ-KKYK (green). **(C)** HA-CAV1-KKYK (green). **(D)** Colocalization was quantified with Pearson's correlation coefficient (PCC). P-values were calculated with a two-tailed student's T-test. ***=p<0.0001. Scale bars represent 10μm.

4.2.5 CAV1-P158 Functions as a Dominant Negative and Disrupts Wild Type CAV1 Trafficking in Cav1$^{-/-}$ MEFs

The naturally occurring P158 CAV1 mutant is co-expressed with a wild type copy of CAV1 in heterozygous PAH patients. Caveolins are known to oligomerize, which could sterically mask ER-retention signal, but it is unclear how co-expression will affect either forms of the CAV1 proteins. Thus, I next co-expressed wild type CAV1 and CAV1-P158 in *Cav1*$^{-/-}$ MEFs in order to determine if CAV1-P158 has a dominant negative effect on wild type CAV1 or if the mutant trafficking defect is rescued by wild type CAV1. Wild type CAV1 and CAV1-P158 were differentially tagged in order to distinguish them in co-transfected *Cav1*$^{-/-}$ MEFs. *Cav1*$^{-/-}$ MEFs co-transfected with two differentially tagged wild type CAV1 constructs were included as controls.

First, I used co-immunoprecipitation to determine if the wild type and mutant form hetero-oligomers. Control co-immunoprecipitation (co-IP) experiments confirmed that as expected, two differentially tagged versions of wild type CAV1 protein could be co-immunoprecipitated in co-transfected *Cav1*$^{-/-}$ MEFs. Wild type CAV1 and CAV1-P158 also co-immunoprecipitated with each other in reciprocal pull-down experiments, similar to controls. This indicates that co-transfected CAV1 proteins co-assemble into hetero-oligomeric complexes in *Cav1*$^{-/-}$ MEFs (Figure 26A).

In a second set of experiments, I examined subcellular distribution of the exogenous CAV1 proteins in co-transfected *Cav1*$^{-/-}$ MEFs stained to mark the ER, lipid droplets, or caveolae. In control co-transfected *Cav1*$^{-/-}$ MEFs, colocalization of wild type CAV1 proteins with the ER and lipid droplet markers is not detected (Figure 26B, F; 26D, G). However, an increased amount of wild type CAV1 colocalizes with both the ER and lipid droplets when it is co-expressed with CAV1-P158 (Figure 26C, F) (Figure 26E, G). Taken together, these results support the hypothesis that CAV1-P158 behaves as a dominant negative.

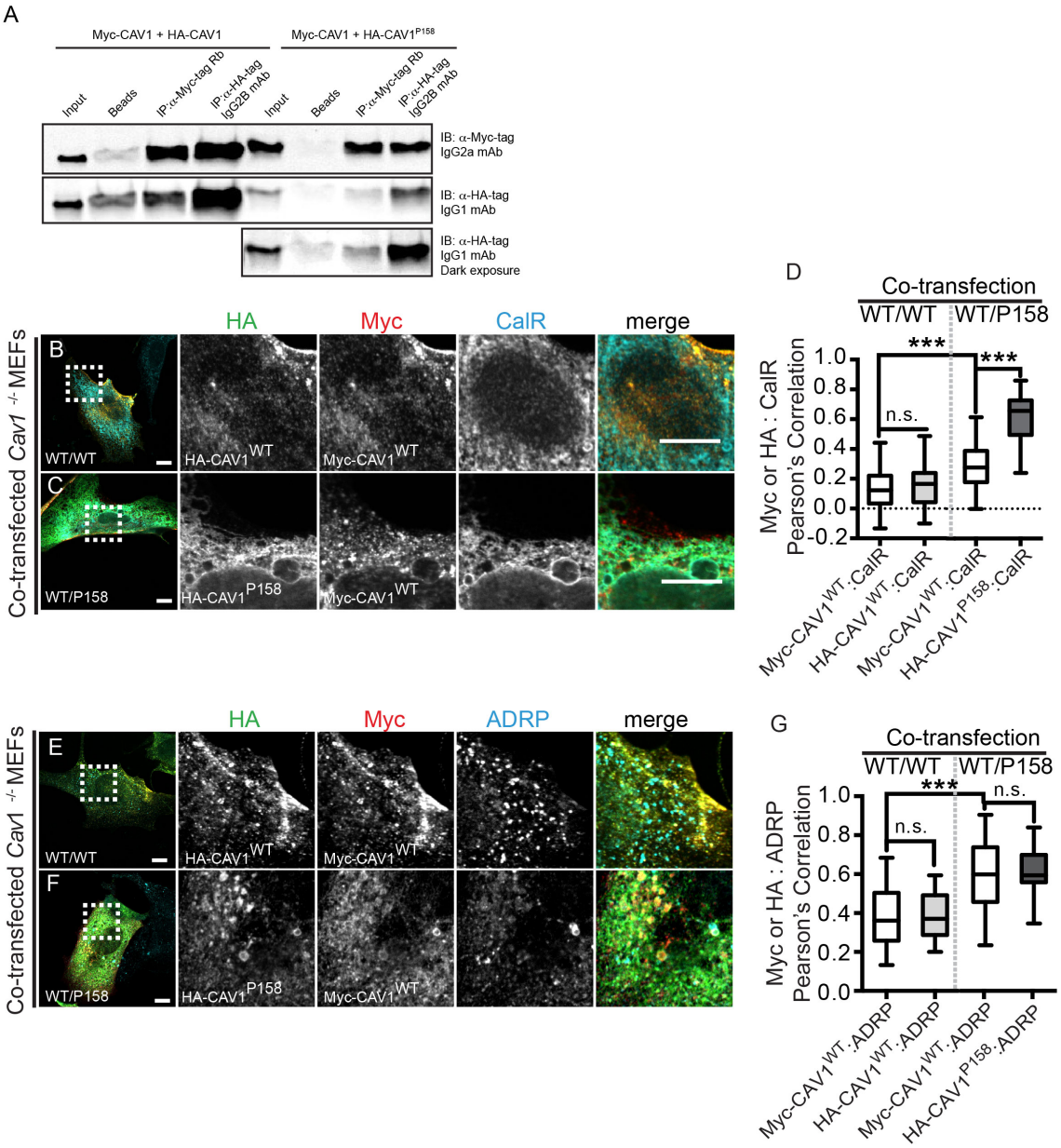

Figure 26. Wild Type CAV1 is Partially Mislocalized to the ER and Lipid Droplets in *Cav1*$^{-/-}$ MEFs Co-Expressing CAV1-P158. (A) Co-IP of wild type HA-CAV1 or HA-CAV1 P158 with wild type Myc-CAV1 using an anti-Myc antibody from lysates of co-transfected *Cav1*$^{-/-}$ MEFs (Wt/Wt and Wt/P158). An anti-HA antibody was used to blot for co-immunoprecipitated proteins. A reciprocal experiment was done using an anti-HA to pull down oligomerized HA-CAV1 or HA-CAV1-P158 and co-immunoprecipitated Myc-CAV1 was detected with an anti-Myc antibody. **(B-D)** Co-staining and colocalization analysis (graph) of the ER marker Calreticulin/CalR (cyan) in *Cav1*$^{-/-}$ MEFs co-expressing wild type Myc-CAV1 (red) and **(E)** wild type HA- CAV1 (green) or **(F)** mutant HA-CAV1-P158 (green). **(G)** Colocalization data is plotted on box and whisker plots for CalR in Wt/Wt and Wt/P158 co-transfected *Cav1*$^{-/-}$ MEFs. **(E-F)** Co-staining and colocalization analysis (graph) of the lipid droplet marker ADRP (cyan) in *Cav1*$^{-/-}$ MEFs co-expressing wild type Myc-CAV1 (red) and **(E)** wild type HA- CAV1 (green) or **(F)** mutant HA-CAV1-P158 (green). **(G)** Colocalization data is plotted on box and whisker plots for ADRP in Wt/Wt and Wt/P158 co-transfected *Cav1*$^{-/-}$ MEFs. (***, p<0.0001). p-values were calculated with a student's T-test. Scale bars represent 10μm.

I went on to assess caveolae formation by measuring the colocalization of the CAV1 constructs with the caveolae marker cavin-1 in co-transfected *Cav1*$^{-/-}$ MEFs. Wild type forms of CAV1 colocalize with each other and cavin-1 in co-transfected *Cav1*$^{-/-}$ MEF controls. Wild type CAV1 also partially colocalizes with cavin-1 when co-expressed with CAV1-P158; however, this is significantly reduced compared to controls (Figure 27B-D). I also found that the degree of colocalization between wild type CAV1 and CAV1-P158 is lower in co-transfected *Cav1*$^{-/-}$ MEFs than that observed between wild type CAV1 constructs in control co-transfections (Figure 27D). Taken together, these findings suggest that co-expression of wild type CAV1 partially corrects the trafficking defects of CAV1-P158, but that CAV1-P158 also causes mislocalization of wild type CAV1. These results further support the conclusion that CAV1-P158 functions as a dominant negative.

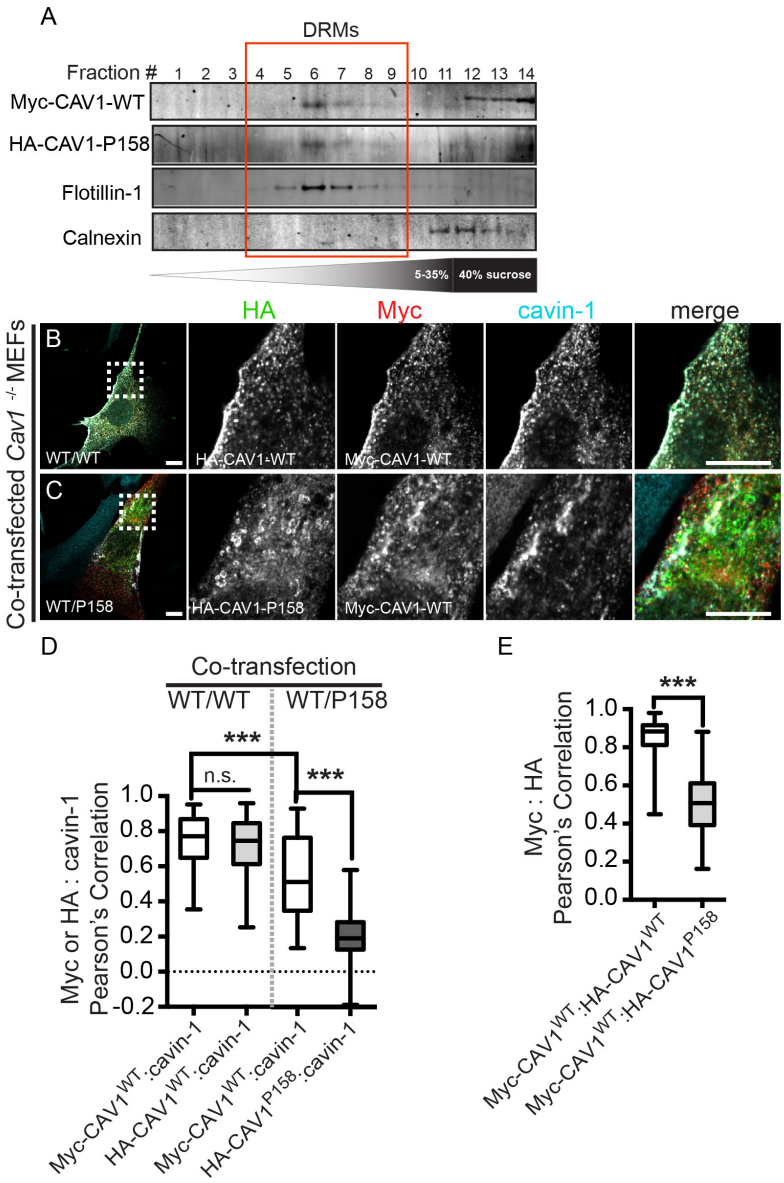

Figure 27. CAV1-P158 is more Detergent-Resistant when Co-Expressed with Wild Type CAV1 but Recruitment of Cavin-1 is Less Efficient in Co-Transfected *Cav1*$^{-/-}$ MEFs. (A) Detection of CAV1-P158 in DRMs is increased when it is co-expressed with wild type CAV1 in *Cav1*$^{-/-}$ MEFs. **(B)** Co-expressed wild type CAV1 constructs (Myc/HA-tagged; Wt/Wt) colocalize with cavin-1. **(C)** Reduced colocalization between wild type CAV1 and cavin-1 is observed in *Cav1*$^{-/-}$ MEFs co-expressing Myc-CAV1 and HA-CAV1P158 (Wt/P158). **(D)** Colocalization analysis of CAV1 constructs and cavin-1 in *Cav1*$^{-/-}$ MEFs co-expressing two wild type CAV1 proteins or a wild type and a mutant CAV1 protein was determined by Pearson's correlation coefficient (PCC). p-values were calculated with a two-tailed student's T-test, and the data plotted as box-and-whisker plots in the graphs (***, $p<0.0001$). Scale bars represent 10μm. (A, Bing Han, Ph.D.)

4.2.6 CAV1 is not Detectible in the ER or Lipid Droplets in Patient Fibroblasts

I wanted to confirm the findings from the co-transfection studies and determine if CAV1 is mistargeted to the ER and lipid droplets in heterozygous patient fibroblasts. To test this, the subcellular distribution of CAV1 in wild type control and patient fibroblasts was analyzed by immunofluorescence microscopy. A caveat to labeling patient cells is that currently available antibodies either detect both wild type and mutant CAV1 or only detect wild type CAV1. Therefore, CAV1-P158 is indistinguishable from wild type CAV1 by antibody labeling in heterozygous patient cells (Figure 21D). With this in mind, I stained control and patient fibroblasts with a CAV1 antibody that is predicted to detect wild type and mutant CAV1. I found that the immuno-staining pattern of CAV1 was indistinguishable in control and patient fibroblasts (Figure 28A); the overall subcellular distribution of CAV1 in patient fibroblasts appeared to be normal and was not detectible in the ER or lipid droplets (Figure 28A-C). This suggests that in patient cells, despite the presence of a mutant copy of CAV1, CAV1 is delivered to the plasma membrane where it appears to form caveolae (Figure 22A).

Control and patient fibroblasts were additionally labeled with a C-terminal anti-CAV1 (156-172) antibody that specifically only detects wild type CAV1 (Figures 22D, 28D-G; Figure S7). This antibody normally only detects CAV1 in the Golgi complex and is unable to label CAV1 in caveolae unless cells have been treated with reagents to deplete cholesterol and lipids [182]. This is because this antibody detects an exposed C-terminal epitope of CAV1 in 8S oligomers that have not fully assembled into 70S complexes in the Golgi compartment. This epitope is masked during the assembly of 70S complexes, after CAV1 undergoes conformational changes and associates with cholesterol as it traffics from the Golgi complex to caveolae [8, 245, 261, 262]. Therefore, this antibody only detects CAV1 in the Golgi complex and not in caveolae unless the conformation of CAV1 is abnormal or the composition of lipids is altered or extracted from cells [194]. In our previous studies in Chapter 3 [13], abnormal epitope accessibility indicated by labeling of extra-Golgi puncta (presumably caveolae) was observed in CAV1-F160X heterozygous patient cells. Extra-Golgi labeling in caveolae with this antibody is therefore indicative of changes in the conformation and/or lipid

composition of caveolae [182]. This led me to use this antibody to test for changes in the organization of wild-type CAV1 complexes that form in CAV1-P158 heterozygous patient fibroblasts. The C-terminal antibody preferentially labeled only Golgi-associated CAV1 in both patient and control cells (Figure 28B-E). However, a significant decrease in colocalization with both Golgi markers was observed. I speculate that this is because the specificity of this antibody is to wild type CAV1, and there is therefore at least half as much wild type CAV1 being labeled in heterozygous patient fibroblasts compared to controls. Thus, the accessibility of the C-terminus of wild-type CAV1 is not noticeably changed in patient cells expressing the frameshift mutant.

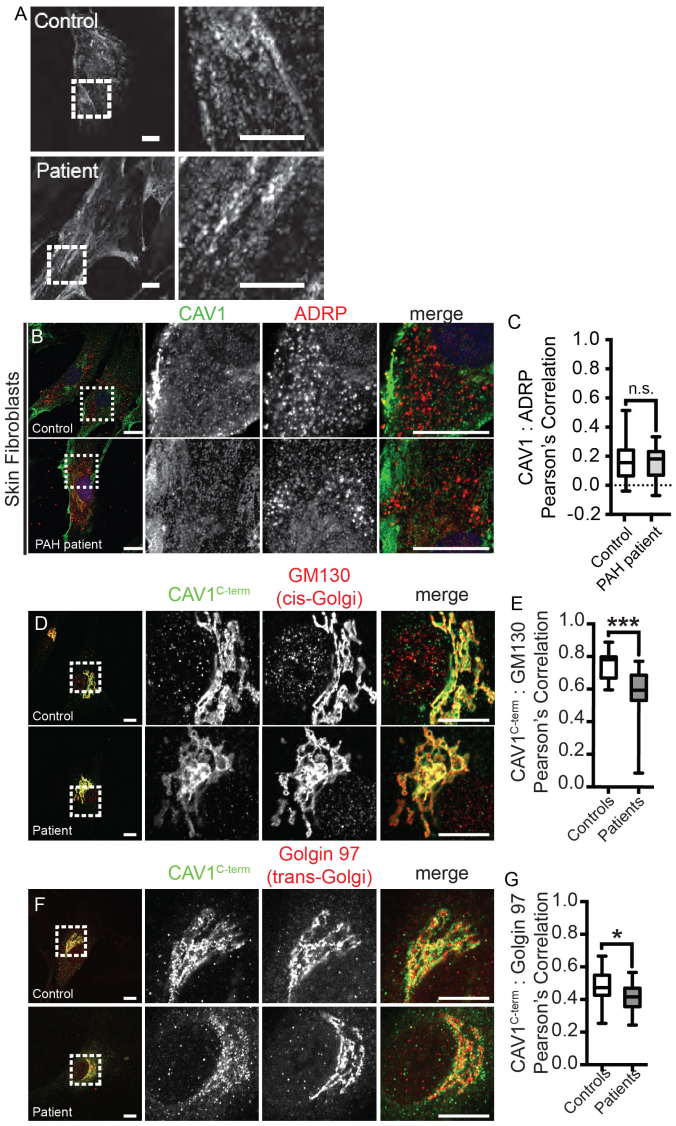

Figure 28. CAV1 is Distributed Normally in Patient Fibroblasts as Detected by Immunofluorescence Microscopy. (A) Cells were labeled with a CAV1 antibody that detects CAV1 in caveolae as well as in the Golgi complex. **(B)** Control (top panel) and patient (bottom panel) cells co-stained with the same CAV1 antibody in **A** and ADRP to label lipid droplets. (**C**) Quantification of CAV1/ADRP colocalization in control (n=41) and patient fibroblasts (n=64). p=0.5488 **(D)** Control (top panel) and patient (bottom panel) cells co-stained with the same C-term-specific CAV1 antibody and the *cis*-Golgi marker GM130. (**E**) Quantification of CAV1/GM130 colocalization control (n=16) and patient fibroblasts (n=18). p=0.0007. (**F)** Control (top panel) and patient (bottom panel) cells co-stained with the same C-term-specific CAV1 antibody and the *trans*-Golgi marker Golgin97. (**G**) Quantification of CAV1/Golgin97 colocalization control (n=31) and patient fibroblasts (n=41). p=0.0111. Images are representative of multiple cell lines observed over 2-3 independent experiments. *, $p < 0.05$, **, $p < 0.01$,***, $p < 0.001$; ns, not significant; T-test. Scale bars, 10 µm.

4.2.7 CAV2 and Caveolar Accessory Protein Expression are Reduced in Patient Fibroblasts but Colocalization with CAV1 is Normal

CAV1 and CAV2 form hetero-oligomers [44, 51, 241], and CAV1 deficiency leads to a concomitant decrease in CAV2 expression levels [11, 263]. Reduced CAV1 levels are also associated with the accumulation of CAV2 in the Golgi complex and its inability to reach the plasma membrane in the absence of CAV1 [11, 263, 264]. Because CAV1 levels are significantly reduced in patient cells, we asked whether this is associated with changes in the expression or subcellular distribution of CAV2. Consistent with this possibility, Western blot analysis showed a 60% reduction of CAV2 levels in control fibroblasts (Figure 29A). However, CAV2 colocalized normally with CAV1 in puncta at the plasma membrane (Figure 29B, C). Some CAV2 was also present in the Golgi complex, but this was also the case in control cells. Thus, although CAV2 levels are decreased in patient cells, the expression of mutant CAV1 does not appear to prevent delivery of CAV2 to caveolae in heterozygous patient fibroblasts.

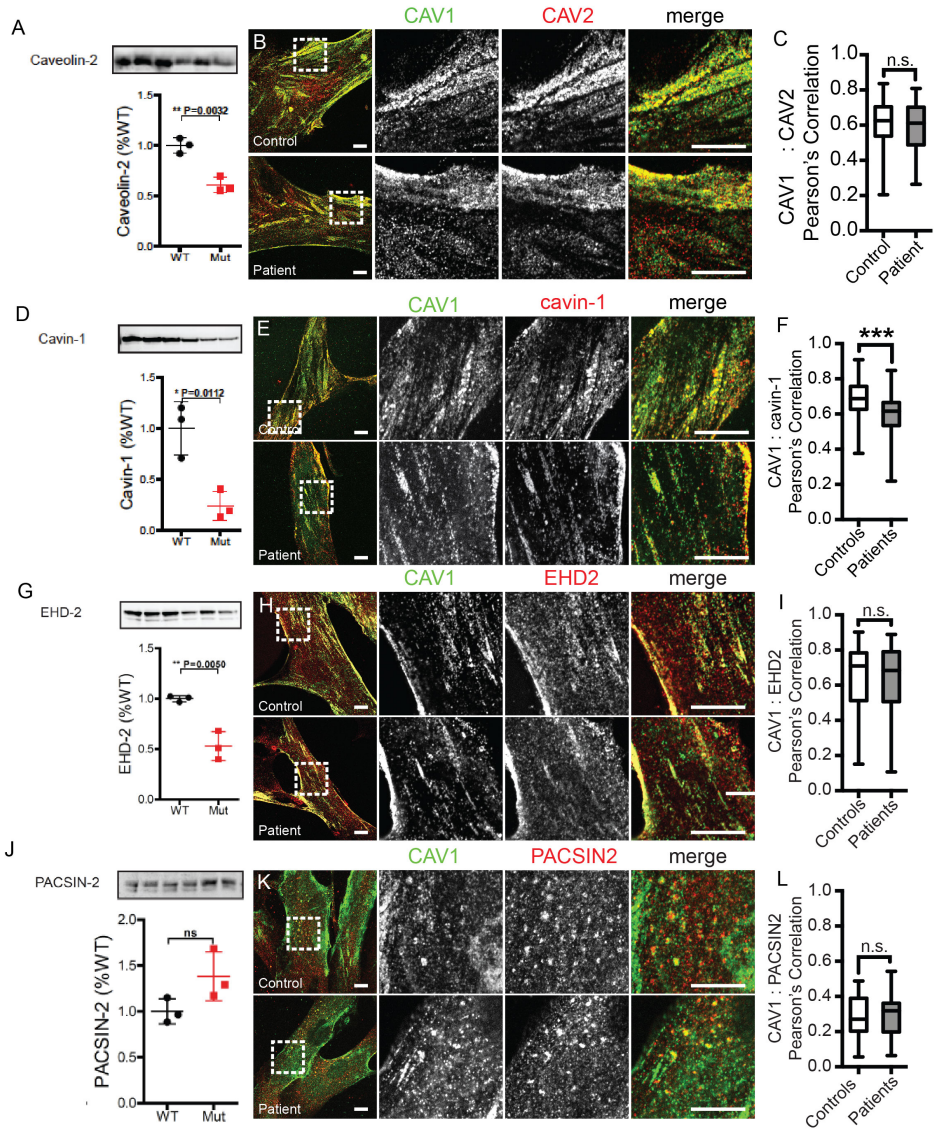

Figure 29. CAV2 and Caveolae Accessory Protein Expression Levels and Localization in Patient and Control Fibroblasts. (A, D, G, J) Western blots of accessory proteins, (B, E, H, K) representative immunofluorescence images and quantification of colocalization of control and patient cells co-stained for caveolin-1 (C, F, I, L). **(A)** CAV2 Western blot and quantification. **(B)** CAV1 (green) and CAV2 (red) immunofluorescence; control (top panel), patient (bottom panel. **(C)** Quantification of CAV1/2 colocalization (p=0.4514; control n=46; patient n=46). **(D)** Cavin-1 Western blot and quantification. **(E)** CAV1 (green) and Cavin-1 (red) immunofluorescence; control (top panel), patient (bottom panel. **(F)** Quantification of CAV1/Cavin-1 colocalization (p< 0.0001; control n=54; patient n=61). **(G)** EHD-2 Western blot and quantification. **(H)** CAV1 (green) and EHD-2 (red) immunofluorescence; control (top panel), patient (bottom panel. **(I)** Quantification of CAV1/EHD-2 colocalization (control n=96; patient n=93; p=0.4780). **(J)** PACSIN2 Western blot and quantification. **(K)** CAV1 (green) and PACSIN2 (red) immunofluorescence; control (top panel), patient (bottom panel. **(L)** Quantification of CAV1/PACSIN2 colocalization (control n=47; patient n=24, p=0.6703). Western blot quantification: bar represents mean ± SD for the 3 control (black squares) or 3 patient (red squares) cell lines. Data represent 3 independent experiments. p-values calculated with Student's T-test. Scale bars, 10 μm. Data represent 2-3 independent experiments for 3 control and 3 patient cells. *, p < 0.05, **, p < 0.01, ***, p < 0.001; ns, not significant; T-test. (Western blots: Bing Han, Ph.D.)

Caveolae are regulated by a series of CAV1 accessory proteins. These include Cavin-1, a protein required for caveolae formation, function and stability [75, 92, 242], EHD-2, which regulates the dynamics of caveolae but that is not required for caveolae formation [76, 79], and PACSIN2, which plays an essential role in sculpting of caveolar membranes [77, 85]. Like CAV2, levels of Cavin-1 are linked to CAV1 expression levels [75]. In agreement with this idea, Western blotting analysis showed that levels of Cavin-1 are reduced in patient cells (Figure 29D). Although this does not affect the distribution of Cavin-1, colocalization of CAV1 with Cavin-1 is reduced in patient fibroblasts (Figure 29E, F). Like Cavin-1, EHD-2 levels are also decreased in patient fibroblasts (Figure 29G), but EHD-2 almost exclusively colocalized with CAV1 in punctate structures in both patient cells and control fibroblasts (Figure 29H, I). PACSIN2 levels were similar in control and patient cells (Figure 29J). In contrast to Cavin-1 and EHD-2, only a partial overlap of PACSIN2 and CAV1 staining was observed in both control and patient fibroblasts (Figure 29K, L). This partial CAV1/PACSIN2 colocalization is consistent with previous studies [85]. Taken together, these results suggest that expression levels of both CAV2 and several caveolar accessory proteins are partially reduced in patient cells. Nevertheless, the fact that CAV1, CAV2, and accessory proteins co-localized in discrete puncta suggests that caveolae are present in the patient cells, and that these caveolae contain the normal complement of known caveolar accessory proteins.

4.2.8 High-Molecular-Weight Oligomers of CAV1 are Detectible in Patient Fibroblasts

Our results up until this point suggest that caveolae form correctly in patient fibroblasts, but the caveolae density is reduced compared to controls. To further test for possible defects in caveolae, we next examined the ability of CAV to form oligomeric complexes using blue native polyacrylamide gel electrophoresis (BN-PAGE). Endogenous CAV1 typically migrates as ~600 kDa complexes using this approach [109, 229]. Defects in oligomerization of CAV1 can also be readily detected using BN-PAGE, which are observed as low molecular weight bands or smearing of bands in the BN-PAGE blot [109, 229].

As a control for these experiments, we assessed HeLa cells transfected with a CAV1 mutant known to disrupt the CAV1 oligomerization, CAV1-P132L [109, 246]. In addition to CAV1-P132L-GFP transfected HeLa cells, we included a series of control cell lysates from untransfected HeLa cells and HeLa cells expressing EGFP or a wild-type Cav1 EGFP fusion protein (Cav1-GFP). Consistent with our recent report [229], we found that when cells are transiently transfected with Cav1-GFP, the exogenous tagged CAV1 and endogenous CAV1 form two separate high-molecular-weight complexes. The former is ~800 kDa (Figure 30A, green arrow) and the latter is ~600 kDa (Figure 30A red arrow). These two bands likely correspond to the core unit of the 8S Cav1 oligomer [229]. In contrast, CAV1-P132L-GFP fails to form a normal ~800 kDa band, instead forming an irregular smear (Figure 30A).

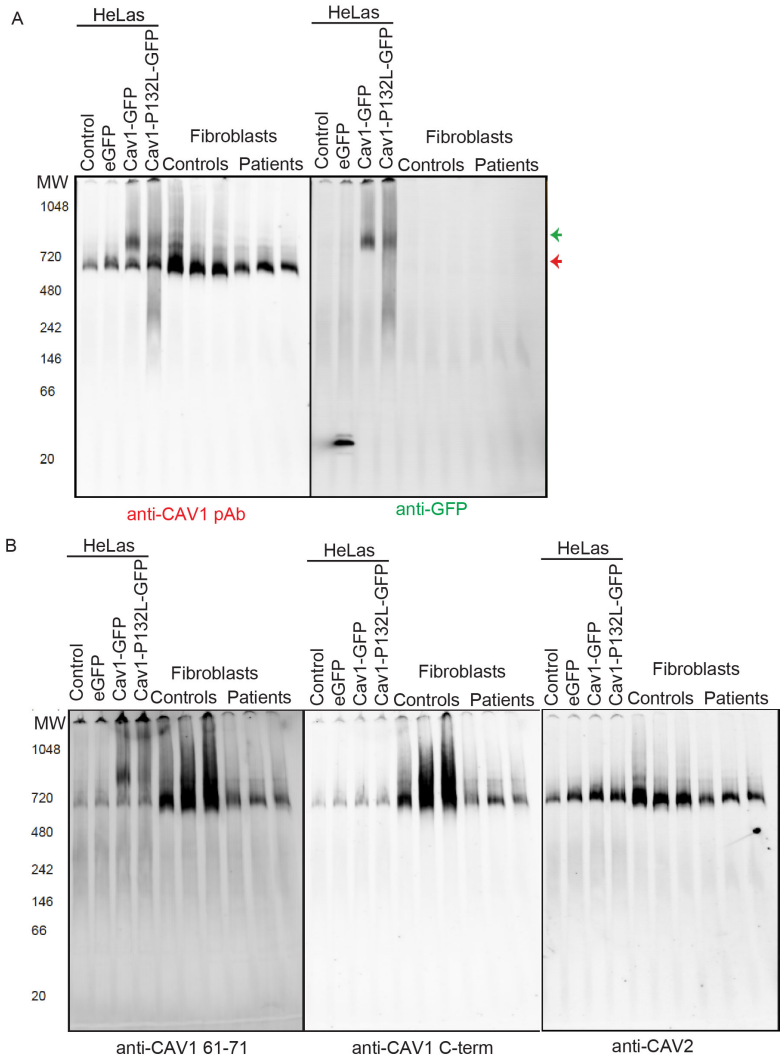

Figure 30. CAV1 Incorporates into CAV1/CAV2 Hetero-Oligomers in Patient Fibroblasts. Control and patient skin fibroblasts were subjected to BN-PAGE and the indicated proteins immunoblotted. Untransfected HeLas and HeLas transiently expressing eGFP, Cav1-GFP, or CAV1-P132L-GFP were used as controls. **(A)** Western blots from BN-PAGE were probed with anti-CAV1 (1-97) (red text and arrow) or anti-GFP (green text and arrow) antibodies. The red arrow indicates the position of complexes containing endogenous CAV1 and the green arrow shows complexes containing Cav1-GFP or CAV1-P132L-GFP. Data are representative of at least 3 independent experiments. **(B)** Blots probed with antibodies against CAV1 oligomerization domain (61-71; first blot), the C-terminal domain (156-172; middle blot) and CAV2 (last blot) are shown. Data are representative of 2-3 independent experiments. (Bing Han, Ph.D.)

In patient fibroblasts, CAV1 formed high-molecular-weight complexes similar to those observed in control fibroblasts and HeLa cells (Figure 30A). This strongly suggests that expression of the mutant CAV1 does not disrupt the oligomerization into the core 8S CAV1 unit. Furthermore, CAV1 and CAV2 co-migrated in both control and patient cells

(Figure 6B). Thus, the presence of the mutant protein also does not appear to interfere with the formation of CAV1/CAV2 hetero-oligomers.

We also probed the blots with two different CAV1 antibodies against the oligomerization domain (61-71; mAb 2297) and the C-terminal domain (156-172; RmAb) (Figure 30B). The oligomerization domain epitope recognized by mAb 2297 is found in both the wild type and mutant form of the protein. As mentioned above, anti-CAV1-C-term can only recognize wild-type CAV1. Both antibodies recognize the same band, which suggests that mutant and wild type CAV1 forms hybrid complexes (Figure 30B). In all cases, we noted that CAV1 isolated from patient fibroblasts is present at lower levels than in control fibroblasts, and also exhibits a slight mobility shift. The exact cause of this shift is unknown but may possibly reflect the presence of the mutant protein (which is one amino acid longer than wild type CAV1) in the complexes. From these experiments, we conclude that CAV1 forms hetero- and homo-oligomeric complexes normally in patient fibroblasts, and that mutant CAV1 and wild-type CAV1 are likely to interact with one another normally as well.

4.2.9 CAV1 and CAV2 Incorporate Normally into 8S and 70S Complexes in Patient Cells

CAV1 oligomerizes into at least two distinct complexes as it traverses the secretory pathway, an 8S complex and a 70S complex [8]. The 8S complexes have been hypothesized to correspond to a hetero-oligomer of CAV1 and CAV2 formed early in the secretory pathway in the ER, whereas the 70S complex has been proposed to represent the formation of a higher order CAV1 scaffold that assembles in the Golgi complex [8]. These two complexes partition in distinct fractions when analyzed by in velocity sucrose gradient centrifugation [8]. This partitioning distribution of these fractionated complexes is disrupted when there is an oligomerization defect in caveolin-1, such as that induced by the P132L mutation [8].

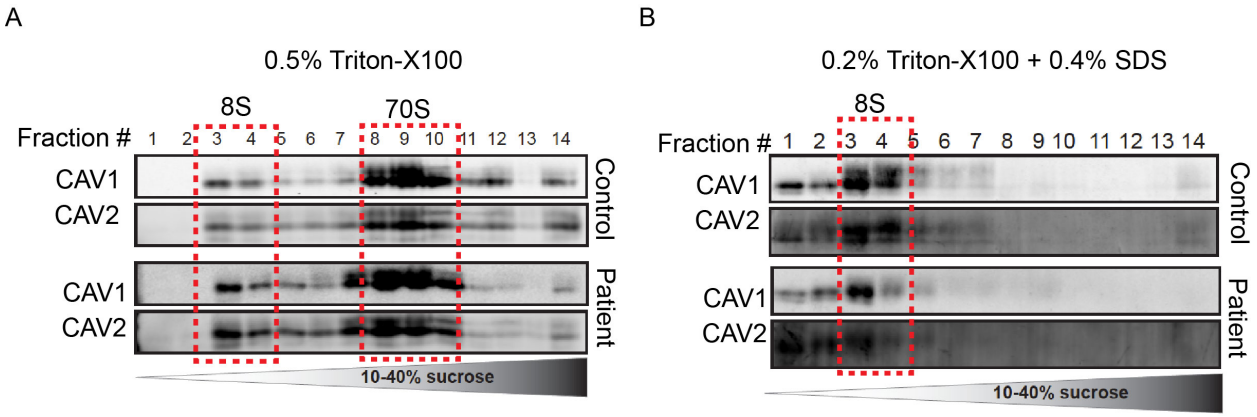

Figure 31. CAV1 Associates with 8S and 70S Complexes in Patient Fibroblasts. (A) Extracts prepared from control and patient fibroblasts were run through 10-40% sucrose velocity gradients and the resulting fractions analyzed by Western blot for CAV1 and CAV2. Both CAV1 and CAV2 associated with 8S and 70S oligomeric species in both control and patient cells. For each fraction, 10 ml of sample was loaded. **(B)** Note that all three patient cells lines contained slightly larger amounts of 8S complexes than were seen in control cells. Data are representative of 1-2 independent experiments per cell line. (Bing Han, Ph.D.)

To determine if the formation of these complexes occurs normally in patient cells, rate-zonal sucrose gradient centrifugation was used to analyze the organization of CAV1 complexes (Figure 31). CAV2, which forms complexes with CAV1, was examined as an internal control. Both CAV1 and CAV2 localize normally to 8S and 70S complexes in patient fibroblasts relative to controls. The finding that 8S and 70S complexes appear to form correctly in patient cells expressing the frameshift mutant of CAV1 further suggests that the mutant protein does not significantly interfere with the ability of CAV1 to form homo- and hetero-oligomers that ultimately are incorporated into caveolae. We did however observe slightly more CAV1 in fractions corresponding to 8S complexes than 70S complexes in patient fibroblast compared to controls (Figure 31A). It is thus possible that in the patient cells there is a subtle defect in the incorporation of 8S complexes into caveolae. To further assess the stability of the 8S complexes, we extracted cells using an SDS-containing lysis buffer (0.2% Triton X-100 + 0.4% SDS), which was previously shown to completely disassemble the 70S complexes into 8S oligomer subunits, which remains intact in wild type CAV1-expressing cells [8]. Under these conditions, almost all of the CAV1 complexes were disassembled to monomers or small oligomers in patient cells, whereas the CAV1 from control fibroblasts remained

associated with intact 8S oligomers (Figure 31B). Thus, the stability of the 8S complexes is decreased in patient cells.

4.2.10 Caveolae from Patient Cells Exhibit Decreased Detergent-Resistance

Detergent resistant membranes (DRMs) have long been considered the *in vitro* biochemical counterpart of caveolae and lipid rafts [8, 246, 265]. Although the interpretation of this assay has a number of limitations, it is a useful way to assess the characteristic biochemical properties of CAV1, a highly detergent-resistant protein. Several additional proteins associated with caveolae are also known to at least partially co-fractionate with DRMs, such as CAV2 [266] and Cavin-1 [93, 266]. We therefore tested whether caveolae-associated proteins from patient cells maintain full detergent resistance. Flotillin-1, a protein whose detergent resistance does not depend on CAV1 expression [267], was used as a positive control for DRMs for these studies, and calnexin served as a marker for detergent soluble fractions (Figure 32).

In cells extracted with cold 0.5% Triton X-100, both CAV1 and CAV2 accumulate in detergent resistant fractions to a similar extent in patient and control cells. CAV2 co-fractionates with CAV1 perfectly in both patient and control cells, and Cavin-1 and EHD-2 partially co-fractionates with CAV1. However, in patient cells, Cavin-1 is completely lost from caveolar fractions, and levels of EHD-2 in DRMs are decreased (Figure 32A, B). These results suggest that expression of the PAH-related mutant CAV1-P158 may weaken the affinity of accessory proteins for caveolae.

We also assessed the effect of increasing detergent concentration to determine whether caveolae/CAV1-rich DRMs in patient cells were equally detergent resistant as controls. When extraction protocol was increased from 0.5% to 1% TX-100, differences between the patient and control cells become more evident. Caveolae from control fibroblasts largely retain their detergent-resistant properties in increased detergent, whereas a substantial shift of CAV1 from detergent resistant to more detergent soluble fractions is observed for the patient cells (Figure 32C). Co-fractionation of EHD-2 with CAV1 in DRMs was also totally lost in patient cells under these conditions. These results

indicate that the PAH-related mutation on C-terminus may not only slightly decrease the affinity of accessory proteins for caveolae, but also impact the biochemical properties of caveolae.

Because CAV1 levels are reduced in patient cells (Figure 21) [16], we also asked whether the absolute amount of CAV1 associated with detergent resistant fractions is different for control and patient cell lines. To carry out this analysis, we loaded equal amounts of DRM-derived protein (Figure 32B, D). These results show approximately 50% less CAV1 is present in DRMs from patient cells than controls isolated in 0.5% TX-100, and even less in patient cells isolated in 1% TX-100. This suggests that the decreased expression of CAV1 levels observed in patient cells also decreases the number of caveolae as estimated by DRM isolation, a result consistent with our EM dataset.

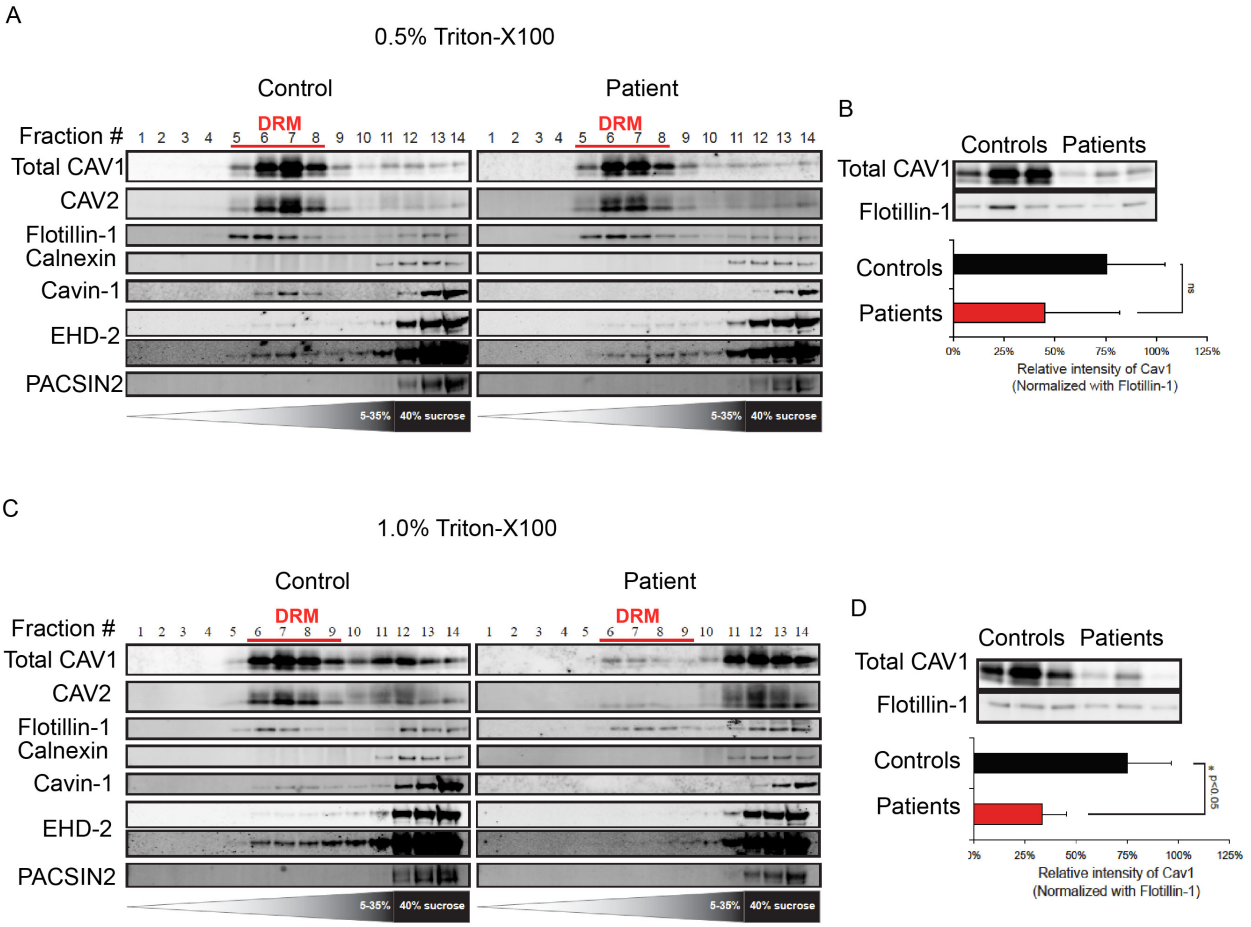

Figure 32. Caveolae are Less Detergent Resistant in Patient Fibroblasts. DRMs were fractionated on sucrose gradients from control and patient fibroblasts extracted using either **(A, B)** 0.5% or **(C, D)** 1.0% of

Figure 32. Continued. cold Triton X-100. **(A, C)** Western blots of fractions from sucrose gradients were probed with antibodies against the indicated proteins. Fraction 1 is the top of the gradient, and fraction 14 is the bottom. Fractions corresponding to DRMs are indicated with red lines. Note the marked decrease in levels of CAV1 in DRMs in patient cells extracted in 1.0% TX-100 relative to control cells. Two different exposures are shown for EHD-2 to show the fraction associated with DRMs. **(B, D) (Top)** DRM fractions were pooled for each cell line and equal amounts of protein were analyzed by SDS-PAGE followed by Western blotting. Samples were blotted for with an anti-CAV1 (1-97) antibody and anti-flotillin-1. Data in A and D are representative of one patient and one control cell line out of the 3 patient and 3 control cell lines examined at each detergent concentration. (Bing Han, Ph.D.)

4.2.11 Patient Fibroblasts Demonstrate Decreased Resistance to Osmotic Stress

Recent studies indicate that one function of caveolae is to serve as a membrane reservoir [268]. Caveolae flatten in response to mechanical or osmotic stress, and cells that contain fewer caveolae show decreased viability following stress [268]. Because patient fibroblasts contain fewer caveolae than wild-type cells, we hypothesized that they may exhibit lower buffering capacity when subjected to oncotic swelling to stretch the plasma membrane. To test this, we subjected cells to osmotic stress by 10 min incubation in hypotonic media (10-fold dilution) (Figure 33). Cell viability was assessed using a live/dead assay. Before treatment, the vast majority of cells were viable and had a fibroblastic spindle shape (green). After 10 minutes treatment, over 50% of wild-type cells were still alive, compared to around 25% of patient cells (Figure 33). These results indicate that the expression of mutant CAV1 sensitizes the fibroblasts to osmotic stress, and by extension likely also shear stress as well.

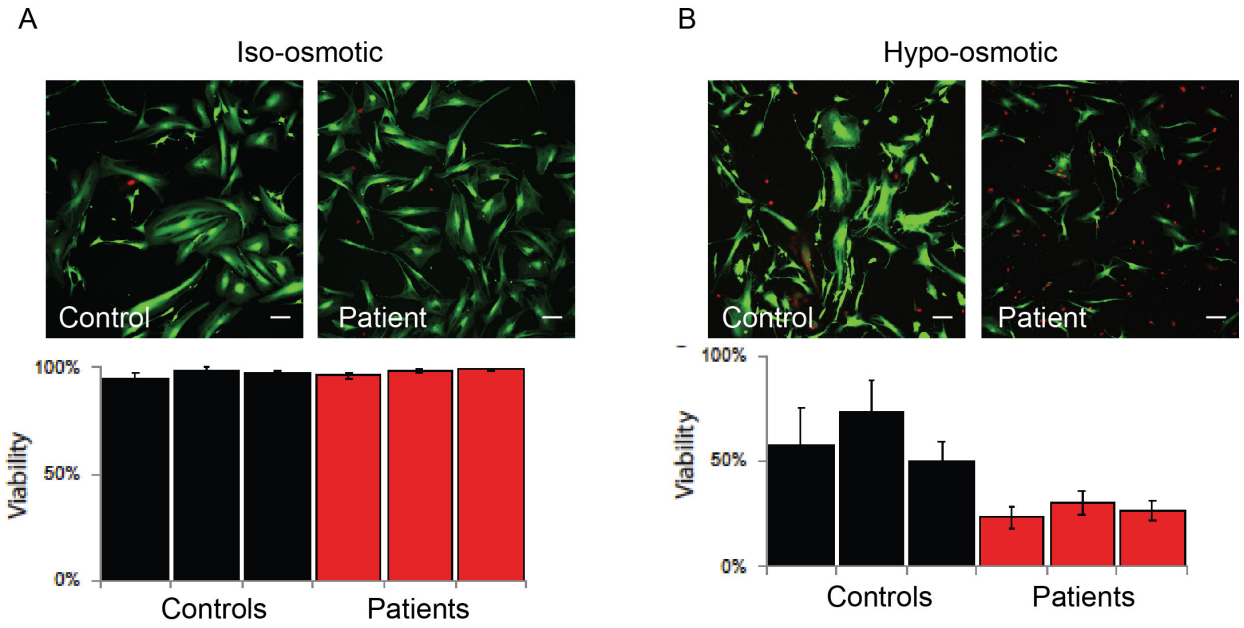

Figure 33. Patient Fibroblasts Demonstrate Increased Susceptibility to Hypo-Osmotic Stress. (A) Representative images of cells before and after 10 minutes of hypo-osmotic challenge. Bar, 10 mm. **(B)** Quantification of cell viability under control and hypo-osmotic conditions. Data represent the mean of at least 4 independent experiments in which at least 9 fields of cells were analyzed for each cell line. (Bing Han, Ph.D.)

4.3 Discussion

Although CAV1 has been linked to a number of diseases, relatively few examples of disease-associated mutations of the protein have been identified. The recent discovery of mutations in CAV1 associated with PAH [16] thus offers a unique opportunity to study the role of CAV1 and caveolae in both normal cellular function and disease. In the current study, we investigated the impact of the expression of a familial PAH-associated frameshift CAV1 mutant, CAV1-P158, on caveolae assembly in patient skin fibroblasts co-expressing a wild-type form of CAV1 and in reconstituted *Cav1*$^{-/-}$ MEFs. Here, we report that a PAH-associated mutant of CAV1 (CAV1-P158) contains an ER-retention/retrieval motif, targets to lipid droplets and does not form caveolae. These defects in turn negatively impact the ability of wild type CAV1 to form caveolae when co-expressed in *Cav1*$^{-/-}$ MEFs. These findings thus reveal a novel dominant-negative role of CAV1-P158 in the pathogenesis of PAH and offer a mechanism by which CAV1 mutations may contribute to human disease.

We determined that the mutant protein is expressed in patient fibroblasts with mass spectrometry (Figure 21D) and CAV1 correctly forms both homo-oligomers and hetero-oligomers with CAV2 (Figure 30). CAV1 also forms 8S and 70S complexes correctly and is targeted to the plasma membrane, where it recruits multiple accessory proteins known to normally associate with caveolae (Figures 29-32). Moreover, by electron microscopy, intact caveolae are readily observed in patient fibroblasts, despite reduced CAV1 expression in patient fibroblasts (Figure 21A) [16]. We could not distinguish the wild type protein from the mutant with the antibodies used in these studies. Therefore we expressed a plasmid encoding CAV1-P158 in *Cav1*$^{-/-}$ MEFs to independently investigate the mutant further.

I identified a C-terminal dilysine motif in the PAH-associated CAV1-P158 mutant (Figure 23). C-terminal dilysine motifs (*KKXX; KXKXX*) function as sorting signals that promote retrieval of ER-resident proteins, which have escaped from the ER [258, 259]. In order for dilysine motifs to be recognized by COPI machinery for ER-retrieval, the signal peptide must be on the distal C-terminus [269]. This signal becomes masked in the CAV-P158-mEmerald construct as a consequence of a C-terminal fusion protein tag, nicely explaining why this mutant is normally distributed and associates with DRMs (Figure S5) [260]. As a result of the presence of the dilysine motif, the N-terminally tagged CAV1-P158 mutant is predominantly localized to the ER and lipid droplets (Figure 23). Lipid droplet trafficking of CAV1 is a secondary consequence of ER-accumulation [270]. Additionally, the ER-retained CAV1-P158 mutant is not observed in DRMs and less efficiently forms 8S and 70S complexes that are unstable (Figure 22, S5, S7) in support of the hypothesis that CAV1 acquires DRM properties during transport from late-Golgi compartments to the PM in caveolae [8]. However, further experiments will be required to determine how the mutant C-terminus and/or mislocalization contribute to the loss of DRM affinity.

To determine if the CAV1-P158 dilysine motif was sufficient to abrogate caveolae targeting and promote ER and lipid droplet accumulation of wild type CAV1, we generated a CAV1-KKYK construct. Another group used a similar mutant (CAV1-KKSL)

previously to study the consequences of CAV1 accumulation in the ER [270]. As expected, CAV1-KKYK was observed in lipid droplets. These results imply that the mutant residues 158-176 of CAV1-P158 (which differ from residues158-176 in wild type CAV1) contribute to ER-accumulation in addition to the KKYK ER-retention signal. In support of this hypothesis, an increased amount of colocalization between CAV1-P158-AAYK and CAV1-P158-ΔKKYK with the ER are detected despite their ability to traffic to caveolae, further suggesting that the remaining mutated residues of CAV1-P158 (aa. 158-175) influence the rate of ER exit. Surprisingly, this mutant also colocalized with cavin-1 in presumable caveolae.

Why is CAV1-KKYK able to traffic to caveolae? The conformation of the CAV1 C-terminus undergoes changes during the assembly of 8S complexes, which are later organized into 70S complexes via the C-terminus [8, 109, 111, 194]. One possibility is that the ER-retrieval signal in CAV1-KKYK is susceptible to oligomerization-induced masking because it more efficiently assembles into 8S and 70S complexes. This would allow some of CAV1-KKYK to exit the ER and traffic to the plasma membrane (Figure 1, 25) [8, 48, 109, 111, 271]. Examination of the biochemical properties of the experimental mutants will further address this question, and will require additional investigation.

The colocalization of CAV1-P158-AAYK, CAV1-P158-ΔKKYK, and CAV1-KKYK with endogenous cavin-1 in *Cav1*$^{-/-}$ MEFs is indicative of caveolae formation. We did not specifically assess whether these caveolae are morphologically and functionally normal. However, preliminary studies using a conformation specific antibody suggest there may be some defects in the organization of CAV1 within caveolae (Figure S.8). This antibody normally only detects CAV1 in the Golgi complex and is unable to label CAV1 in caveolae unless cells have been treated with reagents to deplete cholesterol and lipids [182]. Extra-Golgi labeling in caveolae with this antibody is therefore indicative of changes in the conformation and lipid composition of caveolae [182]. This strongly suggests that there are compositional/conformational defects in the caveolae formed in *Cav1*$^{-/-}$ MEFs co-expressing wild type CAV1 with the experimental mutant constructs.

Additional tests to measure the biochemical properties of CAV1 and the lipid composition of caveolae under these conditions will be needed in order to support this interpretation of our experimental results.

After characterizing the mutant protein independently in *Cav1*$^{-/-}$ MEFs, we wanted to determine if co-expressing wild type CAV1 with CAV1-P158 rescued the trafficking defect of the mutant protein or caused the wild type protein to be mistrafficked. Caveolins are generally found in 70S complexes within caveolae, of which the 8S CAV1 oligomer serves as a fundamental building block [8]. Based on the fact that caveolins readily assemble into oligomers, I tested the hypothesis that hetero-oligomers of wild type CAV1 and CAV1-P158 are formed in cells co-expressing the proteins. I show that that wild type CAV1 and CAV1-P158 co-immunoprecipitate and that wild type CAV1 was partially mistargeted to the ER and lipid droplets in *Cav1*$^{-/-}$ MEFs co-expressing CAV1-P158 (Figure 26). Cavin-1 colocalization with CAV1-P158 was not improved in co-transfected cells and in fact (Figure 27), less colocalization between wild type CAV1 and cavin-1 was observed compared *Cav1*$^{-/-}$ MEFs co-transfected with two wild type CAV1 plasmids. This further supports the conclusion that CAV1-P158 is unable to form caveolae and negatively influences the recruitment of wild type CAV1 to cavin-1-positive spots. Taken together, these findings support the hypothesis that wild type and mutant CAV1 can co-assemble into hetero-oligomers and also suggests that the mutant CAV1 protein behaves as a dominant negative in co-transfected *Cav1*$^{-/-}$ MEFs.

We then examined the subcellular distribution of CAV1 in heterozygous PAH patient in order to determine whether CAV1 was mislocalized. Unlike the *Cav1*$^{-/-}$ MEFs, in patient fibroblasts CAV1 is neither detectible in lipid droplets nor observed reticular pattern indicative of the ER by immunofluorescence microscopy (Figure 28). One possible explanation for this finding is that in patient cells, under physiological conditions, the mutant protein and/or hetero-oligomers containing wild type CAV1 and CAV1-P158 may be targeted for degradation, thereby limiting detection of CAV1 in the ER and lipid droplets. In support of this idea, we found that CAV1-P158 was expressed at lower levels than wild type CAV1 in *Cav1*$^{-/-}$ MEFs and that total CAV1 protein levels were also

reduced in patient fibroblasts. In fact, we estimate that the mutant protein only represents about 25% of the total CAV1 protein levels in heterozygous patient cells (Figure 21). In further support of this hypothesis, preliminary data in *Cav1*$^{-/-}$ MEFs indicate that CAV1-P158 colocalizes with VCP/p97, a protein that chaperones candidate proteins to the proteasome for degradation (Figure S.9).

An alternative model explaining the apparent "normal" subcellular distribution of CAV1 in the heterozygous patient cells compared to co-transfected *Cav1*$^{-/-}$ MEFs is that a portion of hetero-oligomers are able to assemble into 70S complexes thereby masking the ER retrieval signal of the CAV1 mutant. This model is supported by biochemical experiments showing that compared to CAV1-P158 single transfection in *Cav1*$^{-/-}$ MEFs, co-expression with wild type CAV1 resulted in an increased amount of CAV1-P158 in DRMs which are thought to be enriched in 70S CAV1 and caveolae [8]. However, at the cellular level, CAV1-P158 was not detected in caveolae in *Cav1*$^{-/-}$ MEFs co-expressing wild type CAV1 with CAV1-P158. In fact, compared to control co-transfected cells, caveolae localization of wild type CAV1 was significantly reduced in cells co-expressing CAV1-P158. Further analysis will be required to resolve these discrepancies.

Although caveolae could be detected in patient fibroblasts, several features of caveolae and their associated proteins did however differ in the patient and control fibroblasts. First, decreased levels of CAV1 and fewer caveolae were present in patient cells. This is consistent with the observation that CAV1 protein levels are approximately 50% of control values. Second, decreased expression of CAV2 and several caveolae accessory proteins was also observed in patient cells. This is in agreement with reports of stabilization of CAV2 by CAV1 [11, 263], correlations between CAV1 and Cavin-1 expression levels [75], and relationships between Flotillins and caveolin expression [272-274]. Finally, CAV1 was less detergent resistant in patient fibroblasts compared to controls, and several accessory proteins also appeared to dissociate more readily from DRMs. The mechanism underlying this shift in detergent resistance is not yet known, but could potentially be indicative of changes in the lipid composition of caveolae in the patient cells.

Based on our experimental findings, we propose the following working model (Figure 34). First, in patient cells newly synthesized CAV1 monomers quickly oligomerize in the ER. Correctly assembled wild type CAV1 homo-oligomers exit the ER and are normally trafficked, while homo-oligomers of CAV1-P158 are retained in the ER where they are rapidly targeted for degradation thus reducing the available pool of functional CAV1 by 50%. Hetero-oligomers composed of both wild type CAV1 and CAV1-P158 are likely retrieved to the ER (supported by our data) and efficiently degraded. It is unclear if this occurs by ubiquitin-dependent/-independent proteasomal degradation, however preliminary cycloheximide chase experiments (not shown) suggest the mutant protein does indeed have a shortened half-life. This would result in haploinsufficiency, supporting the previous reports of reduced protein levels in these patients [16], and offers a possible explanation of why CAV1 is not detectible in the ER and lipid droplets in PAH patient fibroblasts. Experiments to assess the half-life and studies to identify the mechanism CAV1-P158 turnover are currently underway.

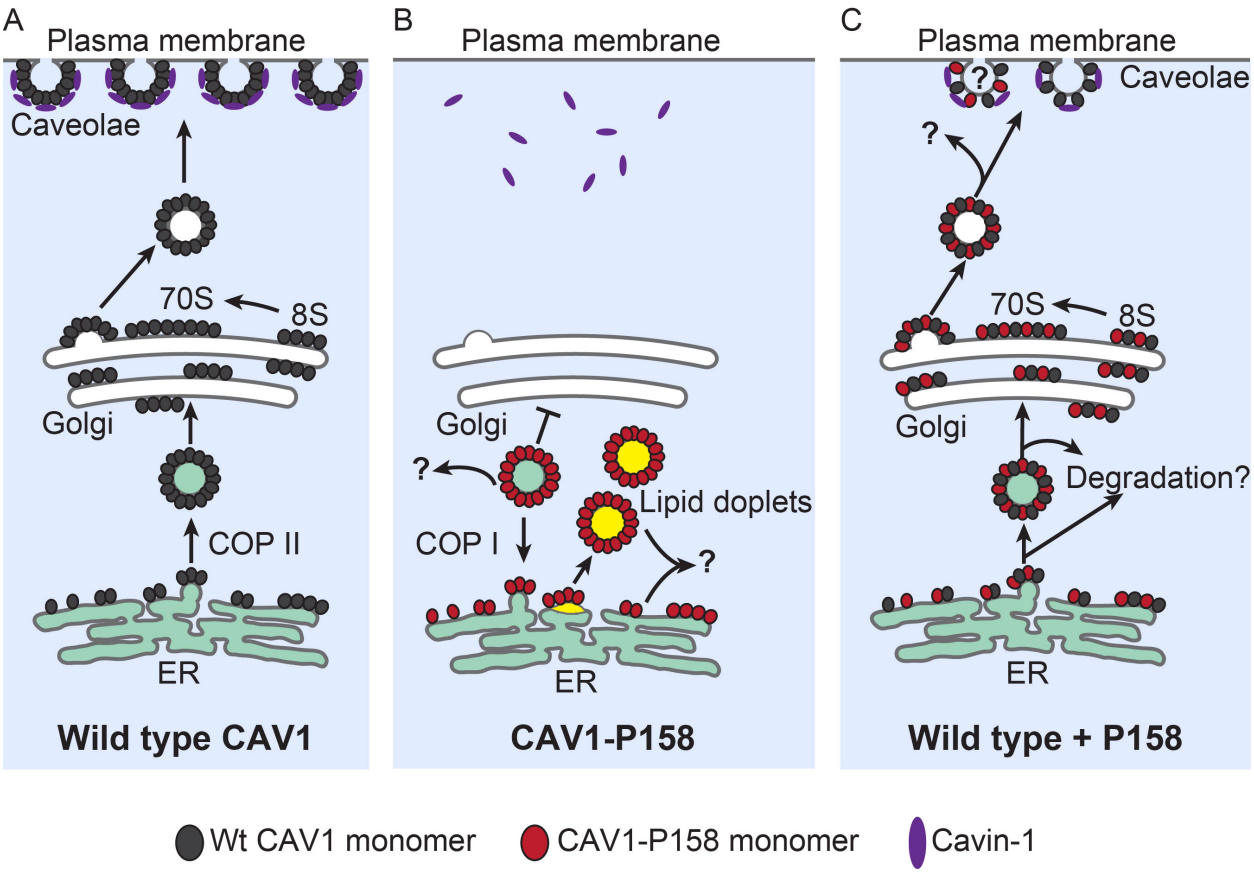

Figure 34. Proposed Model of CAV1-P158 Behavior, Trafficking and Subcellular Distribution in the Absence or Presence of Wild Type CAV1. **(A)** In control cells, wild type CAV1 efficiently exits the ER and is transported from the Golgi complex to the plasma membrane where it recruits Cavin-1 and forms caveolae. **(B)** Unlike wild type CAV1, CAV1-P158 is incapable of supporting caveolae formation or Cavin-1 recruitment when expressed on its own due to ER retention and lipid droplet targeting in *Cav1*$^{-/-}$ MEFs. **(C)** In heterozygous patient cells and co-transfected *Cav1*$^{-/-}$ MEFs, CAV1-P158 can form both 8S and 70S complexes, but these complexes are less stable compared to those formed by wild type CAV1. CAV1-P158 appears to be mostly excluded from caveolae, which are composed primarily of wild type CAV1 but also display defects in detergent resistance and Cavin-1 recruitment.

Our findings allow us to propose several potential mechanisms by which the PAH mutant form of CAV1 may contribute to disease. First, expression of the CAV1 mutant in patient cells impacts the ability of caveolae to function as membrane reservoirs in response to membrane stretching following hypo-osmotic challenge. The simplest explanation for this finding is that the decreased number of caveolae in patient cells decreases the amount of plasma membrane reserve that can be released in response to increased membrane tension induced by oncotic swelling, leading to more rapid rupture of the plasma membrane. Because the lung is composed of cells that are

especially rich in CAV1, decreased numbers of caveolae in the pulmonary arteries may help explain why the CAV1 mutation causes defects in pulmonary-vascular function [16]. Indeed, there is evidence that in both experimental and clinical forms of PAH, there is a loss of endothelial CAV1 [253]. In response to mechanical stress-induced membrane stretch, caveolae flatten and the caveolar accessory protein Cavin-1 is quickly released [268, 275]. Although the downstream consequences of the release of Cavin-1 and flattening are still not fully understood, it is likely that they are important for cell's adaptive responses to mechanical stimuli. In patient tissues primarily affected by disease, elevated vessel pressure/resistance associated with PAH may thus provide a persistent mechanical stimulus that triggers the pathological compensatory tissue remodeling observed in PAH. Further evaluation of the effects of mechanical stress on caveolae in endothelial and smooth muscle cells and mouse models should be able to verify this hypothesis in the future.

Secondly, CAV1 coordinates the activity of key modulators of vasoreactive pathways in endothelial cells in order to maintain vascular tone [276]. CAV1 deficiency causes pathological vascular remodeling and induces pulmonary hypertension in mice and humans [276]. In addition to down regulation of CAV1, we also observed decreased levels of CAV2 and the caveolar accessory proteins Cavin-1 and EHD-2 in patient cells. Flotillin-1 and Flotillin-2 levels were also decreased. These changes may also contribute to disease pathology given that several of these proteins are themselves key regulators of human health and disease [277-279]. Thus, down regulation of CAV1 and/or caveolae accessory proteins may have multiple consequences in signaling pathways relevant to PAH. Changes in CAV1 expression in patient cells may also differ between cell types. For example, although decreased levels of CAV1 were observed in endothelial cells in sections obtained from a lung biopsy from a PAH patient expressing the P158 frameshift mutant, CAV1 staining was still present in surrounding cell types [16]. Further work will be required to determine how expression of the CAV1 mutant impacts caveolae formation on a cell and tissue-specific level and contributes to the development of PAH.

CHAPTER 5

DISCUSSION AND FUTURE DIRECTIONS

5.1 General Discussion

5.1.1 Overview

The projects described in this dissertation were initiated on the basis of the discovery of novel CAV1 mutations associated with PAH and CGL. The goal of these studies was to characterize the mutant proteins and their effects on caveolae formation. Reduced CAV1 and caveolae have been previously implicated in clinical and experimental cases of CGL and PAH in the absence of preexisting CAV1 mutations. C-terminal mutations in CAV1 have also been shown to disrupt trafficking and the biochemical stability of CAV1 and CAV1 complexes. We therefore set out to test the hypothesis that the expression of CAV1-F160X and CAV1-P158 disrupts caveolae assembly and function as a consequence of defects in trafficking and CAV1 complex formation by these mutants. Our results indicate that CAV1-F160X is a novel example of a disease-associated mutant that causes caveolae defects without decreasing the overall cellular density of caveolae or disrupting their function as membrane buffers. We go on to report that CAV1-P158 functions as a dominant negative that ultimately reduces caveolae density. This disrupts the mechano-protective influence of caveolae on patient fibroblasts.

5.1.2 CAV1-F160X Truncation Mutant Associated with PAH and CGL

In chapter 3, the characterization of a CAV1-F160X mutant associated with PAH and CGL was described. Soon after we began studying this mutant, two groups independently reported the identification of CAV1-F160X associated with PAH and CGL in the same patient reported in our studies [14, 15]. Both groups reported reduced CAV1 protein levels in patient cells. However, the effects of the expression of this mutant protein on caveolae formation and function were not yet known. We tested the hypothesis that the decreased expression of CAV1 reduces caveolae formation and function as mechanical buffers in patient fibroblasts and reconstituted *Cav1*$^{-/-}$ MEFs

expressing CAV1-F160X. Contrary to our initial hypothesis, our studies show that expression of CAV1-F160X is not associated with reduced CAV1 protein levels or caveolae, and the function of caveolae in mechano-protection remained intact in CAV1-F160X patient cells. Despite an apparent normal caveolae density and morphology, CAV1-F160X co-assembles with wild type CAV1 into hybrid caveolae that show evidence of alterations in composition and decreased recruitment of the stabilizing caveolae accessory protein, Cavin-1, in patient cells. This shows that CAV1-F160X does not impact the abundance of caveolae but negatively affects the conformation of CAV1 and composition of caveolae.

I conclude that this mutant is behaving as a dominant negative and destabilizes CAV1 oligomers and caveolae. This finding expands on the current breadth of knowledge of known human phenotypes associated with CAV1 mutations and indicates that the CAV1-F160X is a novel example of a disease-associated CAV1 mutant that causes caveolae defects without decreasing the overall cellular density of caveolae. These findings further suggest that the formation of aberrant caveolae with decreased stability of CAV1 oligomers and/or weakened interactions between Cavin-1 and CAV1 in caveolae may contribute to the development of both PAH and CGL in this patient.

5.1.3 The Dominant Negative CAV1-P158 Mutant Associated with PAH

I began my research on CAV1-P158 after it was identified in a family of patients with PAH and no other known PAH-associated mutations [16]. Patients with this heterozygous mutation have reduced CAV1 protein levels in endothelial cells and skin fibroblasts, but it was unknown how this impacts caveolae formation and function. PAH primarily affects pulmonary microvascular endothelial cells [280], where endothelial caveolae play a role in protecting the these cells from mechanical stress and modulating the activity of signaling pathways that are important for maintaining vascular tone [3, 281-283], and are elevated in PAH. In order to address whether CAV1-P158 contributes to PAH by disrupting the mechano-protective properties, we wanted to test if this mutant disrupted caveolae formation and function as membrane buffers during mechanical stress. In Chapter 4, we show that a PAH-associated mutant of CAV1 (CAV1-P158)

contains an ER-retention/retrieval motif, targets to lipid droplets and does not form caveolae. These defects in turn negatively impact the ability of wild type CAV1 to form caveolae due to the formation of hetero-oligomers when co-expressed in *Cav1*$^{-/-}$ MEFs and presumably in heterozygous patient cells.

These findings thus reveal a novel dominant negative role of CAV1-P158 in disrupting caveolae formation and offer an explanation for the reduced CAV1 and caveolae levels observed in patient cells. Our findings also suggest that expression of the CAV1-P158 results in haploinsufficiency that reduces caveolae density in the heterozygous patient fibroblasts. Furthermore, the caveolae and CAV1 complexes that are present in patient cells show evidence of increased detergent solubility, as well as reduced Cavin-1 recruitment. As a consequence of caveolae deficiency, caveolae-dependent mechano-protection during osmotic swelling is diminished in patient fibroblasts. Consistent with the finding that endothelial mechano-protection is lost in mice with PAH [3], the negative effects of CAV1-P158 on caveolae density may be an underlying factor promoting the pathogenesis of PAH. However, ruling out other potential defects will require additional investigation. Taken together, I conclude that the dominant negative behavior of CAV1-P158 reduces caveolae formation and stability in heterozygous patient cells and this is a contributing factor to PAH.

5.1.4 Significance and Implications of Our Findings

A major challenge in defining the necessary requirements for caveolae function is that most routine experimental approaches either prevent caveolae formation from occurring or completely disrupt existing caveolae, promoting the disassembly of caveolae-related protein components. *Cav1* gene ablation in mice is associated with several comorbidities and phenotypic changes observed at the tissue/cell level that have established the importance of CAV1/caveolae expression in modulating many cellular pathways. Despite this breadth of knowledge gained from experiments that disrupt caveolae, the molecular basis of the observed abnormalities is poorly understood and remains an obstacle in the field. Our work to determine the impact of novel caveolin-1 frameshift mutants on caveolae assembly and function has not only expanded on our

knowledge of caveolin mutations associated with human disease, but has also provided insights into novel elements of caveolae biology that are important for the function of caveolae.

PAH is associated with elevated arterial pressure, a force that mechanically stretches endothelial cells lining vessel walls as they expand and contract to accommodate fluctuations in pressure. Caveolae buffer membranes from mechanical stress and we found that reduced caveolae formation in patient fibroblasts expressing CAV1-P158 is associated with reduced membrane buffering capacity. I propose that in the endothelium of these patients, diminished buffering capacity in this environment would negatively impact endothelial membrane integrity, and may be a contributing factor to the vascular damage/remodeling observed in PAH. Results from reconstitution experiments also suggest that the ER-retained mutant is rapidly turned over and behaves as a dominant negative. I hypothesize that in heterozygous patient cells, reduced CAV1 protein levels is a consequence of the formation of hybrid CAV1 oligomers composed of wild type CAV1 and CAV1-P158 that are retained in the ER and efficiently turned over. This is a plausible explanation for reduced CAV1-dependent caveolae formation.

Until now, an example of a naturally occurring CAV1 mutation that has no effect on the density of caveolae in cells yet results in severe comorbidities had not been described. Here, I show that this is the case for CAV1-F160X. Unlike CAV1-P158, caveolae formation is not reduced in CAV1-F160X fibroblasts and the function of caveolae as membrane buffers does not appear to be compromised. This shows that caveolar defects can exist with no obvious consequence on caveolae morphology and quantity. Additional results also suggest that the conformation of caveolae-associated CAV1 and/or the lipid composition of caveolae are abnormal in the patient's cells. This indicates that the appearance of morphological caveolae is not a sufficient determinant of caveolae function and it also implies that additional features of caveolae influence their functional capacity. However, how these changes affect other functions of

caveolae (compartmentalization and modulation of signaling molecules) is unclear and well need to be assessed in future studies.

Finally, both the CAV1-P158 and CAV1-F160X mutants exhibit reduced raft affinity in addition to notable defects in the biochemical properties of oligomers and higher order CAV1 complexes, without entirely disrupting the presence of morphological caveolae. This challenges the previous consensus that unstable oligomers formed by CAV1 mutants do not support caveolae formation and are generally intracellularly retained, never reaching the PM. Furthermore, reduced recruitment of the stabilizing accessory protein Cavin-1 (a PS and PIP_2-binding protein) was observed in patient and reconstituted cells, indicating further caveolar abnormalities. While additional experiments are needed to elucidate the underlying cause giving rise to these defects, a possible explanation is that the abnormalities negatively impact the structural stability of caveolae. Thus the molecular organization of caveolae structural components, and composition of lipids may represent new aspects of caveolae biology that are important for caveolae function.

These studies have led to the discovery of new components of caveolae organization that are important for function and identified additional elements that contribute to PAH and CGL that were previously unknown. With a better understanding of how the mutants impact caveolae, future investigation to determine now the defects impact cellular pathways that give rise to disease will be beneficial in identifying new therapeutic targets for the development of new drugs to treat PAH and CGL.

5.1.5 Concluding Remarks

The discovery of previously unidentified CAV1 mutants used in our studies gave us the exciting opportunity to expand on what is known about how CAV1 and caveolae can contribute to cellular defects underlying PAH and CGL. We examined the impact of the mutations on CAV1 oligomerization, DRM affinity, trafficking and localization. Our work revealed that altered stability of CAV1 oligomers and the assembly of caveolae with abnormal recruitment of accessory proteins gives rise to CAV1/caveolar defects without

entirely abrogating the formation of morphological caveolae. However, the reduced caveolae density in patient cells with the CAV1-P158 mutation appears to disrupt the buffering capacity of the plasma membrane during oncotic stretch experiments. Additionally, our experiments suggest that the lipid composition of caveolae and the conformation of CAV1 in caveolae are altered in patient cells expressing CAV1-F160X. We conclude that these defects are important contributing factors in the pathogenesis of disease. While it is unclear exactly why CAV1-F160X is associated with a more severe disease phenotype, further work will be necessary to begin assessing the underlying mechanisms that give rise to disease.

5.2 Future Directions

In this dissertation, the goal of my studies was to characterize newly identified disease-associated mutations affecting the C-terminus of CAV1 and their impact on caveolae assembly and function in order to delineate the contributions of these mutants to the pathogenesis of disease, which was previously unknown. Our work has expanded on what is currently known about disease-associated CAV1 mutations and shows that in addition to caveolae density, the mutants negatively impact the stability of CAV1 oligomers that are required to form caveolae and the recruitment of a stabilizing caveolae accessory protein (Cavin-1). While our work sheds light on underlying caveolar defects in patient cells, the experiments described in this dissertation do not address how these CAV1/caveolae defects give rise to disease. Therefore, in order understand how the caveolae defects described in this dissertation translate to the pathogenesis of PAH/CGL, it will be important to expand on our findings by studying additional functions or pathways modulated by CAV1/caveolae that are dysregulated during the development of disease.

Caveolae are important for maintaining the balance and organization of cholesterol in cellular membranes, which regulates the fluidity and lateral mobility of signaling molecules. Compartmentalization of signaling molecules and receptors in caveolae is important for modulating their activity and downstream signal transduction. An

appropriate next step to expand on this project is to define the underlying mechanisms of disease resulting from caveolae defects. It will be important to carry out future experiments that address the lipid composition of patient cells and activity of signaling pathways relevant to CGL/PAH in the next set of experiments.

5.2.1 Assessing the Lipid Composition of Patient Fibroblasts

We show that CAV1, CAV1 complexes and caveolae are abnormal in their composition and biochemical stability in patient fibroblasts. CAV1 is a cholesterol-binding protein [193], caveolae are enriched in cholesterol and membrane cholesterol modulates receptor activity. Cholesterol composition and receptor activity can become impaired when there is an imbalance in intracellular free cholesterol levels. Several lines of evidence from our studies suggest that the lipid and cholesterol composition of caveolae formed in patient cells are abnormal, which offers an explanation for the molecular and biochemical abnormalities we observed. First, the oligomers of CAV1 and DRMs in patient cells were less resistant to detergent extraction. Cholesterol is a contributing factor to the characteristic insolubility of CAV1 complexes and DRMs, which are efficiently disassembled when cholesterol/glycosphingolipid levels, or binding is perturbed [284-287]. Next, CAV1 was detectible at the plasma membrane of CAV1-F160X patient cells with an antibody that generally only detects CAV1 in the Golgi complex, before cholesterol binding and further oligomerization masks the epitope during transport from the Golgi to the PM. Only after cholesterol/lipid removal from cell membranes is this antibody able to label CAV1 at the plasma membrane in control cells [194]. This supports the hypothesis that the caveolae in the patient cells have an altered cholesterol composition. Lastly, reduced recruitment of Cavin-1 to caveolae, observed both biochemically and at the cellular level in CAV1-P158 and CAV-F160X patient cells, strongly suggests that PS and PIP_2 enrichment may be reduced because Cavin-1 binds to these lipid moieties and they are enriched in caveolae [85, 86].

To determine if instability of CAV1 complexes is the result of changes in the lipid composition in patient cells compared to controls, measurements of the levels and distribution of cholesterol, glycosphingolipids, sphingomyelin, PS and PIP_2 in isolated

CAV1-enriched DRMs by mass spectrometry could be performed. To complement this experiment, labeling cholesterol with filipin in control and patient labeled with CAV1 and Cavin-1 antibodies should be included in order to assess the distribution of cholesterol in caveolae. Comparing the colocalization by Pearson's Correlation between CAV1/Cavin-1 and filipin in control and patient cells will be useful to determine if cholesterol is inefficiently clustered in caveolae. It will also be beneficial to determine if the stability of CAV1 complexes in patient cells can be increased by modulating the levels of free cholesterol in patient cells. The levels of cholesterol can be increased by exogenous addition, or activation/inhibition of biosynthetic enzymes. Inhibition of these enzymes or pharmacological treatment of cells with statins or Methyl-β-cyclodextrin can effectively remove of free cholesterol from cells. If cholesterol influences the stability of CAV1 complexes and DRMs in patient fibroblasts, I would expect to observe an increased resistance to detergent solubilization.

Additional evidence that the stability of caveolae is abnormal in patient fibroblasts is indicated by reduced colocalization of the stabilizing caveolae accessory protein, Cavin-1 with CAV1 observed in patient fibroblasts. This suggests that Cavin-1 is inefficiently recruited to caveolae. Cavin-1 is a PS/PIP_2-binding protein and these lipids are abundant in caveolae [85, 86]. Thus, if the results of the experiments described above indicate reduced PS and PIP_2, this would support our previous finding of reduced recruitment of Cavin-1 to caveolae in patient fibroblast. If this is the case, including experiments to determine if Cavin-1 recruitment can be restored by enhancing the levels of PS and/or PIP_2 will further help establish the underlying cause of reduced Cavin-1 recruitment to caveolae. It will also be beneficial to include reciprocal experiments in control fibroblasts and test if depleting cellular PS/PIP_2 levels can disrupt Cavin-1 recruitment to caveolae. Addressing the lipid composition and Cavin-1 in the patient cells will be useful future directions to provide a better understanding of how CAV1 defects described in Chapters 3 and 4 affect caveolae, and possibly identify new therapeutic targets that can be used to augment caveolae function, and prevent disease.

5.2.2 Determining the Distribution and Activity of Signaling Molecules Found in Caveolae

In our characterization of the mutant proteins, we investigated the function of caveolae as membrane buffers due to their importance in protecting cells from mechanical stress, which is a pathophysiologically relevant process in the primary tissues affected by PAH. We found that the diminished amount of caveolae in PAH-patient cells expressing CAV1-P158 led to reduced mechano-protection. This was not the case for CAV1-F160X-expressing cells, which contain normal levels of caveolae. However, the fact that the CAV1-F160X is associated with a more severe phenotype including both PAH and CGL suggests that the caveolae defects we observed may negatively influence other functions of caveolae that remain unidentified. CAV1/caveolae have been shown to modulate numerous signaling pathways by compartmentalizing signaling molecules and receptors, many of which are known to be dysregulated in association with PAH and CGL. Caveolae-dependent spatial organization of signaling molecules is important for coordinating signal transduction. Based on the finding that the caveolae composition and recruitment of accessory proteins is altered in patient cells, it is reasonable to hypothesize that other proteins that localize to caveolae to modulate their functional/signaling activity are also inefficiently targeted to caveolae.

The development of PAH and CGL are accompanied by the dysregulation of several key regulators of vascular tone/remodeling (Ca^{2+} permeability, eNOS, BMPR2), metabolism (insulin receptor, fatty acid and glucose transporter) and proliferation/survival (cSrc, AKT) in the endothelium and adipose tissue [130, 136, 144, 213, 276, 288-290]. The highest amounts of caveolae are found in these tissues and CAV1/caveolae influence the signaling activity of the aforementioned “key regulators”. Caveolae deficiency is associated with mislocalization of signaling molecules and aberrant cell signaling that causes cellular dysfunction [130, 136, 144, 213, 276, 288-290]. Hence, in the context of cell types in the pulmonary microvasculature and adipose tissue, caveolae-dependent cellular dysfunction promotes the development of PAH and CGL, respectively. It will be imperative to assess whether the caveolae defects associated with CAV1-P158 and CAV1-F160X impair the localization and function of

known potentiators of PAH and CGL in future experiments as a step towards understanding the underlying mechanisms that promote the pathogenesis of both diseases in patient cells. It will also be important to determine if any potential signaling defects identified can be rescued by excessive ligand stimulation, by altering the membrane composition, or by augmenting caveolae formation.

Adipocyte caveolae compartmentalize the insulin receptor, which is critically important for coordinating the activation of signaling cascades that promote lipid storage, lipid mobilization, and glucose transport in response to insulin stimulation. Adipocyte dysfunction that causes lipodystrophy is associated with deficient lipid storage that is the result of diminished insulin signaling. Genetic mutations giving rise to caveolin-1 deficiency can cause CGL. The identification of CAV1-F160X in a patient with CGL has strong implications in defective lipid transport, storage, and utilization. However, these were not tested in our studies. I propose that the next step towards establishing a connection between the current findings, and the development of CGL is to investigate insulin receptor localization and activity in patient fibroblasts expressing CAV1-F160X, at the cellular level and biochemically. The insulin receptor phosphorylation occurs independently of caveolae localization; however, initiation of lipogenic signaling cascades and glucose transport only occurs when the receptor is in caveolae [144]. To determine if the insulin receptor is functioning properly in the abnormal caveolae present in patient cells, the localization of the receptor to caveolae will need to be assessed. In addition, testing the ability of insulin stimulation to recruit glucose transporters to caveolae will further indicate whether insulin signaling is intact in CAV1-F160X patient fibroblasts. Caveolae also protect adipocytes from lipotoxicity [199] and modulate fatty acid uptake [198], which may also be useful processes to explore as alternative approaches.

In the endothelium, in addition to providing mechano-protection, caveolae are important for mediating the activity of molecules that are implicated in vasoreactivity and vascular remodeling. These include BMPR2, eNOS, and cSrc, which all localize to caveolae [136, 276]. eNOS is not highly expressed in non-endothelial cells; however, BMPR2 and

cSrc expression is present in numerous cell types including human dermal fibroblasts. Therefore BMPR2 and cSrc are the best initial candidates to explore in order to gain the most meaningful insights from experiments carried out in the patient fibroblasts. Determining if these molecules are properly localized and activated in patient cells will be useful for understanding whether CAV1-related defects associated CAV1-P158 and CAV1-F160X expression disrupts these signaling pathways, which are also relevant in endothelial cells. Translating the results generated from these types of experiments in the context of endothelial cells could be used to predict the downstream effects on cellular function that are important for the pathogenesis PAH.

5.2.3 Investigating Lipid Droplet Function in Patient-Derived Cells

The accumulation of CAV1-P158 the ER and lipid droplets in reconstituted *Cav1*$^{-/-}$ cells was also an interesting finding but I did not address how the accumulation of the mutant protein affects the functions of this organelle. This phenotype was not detected in CAV1-P158 patient cells under basal conditions, likely because the mutant protein is efficiently turned over and has a shortened half-life when the protein is expressed under endogenous conditions. However, under conditions that promote ER-stress, ER-export is delayed and newly synthesized proteins such as caveolins accumulate in this compartment [270]. This eventually leads to secondary off-target trafficking of CAV1 to lipid droplets [270]. Furthermore, ER-stress is implicated in cell dysfunction that is associated with PAH [291]. While the expression of CAV1-P158 is low in patient cells, ER-stress associated with PAH, or enhancing CAV1 expression (as an attempt to treat PAH) in these patient cells may result in the accumulation of the mutant protein in the ER and have off target consequences on lipid droplet function. Caveolins can influence the size and morphology of lipid droplets [197]. This could also potentially influence the protein composition of the lipid droplet monolayer, which is important for modulating lipid droplet storage and mobilization. I propose that a logical test to perform next is to measure the lipid droplet protein composition in the presence and absence of CAV1-P158 as an indicator for potential defects in lipogenesis and lipolysis.

Taken together, the proposed experiments described in this section well be beneficial for delineating the underlying mechanisms of PAH and CGL as a result of heterozygous *CAV1* mutations and will also help identify potential therapeutic targets for treating both diseases.

Appendix

A

SUPPLEMENTARY FIGURES

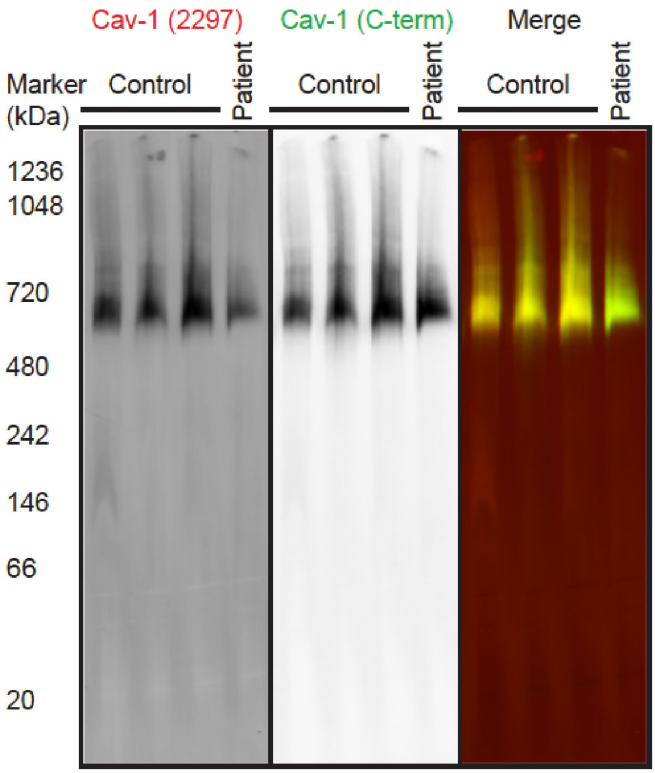

Supplemental Figure 1. BN-PAGE of CAV1 Oligomers in Control and Patient Fibroblasts. Associated with Figure 12. The epitope accessibility of CAV1 in high-molecular-weight oligomers is altered in patient cells. Control and patient skin fibroblasts were subjected to BN-PAGE followed by western blotting using CAV1 mAb 2297 (red in merge) and a C-terminally directed CAV1 antibody (green in merge). Note the relative decreased in labeling by mAb 2297 compared with labeling by the C-terminal antibody in patient cells relative to controls. Data are representative of 2 independent experiments. (Bing Han, Ph.D.)

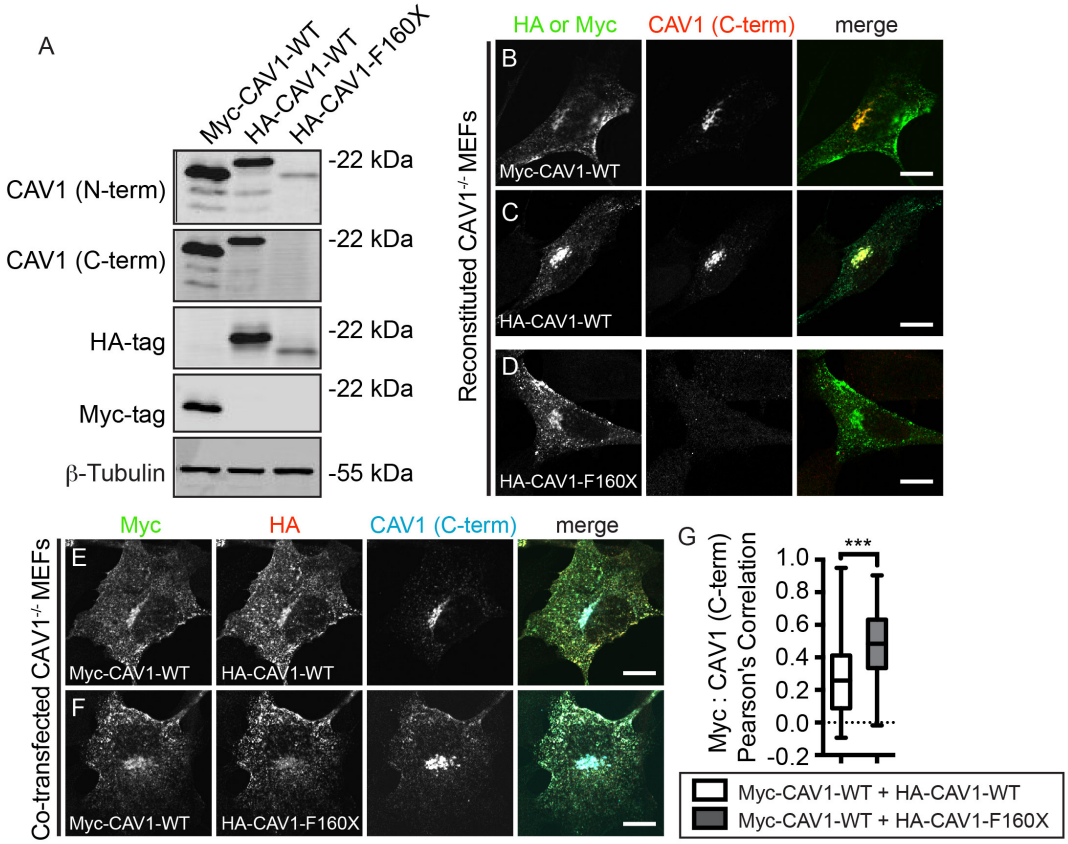

Supplemental Figure 2. Molecular Characterization of CAV1-F160X in *Cav1*$^{-/-}$ MEFs. Associated with Figures 15 and 16. A-C, The CAV1 C-terminal truncation mutant F160X is not recognized by a CAV1 C-term antibody. **(A)** Western blot of transfected *Cav1*$^{-/-}$ MEFs expressing the indicated CAV1 constructs. Antibodies to detect CAV1 or the epitope tags are indicated adjacent to each panel. β-tubulin was used as a control for equal loading. The C-terminally directed CAV1 antibody detects Myc-CAV1 **(B)** and HA-CAV1 **(C)** in transfected *Cav1*$^{-/-}$ MEFs, but does not label HA-F160X CAV1 **(D)** as detected by immunofluorescence microscopy. Scale bar, 10 μm. E and F, The C-terminus of wild-type CAV1 is exposed in extra-Golgi puncta in cells co-expressing wild-type CAV1 and CAV1-F160X. In these experiments, *Cav1*$^{-/-}$ MEFs co-expressing wild-type Myc-CAV1 and HA-CAV1 **(E)** or Myc-CAV1 and HA-CAV1-F160X **(F)** were labeled for Myc (green), HA (red), and the C-terminus of CAV1 (cyan). **G**, Myc-CAV1 colocalizes more strongly with anti-CAV1Cterm labeling when it is co-expressed with HA-CAV1-F160X than when it is co-expressed with wild-type HA-CAV1 (n = 77-90 ROIs from 3 independent experiments) (***P < .0001, Student's t test). Scale bars, 10 μm.

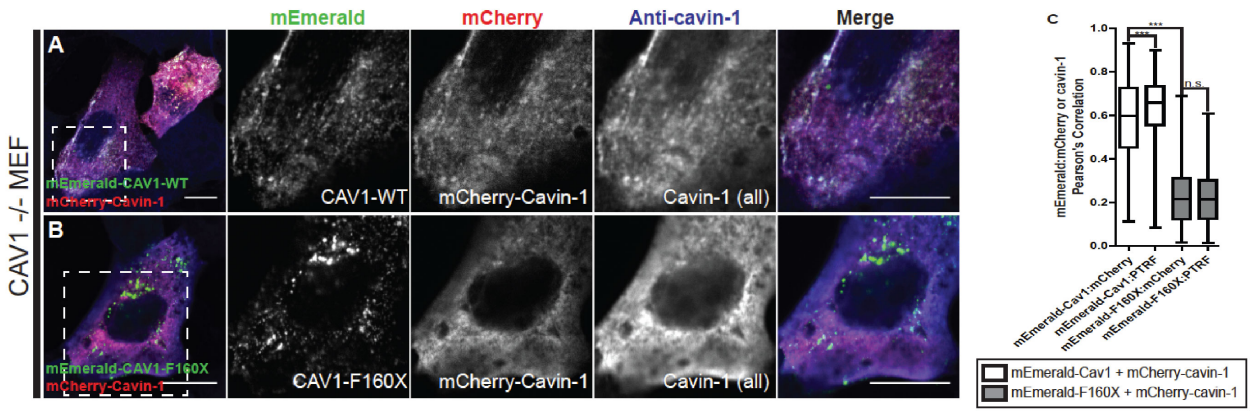

Supplemental Figure 3. Reconstitution of Exogenous CAV1 and Cavin-1 in *Cav1*$^{-/-}$ MEFs. Associated with Figure 16. A and B, Representative images of *Cav1*$^{-/-}$ MEFs cells co-transfected with mCherry-cavin1 (red) and either (A) wild-type mEmerald-CAV1 (green) or (B) mEmerald-F160X (green). Anti-cavin-1 antibody was used to label both endogenous and overexpressed cavin-1 (blue). C, unlike mEmerald-CAV1, mEmerald-CAV1-F160X fails to colocalize with either mCherry-cavin-1 or endogenous cavin-1 (n = 38-63 ROIs from 3 independent experiments) (***P < .0001, n.s., not significant, Student's t test). Scale bars, 10 μm. (Bing Han, Ph. D)

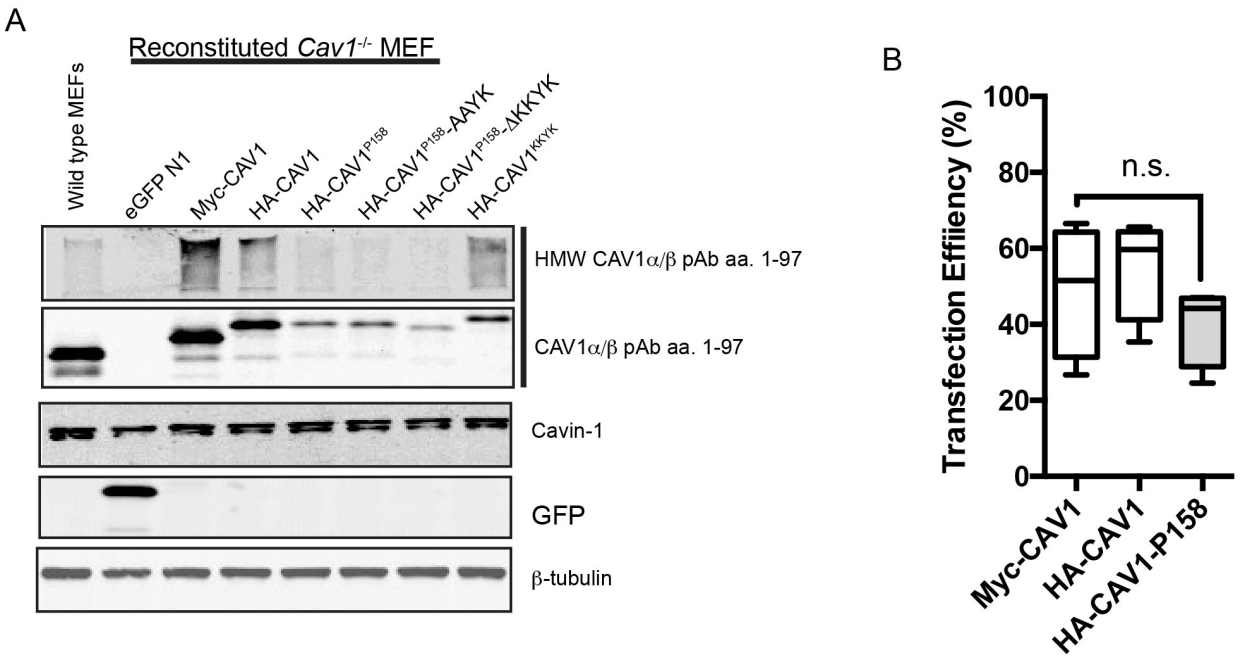

Supplemental Figure 4. CAV1-P158 Constructs are Detected at low Levels in *Cav1*$^{-/-}$ MEFs. Associated with Figures 21, 22, 24 and 25. **(A)** Western blot of transfected *Cav1*$^{-/-}$ MEFs. All reactions were transfected at the same time with the same transfection protocol. All samples were collected at the same time. As a control, wild type MEFs expressing endogenous Cav1 were included. CAV1 constructs were transfected into *Cav1*$^{-/-}$ MEFs and detected with the anti-CAV1 pAB (aa. 1-97) in the first two panels. Panel 1 and 2 depict high and low molecular weight CAV1 species, respectively. Panel 3: Endogenous Cavin-1. Panel 4: *Cav1*$^{-/-}$ MEFs transfected with an empty eGFP vector was used a transfection control, and eGFP was detected with a specific antibody. Panel 5: loading control. **(B)** The amount of transfected cells per total nuclei in an ROI (5 fields per coverslip) was calculated to quantify the transfection efficiency of wild type and CAV1-P158 constructs. The p-value between 3 replicate experiments was calculated using an ordinary one-way ANOVA. p=0.3528, not statistically significant.

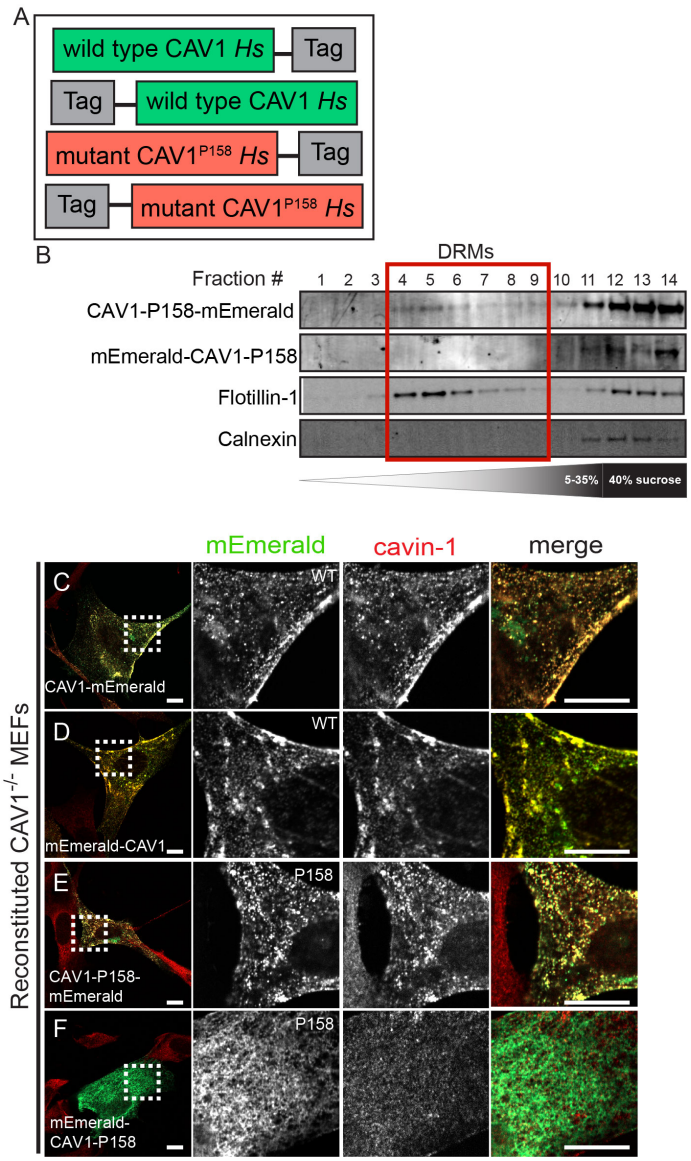

Supplemental Figure 5. Tag Orientation Influences the Trafficking and DRM Affinity of CAV1-P158 in *Cav1*$^{-/-}$ MEFs. Associated with Figure 22. **(A)** Schematic depicting wild type and mutant CAV1 constructs and respective tag orientations. **(B)** (Panel 1) C-terminally tagged CAV1-P158-mEmerald is detectible in DRMs (fractions 4-9) isolated transfected *Cav1*$^{-/-}$ MEFs. (Panel 2) N-terminally tagged mEmerald-CAV1-P158 is not associated with DRMs. (Panel 3) Detection of a positive control raft protein, Flotillin-1 in DRMs. (Panel 4) The non-raft protein, Calnexin is not detected in fractions corresponding to DRMs and served as a negative control. **(C-F)** Immunofluorescence staining of endogenous Cavin-1 in *Cav1*$^{-/-}$ MEFs (red) transfected with mEmerald constructs (green). **(C)** C-terminally tagged wild type CAV1-mEmerald. **(D)** N-terminally tagged wild type mEmerald-CAV1. **(E)** C-terminally tagged mutant CAV1-P158-mEmerald. **(F)** N-terminally tagged mutant mEmerald-CAV1-P158. Note the lack of colocalization between Cavin-1 and mEmerald-CAV1-P158 (F) compared to the other constructs (C-E). Scale bars represent 10μm. (B, Bing Han, Ph.D.)

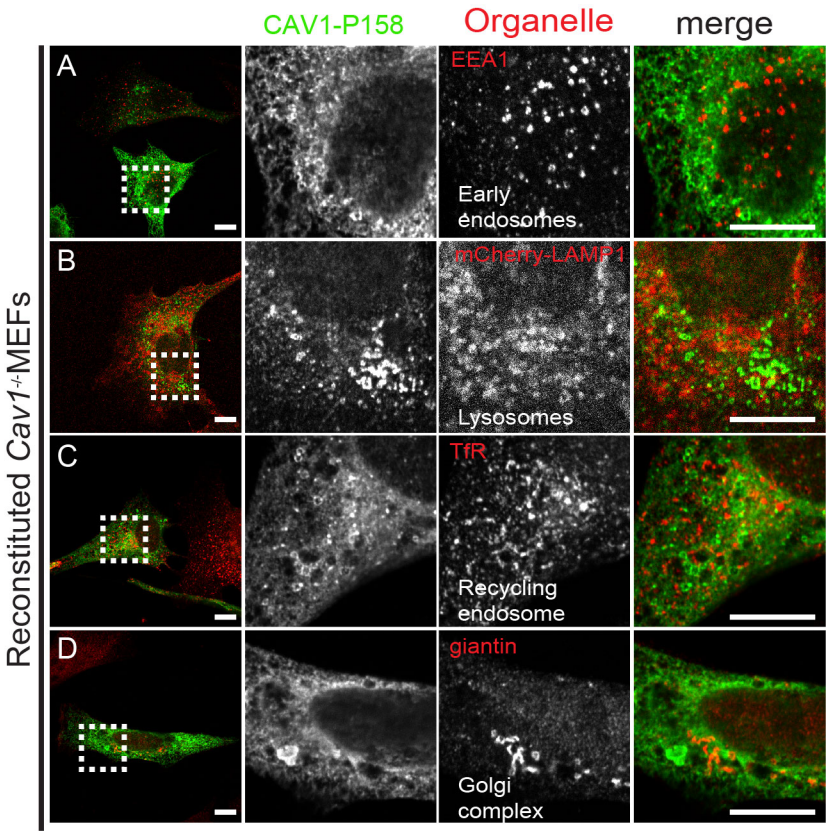

Supplemental Figure 6. CAV1-P158 Localizes to a Compartment that is Distinct from Several Organelles Examined. Associated with Figures 22 and 23. (**A-D)** *Cav1*$^{-/-}$ MEFs transfected with HA-CAV1-P158 (green) shows minimal colocalization with non-ER/lipid droplet compartments. **(A)** EEA1 immunofluorescence labeling early endosomes (red). **(B)** Lysosomes were labeled with a co-transfected plasmid encoding mCherry-LAMP1 (red). **(C)** Transferrin-receptor (TfR) immunofluorescence was used as an indicator for the recycling endosome (red). **(D)** Giantin immunofluorescence was used to label the Golgi complex. Scale bars represent 10μm.

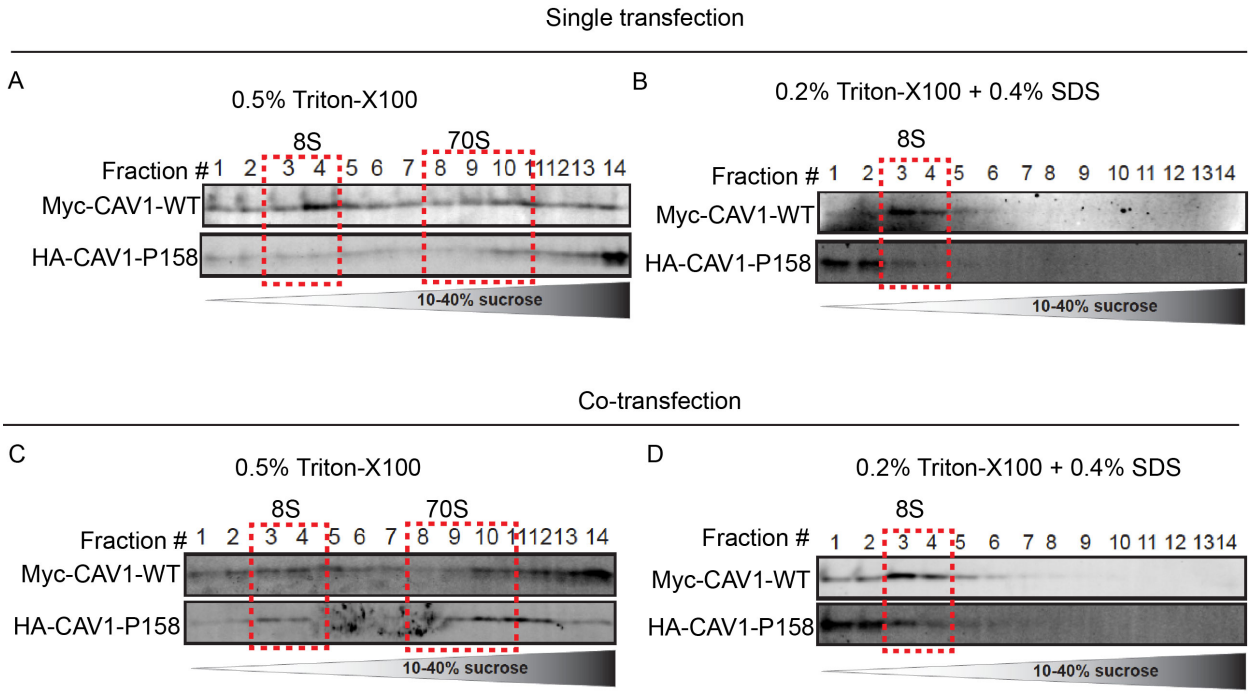

Supplemental Figure 7. Reduced Stability of CAV1 Complexes Containing CAV1-P158 in *Cav1*$^{-/-}$ MEFs. Associated with Figures 22 and 27. Samples were lysed in either 0.5% Triton X-100 **(A, C)** or 0.2% Triton X-100 and 0.4% SDS **(B, D)** at room temperature. Extracts were run though 10-40% sucrose velocity gradients and fractions were analyzed by SDS-PAGE followed by Western blotting. *Cav1*$^{-/-}$ MEFs expressing **(A, B)** Myc-CAV1 (top panel) or HA-CAV1-P158 (bottom panel). **(A)** CAV1 is readily detected in fractions corresponding to 8S and 70S complexes in *Cav1*$^{-/-}$ MEFs co-transfected with wild type CAV1 (top panel), and to a lesser extent when transfected with CAV1-P158 (bottom panel). **(B)** SDS has no effect on wild type CAV1, and CAV1 remains detectible in fractions corresponding to 8S complexes (top panel). A diminished amount of CAV1-P158 is detectible in 8S fractions upon addition of SDS (bottom panel). **(C, D)** *Cav1*$^{-/-}$ MEFs co-expressing HA-CAV1-P158 and Myc-CAV1. **(C)** In the absence, both wild type (top panel) and mutant CAV1 (bottom panel) are detectible in fractions corresponding to 8S and 70S complexes. **(D)** Wild type CAV1 (top panel) and CAV1-P158 (bottom panel) are detectible in 8S complexes that are resistant to SDS. Note the increase of CAV1-P158 detected in 8S fractions compared to that in **B**. Despite this apparent enhancement, a large amount of CAV1-P158 is still disassembled by SDS, and a smaller portion of wild type CAV1 also appears to become sensitive to SDS. (Bing Han, Ph.D.)

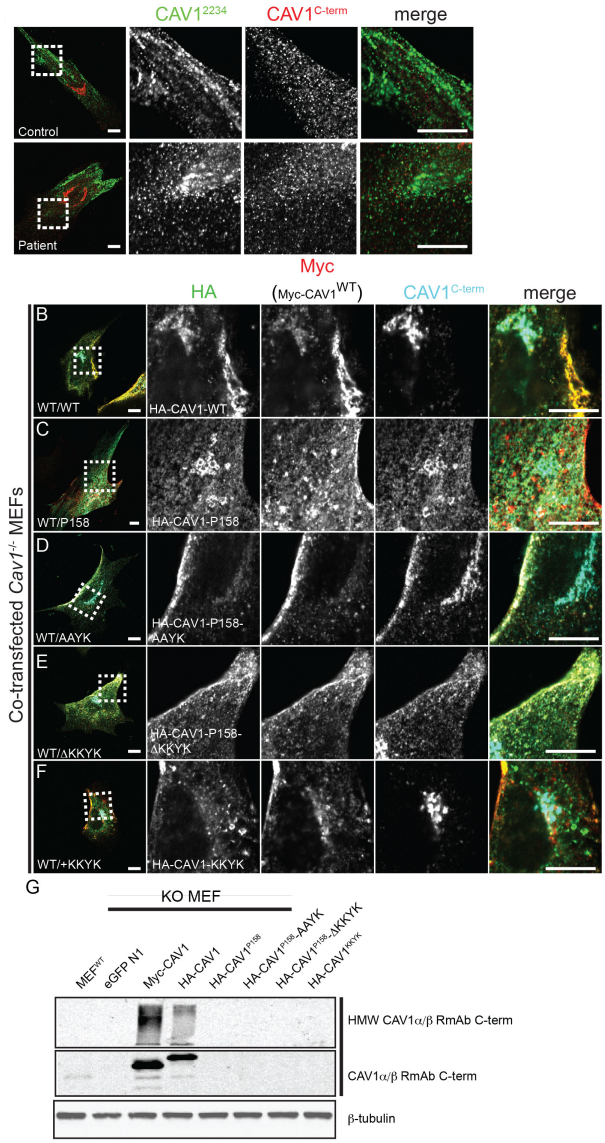

Supplemental Figure 8. The C-Terminus of Wild Type CAV1 is Unmasked in Caveolae Formed in *Cav1*$^{-/-}$ MEFs Co-Expressing Experimental CAV1 Mutants. Associated with Figures 21, and 25-28. **(A)** Control (top) and patient fibroblasts (bottom). Caveolae associated CAV1 labeled with an N-terminally directed CAV1 antibody (green) and Golgi-associated CAV1 labeled with a C-terminally directed antibody (red) do not colocalize. **(B-F)** Anti-CAV1-C-term staining (cyan) in *Cav1*$^{-/-}$ MEFs co-transfected with a wild type CAV1 construct (Myc-CAV1, red) and other HA-tagged CAV1 constructs (green). **(B)** CAV1-Cterm predominantly labels the Golgi complex (cyan) in *Cav1*$^{-/-}$ MEFs co-expressing two wild type forms of CAV1 (Myc-CAV1 and HA-CAV1). **(C-F)** Co-transfections with HA-CAV1-P158, HA-CAV1-P158-AAYK, HA-CAV1-P158-ΔKKYK, and HA-CAV1-KKYK show enhanced epitope accessibility of the C-terminal specific CAV1 antibody labeling of wild type CAV1 (Myc-CAV1, red) in spots indicative of caveolae labeling, outside of the Golgi Complex in co-transfected *Cav1*$^{-/-}$ MEFs co-expressing: **(C)** HA-CAV1-P158 (green), **(D)** HA-CAV1-P158-AAYK (green), **(F)** HA-CAV1-P158-ΔKKYK (green) and **(E)** HA-CAV1-KKYK (green). **(F)** *Cav1*$^{-/-}$ MEFs singly transfected with HA-CAV1-P158, HA-CAV1-P158-AAYK, HA-CAV1-P158-ΔKKYK, and HA-CAV1-KKYK are not recognized by the CAV1C-term antibody via Western blot. β-tubulin served as a control for equal loading. Scale bars represent 10μm.

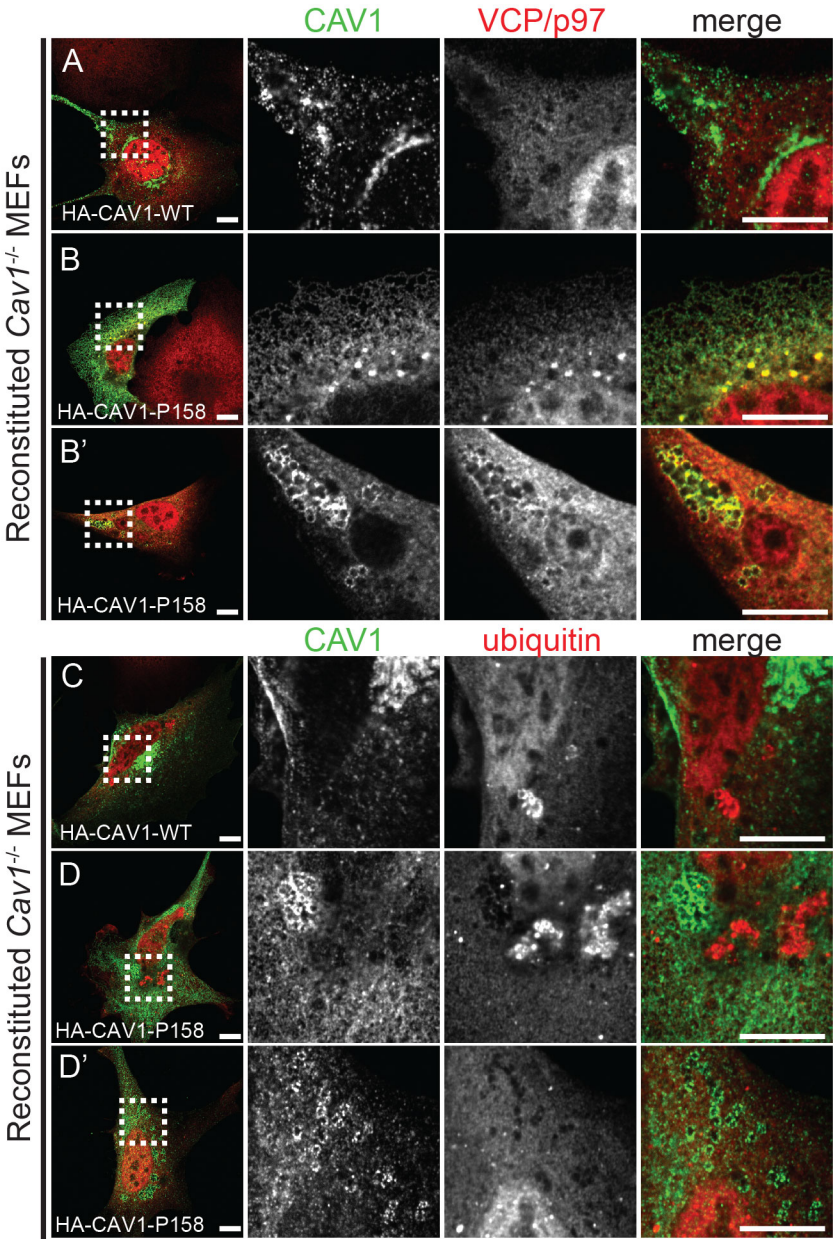

Supplemental Figure 9. Dilysine-Containing CAV1 Constructs Partially Colocalize with a Component of the Ubiquitin-Proteasome System. Associated with Figure 21 and Figure S.4. Immunofluorescence staining of VCP/p97 and ubiquitin labeled in red in transfected *Cav1*$^{-/-}$ MEFs. **(A)** HA-CAV1 (green), VCP/p97 (red) do not colocalize. **(B, B')** HA-CAV1P158 (green) and VCP/p97 partially colocalize with each other. (C-D') No ubiquitin colocalization is detected in wild type CAV1 or CAV1-P158. Scale bars represent 10μm.

REFERENCES

1. Palade GE, Fine structure of blood caillaries. Journal of Applied Physics, 1953. 24: p. 1424.
2. Yamada E, The fine structure of the gall bladder epithelium of the mouse. J Biophys Biochem Cytol, 1955. 1(5): p. 445-458.
3. Cheng JP, Mendoza-Topaz C, Howard G, Chadwick J, Shvets E, Cowburn AS, Dunmore BJ, Crosby A, Morrell NW, Nichols BJ, Caveolae protect endothelial cells from membrane rupture during increased cardiac output. J Cell Biol, 2015. 211(1): p. 53-61.
4. Ariotti N, Fernandez-Rojo MA, Zhou Y, Hill MM, Rodkey TL, Inder KL, Tanner LB, Wenk MR, Hancock JF, Parton RG, Caveolae regulate the nanoscale organization of the plasma membrane to remotely control ras signaling. J Cell Biol, 2014. 204(5): p. 777-792.
5. Blouin CM, Le Lay S, Eberl A, Kofeler HC, Guerrera IC, Klein C, Le Liepvre X, Lasnier F, Bourron O, Gautier JF, Ferre P, Hajduch E, Dugail I, Lipid droplet analysis in caveolin-deficient adipocytes: Alterations in surface phospholipid composition and maturation defects. J Lipid Res, 2010. 51(5): p. 945-956.
6. Galbiati F, Volonte D, Engelman JA, Watanabe G, Burk R, Pestell RG, Lisanti MP, Targeted downregulation of caveolin-1 is sufficient to drive cell transformation and hyperactivate the p42/44 map kinase cascade. EMBO J, 1998. 17(22): p. 6633-6648.
7. Parton RG, Hanzal-Bayer M, Hancock JF, Biogenesis of caveolae: A structural model for caveolin-induced domain formation. J Cell Sci, 2006. 119(Pt 5): p. 787-796.
8. Hayer A, Stoeber M, Bissig C, Helenius A, Biogenesis of caveolae: Stepwise assembly of large caveolin and cavin complexes. Traffic, 2010. 11(3): p. 361-382.
9. Monier S, Parton RG, Vogel F, Behlke J, Henske A, Kurzchalia TV, Vip21-caveolin, a membrane protein constituent of the caveolar coat, oligomerizes in vivo and in vitro. Mol Biol Cell, 1995. 6(7): p. 911-927.
10. Lee H, Park DS, Razani B, Russell RG, Pestell RG, Lisanti MP, Caveolin-1 mutations (p132l and null) and the pathogenesis of breast cancer. The American Journal of Pathology, 2002. 161(4): p. 1357-1369.
11. Razani B, Engelman JA, Wang XB, Schubert W, Zhang XL, Marks CB, Macaluso F, Russell RG, Li M, Pestell RG, Di Vizio D, Hou H, Jr., Kneitz B, Lagaud G, Christ GJ, Edelmann W, Lisanti MP, Caveolin-1 null mice are viable but show evidence of hyperproliferative and vascular abnormalities. J Biol Chem, 2001. 276(41): p. 38121-38138.
12. Cao H, Alston L, Ruschman J, Hegele RA, Heterozygous cav1 frameshift mutations (mim 601047) in patients with atypical partial lipodystrophy and hypertriglyceridemia. Lipids Health Dis, 2008. 7: p. 3-3.
13. Han B, Copeland CA, Kawano Y, Rosenzweig EB, Austin ED, Shahmirzadi L, Tang S, Raghunathan K, Chung WK, Kenworthy AK, Characterization of a caveolin-1 mutation associated with both pulmonary arterial hypertension and congenital generalized lipodystrophy. Traffic, 2016.
14. Schrauwen I, Szelinger S, Siniard AL, Kurdoglu A, Corneveaux JJ, Malenica I, Richholt R, Van Camp G, De Both M, Swaminathan S, Turk M, Ramsey K, Craig DW, Narayanan V, Huentelman MJ, A frame-shift mutation in cav1 is associated with a severe neonatal progeroid and lipodystrophy syndrome. PLoS ONE, 2015. 10(7): p. e0131797.
15. Garg A, Kircher M, Del Campo M, Amato RS, Agarwal AK, University of Washington Center for Mendelian G, Whole exome sequencing identifies de novo heterozygous cav1 mutations associated with a novel neonatal onset lipodystrophy syndrome. Am J Med Genet A, 2015.
16. Austin ED, Ma L, LeDuc C, Berman Rosenzweig E, Borczuk A, Phillips JA, 3rd, Palomero T, Sumazin P, Kim HR, Talati MH, West J, Loyd JE, Chung WK, Whole exome sequencing to identify a novel gene (caveolin-1) associated with human pulmonary arterial hypertension. Circ Cardiovasc Genet, 2012. 5(3): p. 336-343.
17. Bernardino de la Serna J, Schütz GJ, Eggeling C, Cebecauer M, There is no simple model of the plasma membrane organization. Frontiers in Cell and Developmental Biology, 2016. 4: p. 106.
18. Laude AJ, Prior IA, Plasma membrane microdomains: Organisation, function and trafficking. Mol

Membr Biol, 2004. 21(3): p. 193-205.
19. Shaw AS, Lipid rafts: Now you see them, now you don't. Nat Immunol, 2006. 7(11): p. 1139-1142.
20. McIntosh Thomas J, Stepping between membrane microdomains. Biophys J, 2015. 108(4): p. 783-784.
21. Echarri A, Del Pozo MA, Caveolae - mechanosensitive membrane invaginations linked to actin filaments. J Cell Sci, 2015. 128(15): p. 2747-2758.
22. Corrotte M, Almeida PE, Tam C, Castro-Gomes T, Fernandes MC, Millis BA, Cortez M, Miller H, Song W, Maugel TK, Andrews NW, Caveolae internalization repairs wounded cells and muscle fibers. Elife, 2013. 2: p. e00926.
23. Singh RD, Puri V, Valiyaveettil JT, Marks DL, Bittman R, Pagano RE, Selective caveolin-1-dependent endocytosis of glycosphingolipids. Mol Biol Cell, 2003. 14(8): p. 3254-3265.
24. Sharma DK, Brown JC, Choudhury A, Peterson TE, Holicky E, Marks DL, Simari R, Parton RG, Pagano RE, Selective stimulation of caveolar endocytosis by glycosphingolipids and cholesterol. Mol Biol Cell, 2004. 15(7): p. 3114-3122.
25. Chaudhary N, Gomez GA, Howes MT, Lo HP, McMahon KA, Rae JA, Schieber NL, Hill MM, Gaus K, Yap AS, Parton RG, Endocytic crosstalk: Cavins, caveolins, and caveolae regulate clathrin-independent endocytosis. PLoS Biol, 2014. 12(4): p. e1001832.
26. Shaul PW, Anderson RG, Role of plasmalemmal caveolae in signal transduction. Am J Physiol, 1998. 275(5 Pt 1): p. L843-851.
27. Pohl J, Ring A, Stremmel W, Uptake of long-chain fatty acids in hepg2 cells involves caveolae: Analysis of a novel pathway. J Lipid Res, 2002. 43(9): p. 1390-1399.
28. Pohl J, Ring A, Ehehalt R, Schulze-Bergkamen H, Schad A, Verkade P, Stremmel W, Long-chain fatty acid uptake into adipocytes depends on lipid raft function. Biochemistry, 2004. 43(14): p. 4179-4187.
29. Roy S, Luetterforst R, Harding A, Apolloni A, Etheridge M, Stang E, Rolls B, Hancock JF, Parton RG, Dominant-negative caveolin inhibits h-ras function by disrupting cholesterol-rich plasma membrane domains. Nat Cell Biol, 1999. 1(2): p. 98-105.
30. Yu J, Bergaya S, Murata T, Alp IF, Bauer MP, Lin MI, Drab M, Kurzchalia TV, Stan RV, Sessa WC, Direct evidence for the role of caveolin-1 and caveolae in mechanotransduction and remodeling of blood vessels. J Clin Invest, 2006. 116(5): p. 1284-1291.
31. Sinha B, Köster D, Ruez R, Gonnord P, Bastiani M, Abankwa D, Stan RV, Butler-Browne G, Vedie B, Johannes L, Morone N, Parton RG, Raposo G, Sens P, Lamaze C, Nassoy P, Cells respond to mechanical stress by rapid disassembly of caveolae. Cell, 2011. 144(3): p. 402-413.
32. Mercier I, Jasmin JF, Pavlides S, Minetti C, Flomenberg N, Pestell RG, Frank PG, Sotgia F, Lisanti MP, Clinical and translational implications for the caveolin gene family: Lessons from mouse models and human genetic disorders. Laboratory investigation; a journal of technical methods and pathology, 2009. 89(6): p. 614-623.
33. Kwon H, Jeong K, Hwang EM, Park JY, Pak Y, A novel domain of caveolin-2 that controls nuclear targeting: Regulation of insulin-specific erk activation and nuclear translocation by caveolin-2. J Cell Mol Med, 2011. 15(4): p. 888-908.
34. Fuhs SR, Insel PA, Caveolin-3 undergoes sumoylation by the sumo e3 ligase piasy: Sumoylation affects g-protein-coupled receptor desensitization. J Biol Chem, 2011. 286(17): p. 14830-14841.
35. Venema VJ, Ju H, Zou R, Venema RC, Interaction of neuronal nitric-oxide synthase with caveolin-3 in skeletal muscle. Identification of a novel caveolin scaffolding/inhibitory domain. J Biol Chem, 1997. 272(45): p. 28187-28190.
36. Sverdlov M, Shajahan AN, Minshall RD, Tyrosine phosphorylation-dependence of caveolae-mediated endocytosis. J Cell Mol Med, 2007. 11(6): p. 1239-1250.
37. Scherer PE, Tang Z, Chun M, Sargiacomo M, Lodish HF, Lisanti MP, Caveolin isoforms differ in their n-terminal protein sequence and subcellular distribution. Identification and epitope mapping of an isoform-specific monoclonal antibody probe. J Biol Chem, 1995. 270(27): p. 16395-16401.
38. Fujimoto T, Kogo H, Nomura R, Une T, Isoforms of caveolin-1 and caveolar structure. J Cell Sci, 2000. 113 Pt 19: p. 3509-3517.
39. Ramirez MI, Pollack L, Millien G, Cao YX, Hinds A, Williams MC, The alpha-isoform of caveolin-1

is a marker of vasculogenesis in early lung development. J Histochem Cytochem, 2002. 50(1): p. 33-42.
40. Nohe A, Keating E, Underhill TM, Knaus P, Petersen NO, Dynamics and interaction of caveolin-1 isoforms with bmp-receptors. J Cell Sci, 2005. 118(Pt 3): p. 643-650.
41. Sargiacomo M, Scherer PE, Tang Z, Kubler E, Song KS, Sanders MC, Lisanti MP, Oligomeric structure of caveolin: Implications for caveolae membrane organization. Proc Natl Acad Sci U S A, 1995. 92(20): p. 9407-9411.
42. Li S, Couet J, Lisanti MP, Src tyrosine kinases, galpha subunits, and h-ras share a common membrane-anchored scaffolding protein, caveolin. Caveolin binding negatively regulates the auto-activation of src tyrosine kinases. J Biol Chem, 1996. 271(46): p. 29182-29190.
43. Couet J, Li S, Okamoto T, Ikezu T, Lisanti MP, Identification of peptide and protein ligands for the caveolin-scaffolding domain. Implications for the interaction of caveolin with caveolae-associated proteins. J Biol Chem, 1997. 272(10): p. 6525-6533.
44. Das K, Lewis RY, Scherer PE, Lisanti MP, The membrane-spanning domains of caveolins-1 and -2 mediate the formation of caveolin hetero-oligomers. Implications for the assembly of caveolae membranes in vivo. J Biol Chem, 1999. 274(26): p. 18721-18728.
45. Root KT, Plucinsky SM, Glover KJ, Recent progress in the topology, structure, and oligomerization of caveolin: A building block of caveolae. Curr Top Membr, 2015. 75: p. 305-336.
46. Aoki S, Thomas A, Decaffmeyer M, Brasseur R, Epand RM, The role of proline in the membrane re-entrant helix of caveolin-1. J Biol Chem, 2010. 285(43): p. 33371-33380.
47. Rui H, Root KT, Lee J, Glover KJ, Im W, Probing the u-shaped conformation of caveolin-1 in a bilayer. Biophys J, 2014. 106(6): p. 1371-1380.
48. Schlegel A, Lisanti MP, A molecular dissection of caveolin-1 membrane attachment and oligomerization. Two separate regions of the caveolin-1 c-terminal domain mediate membrane binding and oligomer/oligomer interactions in vivo. J Biol Chem, 2000. 275(28): p. 21605-21617.
49. Monier S, Dietzen DJ, Hastings WR, Lublin DM, Kurzchalia TV, Oligomerization of vip21-caveolin in vitro is stabilized by long chain fatty acylation or cholesterol. FEBS Lett, 1996. 388(2-3): p. 143-149.
50. Fujimoto T, Kogo H, Ishiguro K, Tauchi K, Nomura R, Caveolin-2 is targeted to lipid droplets, a new “membrane domain” in the cell. J Cell Biol, 2001. 152(5): p. 1079-1086.
51. Scherer PE, Lewis RY, Volonte D, Engelman JA, Galbiati F, Couet J, Kohtz DS, van Donselaar E, Peters P, Lisanti MP, Cell-type and tissue-specific expression of caveolin-2. Caveolins 1 and 2 co-localize and form a stable hetero-oligomeric complex in vivo. J Biol Chem, 1997. 272(46): p. 29337-29346.
52. Sowa G, Novel insights into the role of caveolin-2 in cell- and tissue-specific signaling and function. Biochemistry Research International, 2011. 2011: p. 809259.
53. Mora R, Caveolin-2 localizes to the golgi complex but redistributes to plasma membrane, caveolae, and rafts when co-expressed with caveolin-1. Journal of Biological Chemistry, 1999. 274(36): p. 25708-25717.
54. Razani B, Wang XB, Engelman JA, Battista M, Lagaud G, Zhang XL, Kneitz B, Hou H, Christ GJ, Edelmann W, Lisanti MP, Caveolin-2-deficient mice show evidence of severe pulmonary dysfunction without disruption of caveolae. Molecular and Cellular Biology, 2002. 22(7): p. 2329-2344.
55. Sowa G, Pypaert M, Fulton D, Sessa WC, The phosphorylation of caveolin-2 on serines 23 and 36 modulates caveolin-1-dependent caveolae formation. Proc Natl Acad Sci U S A, 2003. 100(11): p. 6511-6516.
56. Liu Y, Jang S, Xie L, Sowa G, Host deficiency in caveolin-2 inhibits lung carcinoma tumor growth by impairing tumor angiogenesis. Cancer Res, 2014. 74(22): p. 6452-6462.
57. de Almeida CJ, Jasmin JF, Del Galdo F, Lisanti MP, Genetic ablation of caveolin-2 sensitizes mice to bleomycin-induced injury. Cell Cycle, 2013. 12(14): p. 2248-2254.
58. Xie L, Frank PG, Lisanti MP, Sowa G, Endothelial cells isolated from caveolin-2 knockout mice display higher proliferation rate and cell cycle progression relative to their wild-type counterparts. American Journal of Physiology - Cell Physiology, 2010. 298(3): p. C693-C701.

59. Lee S, Kwon H, Jeong K, Pak Y, Regulation of cancer cell proliferation by caveolin-2 down-regulation and re-expression. Int J Oncol, 2011. 38(5): p. 1395-1402.
60. de Almeida CJ, Witkiewicz AK, Jasmin J-F, Tanowitz HB, Sotgia F, Frank PG, Lisanti MP, Caveolin-2-deficient mice show increased sensitivity to endotoxemia. Cell Cycle, 2011. 10(13): p. 2151-2161.
61. Way M, Parton RG, M-caveolin, a muscle-specific caveolin-related protein. FEBS Lett, 1996. 378(1): p. 108-112.
62. Song KS, Scherer PE, Tang Z, Okamoto T, Li S, Chafel M, Chu C, Kohtz DS, Lisanti MP, Expression of caveolin-3 in skeletal, cardiac, and smooth muscle cells. Caveolin-3 is a component of the sarcolemma and co-fractionates with dystrophin and dystrophin-associated glycoproteins. J Biol Chem, 1996. 271(25): p. 15160-15165.
63. Minetti C, Sotgia F, Bruno C, Scartezzini P, Broda P, Bado M, Masetti E, Mazzocco M, Egeo A, Donati MA, Volonte D, Galbiati F, Cordone G, Bricarelli FD, Lisanti MP, Zara F, Mutations in the caveolin-3 gene cause autosomal dominant limb-girdle muscular dystrophy. Nat Genet, 1998. 18(4): p. 365-368.
64. Parton RG, Way M, Zorzi N, Stang E, Caveolin-3 associates with developing t-tubules during muscle differentiation. J Cell Biol, 1997. 136(1): p. 137.
65. Ralston E, Ploug T, Caveolin-3 is associated with the t-tubules of mature skeletal muscle fibers. Exp Cell Res, 1999. 246(2): p. 510-515.
66. Galbiati F, Engelman JA, Volonte D, Zhang XL, Minetti C, Li M, Hou H, Jr., Kneitz B, Edelmann W, Lisanti MP, Caveolin-3 null mice show a loss of caveolae, changes in the microdomain distribution of the dystrophin-glycoprotein complex, and t-tubule abnormalities. J Biol Chem, 2001. 276(24): p. 21425-21433.
67. Oshikawa J, Otsu K, Toya Y, Tsunematsu T, Hankins R, Kawabe J, Minamisawa S, Umemura S, Hagiwara Y, Ishikawa Y, Insulin resistance in skeletal muscles of caveolin-3-null mice. Proc Natl Acad Sci U S A, 2004. 101(34): p. 12670-12675.
68. Woodman SE, Park DS, Cohen AW, Cheung MW, Chandra M, Shirani J, Tang B, Jelicks LA, Kitsis RN, Christ GJ, Factor SM, Tanowitz HB, Lisanti MP, Caveolin-3 knock-out mice develop a progressive cardiomyopathy and show hyperactivation of the p42/44 mapk cascade. J Biol Chem, 2002. 277(41): p. 38988-38997.
69. Talukder MAH, Preda M, Ryzhova L, Prudovsky I, Pinz IM, Heterozygous caveolin-3 mice show increased susceptibility to palmitate-induced insulin resistance. Physiological Reports, 2016. 4(6): p. e12736.
70. Galbiati F, Volonte D, Minetti C, Bregman DB, Lisanti MP, Limb-girdle muscular dystrophy (lgmd-1c) mutants of caveolin-3 undergo ubiquitination and proteasomal degradation. Treatment with proteasomal inhibitors blocks the dominant negative effect of lgmd-1c mutanta and rescues wild-type caveolin-3. J Biol Chem, 2000. 275(48): p. 37702-37711.
71. Galbiati F, Razani B, Lisanti MP, Caveolae and caveolin-3 in muscular dystrophy. Trends in Molecular Medicine, 2001. 7(10): p. 435-441.
72. Woodman SE, Sotgia F, Galbiati F, Minetti C, Lisanti MP, Caveolinopathies: Mutations in caveolin-3 cause four distinct autosomal dominant muscle diseases. Neurology, 2004. 62(4): p. 538-543.
73. Galbiati F, Phenotypic behavior of caveolin-3 mutations that cause autosomal dominant limb girdle muscular dystrophy (lgmd-1c). Retention of lgmd-1c caveolin-3 mutants within the golgi complex. Journal of Biological Chemistry, 1999. 274(36): p. 25632-25641.
74. Sotgia F, Woodman SE, Bonuccelli G, Capozza F, Minetti C, Scherer PE, Lisanti MP, Phenotypic behavior of caveolin-3 r26q, a mutant associated with hyperckemia, distal myopathy, and rippling muscle disease. Am J Physiol Cell Physiol, 2003. 285(5): p. C1150-1160.
75. Hill MM, Bastiani M, Luetterforst R, Kirkham M, Kirkham A, Nixon SJ, Walser P, Abankwa D, Oorschot VM, Martin S, Hancock JF, Parton RG, Ptrf-cavin, a conserved cytoplasmic protein required for caveola formation and function. Cell, 2008. 132(1): p. 113-124.
76. Stoeber M, Stoeck IK, Hanni C, Bleck CK, Balistreri G, Helenius A, Oligomers of the atpase ehd2 confine caveolae to the plasma membrane through association with actin. EMBO J, 2012. 31(10):

p. 2350-2364.
77. Senju Y, Itoh Y, Takano K, Hamada S, Suetsugu S, Essential role of pacsin2/syndapin-ii in caveolae membrane sculpting. J Cell Sci, 2011. 124(Pt 12): p. 2032-2040.
78. Senju Y, Suetsugu S, Possible regulation of caveolar endocytosis and flattening by phosphorylation of f-bar domain protein pacsin2/syndapin ii. Bioarchitecture, 2015. 5(5-6): p. 70-77.
79. Moren B, Shah C, Howes MT, Schieber NL, McMahon HT, Parton RG, Daumke O, Lundmark R, Ehd2 regulates caveolar dynamics via atp-driven targeting and oligomerization. Mol Biol Cell, 2012. 23(7): p. 1316-1329.
80. Braun A, Pinyol R, Dahlhaus R, Koch D, Fonarev P, Grant BD, Kessels MM, Qualmann B, Ehd proteins associate with syndapin i and ii and such interactions play a crucial role in endosomal recycling. Mol Biol Cell, 2005. 16(8): p. 3642-3658.
81. Campelo F, Fabrikant G, McMahon HT, Kozlov MM, Modeling membrane shaping by proteins: Focus on ehd2 and n-bar domains. FEBS Lett, 2010. 584(9): p. 1830-1839.
82. Guilherme A, Soriano NA, Bose S, Holik J, Bose A, Pomerleau DP, Furcinitti P, Leszyk J, Corvera S, Czech MP, Ehd2 and the novel eh domain binding protein ehbp1 couple endocytosis to the actin cytoskeleton. J Biol Chem, 2004. 279(11): p. 10593-10605.
83. Kessels MM, Qualmann B, The syndapin protein family: Linking membrane trafficking with the cytoskeleton. J Cell Sci, 2004. 117(Pt 15): p. 3077-3086.
84. Koch D, Westermann M, Kessels MM, Qualmann B, Ultrastructural freeze-fracture immunolabeling identifies plasma membrane-localized syndapin ii as a crucial factor in shaping caveolae. Histochem Cell Biol, 2012. 138(2): p. 215-230.
85. Hansen CG, Howard G, Nichols BJ, Pacsin 2 is recruited to caveolae and functions in caveolar biogenesis. J Cell Sci, 2011. 124(Pt 16): p. 2777-2785.
86. Kovtun O, Tillu VA, Ariotti N, Parton RG, Collins BM, Cavin family proteins and the assembly of caveolae. J Cell Sci, 2015. 128(7): p. 1269-1278.
87. Nassar ZD, Parat MO, Cavin family: New players in the biology of caveolae. Int Rev Cell Mol Biol, 2015. 320: p. 235-305.
88. Jansa P, Mason SW, Hoffmann-Rohrer U, Grummt I, Cloning and functional characterization of ptrf, a novel protein which induces dissociation of paused ternary transcription complexes. EMBO J, 1998. 17(10): p. 2855-2864.
89. Jansa P, Grummt I, Mechanism of transcription termination: Ptrf interacts with the largest subunit of rna polymerase i and dissociates paused transcription complexes from yeast and mouse. Mol Gen Genet, 1999. 262(3): p. 508-514.
90. Jansa P, Burek C, Sander EE, Grummt I, The transcript release factor ptrf augments ribosomal gene transcription by facilitating reinitiation of rna polymerase i. Nucleic Acids Res, 2001. 29(2): p. 423-429.
91. Aboulaich N, Vainonen JP, Stralfors P, Vener AV, Vectorial proteomics reveal targeting, phosphorylation and specific fragmentation of polymerase i and transcript release factor (ptrf) at the surface of caveolae in human adipocytes. Biochem J, 2004. 383(Pt 2): p. 237-248.
92. Vinten J, Johnsen AH, Roepstorff P, Harpoth J, Tranum-Jensen J, Identification of a major protein on the cytosolic face of caveolae. Biochim Biophys Acta, 2005. 1717(1): p. 34-40.
93. Liu L, Pilch PF, A critical role of cavin (polymerase i and transcript release factor) in caveolae formation and organization. J Biol Chem, 2008. 283(7): p. 4314-4322.
94. Wei Z, Zou X, Wang H, Lei J, Wu Y, Liao K, The n-terminal leucine-zipper motif in ptrf/cavin-1 is essential and sufficient for its caveolae-association. Biochem Biophys Res Commun, 2015. 456(3): p. 750-756.
95. Hayer A, Stoeber M, Ritz D, Engel S, Meyer HH, Helenius A, Caveolin-1 is ubiquitinated and targeted to intralumenal vesicles in endolysosomes for degradation. J Cell Biol, 2010. 191(3): p. 615-629.
96. Zhu H, Lin P, De G, Choi KH, Takeshima H, Weisleder N, Ma J, Polymerase transcriptase release factor (ptrf) anchors mg53 protein to cell injury site for initiation of membrane repair. J Biol Chem, 2011. 286(15): p. 12820-12824.

97. Ardissone A, Bragato C, Caffi L, Blasevich F, Maestrini S, Bianchi ML, Morandi L, Moroni I, Mora M, Novel ptrf mutation in a child with mild myopathy and very mild congenital lipodystrophy. BMC Med Genet, 2013. 14: p. 89-89.
98. Shastry S, Delgado MR, Dirik E, Turkmen M, Agarwal AK, Garg A, Congenital generalized lipodystrophy, type 4 (cgl4) associated with myopathy due to novel ptrf mutations. Am J Med Genet A, 2010. 152A(9): p. 2245-2253.
99. Gustincich S, Schneider C, Serum deprivation response gene is induced by serum starvation but not by contact inhibition. Cell Growth Differ, 1993. 4(9): p. 753-760.
100. Hansen CG, Bright NA, Howard G, Nichols BJ, Sdpr induces membrane curvature and functions in the formation of caveolae. Nat Cell Biol, 2009. 11(7): p. 807-814.
101. Burgener R, Wolf M, Ganz T, Baggiolini M, Purification and characterization of a major phosphatidylserine-binding phosphoprotein from human platelets. Biochemical Journal, 1990. 269(3): p. 729-734.
102. Gustincich S, Vatta P, Goruppi S, Wolf M, Saccone S, Della Valle G, Baggiolini M, Schneider C, The humanserum deprivation responsegene (sdpr) maps to 2q32–q33 and codes for a phosphatidylserine-binding protein. Genomics, 1999. 57(1): p. 120-129.
103. McMahon K-A, Zajicek H, Li W-P, Peyton MJ, Minna JD, Hernandez VJ, Luby-Phelps K, Anderson RGW, Srbc/cavin-3 is a caveolin adapter protein that regulates caveolae function. EMBO J, 2009. 28(8): p. 1001-1015.
104. Ogata T, Ueyama T, Isodono K, Tagawa M, Takehara N, Kawashima T, Harada K, Takahashi T, Shioi T, Matsubara H, Oh H, Murc, a muscle-restricted coiled-coil protein that modulates the rho/rock pathway, induces cardiac dysfunction and conduction disturbance. Molecular and Cellular Biology, 2008. 28(10): p. 3424-3436.
105. Naito D, Ogata T, Hamaoka T, Nakanishi N, Miyagawa K, Maruyama N, Kasahara T, Taniguchi T, Nishi M, Matoba S, Ueyama T, The coiled-coil domain of murc/cavin-4 is involved in membrane trafficking of caveolin-3 in cardiomyocytes. American Journal of Physiology - Heart and Circulatory Physiology, 2015. 309(12): p. H2127.
106. Rodriguez G, Ueyama T, Ogata T, Czernuszewicz G, Tan Y, Dorn GW, Bogaev R, Amano K, Oh H, Matsubara H, Willerson JT, Marian AJ, Molecular genetic and functional characterization implicate muscle-restricted coiled-coil gene (murc) as a causal gene for familial dilated cardiomyopathy. Circ Cardiovasc Genet, 2011. 4(4): p. 349-358.
107. Bastiani M, Liu L, Hill MM, Jedrychowski MP, Nixon SJ, Lo HP, Abankwa D, Luetterforst R, Fernandez-Rojo M, Breen MR, Gygi SP, Vinten J, Walser PJ, North KN, Hancock JF, Pilch PF, Parton RG, Murc/cavin-4 and cavin family members form tissue-specific caveolar complexes. J Cell Biol, 2009. 185(7): p. 1259-1273.
108. Shu L, Shayman JA, Glycosphingolipid mediated caveolin-1 oligomerization. Journal of glycomics & lipidomics, 2012. Suppl 2: p. 1-6.
109. Ren X, Ostermeyer AG, Ramcharan LT, Zeng Y, Lublin DM, Brown DA, Conformational defects slow golgi exit, block oligomerization, and reduce raft affinity of caveolin-1 mutant proteins. Mol Biol Cell, 2004. 15(10): p. 4556-4567.
110. Machleidt T, Li W-P, Liu P, Anderson RGW, Multiple domains in caveolin-1 control its intracellular traffic. J Cell Biol, 2000. 148(1): p. 17-28.
111. Song KS, Tang Z, Li S, Lisanti MP, Mutational analysis of the properties of caveolin-1. A novel role for the c-terminal domain in mediating homo-typic caveolin-caveolin interactions. J Biol Chem, 1997. 272(7): p. 4398-4403.
112. Machleidt T, Li WP, Liu P, Anderson RG, Multiple domains in caveolin-1 control its intracellular traffic. J Cell Biol, 2000. 148(1): p. 17-28.
113. Stahlhut M, van Deurs B, Identification of filamin as a novel ligand for caveolin-1: Evidence for the organization of caveolin-1–associated membrane domains by the actin cytoskeleton. Mol Biol Cell, 2000. 11(1): p. 325-337.
114. Nomura R, Fujimoto T, Tyrosine-phosphorylated caveolin-1: Immunolocalization and molecular characterization. Mol Biol Cell, 1999. 10(4): p. 975-986.
115. Aoki T, Nomura R, Fujimoto T, Tyrosine phosphorylation of caveolin-1 in the endothelium. Exp

Cell Res, 1999. 253(2): p. 629-636.
116. Volonte D, Galbiati F, Pestell RG, Lisanti MP, Cellular stress induces the tyrosine phosphorylation of caveolin-1 (tyr(14)) via activation of p38 mitogen-activated protein kinase and c-src kinase. Evidence for caveolae, the actin cytoskeleton, and focal adhesions as mechanical sensors of osmotic stress. J Biol Chem, 2001. 276(11): p. 8094-8103.
117. Pelkmans L, Püntener D, Helenius A, Local actin polymerization and dynamin recruitment in sv40-induced internalization of caveolae. Science, 2002. 296(5567): p. 535.
118. Radel C, Rizzo V, Integrin mechanotransduction stimulates caveolin-1 phosphorylation and recruitment of csk to mediate actin reorganization. Am J Physiol Heart Circ Physiol, 2005. 288(2): p. H936-945.
119. Fagerholm S, Örtegren U, Karlsson M, Ruishalme I, Strålfors P, Rapid insulin-dependent endocytosis of the insulin receptor by caveolae in primary adipocytes. PLoS One, 2009. 4(6): p. e5985.
120. Shajahan AN, Tiruppathi C, Smrcka AV, Malik AB, Minshall RD, Gbetagamma activation of src induces caveolae-mediated endocytosis in endothelial cells. J Biol Chem, 2004. 279(46): p. 48055-48062.
121. Zimnicka AM, Husain YS, Shajahan AN, Sverdlov M, Chaga O, Chen Z, Toth PT, Klomp J, Karginov AV, Tiruppathi C, Malik AB, Minshall RD, Src-dependent phosphorylation of caveolin-1 tyr-14 promotes swelling and release of caveolae. Mol Biol Cell, 2016. 27(13): p. 2090-2106.
122. Lapierre LA, Ducharme NA, Drake KR, Goldenring JR, Kenworthy AK, Coordinated regulation of caveolin-1 and rab11a in apical recycling compartments of polarized epithelial cells. Exp Cell Res, 2012. 318(2): p. 103-113.
123. Shang F, Taylor A, Ubiquitin-proteasome pathway and cellular responses to oxidative stress. Free radical biology & medicine, 2011. 51(1): p. 5-16.
124. Dunne KA, Allam A, McIntosh A, Houston SA, Cerovic V, Goodyear CS, Roe AJ, Beatson SA, Milling SW, Walker D, Wall DM, Increased s-nitrosylation and proteasomal degradation of caspase-3 during infection contribute to the persistence of adherent invasive escherichia coli (aiec) in immune cells. PLoS One, 2013. 8(7): p. e68386.
125. Mougeolle A, Poussard S, Decossas M, Lamaze C, Lambert O, Dargelos E, Oxidative stress induces caveolin 1 degradation and impairs caveolae functions in skeletal muscle cells. PLoS One, 2015. 10(3): p. e0122654.
126. Bakhshi FR, Mao M, Shajahan AN, Piegeler T, Chen Z, Chernaya O, Sharma T, Elliott WM, Szulcek R, Bogaard HJ, Comhair S, Erzurum S, van Nieuw Amerongen GP, Bonini MG, Minshall RD, Nitrosation-dependent caveolin 1 phosphorylation, ubiquitination, and degradation and its association with idiopathic pulmonary arterial hypertension. Pulm Circ, 2013. 3(4): p. 816-830.
127. Sotgia F, Woodman SE, Bonuccelli G, Capozza F, Minetti C, Scherer PE, Lisanti MP, Phenotypic behavior of caveolin-3 r26q, a mutant associated with hyperckemia, distal myopathy, and rippling muscle disease. American Journal of Physiology - Cell Physiology, 2003. 285(5): p. C1150.
128. Cheng JPX, Nichols BJ, Caveolae: One function or many? Trends Cell Biol, 2016. 26(3): p. 177-189.
129. Cohen AW, Park DS, Woodman SE, Williams TM, Chandra M, Shirani J, Pereira de Souza A, Kitsis RN, Russell RG, Weiss LM, Tang B, Jelicks LA, Factor SM, Shtutin V, Tanowitz HB, Lisanti MP, Caveolin-1 null mice develop cardiac hypertrophy with hyperactivation of p42/44 map kinase in cardiac fibroblasts. Am J Physiol Cell Physiol, 2003. 284(2): p. C457-474.
130. Ryter SW, Choi AM, Caveolin-1: A critical regulator of pulmonary vascular architecture and nitric oxide bioavailability in pulmonary hypertension. Am J Physiol Lung Cell Mol Physiol, 2008. 294(5): p. L862-864.
131. Zhao YY, Liu Y, Stan RV, Fan L, Gu Y, Dalton N, Chu PH, Peterson K, Ross J, Jr., Chien KR, Defects in caveolin-1 cause dilated cardiomyopathy and pulmonary hypertension in knockout mice. Proc Natl Acad Sci U S A, 2002. 99(17): p. 11375-11380.
132. Head BP, Patel HH, Roth DM, Murray F, Swaney JS, Niesman IR, Farquhar MG, Insel PA, Microtubules and actin microfilaments regulate lipid raft/caveolae localization of adenylyl cyclase signaling components. J Biol Chem, 2006. 281(36): p. 26391-26399.

133. Patel HH, Tsutsumi YM, Head BP, Niesman IR, Jennings M, Horikawa Y, Huang D, Moreno AL, Patel PM, Insel PA, Roth DM, Mechanisms of cardiac protection from ischemia/reperfusion injury: A role for caveolae and caveolin-1. The FASEB Journal, 2007. 21(7): p. 1565-1574.
134. Hassan GS, Jasmin JF, Schubert W, Frank PG, Lisanti MP, Caveolin-1 deficiency stimulates neointima formation during vascular injury. Biochemistry, 2004. 43(26): p. 8312-8321.
135. Miyasato SK, Loeffler J, Shohet R, Zhang J, Lindsey M, Le Saux CJ, Caveolin-1 modulates tgf-β1 signaling in cardiac remodeling. Matrix Biol, 2011. 30(0): p. 318-329.
136. Wertz JW, Bauer PM, Caveolin-1 regulates bmprii localization and signaling in vascular smooth muscle cells. Biochem Biophys Res Commun, 2008. 375(4): p. 557-561.
137. Hassan GS, Williams TM, Frank PG, Lisanti MP, Caveolin-1-deficient aortic smooth muscle cells show cell autonomous abnormalities in proliferation, migration, and endothelin-based signal transduction. American Journal of Physiology - Heart and Circulatory Physiology, 2006. 290(6): p. H2393.
138. Wunderlich C, Schober K, Lange SA, Drab M, Braun-Dullaeus RC, Kasper M, Schwencke C, Schmeisser A, Strasser RH, Disruption of caveolin-1 leads to enhanced nitrosative stress and severe systolic and diastolic heart failure. Biochem Biophys Res Commun, 2006. 340(2): p. 702-708.
139. Park DS, Cohen AW, Frank PG, Razani B, Lee H, Williams TM, Chandra M, Shirani J, De Souza AP, Tang B, Jelicks LA, Factor SM, Weiss LM, Tanowitz HB, Lisanti MP, Caveolin-1 null (–/–) mice show dramatic reductions in life span. Biochemistry, 2003. 42(51): p. 15124-15131.
140. Razani B, Combs TP, Wang XB, Frank PG, Park DS, Russell RG, Li M, Tang B, Jelicks LA, Scherer PE, Lisanti MP, Caveolin-1-deficient mice are lean, resistant to diet-induced obesity, and show hypertriglyceridemia with adipocyte abnormalities. J Biol Chem, 2002. 277(10): p. 8635-8647.
141. Martin S, Fernandez-Rojo MA, Stanley AC, Bastiani M, Okano S, Nixon SJ, Thomas G, Stow JL, Parton RG, Caveolin-1 deficiency leads to increased susceptibility to cell death and fibrosis in white adipose tissue: Characterization of a lipodystrophic model. PLoS One, 2012. 7(9): p. e46242.
142. Del Galdo F, Lisanti MP, Jimenez SA, Caveolin-1, transforming growth factor-beta receptor internalization, and the pathogenesis of systemic sclerosis. Curr Opin Rheumatol, 2008. 20(6): p. 713-719.
143. Le Lay S, Briand N, Blouin CM, Chateau D, Prado C, Lasnier F, Le Liepvre X, Hajduch E, Dugail I, The lipoatrophic caveolin-1 deficient mouse model reveals autophagy in mature adipocytes. Autophagy, 2010. 6(6): p. 754-763.
144. Gonzalez-Munoz E, Lopez-Iglesias C, Calvo M, Palacin M, Zorzano A, Camps M, Caveolin-1 loss of function accelerates glucose transporter 4 and insulin receptor degradation in 3t3-l1 adipocytes. Endocrinology, 2009. 150(8): p. 3493-3502.
145. Bastiani M, Parton RG, Caveolae at a glance. J Cell Sci, 2010. 123(Pt 22): p. 3831-3836.
146. Chidlow JH, Jr., Sessa WC, Caveolae, caveolins, and cavins: Complex control of cellular signalling and inflammation. Cardiovasc Res, 2010. 86(2): p. 219-225.
147. Oka N, Yamamoto M, Schwencke C, Kawabe J, Ebina T, Ohno S, Couet J, Lisanti MP, Ishikawa Y, Caveolin interaction with protein kinase c. Isoenzyme-dependent regulation of kinase activity by the caveolin scaffolding domain peptide. J Biol Chem, 1997. 272(52): p. 33416-33421.
148. Ju H, Zou R, Venema VJ, Venema RC, Direct interaction of endothelial nitric-oxide synthase and caveolin-1 inhibits synthase activity. J Biol Chem, 1997. 272(30): p. 18522-18525.
149. Trane AE, Pavlov D, Sharma A, Saqib U, Lau K, van Petegem F, Minshall RD, Roman LJ, Bernatchez PN, Deciphering the binding of caveolin-1 to client protein endothelial nitric-oxide synthase (enos): Scaffolding subdomain identification, interaction modeling, and biological significance. J Biol Chem, 2014. 289(19): p. 13273-13283.
150. Yamamoto M, Toya Y, Jensen RA, Ishikawa Y, Caveolin is an inhibitor of platelet-derived growth factor receptor signaling. Exp Cell Res, 1999. 247(2): p. 380-388.
151. Couet J, Sargiacomo M, Lisanti MP, Interaction of a receptor tyrosine kinase, egf-r, with caveolins. Caveolin binding negatively regulates tyrosine and serine/threonine kinase activities. J

Biol Chem, 1997. 272(48): p. 30429-30438.
152. Razani B, Zhang XL, Bitzer M, von Gersdorff G, Bottinger EP, Lisanti MP, Caveolin-1 regulates transforming growth factor (tgf)-beta/smad signaling through an interaction with the tgf-beta type i receptor. J Biol Chem, 2001. 276(9): p. 6727-6738.
153. Zhang B, Peng F, Wu D, Ingram AJ, Gao B, Krepinsky JC, Caveolin-1 phosphorylation is required for stretch-induced egfr and akt activation in mesangial cells. Cell Signal, 2007. 19(8): p. 1690-1700.
154. Gosens R, Stelmack GL, Dueck G, McNeill KD, Yamasaki A, Gerthoffer WT, Unruh H, Gounni AS, Zaagsma J, Halayko AJ, Role of caveolin-1 in p42/p44 map kinase activation and proliferation of human airway smooth muscle. Am J Physiol Lung Cell Mol Physiol, 2006. 291(3): p. L523-534.
155. Park WY, Park JS, Cho KA, Kim DI, Ko YG, Seo JS, Park SC, Up-regulation of caveolin attenuates epidermal growth factor signaling in senescent cells. J Biol Chem, 2000. 275(27): p. 20847-20852.
156. Galbiati F, Volonté D, Gil O, Zanazzi G, Salzer JL, Sargiacomo M, Scherer PE, Engelman JA, Schlegel A, Parenti M, Okamoto T, Lisanti MP, Expression of caveolin-1 and -2 in differentiating pc12 cells and dorsal root ganglion neurons: Caveolin-2 is up-regulated in response to cell injury. Proc Natl Acad Sci U S A, 1998. 95(17): p. 10257-10262.
157. Volonte D, Zhang K, Lisanti MP, Galbiati F, Expression of caveolin-1 induces premature cellular senescence in primary cultures of murine fibroblasts: Stress-induced premature senescence upregulates the expression of endogenous caveolin-1. Mol Biol Cell, 2002. 13(7): p. 2502-2517.
158. Koleske AJ, Baltimore D, Lisanti MP, Reduction of caveolin and caveolae in oncogenically transformed cells. Proc Natl Acad Sci U S A, 1995. 92(5): p. 1381-1385.
159. Song G, Ouyang G, Bao S, The activation of akt/pkb signaling pathway and cell survival. J Cell Mol Med, 2005. 9(1): p. 59-71.
160. Parsons SJ, Parsons JT, Src family kinases, key regulators of signal transduction. Oncogene, 2004. 23(48): p. 7906-7909.
161. Sotgia F, Martinez-Outschoorn UE, Howell A, Pestell RG, Pavlides S, Lisanti MP, Caveolin-1 and cancer metabolism in the tumor microenvironment: Markers, models, and mechanisms. Annu Rev Pathol, 2012. 7: p. 423-467.
162. Williams TM, Lisanti MP, Caveolin-1 in oncogenic transformation, cancer, and metastasis. Am J Physiol Cell Physiol, 2005. 288(3): p. C494-506.
163. Place AT, Chen Z, Bakhshi FR, Liu G, O'Bryan JP, Minshall RD, Cooperative role of caveolin-1 and c-terminal src kinase binding protein in c-terminal src kinase-mediated negative regulation of c-src. Mol Pharmacol, 2011. 80(4): p. 665-672.
164. Podar K, Tai YT, Cole CE, Hideshima T, Sattler M, Hamblin A, Mitsiades N, Schlossman RL, Davies FE, Morgan GJ, Munshi NC, Chauhan D, Anderson KC, Essential role of caveolae in interleukin-6- and insulin-like growth factor i-triggered akt-1-mediated survival of multiple myeloma cells. J Biol Chem, 2003. 278(8): p. 5794-5801.
165. Engelman JA, Zhang XL, Lisanti MP, Sequence and detailed organization of the human caveolin-1 and -2 genes located near the d7s522 locus (7q31.1): Methylation of a cpg island in the 5′ promoter region of the caveolin-1 gene in human breast cancer cell lines. FEBS Lett, 1999. 448(2–3): p. 221-230.
166. Lee SW, Reimer CL, Oh P, Campbell DB, Schnitzer JE, Tumor cell growth inhibition by caveolin re-expression in human breast cancer cells. Oncogene, 1998. 16(11): p. 1391-1397.
167. Hayashi K, Matsuda S, Machida K, Yamamoto T, Fukuda Y, Nimura Y, Hayakawa T, Hamaguchi M, Invasion activating caveolin-1 mutation in human scirrhous breast cancers. Cancer Res, 2001. 61(6): p. 2361-2364.
168. Bonuccelli G, Casimiro MC, Sotgia F, Wang C, Liu M, Katiyar S, Zhou J, Dew E, Capozza F, Daumer KM, Minetti C, Milliman JN, Alpy F, Rio MC, Tomasetto C, Mercier I, Flomenberg N, Frank PG, Pestell RG, Lisanti MP, Caveolin-1 (p132l), a common breast cancer mutation, confers mammary cell invasiveness and defines a novel stem cell/metastasis-associated gene signature. Am J Pathol, 2009. 174(5): p. 1650-1662.

169. Mercier I, Bryant KG, Sotgia F, Bonuccelli G, Witkiewicz AK, Dasgupta A, Jasmin JF, Pestell RG, Lisanti MP, Using caveolin-1 epithelial immunostaining patterns to stratify human breast cancer patients and predict the caveolin-1 (p132l) mutation. Cell Cycle, 2009. 8(9): p. 1396-1401.
170. Tiwari A, Copeland CA, Han B, Hanson CA, Raghunathan K, Kenworthy AK, Caveolin-1 is an aggresome-inducing protein. Sci Rep, 2016. 6: p. 38681.
171. Rieth MD, Lee J, Glover KJ, Probing the caveolin-1 p132l mutant: Critical insights into its oligomeric behavior and structure. Biochemistry, 2012. 51(18): p. 3911-3918.
172. Shatz M, Lustig G, Reich R, Liscovitch M, Caveolin-1 mutants p132l and y14f are dominant negative regulators of invasion, migration and aggregation in h1299 lung cancer cells. Exp Cell Res, 2010. 316(10): p. 1748-1762.
173. Li S, Seitz R, Lisanti MP, Phosphorylation of caveolin by src tyrosine kinases. The alpha-isoform of caveolin is selectively phosphorylated by v-src in vivo. J Biol Chem, 1996. 271(7): p. 3863-3868.
174. Schlegel A, Arvan P, Lisanti MP, Caveolin-1 binding to endoplasmic reticulum membranes and entry into the regulated secretory pathway are regulated by serine phosphorylation. Protein sorting at the level of the endoplasmic reticulum. J Biol Chem, 2001. 276(6): p. 4398-4408.
175. Liu P, Li WP, Machleidt T, Anderson RG, Identification of caveolin-1 in lipoprotein particles secreted by exocrine cells. Nat Cell Biol, 1999. 1(6): p. 369-375.
176. Gargalovic P, Dory L, Caveolin-1 and caveolin-2 expression in mouse macrophages. High density lipoprotein 3-stimulated secretion and a lack of significant subcellular co-localization. J Biol Chem, 2001. 276(28): p. 26164-26170.
177. Wu D, Terrian DM, Regulation of caveolin-1 expression and secretion by a protein kinase cepsilon signaling pathway in human prostate cancer cells. J Biol Chem, 2002. 277(43): p. 40449-40455.
178. Tahir SA, Yang G, Ebara S, Timme TL, Satoh T, Li L, Goltsov A, Ittmann M, Morrisett JD, Thompson TC, Secreted caveolin-1 stimulates cell survival/clonal growth and contributes to metastasis in androgen-insensitive prostate cancer. Cancer Res, 2001. 61(10): p. 3882-3885.
179. Tahir SA, Frolov A, Hayes TG, Mims MP, Miles BJ, Lerner SP, Wheeler TM, Ayala G, Thompson TC, Kadmon D, Preoperative serum caveolin-1 as a prognostic marker for recurrence in a radical prostatectomy cohort. Clin Cancer Res, 2006. 12(16): p. 4872-4875.
180. Bracamontes CG, Lopez-Valdez R, Subramani R, Arumugam A, Nandy S, Rajamanickam V, Ravichandran V, Lakshmanaswamy R, The serum protein profile of early parity which induces protection against breast cancer. Oncotarget, 2016.
181. Erdemli HK, Kocabas R, Salis O, Sen F, Akyol S, Eskin F, Akyol O, Bedir A, Sahin AF, Is serum caveolin-1 a useful biomarker for progression in patients with colorectal cancer? Clin Lab, 2016. 62(3): p. 401-408.
182. Teixeira A, Chaverot N, Schroder C, Strosberg AD, Couraud PO, Cazaubon S, Requirement of caveolae microdomains in extracellular signal-regulated kinase and focal adhesion kinase activation induced by endothelin-1 in primary astrocytes. J Neurochem, 1999. 72(1): p. 120-128.
183. Navarro A, Anand-Apte B, Parat MO, A role for caveolae in cell migration. FASEB J, 2004. 18(15): p. 1801-1811.
184. Luan TY, Zhu TN, Cui YJ, Zhang G, Song XJ, Gao DM, Zhang YM, Zhao QL, Liu S, Su TY, Zhao RJ, Expression of caveolin-1 is correlated with lung adenocarcinoma proliferation, migration, and invasion. Med Oncol, 2015. 32(7): p. 207.
185. Diaz-Valdivia N, Bravo D, Huerta H, Henriquez S, Gabler F, Vega M, Romero C, Calderon C, Owen GI, Leyton L, Quest AFG, Enhanced caveolin-1 expression increases migration, anchorage-independent growth and invasion of endometrial adenocarcinoma cells. BMC Cancer, 2015. 15: p. 463.
186. Nunez-Wehinger S, Ortiz RJ, Diaz N, Diaz J, Lobos-Gonzalez L, Quest AF, Caveolin-1 in cell migration and metastasis. Curr Mol Med, 2014. 14(2): p. 255-274.
187. Parton RG, del Pozo MA, Caveolae as plasma membrane sensors, protectors and organizers. Nat Rev Mol Cell Biol, 2013. 14(2): p. 98-112.
188. Pelkmans L, Helenius A, Endocytosis via caveolae. Traffic, 2002. 3(5): p. 311-320.

189. Henley JR, Krueger EW, Oswald BJ, McNiven MA, Dynamin-mediated internalization of caveolae. J Cell Biol, 1998. 141(1): p. 85-99.
190. Jiang Y, Sverdlov MS, Toth PT, Huang L, Du G, Liu Y, Natarajan V, Minshall RD, Phosphatidic acid produced by rala-activated pld2 stimulates caveolae-mediated endocytosis and trafficking in endothelial cells. J Biol Chem, 2016.
191. Shi F, Sottile J, Caveolin-1-dependent β1 integrin endocytosis is a critical regulator of fibronectin turnover. J Cell Sci, 2008. 121(Pt 14): p. 2360-2371.
192. Simionescu M, Popov D, Sima A, Endothelial transcytosis in health and disease. Cell Tissue Res, 2009. 335(1): p. 27-40.
193. Murata M, Peranen J, Schreiner R, Wieland F, Kurzchalia TV, Simons K, Vip21/caveolin is a cholesterol-binding protein. Proc Natl Acad Sci U S A, 1995. 92(22): p. 10339-10343.
194. Pol A, Martin S, Fernández MA, Ingelmo-Torres M, Ferguson C, Enrich C, Parton RG, Cholesterol and fatty acids regulate dynamic caveolin trafficking through the golgi complex and between the cell surface and lipid bodies. Mol Biol Cell, 2005. 16(4): p. 2091-2105.
195. Frank PG, Cheung MW, Pavlides S, Llaverias G, Park DS, Lisanti MP, Caveolin-1 and regulation of cellular cholesterol homeostasis. Am J Physiol Heart Circ Physiol, 2006. 291(2): p. H677-686.
196. Shvets E, Bitsikas V, Howard G, Hansen CG, Nichols BJ, Dynamic caveolae exclude bulk membrane proteins and are required for sorting of excess glycosphingolipids. Nat Commun, 2015. 6: p. 6867.
197. Pilch PF, Liu L, Fat caves: Caveolae, lipid trafficking and lipid metabolism in adipocytes. Trends Endocrinol Metab, 2011. 22(8): p. 318-324.
198. Pohl J, Ring A, Korkmaz Ü, Ehehalt R, Stremmel W, Fat/cd36-mediated long-chain fatty acid uptake in adipocytes requires plasma membrane rafts. Mol Biol Cell, 2005. 16(1): p. 24-31.
199. Meshulam T, Breen MR, Liu L, Parton RG, Pilch PF, Caveolins/caveolae protect adipocytes from fatty acid-mediated lipotoxicity. J Lipid Res, 2011. 52(8): p. 1526-1532.
200. Davies PF, Tripathi SC, Mechanical stress mechanisms and the cell. An endothelial paradigm. Circ Res, 1993. 72(2): p. 239-245.
201. Matthews BD, Overby DR, Mannix R, Ingber DE, Cellular adaptation to mechanical stress: Role of integrins, rho, cytoskeletal tension and mechanosensitive ion channels. J Cell Sci, 2006. 119(3): p. 508.
202. Gervasio OL, Phillips WD, Cole L, Allen DG, Caveolae respond to cell stretch and contribute to stretch-induced signaling. J Cell Sci, 2011. 124(Pt 21): p. 3581-3590.
203. Gilbert G, Ducret T, Savineau J-P, Marthan R, Quignard J-F, Caveolae are involved in mechanotransduction during pulmonary hypertension. American Journal of Physiology - Lung Cellular and Molecular Physiology, 2016. 310(11): p. L1078.
204. Sedding DG, Hermsen J, Seay U, Eickelberg O, Kummer W, Schwencke C, Strasser RH, Tillmanns H, Braun-Dullaeus RC, Caveolin-1 facilitates mechanosensitive protein kinase b (akt) signaling in vitro and in vivo. Circ Res, 2005. 96(6): p. 635-642.
205. Briand N, Prado C, Mabilleau G, Lasnier F, Le Lièpvre X, Covington JD, Ravussin E, Le Lay S, Dugail I, Caveolin-1 expression and cavin stability regulate caveolae dynamics in adipocyte lipid store fluctuation. Diabetes, 2014. 63(12): p. 4032-4044.
206. Martinez-Outschoorn UE, Sotgia F, Lisanti MP, Caveolae and signalling in cancer. Nat Rev Cancer, 2015. 15(4): p. 225-237.
207. Del Galdo F, Sotgia F, de Almeida CJ, Jasmin JF, Musick M, Lisanti MP, Jimenez SA, Decreased expression of caveolin 1 in patients with systemic sclerosis: Crucial role in the pathogenesis of tissue fibrosis. Arthritis Rheum, 2008. 58(9): p. 2854-2865.
208. Wang XM, Zhang Y, Kim HP, Zhou Z, Feghali-Bostwick CA, Liu F, Ifedigbo E, Xu X, Oury TD, Kaminski N, Choi AM, Caveolin-1: A critical regulator of lung fibrosis in idiopathic pulmonary fibrosis. J Exp Med, 2006. 203(13): p. 2895-2906.
209. Walther TC, Farese RV, Jr., Lipid droplets and cellular lipid metabolism. Annu Rev Biochem, 2012. 81: p. 687-714.
210. Machado RD, Eickelberg O, Elliott CG, Geraci MW, Hanaoka M, Loyd JE, Newman JH, Phillips JA, 3rd, Soubrier F, Trembath RC, Chung WK, Genetics and genomics of pulmonary arterial

hypertension. J Am Coll Cardiol, 2009. 54(1 Suppl): p. S32-42.
211. Garg A, Kircher M, Del Campo M, Amato RS, Agarwal AK, University of Washington Center for Mendelian G, Whole exome sequencing identifies de novo heterozygous cav1 mutations associated with a novel neonatal onset lipodystrophy syndrome. Am J Med Genet A, 2015. 167A(8): p. 1796-1806.
212. Razani B, Wang XB, Engelman JA, Battista M, Lagaud G, Zhang XL, Kneitz B, Hou H, Jr., Christ GJ, Edelmann W, Lisanti MP, Caveolin-2-deficient mice show evidence of severe pulmonary dysfunction without disruption of caveolae. Mol Cell Biol, 2002. 22(7): p. 2329-2344.
213. Cohen AW, Razani B, Wang XB, Combs TP, Williams TM, Scherer PE, Lisanti MP, Caveolin-1-deficient mice show insulin resistance and defective insulin receptor protein expression in adipose tissue. Am J Physiol Cell Physiol, 2003. 285(1): p. C222-235.
214. Cohen AW, Razani B, Schubert W, Williams TM, Wang XB, Iyengar P, Brasaemle DL, Scherer PE, Lisanti MP, Role of caveolin-1 in the modulation of lipolysis and lipid droplet formation. Diabetes, 2004. 53(5): p. 1261-1270.
215. Cohen AW, Combs TP, Scherer PE, Lisanti MP, Role of caveolin and caveolae in insulin signaling and diabetes. Am J Physiol Endocrinol Metab, 2003. 285(6): p. E1151-1160.
216. Ariotti N, Parton RG, Snapshot: Caveolae, caveolins, and cavins. Cell, 2013. 154(3): p. 704-704.e701.
217. Dwianingsih EK, Takeshima Y, Itoh K, Yamauchi Y, Awano H, Malueka RG, Nishida A, Ota M, Yagi M, Matsuo M, A japanese child with asymptomatic elevation of serum creatine kinase shows ptrf-cavin mutation matching with congenital generalized lipodystrophy type 4. Mol Genet Metab, 2010. 101(2-3): p. 233-237.
218. Hayashi YK, Matsuda C, Ogawa M, Goto K, Tominaga K, Mitsuhashi S, Park Y-E, Nonaka I, Hino-Fukuyo N, Haginoya K, Sugano H, Nishino I, Human ptrf mutations cause secondary deficiency of caveolins resulting in muscular dystrophy with generalized lipodystrophy. J Clin Invest, 2009. 119(9): p. 2623-2633.
219. Rajab A, Straub V, McCann LJ, Seelow D, Varon R, Barresi R, Schulze A, Lucke B, Lützkendorf S, Karbasiyan M, Bachmann S, Spuler S, Schuelke M, Fatal cardiac arrhythmia and long-qt syndrome in a new form of congenital generalized lipodystrophy with muscle rippling (cgl4) due to ptrf-cavin mutations. PLoS Genetics, 2010. 6(3): p. e1000874.
220. Jelani M, Ahmed S, Almramhi MM, Mohamoud HS, Bakur K, Anshasi W, Wang J, Al-Aama JY, Novel nonsense mutation in the ptrf gene underlies congenital generalized lipodystrophy in a consanguineous saudi family. Eur J Med Genet, 2015. 58(4): p. 216-221.
221. Murakami N, Hayashi YK, Oto Y, Shiraishi M, Itabashi H, Kudo K, Nishino I, Nonaka I, Nagai T, Congenital generalized lipodystrophy type 4 with muscular dystrophy: Clinical and pathological manifestations in early childhood. Neuromuscul Disord, 2013. 23(5): p. 441-444.
222. Kim CA, Delepine M, Boutet E, El Mourabit H, Le Lay S, Meier M, Nemani M, Bridel E, Leite CC, Bertola DR, Semple RK, O'Rahilly S, Dugail I, Capeau J, Lathrop M, Magre J, Association of a homozygous nonsense caveolin-1 mutation with berardinelli-seip congenital lipodystrophy. J Clin Endocrinol Metab, 2008. 93(4): p. 1129-1134.
223. Scherer PE, Okamoto T, Chun M, Nishimoto I, Lodish HF, Lisanti MP, Identification, sequence, and expression of caveolin-2 defines a caveolin gene family. Proc Natl Acad Sci U S A, 1996. 93(1): p. 131-135.
224. Ludwig A, Howard G, Mendoza-Topaz C, Deerinck T, Mackey M, Sandin S, Ellisman MH, Nichols BJ, Molecular composition and ultrastructure of the caveolar coat complex. PLoS Biol, 2013. 11(8): p. e1001640.
225. Gambin Y, Ariotti N, McMahon K-A, Bastiani M, Sierecki E, Kovtun O, Polinkovsky ME, Magenau A, Jung W, Okano S, Zhou Y, Leneva N, Mureev S, Johnston W, Gaus K, Hancock JF, Collins BM, Alexandrov K, Parton RG, Single-molecule analysis reveals self assembly and nanoscale segregation of two distinct cavin subcomplexes on caveolae. Elife, 2014. 3: p. e01434.
226. Mohan J, Moren B, Larsson E, Holst MR, Lundmark R, Cavin3 interacts with cavin1 and caveolin1 to increase surface dynamics of caveolae. J Cell Sci, 2015. 128(5): p. 979-991.
227. Oberhuber G, Histopathology of celiac disease. Biomed Pharmacother, 2000. 54(7): p. 368-372.

228. Fennessey CM, Sheng J, Rubin DH, McClain MS, Oligomerization of clostridium perfringens epsilon toxin is dependent upon caveolins 1 and 2. PLoS One, 2012. 7(10): p. e46866.
229. Han B, Tiwari A, Kenworthy AK, Tagging strategies strongly affect the fate of overexpressed caveolin-1. Traffic, 2015. 16(4): p. 417-438.
230. Lajoie P, Partridge EA, Guay G, Goetz JG, Pawling J, Lagana A, Joshi B, Dennis JW, Nabi IR, Plasma membrane domain organization regulates egfr signaling in tumor cells. J Cell Biol, 2007. 179(2): p. 341-356.
231. Parton RG, Simons K, The multiple faces of caveolae. Nat Rev Mol Cell Biol, 2007. 8(3): p. 185-194.
232. Kirkham M, Nixon SJ, Howes MT, Abi-Rached L, Wakeham DE, Hanzal-Bayer M, Ferguson C, Hill MM, Fernandez-Rojo M, Brown DA, Hancock JF, Brodsky FM, Parton RG, Evolutionary analysis and molecular dissection of caveola biogenesis. J Cell Sci, 2008. 121(Pt 12): p. 2075-2086.
233. Ariotti N, Rae J, Leneva N, Ferguson C, Loo D, Okano S, Hill MM, Walser P, Collins BM, Parton RG, Molecular characterization of caveolin-induced membrane curvature. J Biol Chem, 2015. 290(41): p. 24875-24890.
234. Bush WS, Ihrke G, Robinson JM, Kenworthy AK, Antibody-specific detection of caveolin-1 in subapical compartments of mdck cells. Histochem Cell Biol, 2006. 126(1): p. 27-34.
235. Hanson CA, Drake KR, Baird MA, Han B, Kraft LJ, Davidson MW, Kenworthy AK, Overexpression of caveolin-1 is sufficient to phenocopy the behavior of a disease-associated mutant. Traffic, 2013. 14(6): p. 663-677.
236. Drab M, Verkade P, Elger M, Kasper M, Lohn M, Lauterbach B, Menne J, Lindschau C, Mende F, Luft FC, Schedl A, Haller H, Kurzchalia TV, Loss of caveolae, vascular dysfunction, and pulmonary defects in caveolin-1 gene-disrupted mice. Science, 2001. 293(5539): p. 2449-2452.
237. Liu L, Pilch PF, Ptrf/cavin-1 promotes efficient ribosomal rna transcription in response to metabolic challenges. Elife, 2016. 5: p. e17508.
238. Rothberg KG, Heuser JE, Donzell WC, Ying YS, Glenney JR, Anderson RG, Caveolin, a protein component of caveolae membrane coats. Cell, 1992. 68(4): p. 673-682.
239. Collins BM, Davis MJ, Hancock JF, Parton RG, Structure-based reassessment of the caveolin signaling model: Do caveolae regulate signaling through caveolin-protein interactions? Dev Cell, 2012. 23(1): p. 11-20.
240. Monier S, Parton RG, Vogel F, Behlke J, Henske A, Kurzchalia TV, Vip21-caveolin, a membrane protein constituent of the caveolar coat, oligomerizes in vivo and in vitro. Mol Biol Cell, 1995. 6(7): p. 911-927.
241. Scheiffele P, Verkade P, Fra AM, Virta H, Simons K, Ikonen E, Caveolin-1 and -2 in the exocytic pathway of mdck cells. J Cell Biol, 1998. 140(4): p. 795-806.
242. Liu L, Brown D, McKee M, Lebrasseur NK, Yang D, Albrecht KH, Ravid K, Pilch PF, Deletion of cavin/ptrf causes global loss of caveolae, dyslipidemia, and glucose intolerance. Cell Metab, 2008. 8(4): p. 310-317.
243. Song KS, Tang ZL, Li SW, Lisanti MP, Mutational analysis of the properties of caveolin-1. A novel role for the c-terminal domain in mediating homo-typic caveolin-caveolin interactions. J Biol Chem, 1997. 272(7): p. 4398-4403.
244. Lee H, Woodman SE, Engelman JA, Volonte D, Galbiati F, Kaufman HL, Lublin DM, Lisanti MP, Palmitoylation of caveolin-1 at a single site (cys-156) controls its coupling to the c-src tyrosine kinase: Targeting of dually acylated molecules (gpi-linked, transmembrane, or cytoplasmic) to caveolae effectively uncouples c-src and caveolin-1 (tyr-14). J Biol Chem, 2001. 276(37): p. 35150-35158.
245. Luetterforst R, Stang E, Zorzi N, Carozzi A, Way M, Parton RG, Molecular characterization of caveolin association with the golgi complex: Identification of a cis-golgi targeting domain in the caveolin molecule. J Cell Biol, 1999. 145(7): p. 1443-1459.
246. Lee H, Park DS, Razani B, Russell RG, Pestell RG, Lisanti MP, Caveolin-1 mutations (p132l and null) and the pathogenesis of breast cancer: Caveolin-1 (p132l) behaves in a dominant-negative manner and caveolin-1 (-/-) null mice show mammary epithelial cell hyperplasia. Am J Pathol,

2002. 161(4): p. 1357-1369.
247. Razani B, Lisanti MP, Caveolin-deficient mice: Insights into caveolar function human disease. J Clin Invest, 2001. 108(11): p. 1553-1561.
248. Cao H, Alston L, Ruschman J, Hegele RA, Heterozygous cav1 frameshift mutations (mim 601047) in patients with atypical partial lipodystrophy and hypertriglyceridemia. Lipids Health Dis, 2008. 7: p. 3.
249. Pol A, Luetterforst R, Lindsay M, Heino S, Ikonen E, Parton RG, A caveolin dominant negative mutant associates with lipid bodies and induces intracellular cholesterol imbalance. J Cell Biol, 2001. 152(5): p. 1057-1070.
250. Mathew R, Huang J, Gewitz MH, Pulmonary artery hypertension: Caveolin-1 and enos interrelationship: A new perspective. Cardiol Rev, 2007. 15(3): p. 143-149.
251. Austin ED, Loyd JE, The genetics of pulmonary arterial hypertension. Circ Res, 2014. 115(1): p. 189-202.
252. Patel HH, Zhang S, Murray F, Suda RY, Head BP, Yokoyama U, Swaney JS, Niesman IR, Schermuly RT, Pullamsetti SS, Thistlethwaite PA, Miyanohara A, Farquhar MG, Yuan JX, Insel PA, Increased smooth muscle cell expression of caveolin-1 and caveolae contribute to the pathophysiology of idiopathic pulmonary arterial hypertension. FASEB J, 2007. 21(11): p. 2970-2979.
253. Mathew R, Cell-specific dual role of caveolin-1 in pulmonary hypertension. Pulm Med, 2011. 2011: p. 573432.
254. Prewitt AR, Ghose S, Frump AL, Datta A, Austin ED, Kenworthy AK, de Caestecker MP, Heterozygous null bone morphogenetic protein receptor type 2 mutations promote src kinase-dependent caveolar trafficking defects and endothelial dysfunction in pulmonary arterial hypertension. J Biol Chem, 2015. 290(2): p. 960-971.
255. Mathew R, Huang J, Shah M, Patel K, Gewitz M, Sehgal PB, Disruption of endothelial-cell caveolin-1alpha/raft scaffolding during development of monocrotaline-induced pulmonary hypertension. Circulation, 2004. 110(11): p. 1499-1506.
256. Hoeper MM, Bogaard HJ, Condliffe R, Frantz R, Khanna D, Kurzyna M, Langleben D, Manes A, Satoh T, Torres F, Wilkins MR, Badesch DB, Definitions and diagnosis of pulmonary hypertension. J Am Coll Cardiol, 2013. 62(25 Suppl): p. D42-50.
257. Jasmin JF, Mercier I, Dupuis J, Tanowitz HB, Lisanti MP, Short-term administration of a cell-permeable caveolin-1 peptide prevents the development of monocrotaline-induced pulmonary hypertension and right ventricular hypertrophy. Circulation, 2006. 114(9): p. 912-920.
258. Cosson P, Lefkir Y, Demolliere C, Letourneur F, New cop1-binding motifs involved in er retrieval. EMBO J, 1998. 17(23): p. 6863-6870.
259. Benghezal M, Wasteneys GO, Jones DA, The c-terminal dilysine motif confers endoplasmic reticulum localization to type i membrane proteins in plants. Plant Cell, 2000. 12(7): p. 1179-1201.
260. Lontok E, Corse E, Machamer CE, Intracellular targeting signals contribute to localization of coronavirus spike proteins near the virus assembly site. J Virol, 2004. 78(11): p. 5913-5922.
261. Pol A, Martin S, Fernandez MA, Ingelmo-Torres M, Ferguson C, Enrich C, Parton RG, Cholesterol and fatty acids regulate dynamic caveolin trafficking through the golgi complex and between the cell surface and lipid bodies. Mol Biol Cell, 2005. 16: p. 2091-2105.
262. Dupree P, Parton RG, Raposo G, Kurzchalia TV, Simons K, Caveolae and sorting in the trans-golgi network of epithelial cells. EMBO J, 1993. 12(4): p. 1597-1605.
263. Parolini I, Sargiacomo M, Galbiati F, Rizzo G, Grignani F, Engelman JA, Okamoto T, Ikezu T, Scherer PE, Mora R, Rodriguez-Boulan E, Peschle C, Lisanti MP, Expression of caveolin-1 is required for the transport of caveolin-2 to the plasma membrane. Retention of caveolin-2 at the level of the golgi complex. J Biol Chem, 1999. 274(36): p. 25718-25725.
264. Mora R, Bonilha VL, Marmorstein A, Scherer PE, Brown D, Lisanti MP, Rodriguez-Boulan E, Caveolin-2 localizes to the golgi complex but redistributes to plasma membrane, caveolae, and rafts when co-expressed with caveolin-1. J Biol Chem, 1999. 274(36): p. 25708-25717.
265. Lingwood D, Simons K, Detergent resistance as a tool in membrane research. Nat Protoc, 2007. 2(9): p. 2159-2165.

266. Davalos A, Fernandez-Hernando C, Sowa G, Derakhshan B, Lin MI, Lee JY, Zhao H, Luo R, Colangelo C, Sessa WC, Quantitative proteomics of caveolin-1 regulated proteins: Characterization of ptrf/cavin-1 in endothelial cells. Mol Cell Proteomics, 2010. 9: p. 2109-2124.
267. Rajendran L, Le Lay S, Illges H, Raft association and lipid droplet targeting of flotillins are independent of caveolin. Biol Chem, 2007. 388(3): p. 307-314.
268. Sinha B, Koster D, Ruez R, Gonnord P, Bastiani M, Abankwa D, Stan RV, Butler-Browne G, Vedie B, Johannes L, Morone N, Parton RG, Raposo G, Sens P, Lamaze C, Nassoy P, Cells respond to mechanical stress by rapid disassembly of caveolae. Cell, 2011. 144(3): p. 402-413.
269. Kabuss R, Ashikov A, Oelmann S, Gerardy-Schahn R, Bakker H, Endoplasmic reticulum retention of the large splice variant of the udp-galactose transporter is caused by a dilysine motif. Glycobiology, 2005. 15(10): p. 905-911.
270. Ostermeyer AG, Paci JM, Zeng Y, Lublin DM, Munro S, Brown DA, Accumulation of caveolin in the endoplasmic reticulum redirects the protein to lipid storage droplets. J Cell Biol, 2001. 152(5): p. 1071-1078.
271. Steric masking of a dilysine endoplasmic reticulum retention motif during assembly of the human high affinity receptor for immunoglobulin e. J Cell Biol, 1995. 129(4): p. 971-978.
272. Frick M, Bright NA, Riento K, Bray A, Merrified C, Nichols BJ, Coassembly of flotillins induces formation of membrane microdomains, membrane curvature, and vesicle budding. Curr Biol, 2007. 17(13): p. 1151-1156.
273. Vassilieva EV, Ivanov AI, Nusrat A, Flotillin-1 stabilizes caveolin-1 in intestinal epithelial cells. Biochem Biophys Res Commun, 2009. 379(2): p. 460-465.
274. Volonte D, Galbiati F, Li S, Nishiyama K, Okamoto T, Lisanti MP, Flotillins/cavatellins are differentially expressed in cells and tissues and form a hetero-oligomeric complex with caveolins in vivo. Characterization and epitope-mapping of a novel flotillin-1 monoclonal antibody probe. J Biol Chem, 1999. 274(18): p. 12702-12709.
275. Gambin Y, Ariotti N, McMahon KA, Bastiani M, Sierecki E, Kovtun O, Polinkovsky ME, Magenau A, Jung W, Okano S, Zhou Y, Leneva N, Mureev S, Johnston W, Gaus K, Hancock JF, Collins BM, Alexandrov K, Parton RG, Single-molecule analysis reveals self assembly and nanoscale segregation of two distinct cavin subcomplexes on caveolae. Elife, 2014. 3: p. e01434.
276. Zhao YY, Zhao YD, Mirza MK, Huang JH, Potula HH, Vogel SM, Brovkovych V, Yuan JX, Wharton J, Malik AB, Persistent enos activation secondary to caveolin-1 deficiency induces pulmonary hypertension in mice and humans through pkg nitration. J Clin Invest, 2009. 119(7): p. 2009-2018.
277. Low JY, Nicholson HD, Epigenetic modifications of caveolae associated proteins in health and disease. BMC Genet, 2015. 16(1): p. 71.
278. Nassar ZD, Moon H, Duong T, Neo L, Hill MM, Francois M, Parton RG, Parat MO, Ptrf/cavin-1 decreases prostate cancer angiogenesis and lymphangiogenesis. Oncotarget, 2013. 4(10): p. 1844-1855.
279. Razani B, Woodman SE, Lisanti MP, Caveolae: From cell biology to animal physiology. Pharmacol Rev, 2002. 54(3): p. 431-467.
280. Budhiraja R, Tuder RM, Hassoun PM, Endothelial dysfunction in pulmonary hypertension. Circulation, 2004. 109(2): p. 159-165.
281. Sowa G, Caveolae, caveolins, cavins, and endothelial cell function: New insights. Front Physiol, 2012. 2: p. 120.
282. Minshall RD, Sessa WC, Stan RV, Anderson RG, Malik AB, Caveolin regulation of endothelial function. Am J Physiol Lung Cell Mol Physiol, 2003. 285(6): p. L1179-1183.
283. Bauer PM, Yu J, Chen Y, Hickey R, Bernatchez PN, Looft-Wilson R, Huang Y, Giordano F, Stan RV, Sessa WC, Endothelial-specific expression of caveolin-1 impairs microvascular permeability and angiogenesis. Proc Natl Acad Sci U S A, 2005. 102(1): p. 204-209.
284. Sengupta D, Cholesterol modulates the structure, binding modes, and energetics of caveolin-membrane interactions. J Phys Chem B, 2012. 116(50): p. 14556-14564.
285. Jansen M, Pietiainen VM, Polonen H, Rasilainen L, Koivusalo M, Ruotsalainen U, Jokitalo E, Ikonen E, Cholesterol substitution increases the structural heterogeneity of caveolae. J Biol

Chem, 2008. 283(21): p. 14610-14618.
286. London E, Brown DA, Insolubility of lipids in triton x-100: Physical origin and relationship to sphingolipid/cholesterol membrane domains (rafts). Biochim Biophys Acta, 2000. 1508(1-2): p. 182-195.
287. Ahmed SN, Brown DA, London E, On the origin of sphingolipid/cholesterol-rich detergent-insoluble cell membranes: Physiological concentrations of cholesterol and sphingolipid induce formation of a detergent-insoluble, liquid-ordered lipid phase in model membranes. Biochemistry, 1997. 36(36): p. 10944-10953.
288. Ring A, Le Lay S, Pohl J, Verkade P, Stremmel W, Caveolin-1 is required for fatty acid translocase (fat/cd36) localization and function at the plasma membrane of mouse embryonic fibroblasts. Biochim Biophys Acta, 2006. 1761(4): p. 416-423.
289. Garg A, Agarwal AK, Caveolin-1: A new locus for human lipodystrophy. J Clin Endocrinol Metab, 2008. 93(4): p. 1183-1185.
290. Frank PG, Woodman SE, Park DS, Lisanti MP, Caveolin, caveolae, and endothelial cell function. Arterioscler Thromb Vasc Biol, 2003. 23(7): p. 1161-1168.
291. Dromparis P, Paulin R, Stenson TH, Haromy A, Sutendra G, Michelakis ED, Attenuating endoplasmic reticulum stress as a novel therapeutic strategy in pulmonary hypertension. Circulation, 2013. 127(1): p. 115-125.